

https://dspace.org/

Wind speed climatology in the northern, western, and Eastern Capes of South Africa: implications for wind power

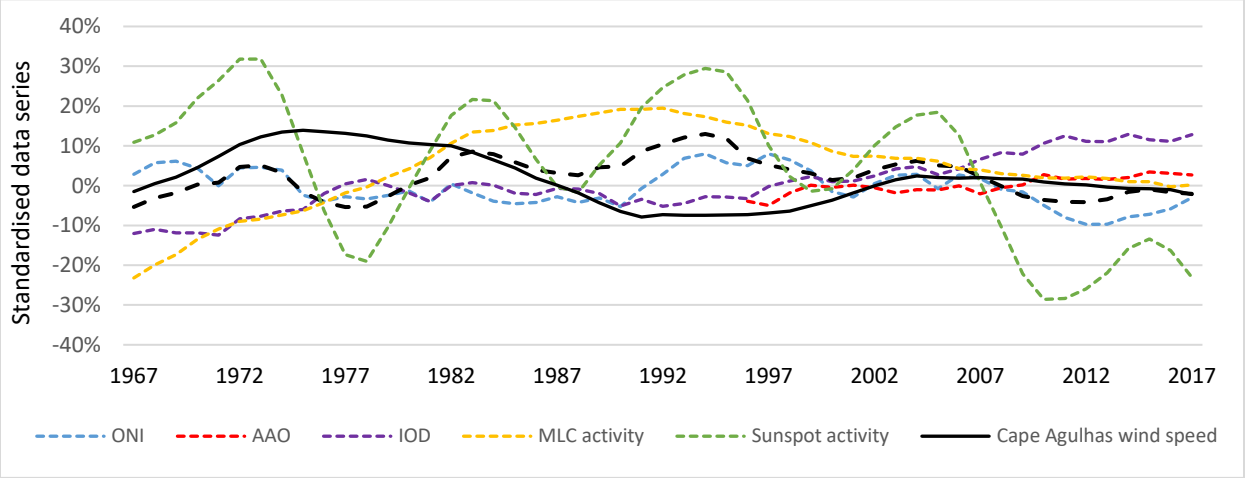
Wright, Marc Alan

2021
https://hdl.handle.net/10539/32391

Downloaded from a DSpace repository. https://dspace.org/

WIND SPEED CLIMATOLOGY IN THE NORTHERN, WESTERN, AND EASTERN CAPES OF SOUTH AFRICA: IMPLICATIONS FOR WIND POWER

Marc Alan Wright



Seventeen–year mean monthly filter for climatic variables, and Cape Agulhas wind speed series (black dashed line presenting the combined influence of all climatic variables).

A Thesis submitted in fulfilment of the academic requirements for the degree of Doctor of Philosophy

School of Geography, Archaeology, and Environmental Studies

University of the Witwatersrand, Johannesburg

16 February 2021

DECLARATION

I declare that this thesis is my own, unaided work, except where otherwise acknowledged. It is being submitted for the degree of Doctor of Philosophy in Science at the University of the Witwatersrand, Johannesburg. I have not submitted this work previously, for the purpose of obtaining any degree, qualification or otherwise, at this or any other university.

Signed this 16 day of February 2021



Marc Alan Wright.

ABSTRACT

The primary aims of this PhD research are to utilise long-term (>20 years), ground measured wind speed records (spanning 1950–2018) available from the Eastern, Northern, and Western Cape provinces of South Africa (the study area), to determine temporal wind speed trends, wind speed profiles, and wind speed teleconnection to global climate modes over these regions. This is achieved through the application of a robust methodology (i.e. data homogenization, quality control procedures, and multiple-geographically dispersed stations) to ensure high quality data series are available for the statistical analysis. Data homogenization, and quality control procedures of data series are conducted using windPRO, PAST4.01, and XLSTAT software. Wind speed trends are determined using the Sen's slope estimator, continuous wavelet analysis, and tested for statistical significance applying nonparametric statistics (i.e. Mann Kendall test). Wind speed profiles, and wind speed teleconnection to climate modes are assessed using correlation, regression, and multiple regression statistics, also tested for statistical significance applying nonparametric statistics (i.e. Mann Kendall test).

The fundamental objective of this thesis is to assess the long-term wind speed trends of the study area at multi-decadal, annual, seasonal, and monthly temporal scales. The second objective is to validate the diurnal, monthly, and seasonal wind speed profiles of the study area in the context of wind power generation. The final objective is to quantify the teleconnections present between wind speed, and large–scale climate modes, and observed wind speed characteristics at an annual, seasonal, and monthly temporal scale.

Long-term wind speed trends for the Cape Agulhas station indicates a statistically non-significant ($P>0.1$) decreasing (-0.06% per year; –0.003 m/s/year) mean annual wind speed trend for adjusted (standardised) data over the study period. For the common period (1995–2018), a statistically significant ($P<0.05$) mean decreasing trend (-0.14% per year; -0.005 m/s/year) is recorded by all stations in the study area, except for Langebaan (0.16% per year;

0.006 m/s/year). Mean seasonal trends also indicate statistically significant (P<0.1) decreasing trends, with the exception of the mean summer trend (0.31% per year; 0.015 m/s/year) at Langebaan. Decreasing mean cyclic trends are identified at most stations at 1–2, and 3–4 year periods, while increasing trends dominate most stations at 4–8 year cycles. Decreasing mean monthly trends are indicated at Cape Agulhas over 8–16 year periods, while, mean increasing monthly trends are present over 16–32 year periods.

Assessment of the diurnal wind resource profile identified ubiquitous statistically significant (P<0.1) correlations between daily electricity load profile, and the wind speed profiles - all positive. The correlations are moderate (i.e. mean r = 0.545) during Eskom high power demand periods, and strong during Eskom low per demand periods (i.e. mean r = 0.742). At a seasonal, and monthly scale, a negative correlation dominates wind speed, and the Eskom demand profile, indicating that the peak wind months correspond inversely to peak Eskom power demand (e.g. Alexander Bay, Langebaan, Tygerhoek). However, the Springbok series stood out being the only series with a positive seasonal (r = 0.833), and monthly (r = 0.739) wind speed correlation to the Eskom load profile.

Teleconnections of five climate modes (El Niño Southern Oscillation (ONI); Indian Ocean Dipole (IOD); Antarctic Oscillation (AAO); Regional Mid–Latitude Cyclones; Solar cycle (sunspot activity)) with wind speed are assessed at a monthly, seasonal, annual, and periodic time-scales. Weak inter–annual, -seasonal and-monthly correlations are observed between the wind speed series, and climate modes. The strongest association is identified between a 5-month lagged ONI, and wind speed, which explains a large percentage of variance at a mean monthly (63.04%) scale, and is particularly strong for the austral seasons of Autumn (97.4%), Winter (94.9%), and Spring (99.9%).

Keywords: wind power, wind speed, trend analysis, wind speed profile, continuous wavelet, Sen's slope, Mann Kendall, historical climate, Western Cape, Northern Cape, Eastern Cape, South Africa, ENSO, ONI.

ACKNOWLEDGEMENTS

I would like to extend my gratitude to my supervisor Professor Stefan Grab for his endless support, motivation, and commitment. I could not have had a better mentor, and I will forever value the lessons learnt throughout this process. It has bettered me as an individual in my personal, and professional capacity.

Importantly this research would not have been possible if my wife, and children, Sian, Keagan, and Chloe had not been so understanding. You helped me pick up my spirits when times were tough, and we have grown stronger as a family together. I am eternally grateful, and the sacrifices made will be dwarfed to the road that lies ahead. We have closed a huge milestone in our book called life, now onward, and upward we go.

To my Mom and Dad, thank you for providing me the resources to become the professional I am today. I am forever grateful for the endless support you have provided over the years.

We acknowledge data provided by the South African Weather Service (SAWS), and financial support from the National Research Foundation of South Africa (grant #102100).

Declaration ii
Abstract iii
Acknowledgements v
List of Figures x
List of Tables xiv
LIST OF ABBREVIATIONS xvi
1 Introduction 1
1.1 Overview, and motivation 1
1.2 Research Rationale 2
1.3 Aims, and objectives 3
1.3.1 Aims 4
1.3.2 Objectives 5
1.4 Wind speed, and power dynamics 7
1.4.1 Sources of wind 8
1.4.2 Wind power statistics 9
1.4.3 Wind power conversion 13
1.4.4 Overview of wind energy technology, and development 15
1.5 An overview of global wind energy 15
1.6 Wind energy in Africa 19
1.7 Wind energy in South Africa 23
2 data, and methods 27
2.1 Introduction 27
2.2 Statistical evaluation techniques 28
2.2.1 Trend analysis 29
2.2.2 Periodicity 31
2.2.3 Covariance, and correlation 35
2.2.4 Multivariate analysis 35
2.2.5 Software 36
2.3 Datasets 37

2.3.1 Wind speed 37
2.3.2 Quality assurance 46
2.3.3 Electricity demand profile 50
2.3.4 Climatic variables 51
2.4 Data limitations 53
3 Spatio–temporal trends of near–surface wind speed in the Northern, Western, and Eastern Cape provinces of South Africa 55
3.1 Introduction 55
3.2 Review of wind speed trend studies 56
3.2.1 Global wind speed trends 61
3.3 Data, and trend tests 67
3.4 Results 68
3.4.1 Annual wind speed trends 68
3.4.2 Monthly, and seasonal wind speed trends 70
3.4.3 Multi-temporal wind speed trends 78
3.5 Discussion 89
3.5.1 Annual wind speed trends 90
3.5.2 Monthly, and seasonal wind speed trends 91
3.5.3 Multi-temporal wind speed trends 92
3.5.4 Limitations 93
3.6 Recommendation for future research 93
4 Characterising near–surface wind speed, and electricity demand profile in the Northern, Western,, and Eastern Cape provinces of South Africa 95
4.1 Introduction 95
4.2 Data 101
4.3 Results 108
4.3.1 Seasonal, and monthly wind speed profile anomalies 110
4.3.2 Diurnal profile anomalies 111
4.4 Discussion 114

4.4.1 Monthly, and seasonal wind speed profile anomalies 115
4.4.2 Diurnal wind speed profile anomalies 117
4.5 Recommendation for future research 121
5 Teleconnections, and near–surface wind speed variability in the Northern, Western, and Eastern Cape provinces of South Africa 123
5.1 Introduction 123
5.2 Review of teleconnection studies 124
5.2.1 El Niño Southern Oscillation 125
5.2.2 Indian Ocean dipole 127
5.2.3 Antarctic Oscillation 129
5.2.4 Mid–latitude cyclones 131
5.2.5 Solar sunspot cycle 132
5.3 Dataset description 134
5.3.1 Spectral analysis 135
5.4 Results 139
5.4.1 Multi–decadal association of station observed wind speed characteristics with key climate indices 139
5.4.2 Periodic association of observed wind speed characteristics with key climate indices 148
5.4.3 Mean monthly association of station observed wind speed characteristics with key climate indices 156
5.5 Discussion 163
5.5.1 Multi–decadal association between station wind speed characteristics, and key climate indices 164
5.5.2 Periodic association between station wind speed characteristics and key climate indices 165
5.5.3 Mean monthly association of wind speed characteristics with key climate indices 167
5.6 Recommendation for future research 170

6 Conclusion 171
6.1 Introduction 171
6.2 Achievement of study aims 172
6.2.1 Aim One: Wind speed trends 172
6.2.2 Aim two: Wind speed profiles 173
6.2.3 Aim three: Wind speed teleconnections 174
6.3 Application, and Importance of Findings 175
6.4 Recommendation for future research 176
6.4.1 Wind speed trends 176
6.4.2 Wind speed profiles 176
6.4.3 Wind speed teleconnections 177
7 REFERENCES 178

LIST OF FIGURES

Figure 1.1: Global wind energy consumption by region (IRENA, 2019). 16

Figure 1.2: Global distribution of onshore wind farm Cf (%) at 100m AGL excluding permanent snow/ice–covered regions (Lu, et al., 2009). 17

Figure 1.3: Global average cost of wind energy (per kWh) procured through tender programmes, and mean cost of confirmed projects by region, and commissioning date (IRENA, 2019). 18

Figure 1.4: Distribution of wind energy across Africa: wind power Cf (%) at 100m elevation (Technical University of Denmark, 2018). 21

Figure 1.5: Distribution of wind energy across South Africa: wind power Cf (%) at 100m elevation (Technical University of Denmark, 2018). 24

Figure 1.6: Price trend of wind power in South Africa for all bid windows to date (Independent Power Producer Office, 2016). 25

Figure 2.1: SAWS weather stations with at least 10 years of automatically recorded 5–minute wind speed data 39

Figure 2.2: 21 SAWS weather stations with at least 20 years of wind speed data, and regional wind project developments 40

Figure 2.3: Standardised mean annual, and 6–year filtered seasonal wind speed for the period 1995 to 2018 (y-axis indicates deviation from the mean presented as a percentage) 43

Figure 2.4: Standardised mean annual, and 6–year filtered seasonal wind speed for the period 1995 to 2018 (y-axis indicates deviation from the mean presented as a percentage) 44

Figure 2.5: Standardised mean annual, and 6–year filtered seasonal wind speed for the period 1995 to 2018 (y-axis indicates deviation from the mean presented as a percentage) 45

Figure 2.6: Standardised mean annual, and 6–year filtered seasonal wind speed for the Cape Agulhas station for the period 1950 to 2018 (y-axis indicates deviation from the mean as a percentage). 46

Figure 2.7: Example of erroneous wind speed series (standardised) for Grahamstown (tree removal), Patensie, and Lamberts Bay (tree growth) stations. 49

Figure 2.8: Eskom mean monthly, and diurnal load profile (Eskom, 2019c). 51

Figure 2.9: Climate indices used in this study. 52

Figure 3.1: MERRA wind speed trends across South Africa between 1980–2014 (Jury, 2018). 60

Figure 3.2: Mean decadal wind speed trends (1995–2018) & Cape Agulhas series (1950–2018), statistical significance is considered at a threshold of P<0.1..... 72

Figure 3.3: Mean monthly Sen's slope wind speed trend of all stations considering 1995–2018 period..... 73

Figure 3.4: Mean annual, and seasonal Sen's slope wind speed trends presented for each region in m/s, and percentage per year (1995–2018)..... 75

Figure 3.5: Mean seasonal wind speed trends per year (1995–2018) & Cape Agulhas series (1950–2018), statistical significance is considered at a threshold of P<0.1..... 76

Figure 3.6: Station continuous wavelet transform plots (lag–1) applying a 12–month Gaussian filter to the wind speed series between 1995–2018. The shaded scale indicates the wavelet power scaled from lowest to highest. The black boundary defines periods of statistical significance (P<0.05), and the cone of influence is within the U–shaped area. 79

Figure 3.7: Station continuous wavelet transform plots (lag–1) applying a 12–month Gaussian filter to the wind speed series between 1995–2018. The shaded scale indicates the wavelet power scaled from lowest to highest. The black boundary defines periods of statistical significance (P<0.05), and the cone of influence is within the U–shaped area. 80

Figure 3.8: Inter–annual 48 month Gaussian filtered wind speed trends (1995–2018). Y-axis presents observed Sen's slope statistic as a percent (%) per year. The MK test was performed on each series with the dashed lines indicating the upper, and lower 95% statistical significance levels (red: decreasing trend; blue: increasing trend)..... 81

Figure 3.9: Monthly, and seasonal continuous wavelet transform plots (lag–0) for the Cape Agulhas station applying a mean annual filter to the wind speed series between 1950–2018. The shaded scale indicates the wavelet power scaled from lowest to highest. The black boundary defines periods of statistical significance (P<0.05), and the cone of influence is within the U–shaped area. 85

Figure 3.10: Monthly, and seasonal wind speed trend (24–year Gaussian filtered) of the Cape Agulhas station between 1950–2018. Y-axis presents observed Sen's slope statistic as a percent (%) per year. The MK test was performed on each series with the dashed lines indicating the upper, and lower 95% statistical significance levels (red: decreasing trend; blue: increasing trend)..... 86

Figure 3.11: Cape Agulhas station mean annual a) CWT plot (lag–0) for the period 1950–2018. The shaded scale indicates the wavelet power scaled from lowest to highest. The black boundary defines periods of statistical significance (P<0.05), and the cone of influence is within the U–shaped area. b) 24–year Gaussian

filtered wind speed trend between 1950–2018. Y-axis presents observed Sen's slope statistic as a percent (%) per year. The MK test was performed with the dashed lines indicating the upper, and lower 95% statistical significance levels (red: decreasing trend; blue: increasing trend).....87

Figure 3.12: Multi–decadal trend analysis for annual wind speed at the Cape Agulhas station, ranging 1–6 decades over the period 1950–2018. Y-axis presents observed Sen's slope statistic in percent (%) per year, and m/s/year. The MK test was performed on each decadal record with the dashed lines indicating the upper, and lower 95% statistical significance level (red-dashed line: decreasing trend; blue-dashed line: increasing trend). 88

Figure 4.1: Eskom diurnal electricity demand profile (Eskom, 2017b).....103

Figure 4.2: Mean a) Monthly;, and b) Diurnal wind speed, and electricity load anomalies. 103

Figure 4.3: Mean monthly wind speed anomalies a) Province b) Region c) Sub-region. 104

Figure 4.4: Mean diurnal wind speed, and Eskom load anomalies a) Province b) Region c) Sub-region. 105

Figure 4.5: Mean inter-annual wind speed correlation (r) as a function of the distance between stations.....109

Figure 4.6: Mean hourly wind speed autocorrelation as a function of temporal lag.....110

Figure 4.7: Mean inter-station a) monthly b) seasonal, and c) diurnal wind speed profile correlation as a function of the distance between stations.....113

Figure 4.8: Springbok, Langebaan, and Eskom load to the monthly data anomalies. 116

Figure 4.9: Inter-monthly wind speed correlation (r) of stations in the study area ranging 50km - 1100km apart. 117

Figure 4.10: Mean inter-hourly station wind speed variance. 119

Figure 4.11: Inter-hourly wind speed correlation (r) of stations in the study area ranging 80km - 1100km apart. 120

Figure 4.12: Hourly power correlation of sites in the Nordic countries ranging 10km - 2000km apart (Holttinen, 2004).....121

Figure 5.1: Drivers of regional climate (EMD, 2015). 125

Figure 5.2: Monthly (left), and annual (right) data spectral density for all available data series. 136

Figure 5.3: ONI, IOD,, and Sunspot activity Gaussian filtered monthly data anomalies (1950 – 2018).....137

Figure 5.4: Mid–latitude cyclone activity, Cape Agulhas wind station, and AAO Gaussian filtered monthly data anomalies (1950–2018). 138

Figure 5.5: Anomalous high, and low wind speed change points (larger circles indicate stronger anomalies relative to station mean wind speed). 148

Figure 5.6: Seventeen–year mean monthly filter for climatic variables, and Cape Agulhas wind speed series (black dashed line presenting the combined influence of all climatic variables). 154

* All diagrams, graphs, and images are the authors own unless stated otherwise

LIST OF TABLES

Table 1.1: Topography roughness classes, and corresponding spatial scale lengths (Windgiant, 2013). 11

Table 1.2: Wind turbine class defined by the IEC 61 400–1 (IEC, 2019). 15

Table 2.1: Meta–data for the 16 SAWS weather stations used in this thesis. 41

Table 2.2: Stations disregarded due to data anomalies not resulting from poor data capture. 47

Table 2.3: Stations disregarded due to data anomalies not resulting from poor data capture. 48

Table 3.1: Recent wind speed trends across Africa. 61

Table 3.2: Recent global wind speed trends (excluding Africa). 62

Table 3.3: Annual, and seasonal Sen's slope wind speed trend (%) per station, and region (1995–2018) 71

Table 3.4: Monthly station Sen's slope wind speed trend (%) per year (1995–2018) 77

Table 3.5: Station inter-annual cycle period lengths, and dates (at 10% statistical significance level) for continuous cycles lasting at least two periods when applying a continuous wavelet analysis between 1995–2018 (red: decreasing trend; blue: increasing trend). 83

Table 3.6: Seasonal, and monthly Cape Agulhas cycle period lengths, and dates (at 10% statistical significance level) for continuous cycles lasting at least two periods when applying a continuous wavelet analysis between 1950–2018 (red: decreasing trend; blue: increasing trend). 87

Table 4.1: Eskom 2018 electricity source by technology (Eskom, 2019b) 102

Table 4.2: Diurnal, monthly, and seasonal wind resource correlation (r) with Eskom load profile. 106

Table 4.3: Mean seasonal, and monthly wind speed, and Eskom electricity load anomalies. 107

Table 5.1: Primary harmonic, and period observed in each data series 135

Table 5.2: Inter–annual wind speed correlation (r), and multiple regression (multiple R) for each climatic mode 142

Table 5.3: Seasonal multiple regression statistics to all climatic modes per station, and region 143

Table 5.4: Inter–month wind speed correlation (r), and multiple regression (multiple R) statistics for each climate mode. 146
Table 5.5: Periodic climatic mode correlation (r) with wind speed series..... 149
Table 5.6: Seventeen–year periodic climatic mode correlation (r), and multiple regression (multiple R) statistics..... 155
Table 5.7: Mean monthly correlation, and multiple regression (multiple R) for all series.. 157
Table 5.8: Mean regional monthly correlation, and multiple regression (multiple R). 158
Table 5.9: Mean wind speed variance explains by climate mode data series at different periods (statistical significance P<0.1)..... 164

LIST OF ABBREVIATIONS

°C	:	Degrees centigrade
AAO	:	Antarctic Oscillation
AEP	:	Annual energy production
amsl	:	Above Mean Sea Level
AOI	:	Antarctic Oscillation Index
bn	:	Billion
BW	:	Bid window
Cf	:	Capacity factor
CFSR	:	Climate Forecast System Reanalysis
CWA	:	Continuous wavelet analysis
DFT	:	Discrete Fourier Transform
DoE	:	Department of Energy
E	:	Energy
EC	:	Eastern Cape
ENSO	:	El Niño Southern Oscillation
FIT	:	Feed-in-tariff
FT	:	Fourier Transform
GW	:	Gigawatt
IEC	:	International Electrotechnical Commission
IO	:	Indian ocean
IO	:	Indian Ocean
IOD	:	Indian Ocean Dipole
IPP	:	Independent power producers
IRP	:	Integrated resource plan
ITCZ	:	Inter-Tropical Convergence Zone
kg	:	Kilogram
kW	:	Kilowatt (1000w)
kWh	:	Kilowatt hour

m/s	:	Meter per second
m	:	Meter
m^3	:	Cubic meters
ME	:	Moderate El Niño
MERRA	:	Modern-Era Retrospective for Research, and Analysis
MLC	:	mid-latitude cyclone
MK	:	Mann Kendall
ML	:	Moderate La Niña
MW	:	Megawatt
NOAA	:	National Oceanic, and Atmospheric Administration
NC	:	Northern Cape
ONI	:	Oceanic Nino Index
PO	:	Pacific Ocean
PC	:	Principle components
PCA	:	Principal Component Analysis
PM	:	Particulate matter
PPA	:	Power purchase agreement
R^2	:	Multiple regression statistic
REIPPPP	:	Renewable Energy Independent Power Producer Procurement programme
SAST	:	South African Standard Time
SAWS	:	South African Weather Service
SC	:	Serial correlation
SD	:	Standard deviation
SE	:	Strong El Niño
SL	:	Strong La Niña
SO	:	Southern oscillation
SST	:	Sea surface temperature
TW	:	Terawatt (1000 GW)
TWh	:	Terawatt hours
USD	:	United States Dollar

VSE	:	Very strong El Niño events
W/m^2	:	Power density
WE	:	Weak El Niño
WC	:	Western Cape
WL	:	Weak La Niña
WTG	:	Wind turbine generator
ZAR	:	South african rand

1 INTRODUCTION

1.1 Overview, and motivation

The most remarkable characteristic of wind is its inherent variability in both the spatial, and temporal domain. Wind speed is a function of atmospheric pressure gradient with the ultimate driver being the sun (Lindsey, 2009). Varied heating of the earth results in global circulation patterns with Coriolis forces fundamentally driving large–scale motion of the air (Neuberger, 1981). Wind variability at a regional scale is influenced by micro, synoptic, and global scale factors such as topography, water bodies, the Indian Ocean Dipole (IOD), and El Niño Southern Oscillation (ENSO). As part of an international effort to quantify climate, and related circulation changes, several studies have focused on wind speed anomalies at various global locations (Breslow & Sailor, 2002; de Lucena, et al., 2010; Wan, et al., 2010; Abdraman, et al., 2016; Azeroual, et al., 2018; Jung, et al., 2019). Determining a suitable location for a wind farm is in itself a difficult task as several aspects such as grid, environmental, and social aspects should be considered, given that the most important dynamic is the wind resource (Köse, 2004; Dincer, 2011; Awad, et al., 2017; Bayer, 2018). A wind project typically operates for 20–25 years, and will endure wind speed variance at a daily, monthly, annual, and decadal temporal scale. Wind speed variance occurs due to the impact of climatic mode fluctuation, and in the context of a wind turbine generator, is important to define when, and how much power is generated. In this respect, after an extensive literature review, it was felt that a knowledge gap still exists in understanding South Africa's wind climate trends, profile, and drivers; hence the undertaking of this PhD project.

Over recent decades there has been an increased awareness of climate change globally, with renewable electricity generation alternatives being implemented more frequently, and widely. Wind power, as one such alternative, has recorded global growth rates of up to 15% per year in recent years, despite the associated temporal uncertainty of wind resources (World Wind Energy Association, 2018a). The procurement of wind-generated electricity has primarily been a feed-in–tariff (FIT) or tender, which have enabled the growth of the industry (World Energy Council, 2017; Kruger, et al., 2018; IRENA, 2019; Rosales-Asensioa, et al.,

2019).Globally, the largest additional (60 gigawatts (GW)) new wind capacity was installed in 2017, and by the end of 2018 had grown the global industry to 600GW (IEC, 2019). Countries with the largest installed wind power generation capacity include China (220GW), the USA (100GW), Germany (60GW), and India (35GW) (World Wind Energy Association, 2018a).

This global uptake of wind power has encouraged the international scientific community to research wind speed distribution with associated trends, and global climate linkages (Beer, et al., 2010; Misios, 2012; Huang, et al., 2015; Sato, et al., 2018; Calitz & Wright, 2019). The earth's climate is a complex system with multiple micro, meso, synoptic, and global scale forcings. Changes in one or more forcings can have cumulative large, and global climate impacts which are quantifiable, and observable in several features such as ocean currents, rainfall patterns, and wind speed. Understanding wind speed profile, variance, and climate teleconnections are fundamentally important to ensure energy security from wind power generation perspective (Barthelmie, et al., 2006; Patra & K, 2016; Slot, et al., 2018). To this end, information relating to near-surface wind speed can be applied in various fields of interest, such as pollen dispersal alerts, wind erosion in agricultural settings, building engineering, and the design of wind farms.

This introductory chapter provides an overview of wind, and energy fundamentals, and the evolution of the global wind power industry. Thereafter, a literature review of relevant scientific research findings concerning wind energy is presented at a global, African, and regional scale. Key concepts presented include wind resource distribution, associated cost, wind power growth, and the sources of wind speed variation.

1.2 Research Rationale

South Africa is a developing country which requires energy security for current, and future needs. Considering the global uptake of renewable power generation, the South African government through the Department of Energy (DoE) developed the Renewable Energy Independent Power Producer Procurement Programme (REIPPPP). This programme is

aimed at diversifying, and expanding South Africa's electricity generation sources through independent power producers (IPPs). Prior to the implementation of the REIPPPP (2011), wind power was not sought as an electricity source in South Africa (Lombard & Ferreira, 2015; Pollet, et al., 2015). South Africa received the first wind-generated electricity from IPPs at the end of 2013. This has since increased to 3,346 mega-watts (MW), accounting for 6.3% of the country's installed power station capacity (Calitz & Wright, 2019). The current Ministerial determinations include 6,360MW of wind (approximately 6% of national capacity) to be procured under the REIPPPP, which accounts for 48% of all technologies (DoE, 2015b). Further, South Africa's integrated resource plan (IRP) projects an uptake of up to 25GW of wind power by 2050.

The uptake of wind-generated electricity in South Africa justifies the need for additional scientific research to quantify statistically significant wind speed variability, wind profile, and wind speed teleconnections to climatic phenomena. Quantifiable scientific knowledge of wind speed at a daily, monthly, seasonal, annual, and periodic temporal scale remains relatively limited for South Africa. A failure to provide sufficient, and appropriate country specific data in the planning of wind electricity generation, would negate the attempt to achieve electricity generation security. It is for this reason that wind speed is an important parameter to which further research will add essential scientific information.

1.3 Aims, and objectives

This thesis contemplates important scientific issues by addressing temporal wind speed variance, diurnal wind profile, and teleconnections to synoptic, and global climate forcing. This is achieved through the statistical analysis of recorded wind speed data while considering climate mode anomalies for the same period. The foremost goal of this thesis is to quantify teleconnections between climatic modes which is influenced by large scale wind speed variations. The analysis is based on wind speed records from 21 stations, with series ranging from 20 to 68 years. The stations are all located in the Northern (NC), Western (WC), and Eastern Cape (EC) provinces of South Africa (the study area). To achieve this goal, it is necessary to statistically assess the recorded wind speed data, and investigate the circulation

features which drive extended high, and low mean wind speed periods at a decadal temporal scale.

1.3.1 Aims

The specific aims which form the framework to achieve the objectives of this thesis are detailed below:

1.3.1.1 Aim 1

One of the aims of this thesis is to explore, and quantify station wind speed trends in the study area. Literature specific to annual, and seasonal wind speed trends in South Africa is relatively sparse, hence, the study aims to supplement, and build on previous work. To date, no scientifically documented references are available which deal with monthly, decadal, and multi-temporal wind speed trends in the study regions. This research documents these findings for the first time through the application of continuous wavelet transform, which is an advanced statistical approach. Reference is made to international work assessing wind climatology as a guide to specific methodology, and general approach.

1.3.1.2 Aim 2

The secondary aim of this thesis is to establish station-based wind speed profiles which concern the Eskom demand profile. Several reports published by Eskom, and the WASA project document operational wind power supply in consideration of power demand. However, regional development plans based on a wind speed profile do not exist. For the first time, this thesis identifies geographical locations which should be considered for strategic development to support the long–term sustainability of wind power generation in South Africa.

1.3.1.3 Aim 3

The third aim of this thesis is to quantify teleconnections between large-scale climate modes, and observed wind speed variance in the study area. Extensive literature is available, which contemplates southern African climate forcing modes, their associated variance, and impact

on factors such as temperature, and rainfall. Yet, limited research quantifies the teleconnection between these modes, and wind speed. Specifically, no literature to date has quantified the multi-temporal teleconnections in this regard. The thesis presents key modes which may forecast regional wind speed trend, the quantified teleconnection between each mode, and wind speed as well as the observed multi-temporal teleconnections.

1.3.2 Objectives

Some important concepts to expand existing scientific knowledge gaps in the context of wind speed in South Africa are raised through three core objectives:

Objective 1

1.1. To identify, and review available SAWS wind speed records, and quantify wind speed trends is the study area;

1.2. To quantify wind speed trends at multi-decadal, annual, seasonal, and monthly temporal scales;

1.3. To identify, and quantify stational multi-temporal wind speed trends; and

1.4. To quantify the interannual variability of station recorded wind speed over a typical power purchase agreement (PPA) agreement period of 20 years.

Objective 2:

2.1 To assess station-based diurnal, monthly, and seasonal wind speed profiles in the context of wind power generation, considering South Africa's electricity demand profile;

2.2 To determine the variability between station series considering spatial dispersion in the context of dynamic power generation.

Objective 3:

3.1 To identify, and evaluate potential teleconnections between large–scale climate modes, and wind speed characteristics at an annual, seasonal, and monthly temporal scale;

3.2 To identify, and quantify multi-temporal wind speed teleconnections between large–scale climate modes, and observed wind speed;

3.3 To determine if any of the climate indices could potentially be used to forecast wind speed in the NC, WC, and EC provinces.

Station-based wind speed records were statistically analysed to identify inherent trends, profiles, and teleconnections to climatic drivers. Results are compared between stations on various spatial, and temporal scales. The above-defined thesis objectives are assessed in six chapters.

Chapter 1 provides a motivation, overview, and scope to this thesis presenting the specific aims, and objectives. Thereafter, a literature review of associated research at a global, regional, and country-specific scale are considered. The distribution of wind resource at the same spatial scale is then discussed. The characteristics of South African wind resources, and known driving mechanisms are identified. The chapter is closed by presenting an overview of wind power fundamentals.

Chapter 2 presents an overview of the data, and statistical techniques applied. Scientifically proven techniques, which are commonly used to identify temporal, and spatial structure of variability in climate features are spectral, correlation, trend, and regression analysis, as well as the root, mean square, mean absolute, cycle amplitude, and monthly mean error statistics. The climate features, data sources, and associated key indicators used in the analysis are discussed. Further, an overview of the 22 study stations, data cleaning methodologies, and associated uncertainties along with their limitations are presented.

Chapter 3 documents the spatio–temporal dynamics of wind speeds over the past 24 years (1995–2018), which is representative of a typical wind PPA term. The stations are assessed at an annual, seasonal, and monthly temporal scale to quantifying 20–year wind speed variability trends. The results are assessed to identify potential implications to electricity generation from wind.

Chapter 4 defines the national electricity load profile, and quantifies wind speed profile characteristics. The profiles are then assessed at a daily, monthly, and seasonal temporal scale to quantify wind generation potential in association with power demand. Stations are also grouped per region to identify profile trends.

Chapter 5 identifies the primary climate driver components which impact wind speed in the study regions. Key climate phenomena include ENSO: Oceanic Niño Index (ONI), IOD, Antarctic Oscillation (AAO), regional mid-latitude cyclone (MLC), and Sunspot activity. Statistical analysis was performed to identify teleconnections between climate modes, and their impact on regional wind speed. Interpretation of the potential forcing teleconnections to station-based wind speeds was statistically performed at a monthly, seasonal, annual, and climate–mode harmonic scale.

Finally, conclusions are presented in **Chapter 6** where the research findings are highlighted, and the key objectives, and associated aims of the thesis answered.

1.4 Wind speed, and power dynamics

Prior to the literature review, methodology, and research results, it is necessary to detail fundamental terminology, equations, and characteristics associated with wind, and the power contained therein. The consideration of time, and space essential for any meteorological research, and definitions varies between sources. The bold temporal, and spatial scales are of core focus to this research as detailed in section 1.2.

This thesis shall apply the below-defined scales in reference to temporal variance:

- ultra-high frequency equates an order of seconds;
- high frequency equates an order of minutes;
- medium frequency equates an order of hours;
- **daily/low frequency** equates an order of days;
- **monthly/seasonal frequency** equates an order of months;
    - four austral seasons are defined as summer (DJF), autumn (MAM), winter (JJA), and spring (SON);
- **annual/inter–annual frequency** equates an order of years; and
- **decadal frequency** equates an order of decades.
- **multi–decadal** equates in excess of four decades

This thesis shall use the below defined physical boundaries in reference to spatial variation:

- micro–, small–, and local– scale quantifies an order of meters to hundreds of meters;
- meso–, and regional– scale quantifies an order of kilometres to tens of kilometres;
- **synoptic–, and large– scale** quantifies an order of hundreds of kilometres; and
- **global scale** quantifies an order of thousands of kilometres.

1.4.1 Sources of wind

The concept of wind speed can be defined as the movement of air from one region to another resulting from an atmospheric pressure differential (Barthelmie, et al., 2006; Dadaser-Celik & Cengiz, 2013; Cevallos-Sierra & Ramos-Martin, 2018). Fundamentally at a synoptic scale, air flows from a high- to a low-pressure system where the larger the gradient, the faster the movement is (Shuab, et al., 2018). This flow is impacted by the Coriolis force which is present due to the Earth's rotation. Depending on the hemisphere, the resulting force deflects wind to the right (northern hemisphere) or left (southern hemisphere). Once the Coriolis, and pressure forces are in balance, wind follows the isobars. It is also known as the geostrophic

wind which varies at a low frequency due to associated large scale influences. This is an ideal, yet theoretical concept which governs the majority of wind speed variance (Emeis, 2018).

Dynamic mesoscale phenomena which occur at a medium frequency drive the daily wind speed profile (van Vuuren & Vermeulen, 2019). The most frequent phenomena include land/sea breeze, and topographic (slope) elevation change (Hagermann, 2008). During the day, a sea breeze develops in response to temperature differentials between onshore, and offshore surfaces due to the associated rate of heat absorption. Wind speed is in direct proportion to the surface temperature differential (Tyson & Preston-Whyte, 2000). A land breeze occurs in the opposite direction at night, and driven by the same physical dynamic. This phenomenon is typically weaker than a sea breeze due to the reduced temperature differential as a result of larger static stability which prevails nocturnally (Hagermann, 2008; Shen, et al., 2019). Similarly, slope winds occur due to a temperature differential between higher altitudes, and the presence of valleys. During the day an anabatic upslope breeze develops while at night it is the sinking katabatic downslope breeze (Solari, 2019). Considering the geography of South Africa, and its extensive coastline, the occurrence of land/sea breezes are frequently observed. Further, there are mountain ranges reaching 3,400m above mean sea level (amsl) generating significant slope winds (Tyson & Preston-Whyte, 2000; Cevallos-Sierra & Ramos-Martin, 2018).

1.4.2 Wind power statistics

Wind speed anomalies are a primary focus of this research. Thus, it is essential to understand wind in the context of a mathematical function, specifically those equations of relevance to the analysis methodologies applied. Temporal variance of wind speed is discussed extensively as it is a function of time, and speed, and denoted as:

$$S_i = S(t_i) = V(t_i) \qquad [1]$$

where S is the data series, and t_i is a specific time, and V is the wind speed expressed in meter per second (m/s). Generally, $\Delta t = t_{i+1} - t_i$ is constant, where Δt^{-1} is the sampling frequency.

Wind in its most generalised form is also considered a function of space which results in the four-dimensional expression of:

$$V = V(x, y, z, t) \qquad [2]$$

where (x, y) represents the horizontal, z is the vertical, and t is the moment in time.

Wind speed is impacted by a topographic variation such as elevation, obstacles, and surface roughness which generally affect wind at a local to regional scale. Elevation changes can funnel, detour, slow down or speed upwind depending on the site-specific topography. Obstacles such as large trees or buildings are known to have a significant influence on wind speed. These impacts are directly proportional to the obstacle's height, and influence wind dynamics, and velocity up to 40 times downwind, and 3 times vertically (Diab, 1995). Surface roughness, on the other hand, causes wind speed to decrease due to absorption of kinetic energy. Roughness varies ranging from a smooth water surface to grassland, forest or high–rise city buildings (Table 1.1). The roughness of a region is quantified by using a parameter defined as the roughness length of the surface Z_0, an empiric quantity calculated by measuring the vertical impact on a wind profile. The impact of roughness length 'Z' on wind speed 'V_z' is approximately logarithmic, and described by the equation:

$$V(z) = \frac{1}{k_0} V_* \ln \frac{z}{z_0} \qquad [3]$$

where V_z is the wind speed at a specific height, k_0 (~ 0.4) is the von Kármán constant, and V_* is the friction velocity (generally 0.2–0.4 m/s) defined by the surface stress, and air pressure (Justus & Mikhail, 1976). This statistical equation does not consider zero plane displacement, and is only appropriate for neutral stability regimes, thus it is the most basic expression that defines vertical wind speed extrapolation.

Table 1.1: Topography roughness classes, and corresponding spatial scale lengths (Windgiant, 2013).

Class	Length (m)	Energy index (Useable %)	LandsCape type
0	0.0002	100	Water surface
0.5	0.0024	73	Completely open terrain with a smooth surface, e.g. concrete runways in airports, mowed grass, etc.
1	0.03	52	Open agricultural area without fences, and hedgerows, and very scattered buildings. Only softly rounded hills
1.5	0.055	45	Agricultural land with some houses, and 8m–tall sheltering hedgerows with a distance of approximately 1250m
2	0.1	39	Agricultural land with some houses, and 8m–tall sheltering hedgerows with a distance of approximately 500m
2.5	0.2	31	Agricultural land with many houses, shrubs, and plants, or 8m–tall sheltering hedgerows with a distance of approximately 250m
3	0.4	24	Villages, small towns, agricultural land with many or tall sheltering hedgerows, forests, and very rough, and uneven terrain
3.5	0.8	18	Larger cities with tall buildings
4	1.6	13	Very large cities with tall buildings, and skyscrapers

When analysing wind speed data, the most common statistic is the recorded mean wind speed ($\overline{V}$) defined as:

$$\overline{V} = \frac{1}{n} \sum_{i=1}^{n} V_i \qquad [4]$$

where the standard deviation (SD) thereof is described by the typical expression of:

$$\sigma V = \sqrt{\frac{1}{n} \sum_{i=1}^{n} (V_i - \overline{V})^2} \qquad [5]$$

It is essential that one considers as many years as possible to ensure an accurate representation of the true decadal mean. The data series should ideally span a decade or more to smooth variability at various temporal scales where Δt^{-1} should be a high-frequency record ensuring short term variability is captured.

The diurnal wind speed profile is equally important to quantify, especially when incorporating wind-generated electricity into a power grid. This daily profile is calculated by generating a new wind speed data series V_{24} as follows:

$$V_{24} = \frac{24}{n}\left(\left(\sum_{i=1,\dots}^{n} V_i\right), \left(\sum_{i=2\dots}^{n} V_i\right), \dots, \left(\sum_{i=N\dots}^{n} V_i\right)\right) \quad [6]$$

This assumes that $\Delta t = 1h$, which thereby considers that the 24 elements of the new data series represent averages at every hour of the day. The resulting dataset allows for the visual assessment to identify if a daily cycle exists. To quantify the cycle amplitude, D_a as the delta between minima, and maxima elements of V_{24}:

$$D_a = \max(V_{24}) - \min(V_{24}) \quad [7]$$

Both statistics of t_{max}, and D_a are key indicators for a wind farm as it defines how synchronous diurnal wind speed distribution matches supply, and demand requirements of the electricity offtake operator. In some cases, a PPA offers incentives for electricity generated during specific hours which significantly change the commerciality of a project. Noting the importance of the diurnal profile at a given location, calculation of the Fourier transform G(f) for V(t), where f represents frequency, can provide useful information for site analysis, and comparison.

Finally, the annual wind speed profile at a monthly (V_{12}) scale is frequently assessed which can further consider seasonal changes. The statistical, and visual analysis of V_{12} provides fundamental information of the wind profile in relation to increased power demand seasons of summer, and winter.

1.4.3 Wind power conversion

Power (P_d) from wind varies exponentially at a cubic relation to the wind speed. The resulting equation to quantify P_d is:

$$P_d = \frac{1}{2}\rho V^3 \qquad [8]$$

where P_d indicates the power density (W/m^2), and ρ (kg/m^3) accounts for the air density. This expression is well known, and mathematically referred to as the 'third power law', which is derived through Newtonian principles (Justus & Mikhail, 1976). In case of a wind power generation, each wind turbine generator has specific aerodynamic, and efficiency losses. Further, these are impacted by the 'Betz efficiency limit', which denotes that about 59.3% of the theoretical total power density can be transferred to a rotational force that affects electricity generation potential (Betz, 1966). Noting these influences, the 'third power law' in the case of wind energy generation potential is calculated by:

$$P_d = \frac{1}{2}C_p(V)\rho V^3 \qquad [9]$$

where '$C_p(V)$' considers the two components of a specific wind turbine generator's (WTG) power efficiency coefficient as a function of wind speed. The WTG coefficient indicates the amount of electrical power produced by the generator based on the theoretically available power. The location-specific air density ρ is equally important for power generation, and is a function of air pressure (p), air mixing ratio (q), and absolute temperature (T) while it is calculated by:

$$\rho = \frac{pM_a(1+q)}{R_aT(1+1.608q)} \qquad [10]$$

where the molar mass of dry air (0.029 kg) is denoted by M_a, and the ideal gas constant (8.314 J/K/mol) is denoted by R_a (Guyot & Guyot, 1998). At ideal conditions, the standard density of air equates 1.2265 kg/m^3 at sea level when there is a zero–mixing rate (dry air), standard pressure (1013.25 Pa), and a temperature of 15°C. As with V, the variables, p, q, and T are a

function of time, and space which are recorded in four dimensions so that the values of ρ, and P_d are also four-dimensional. However, in reality, ρ records a fairly constant value (near-surface) at a given point as neither p nor T vary significantly at an absolute temporal scale. Due to this, the calculation of wind power considers the mean recorded $\overline{\rho(t)}$.

The final variable to quantify before calculating the total energy (E) transformed from kinetic to electrical is the WTG swept area (A_r). This is a common expression used for circular area calculation, and accounts for model-specific rotor diameter (D), defined by:

$$A_r = \pi\left(\frac{D}{2}\right)^2 \qquad [11]$$

Considering the afore presented wind speed, pressure, density, and area variables, the actual E generation of a wind turbine generator at a given point (x, y, z), may be defined by:

$$E = \frac{1}{2}A_r\int_{t1}^{t2}\rho(t)C_p(V(t))(V(t))^3dt \qquad [12]$$

where t_1, and t_2 are the start, and end times of the record. If the data series period corresponds to a calendar year, then E is called the Annual Energy Production (AEP) for the associated WTG.

The term capacity factor (C_f) is referred throughout this thesis. This indicates the actual WTG performance between two in time points ($t_2 - t_1$), as a percentage of the maximum (P_{rated}) generation potential, which assumes peak generation between t_1, and t_2. The expression is calculated by:

$$C_f = EP_{rated}(t_2 - t_1)100\% \qquad [13]$$

Considering the variables presented in this section, the most significant change in E results from the power factor dependence on the rotor diameter A_r (square), and wind speed V (cubic). In a scenario where A_r is doubled, the resulting E increases four times. When V is doubled, the resulting E increases eight times (Elmabruk, et al., 2014; Sorensen, et al., 2018).

1.4.4 Overview of wind energy technology, and development

Utility-scale wind farms have been in commercial operation from the early 1980s as the turbines dominated the market, and had a rated capacity of below 200 Kilowatt (kW) (IRENA, 2012). Since then, the wind market has evolved dramatically with ongoing increases in hub height (up to 178m), rotor diameter (up to 164m), and rated capacity (up to 10MW) (World Wind Energy Association, 2018b). Most modern wind turbine generators (WTG's) require a minimum wind speed of 3 m/s to start generating electricity while typically generating maximum power by 12–13 m/s, and cutting out at 25 m/s (European Commission, 2013; World Wind Energy Association, 2018b). Wind turbine selection is driven by variables such as mean annual wind conditions, climate, and topography as they define the type of WTG required for the site (Table 1.2). The International Electrotechnical Commission (IEC) is a globally recognised organisation which developed the IEC 61 400–1, and defines the wind turbine class based on 50–year site-specific variables (IEC, 2019). The wind classes range from I (high wind speed)–IV (low wind speed), and are defined depending on a high or low wind turbulence characteristic. Wind turbine manufacturers define a WTG specification according to these classes, and the correct class WTG must be matched with the appropriate site class to ensure optimal WTG efficiency.

Table 1.2: Wind turbine class defined by the IEC 61 400–1 (IEC, 2019).

	Wind Class			
a–Higher turbulence (18%) **b–Lower turbulence (16%)**	I (a/b)	II (a/b)	III (a/b)	IV
Extreme 50–year gust (m/s)	70	59.5	52.5	42
Annual average wind speed (m/s)	10	8.5	7.5	6

1.5 An overview of global wind energy

The last 30 years has observed exponential growth of the global wind energy sector growing from 1.3GW in 1986 to 597GW in 2018 (Lantz, et al., 2012; World Wind Energy Association, 2018a). Renewable energy accounted for 66% of new energy projects installed globally in 2018 while wind contributes 35.4% (51.3GW) of this new generation (IRENA, 2019). The most recent statistic available for global wind energy consumption is from 2018, where the

regions of Europe, Eurasia, Asia Pacific,, and North America accounted for 99% of global wind power consumption (Figure 1.1) (IRENA, 2019).

Several authors have documented global, and continental-scale wind circulation patterns (Bigg, 1993; Dadaser-Celik & Cengiz, 2013; Grundstrom, et al., 2015; Hui & Zheng, 2018). In these studies, the resource distribution, uptake of wind power, variance, and drivers are quantified. Wind resource quality varies across the globe with the least attractive resource located in the equatorial regions, and the most attractive North (Cancer), and South (Capricorn) of the respective tropics (Figure 1.2). The technical potential of global wind energy is estimated at approximately 50,000 terawatt-hours (TWh) per year (Jung, et al., 2018). Research has quantified that approximately 10.8 terawatts (TW) (equivalent to 2.3% of available wind power globally) would yield enough electricity to fulfil current global energy consumption from all energy forms (Archer & Jacobson, 2005; Rienecker, et al., 2008; Lu, et al., 2009; Dincer, 2011; Gielen, et al., 2019).

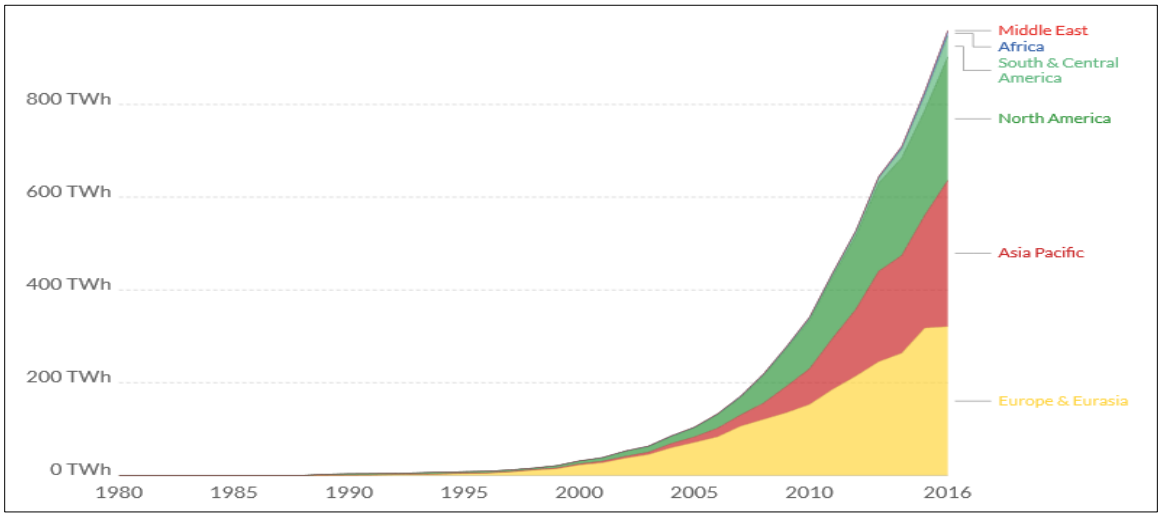


Figure 1.1: Global wind energy consumption by region (IRENA, 2019).

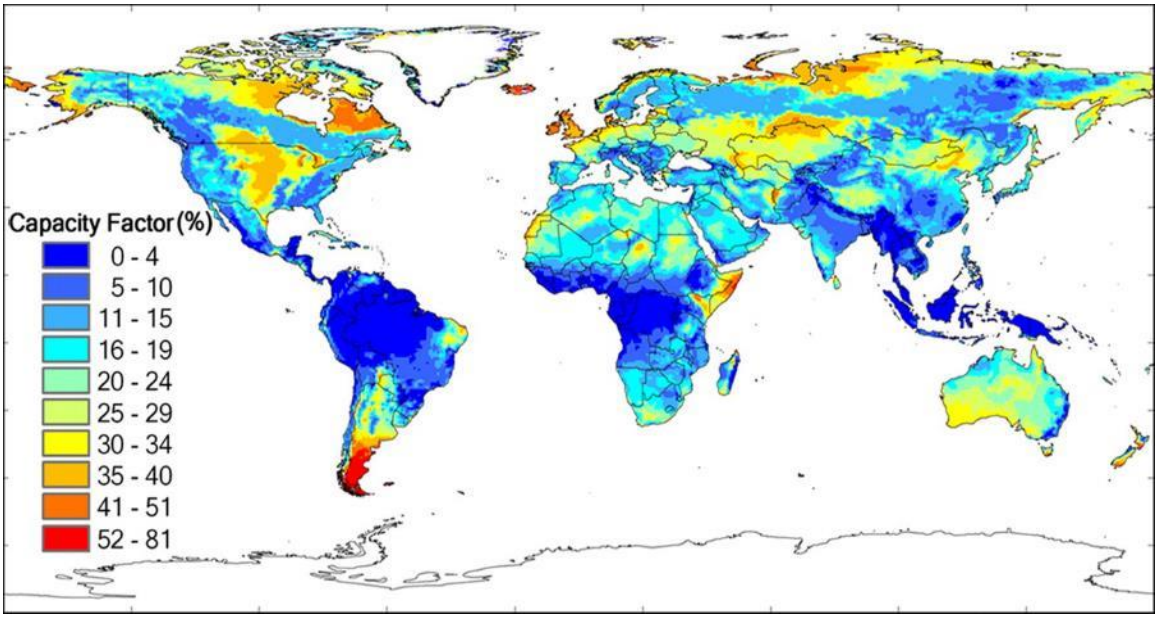


Figure 1.2: Global distribution of onshore wind farm C_f (%) at 100m AGL excluding permanent snow/ice–covered regions (Lu, et al., 2009).

There is a global trend of countries implementing auctions to obtain the most competitive electricity rates, and is now officially the preferred method of procurement (Kruger, et al., 2018). These competitive tenders, along with decreasing technology prices, and increasing efficiencies, are resulting in additional renewable energy globally (Rosales-Asensioa, et al., 2019). In 2015, Denmark obtained over 40% of its electricity generation from wind power, which represents the largest annual contribution for any country worldwide (World Energy Council, 2017). In the same year, Portugal, Ireland, and Spain each generated 20% of their electricity needs from wind power, while a further 11 of 28 EU Member States generated above 10% of their energy from wind (International Energy Agency, 2016; WindEurope, 2017).

Brazil is a country, in particular, that has influenced global wind tender programmes between 2009, and 2015, as it held 15 auction windows procuring over 14GW of wind power. The program observed a decrease (50%) in tender price between the first (2009), and seventh (2012) auctions, after which prices began to increase (Bayer, 2018). The price increase is associated with the change in tender structure (increased local content, performance

penalties, and grid connection costs) as well as the external economic factors (currency devaluation, and rising interest rates). The global weighted price of wind projects commissioned in 2018 was USD 0.056/Kilowatt hour (kWh), with the Mexico tender of November 2017 having presented the lowest recorded price of USD 0.017/kWh (IRENA, 2019). The mean cost of wind power globally has continued to decrease, primarily driven by increasing hub height, swept area, and capacity (McVicar, et al., 2012) (Figure 1.3).

It was noted that wind varies at a diurnal, monthly, and seasonal temporal scale depending on the region considered. Between 1971, and 2010, Canada, Australia, and the USA indicated the lowest inter-annual wind speed variance while Bhutan, Micronesia, and Gabon recorded the highest (McVicar, et al., 2012). Africa was cited as a continent likely to record significant inter-annual wind speed fluctuations (Jung, et al., 2019). During the same period, Russia (–2.4%), Canada (–1.1%), and the USA (–1.0%) indicated decreasing wind speed trends while mean global wind speed trends did not record any significant trend (Schindler, et al., 2016; Jung & Schindler, 2018; Jung, et al., 2019).

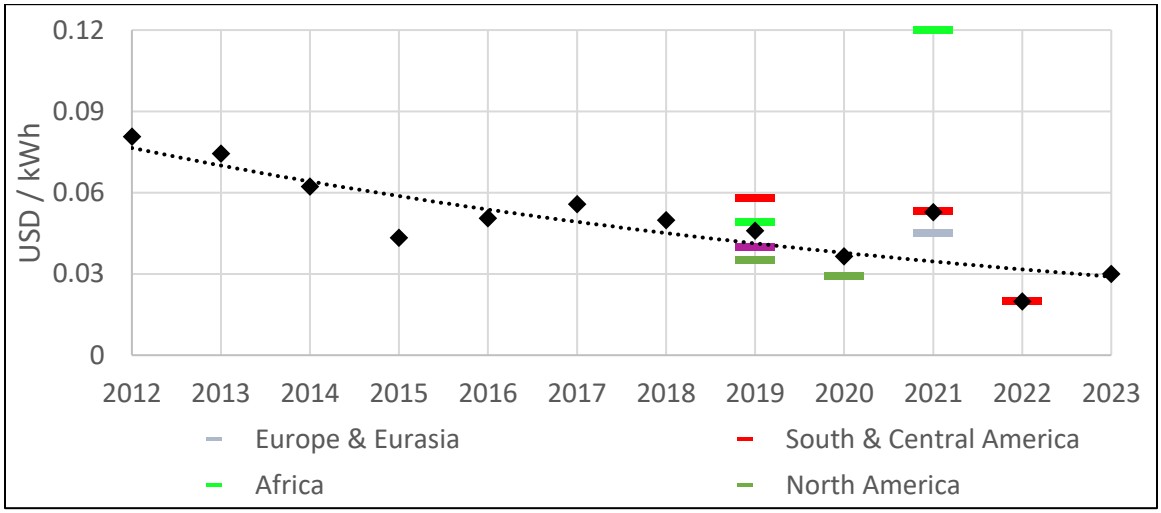


Figure 1.3: Global average cost of wind energy (per kWh) procured through tender programmes, and mean cost of confirmed projects by region, and commissioning date (IRENA, 2019).

An essential aspect to consider with the uptake of wind-generated electricity is to identify the global drivers of wind resource variance. High equatorial temperatures are a key influencing

factor for earth winds while the equatorial latitude is defined by a region of low-pressure Inter-Tropical Convergence Zone (ITCZ), and alternates between high (subtropical), and low (subpolar) pressure regions as the latitudes increase toward the poles. The alternating pressure regions, in turn, drive the predominant westerlies, easterlies, and trade winds associated with the Hadley, Ferrel, and Polar Cells (Saji & Yamagata, 2003). Further, the role of ocean-atmosphere coupling, and the modulating of global, and regional wind speed variance are suggested.

As early as 1924, the concept of global oscillations was presented, which included three primary circulation phenomena at the time as the North Atlantic Oscillation, Southern Oscillation (SO), and North Pacific Oscillation (Walker & Bliss, 1924; Walker & Bliss, 1932). Interaction between El Niño, and tropical oceans was documented in 1966, which for the first time introduced the atmospheric circulation connection to the equatorial Pacific sea surface temperature (SST) (Angell, 1981; Bjerknes, 1969). There is a tropical low-frequency cycle of the zonal air pressure, and wind interaction that exists between the Pacific (PO), and Indian (IO) oceans, defined as the Madden–Julian oscillation (Madden & Julian, 1971). While advancements on the earlier studies considered a possible oscillation in the mid to high latitudes of the southern hemisphere (40°-65°), Gong (1999) defined the AAO, and proposed that the three oscillations of AAO, AO, and SO drive atmospheric circulation globally. Besides, the phenomena of the IOD, and the associated negative, and positive oscillation of the IO SST was defined (Saji, et al., 1999; Webster, et al., 1999).

1.6 Wind energy in Africa

Wind resource to a large extent is an untapped resource on the African continent, accounting for below 1% of total power generation (Mentis, et al., 2017; IRENA, 2019). There are seven countries in Africa which account for over 95% of the continent's installed capacity, including Tunisia (243MW), Tanzania (250MW), Kenya (336MW), Ethiopia (385MW), Egypt (785MW), Morocco (1,344MW), and South Africa (3,428MW) (IRENA, 2019; The Wind Power, 2019). The primary drivers include the wind resource, capacity of governments to support effective policies, political investment risk, and social acceptance of wind power generation (Barry, et

al., 2011). Considering the wind resource distribution, the most favourable regions are primarily located north, and south of the tropics of Cancer, and Capricorn respectively, as well as the East Coast of Africa (Figure 1.4).

Several authors have documented the wind resource potential across Africa. Recently, Olaofe (2017) assessed five wind monitoring stations located along the coast of Nigeria to quantify the potential for wind power generation. This research concluded that the five locations indicated a low mean annual wind speed while only one site could be marginally suitable for electricity generation. Similarly, research in Algeria, which assessed five wind monitoring stations, found only one site that may be able to support electricity generation. The cost of utility-scale generation is uncertain due to the low resource (Benmemdejahed & Mouhadjer, 2016). Assessment of wind measurement stations in Ghana, Burkina Faso, Rwanda, Cameroon, and Zimbabwe identified a low wind resource, generally unsuitable for utility-scale wind power generation (Safari & Gasore, 2010; Adaramola, et al., 2014; Afungchui, 2014; Hove, et al., 2014; Arreyndip, et al., 2016; Asumadu-Sarkodie & Owusu, 2016; Landry, et al., 2017). In contrast, other locations such as in Morocco, Algeria, Chad, Libya, Niger, and Sudan, have been deemed suitable for utility-scale wind power generation (Bekele & Palm, 2009; Elmabruk, et al., 2014; Monjid, et al., 2015; Abdraman, et al., 2016; Elsner, 2019). On the other hand, political instability is hindering the investment of wind power generation in Algeria, Chad, Libya, Niger, and Sudan while Morocco stands as one of the biggest wind power generators in Africa with over 1GW of installed wind power capacity.

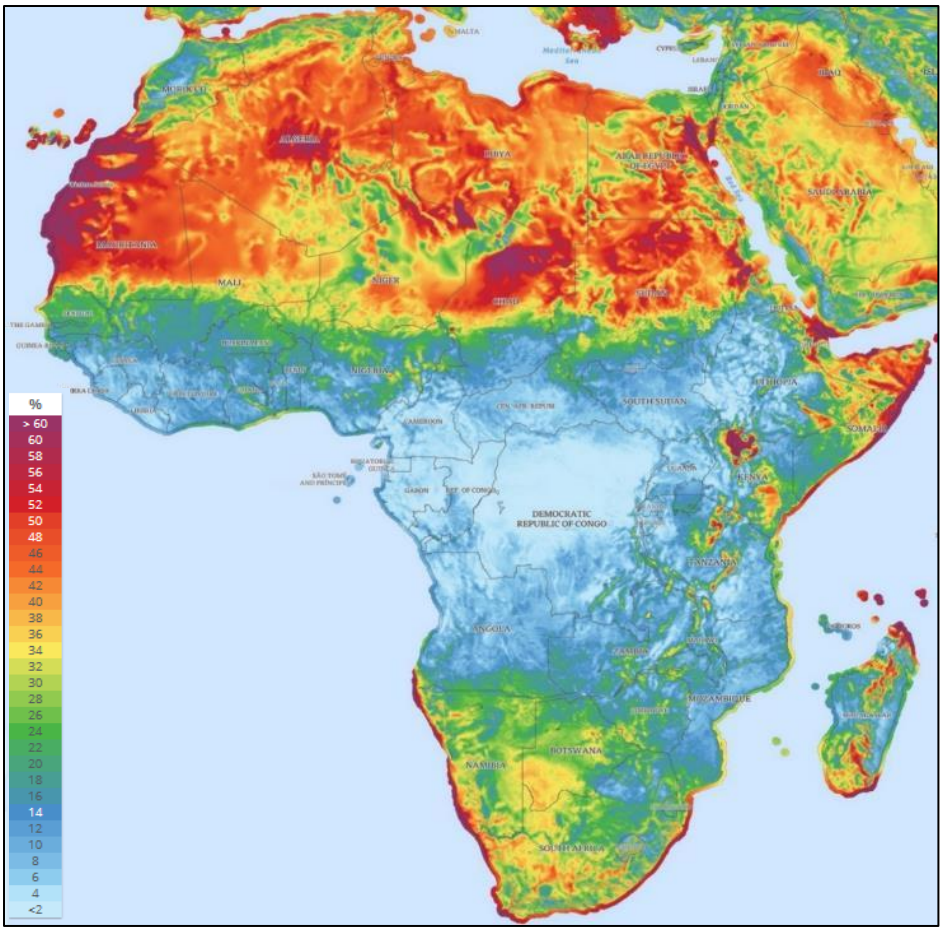


Figure 1.4: Distribution of wind energy across Africa: wind power C_f (%) at 100m elevation (Technical University of Denmark, 2018).

When reviewing the literature on wind as an energy resource in Africa, it becomes evident that a large wind resource variance occurs throughout the continent. This variance primarily depends on the country location, time period assessed, and elevation (Olaofe, 2018). It should be further noted that countries which record low wind speed at a large scale of assessment may contain isolated regions of moderate or high wind speed that may be suitable for utility-scale wind generation (Figure 1.4).

Several African countries have implemented FIT schemes to procure wind, and other renewable energy sources including Algeria, Ghana, Kenya, Tanzania, and Uganda. These programs do not drive competitive bidding, and are generally supported by institutions such

as the African Development Bank or the World Bank. These organisations are able to provide offtake guarantees in many cases when the local government or utility cannot afford investment certainty. FIT PPA terms have a range of 10–20 years. While they are not competitive, they have resulted in the successful procurement of wind power (Meyer-Renschhausen, 2013; International Energy Agency, 2016). The price of wind power in Africa varies. For instance, countries such as Egypt, and Kenya implemented FIT schemes while prices range from USD 0.05/kWh to USD 0.11/kWh, driven by project size (Meyer-Renschhausen, 2013; IEA, 2018). In other cases, countries have implemented a competitive bidding programme, which has observed higher value for money tariffs such as Morocco (USD 0.025/kWh), South Africa (USD 0.04/kWh), and most recently Tunisia (USD 0.04/kWh) (Azeroual, et al., 2018; IEA, 2018).

Similar to global trends, both increasing, and decreasing wind speed trends are identified across Africa. The spatial, and temporal variance of wind speed at a continental scale was examined by multiple researchers (Elsawwaf, et al., 2010; Kainkwa, 2010; Vautard, et al., 2010; Lavaysse, et al., 2016; Jury, 2018). These researchers have identified that countries such as Niger, Tanzania, and Nigeria indicated the largest increasing trend in mean annual wind speed, while Liberia, Ghana, and Cameroon indicated the largest decreasing trend. Chapter 3 presents an extensive literature review of regional wind speed trends while wind speed trends are quantified for the study area.

Wind speed trends are driven by regional, and global climate drivers specific to each geographical location. Several global, and synoptic-scale phenomena influence the African climate. Global phenomena include the ITCZ, and associated Hadley Cell, ENSO,, and the solar sunspot cycle, while regional phenomena include the equatorial cold tongue, African westerly Jet, Arctic Oscillation, IOD,, and seasonal insolation variance (Tyson & Preston-Whyte, 2000; Giannini, et al., 2008; Sonwa, et al., 2017; Shen, et al., 2019).

1.7 Wind energy in South Africa

The study area accounts for 95% of the countries onshore wind resource (Diab, 1995; Hagermann, 2008). Wind remained a largely untapped resource until the first utility-scale wind farms were installed in 2011 (DoE, 2013). The uptake of wind was driven by the REIPPPP to procure electricity from IPP's. The programme has driven the wind industry from non–existent to 3,346MW, comprising 34 of preferred bidder projects.

Several studies in South Africa have evaluated, and quantified the country's wind distribution, and frequency (Diab & Garstang, 1984; Diab, 1995; Hagermann, 2008; CSIR, 2010). Similarly, a recent study statistically assessed wind speed distribution, and power density in Port Elizabeth, concluding that average wind power density is largest during spring (September–October), and lowest during autumn (April–May) (Ayodele, et al., 2012). Wind atlas modelling is an important component when determining a suitable locality for a wind farm. The accuracy of such models has also evolved over time. Historically, such research was of considerable importance in establishing the wind power industry in South Africa (Figure 1.5). Given the distribution of wind resource, all of the wind projects (35 projects, 3346MW) procured to date are located in the NC, WC, and EC provinces, ranging in size from 20.6MW to 140MW.

The IRP of South Africa is a key government planning document that considers the present, and future energy requirements of the country. The updated (November 2013) IRP2010 forecasts several scenarios for the future capacity of wind generation. Eight of the 10 scenarios project a significant uptake of wind power generation ranging from 9GW to 25GW. The two scenarios with a low proportion of wind power are in the circumstance that natural gas fulfils the power demand or where technological, resource or grid integration issues occur with the implementation of wind-generated power.

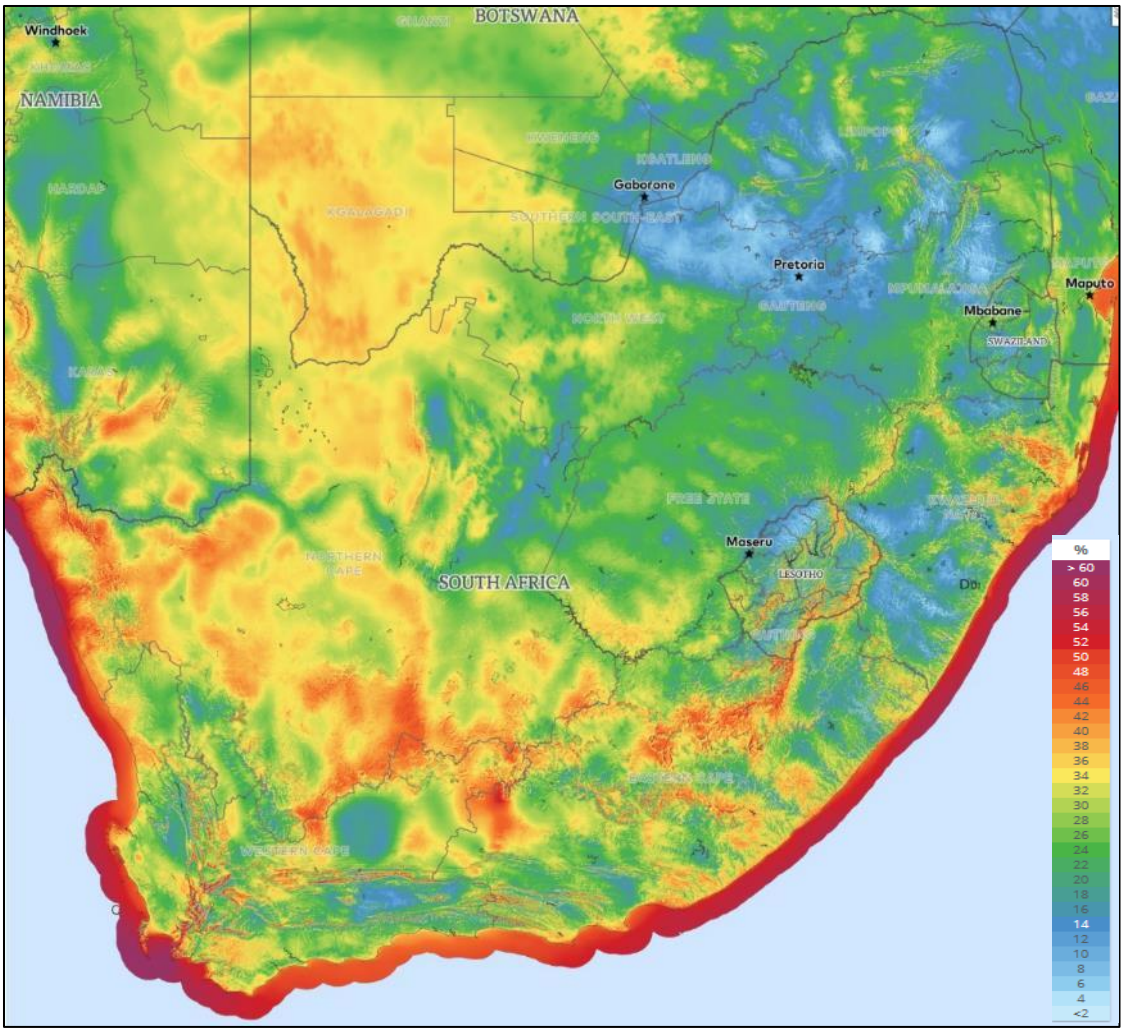


Figure 1.5: Distribution of wind energy across South Africa: wind power C_f (%) at 100m elevation (Technical University of Denmark, 2018).

In order to facilitate investment into utility-scale, grid-connected wind, and other renewable energy projects, the South African government developed the tender process known as the REIPPPP. The programme was extremely effective in facilitating the procurement of multiple technologies including wind, solar, landfill gas, biogas, hydro, and biomass collectively. For a total of 92 projects, the investment is USD 20.5 billion (bn) (ZAR 193bn), and 6,328MW is added to the South African power grid (DoE, 2015b). Due to the competitive nature of the programme, prices have reduced sharply across bid windows (BW) (2011–2015), and contracted project tariffs are now among the lowest in the world. Onshore wind (6,360MW)

accounts for almost half (48%) of the total (14,725MW) capacity allocated for procurement under the REIPPPP by the Minister of Energy under the Ministerial Determinations of 2011, and Government Gazettes No36005, and No 3911 (DoE, 2012; 2015a).

The most recent BW4 winning wind, and solar project tariffs are below Eskom's average cost of supply, and significantly below its new coal facilities of Medupi, and Kusile (Figure 1.6) (DoE, 2015b). There was no subsequent award of additional PPA's as a result of government politics. Eskom is observing IPP, and public unrest, primarily due to the battle between traditional, and renewable power generation. As South Africa reaches its 12th year of load shedding, it is has been announced that the REIPPP programme will recommence with an emergency BW in December 2020 to procure much needed electricity.

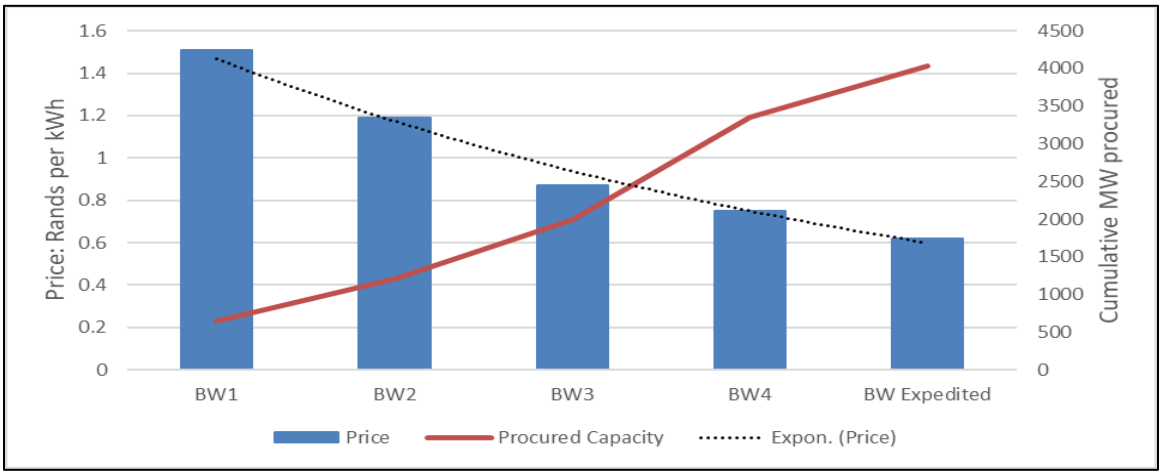


Figure 1.6: Price trend of wind power in South Africa for all bid windows to date[1] (Independent Power Producer Office, 2016).

[1] *Note: All tariffs are contracted to increase by the consumer price index or less per annum over the PPA term. There are four BW 2 projects and one BW 3 project which are partially indexed resulting in a reduced tariff in real terms over the PPA term. The presented prices are indexed based on April 2016 terms.*

Wind speed variability, trends, and climate teleconnections are still poorly documented in South Africa. Specific interest is why, and how wind speeds vary inter-annually, and which climatic phenomena are associated with the observed change. For this reason, the presented research is important for wind power generation which is designed to operate for 20–30 years. The teleconnections of climatic drivers, and wind speed in South Africa has produced limited scientific research compared to that available for the Americas, Asia and Europe (Alexander & Scott, 2002; Barthelmie, et al., 2006; Fu, et al., 2010; Rodrigues, 2015; Westra, et al., 2016; Pepler, et al., 2018). Besides, the drivers of South African climate are well documented including ENSO, IOD, AAO, solar irradiance cycle, and MLC activity (Behera & Yamagata, 2001; Alexander & Emeritus, 2005; Crétat, et al., 2012; Herbst & Lalk, 2014; Lakhraj-Govender & Grab, 2018). This study presents these trends, profiles, and relationships at a greater level of detail, scale, and accuracy than previously published. Stations which passed the selection criteria are distributed across the study area.

2 DATA, AND METHODS

2.1 Introduction

As outlined in section 1.2, the primary aim of this chapter is to present the data, statistical methods, and applied methodology to achieve the research aims, and objectives of this study. These data include wind speed, electricity demand profile, and climatic data (Niño 3.4, AAO, IOD, sunspot, and MLC referred to as ('the variables'). The geographical location of wind speed data encompasses the NC, WC, and EC provinces of South Africa. These provinces are of specific interest given that they encompass every operational wind project in South Africa to date.

Wind speed data were obtained from the SAWS for stations which contain at least 20 years of data located in the study area. Climatic data, historical synoptic charts, and electricity demand data series were obtained from the National Oceanic, and Atmospheric Administration (NOAA), SAWS,, and Eskom respectively. Data series are filtered at a daily, monthly, seasonal, and annual temporal scale, and statistically analysed. Further, the analysis considers station geographic location at a provincial, and regional scale. The three regions are defined by the distance from the shoreline which includes coastal (0–10km), hinterland (10–60km), and inland (> 60km).

The purpose of the statistical techniques presented is to assess the inherent spatial, and temporal wind speed characteristics, and their association with atmospheric, and electricity demand. Standard descriptive statistics are generated to identify the general characteristics of each data series where spectral, and trend analysis are applied to identify the cyclic frequency, and observed variance. Other core descriptive statistics of mean, minimum, and maximum are also used to evaluate the data series.

2.2 Statistical evaluation techniques

The assessment of recorded climate data are of utmost importance to accurately interpret wind speed characteristics, teleconnections, and inter–climatic relationships. This thesis applies proven statistical metrics including Discrete Fourier Transform, filtering, red–noise, standard error, and SD, as all are suited to climatic data interpretation (Erik, et al., 1997; Kruger, et al., 2010; Pishgar-Komleh, et al., 2015; Wang, et al., 2015; Fant, et al., 2016). Additionally, results are tested for statistical significance to ensure the validity of findings.

Several traditional metrics are typically used for data validation (Davis, 1973; Willmott, et al., 1985). When evaluating wind speed data, the most frequently applied metrics include root mean square error standard error ($RMSE_v$), mean bias error (b_v), and the mean absolute error (MAE_v) defined by:

$$RMSE_V = \sqrt{\frac{1}{n}\sum_{i=1}^{n}(V_{mi} - V_{Oi})^2}\ ; \qquad [14]$$

$$b_V = \overline{V_m - V_O}\ ;, \text{and} \qquad [15]$$

$$MAE_V = \frac{1}{n}\sum_{i=1}^{n}|V_{mi} - V_{Oi}| \qquad [16]$$

$RMSE_v$ describes how far apart the variables are from a reference level at any point in time, while b_v defines the difference in the overall average. MAE_v is an alternative to $RMSE_v$ which removes the need to square the result to remove negative values by calculating the associated absolute value. These are key aspects to quantify when analysing the time evolution of time series data.

Spectral analysis techniques are widely applied when investigating climatic data to analyse series frequency (Jenkins & Watts, 1968; Bloomfield, 1976; Yuen & Fraser, 1979; William & Thomson, 1997). Considering the variability, and cyclic nature of meteorological variables, the application of spectral techniques is essential to assess potential teleconnections. This statistical technique identifies the cyclical functions of a data series, and the relative

importance of each cycle's frequency. Spectral analysis methodologies include Discrete Fourier Transform (DFT), Filtering, and Covariance as all are applied during the data scrutiny, and presented in the subsections below.

2.2.1 Trend analysis

Wind speed data variance is of key interest when assessing long-term series to quantify inherent characteristics. This is achieved by calculating the series SD, Sen's slope estimator for trend analysis, and Mann Kendall (MK) test for statistical significance.

SD is a statistic frequently applied as a descriptive statistic defined by:

$$\mathrm{SD} = \sum_{\mathrm{i}-1}^{\mathrm{n}} \frac{(\mathrm{x_i}-\bar{\mathrm{x}})^2}{\mathrm{N}-1} \qquad [17]$$

Sen's slope is applied to quantify the magnitude of a monotonic slope (Q), where a standard linear model $f(t)$ is defined by:

$$f(t) = Q(t) + b \qquad [18]$$

and Q_k is initially calculated by applying:

$$Q_k = \frac{(y_j - y_i)}{j - i}, for\ k = 1, 2, \dots, N, \qquad [19]$$

where y_i, and y_j are data points at times i, and j, and $j > i$.

Sen's slope variance is defined by:

$$|var(S) = \frac{1}{18}\left[n[n-1][2n+5] - \sum_{p=1}^{q} t_p\left[t_p - 1\right]\left[2t_p + 5\right]\right] \qquad [20]$$

where q is the count of tied groups, and t_p is the total series of data points in the pth group, and Q_s is the median of Q_k values calculated by:

$$Q_s = \begin{cases} Q_{\frac{N+1}{2}}, if\ N\ is\ odd \\ \frac{\left(Q_{\frac{N}{2}} + Q_{\frac{N+2}{2}}\right)}{2}, if\ N\ is\ even. \end{cases} \quad [21]$$

In order to determine if the resulting slope significantly differs from zero, the ranks of lower, and upper limits of the confidence interval are calculated as follows:

$$Lower = \frac{N - Z_{1-\frac{\alpha}{2}}\sqrt{var\,(S)}}{2} \quad [22]$$

$$Upper = \frac{N + Z_{1-\frac{\alpha}{2}}\sqrt{var\,(S)}}{2}. \quad [23]$$

The slopes which correspond to Q_L, and Q_U are quantified if zero is not contained between these two quartiles. Such a case refers that the slope significantly differs from zero so that it indicates a significant trend.

The series (y_1, y_2, …, y_n) are further tested for statistical significance applying the MK test to check for a monotonic trend as follows:

$$S = \sum_{i=1}^{n-1} \sum_{j=i+1}^{n} sign\,(y_j - y_i)\ , where \quad [24]$$

$$sign(y_j - y_i) = \begin{cases} +1, if\ y_j - y_i > 0 \\ 0, if\ y_j - y_i = 0 \\ -1, if\ y_j - y_i < 0\,. \end{cases} \quad [25]$$

Thereafter $Var(S)$ is quantified where n is the count of time series data points y_1, y_2, …, y_n, and $i, = 1, 2, \dots, n-1, and\ j = 2, 3, \dots, n, for\ j > i$. The mean of $S, E[S] = 0$, and the variance is defined by:

$$Var(S) = \frac{1}{18}\,[n(n-1)(2n+5)] - \sum_{p=1}^{q} t_p\,(t_p-1)(2t_p+5), \quad [26]$$

where q is the count of tied groups, and t_p is the number of points in the p^th group.

Finally, the test statistic (Z) is calculated by:

$$Z = \begin{cases} \frac{S-1}{\sqrt{var(S)}}, if\ S > 0 \\ 0, if\ y_j - y_i = 0 \\ \frac{S+1}{\sqrt{var(S)}}\ , if\ S < 0\ . \end{cases} \quad [27]$$

The $Z\ statistic$ is normally distributed so that if $|Z| > Z_{1-\frac{a}{2}}$, then the null hypothesis of no trend is rejected, concluding a trend of statistical significance if present in the data series.

Of specific interest when evaluating a wind speed data series is the analysis, and comparison of cycles at a daily, seasonal, annual, and decadal scale. The reader is referred to section 1.3.2 where the concepts of daily $V_{24,\ and}$ annual V_{12} equations are presented. Seasonal scale data are composed of the associated V_{12} monthly filtered data. The following section presents an overview of methodologies applied to these data.

2.2.2 Periodicity

Periodicities in a wind speed time series refer to wind speed variance which is cyclic, and may occur at several frequencies (Sang, et al., 2013). Periodicities can be identified by applying methods which include sine wave regression, Fourier transforms, moving average (filtering), spectral density analysis, and wavelet analysis (Shumway & Stoffer, 2011). Continuous wavelet, Discrete Fourier Transform (DFT), and filtering are widely used to determine wind speed periodicity, and are applied to the current study.

2.2.2.1 Continuous wavelet analysis

One of the spectral density techniques is the continuous wavelet transform analysis (CWT). This is a key methodology applied to identify, and quantify the periodicity of wind speed variance (Yanfei, et al., 2019). The wavelet power is tested for statistical significance under the null hypothesis that the signal results from a stationary series given the background power spectrum. Given that the wind speed series $y(t)$ are continuous, a wavelet function is defined as:

$$\varphi(\omega) = \varphi(s,\tau) = s^{-\frac{1}{2}}\varphi\left(\frac{t-\tau}{s}\right), \qquad [28]$$

where t is time, τis the time step window iteration, and s is the wavelet scale $(0,\infty)$*.*

The function $\varphi(\omega)$ requires a zero mean, and is localised in both time, and space. The convolution of $y(t)$ defines the CWT while localised, and scaled gives the function $W(s,\tau)$ as:

$$W(s,\tau) = s^{-\frac{1}{2}}\int_{-\infty}^{\infty} y(t)\varphi^*\left(\frac{t-\tau}{s}\right)dt. \qquad [29]$$

Gaussian, Meyer, Mexican Hat, and Morlet are all types of wavelet functions which can be applied for CWT. Function selection is based on data series characteristics. Hydrological, climate, and wind studies commonly apply Morlet as it provides a suitable balance between frequency, and time localisation (Grossman & Morlet, 1984). The wavelet power spectrum is obtained by applying $|W(s,\tau)|^2$ against frequency, and time. In such a case, data can be filtered over space, and time to obtain additional insight into the time series.

2.2.2.2 Discrete Fourier Transform (spectral density)

Statistically, continuous functions such as Fourier Transform (FT) provide infinite results. However, practically one needs to obtain a result which accurately approximates the frequencies of most importance. In this regard, one needs to consider the DFT as the results are close to the FT of the time series, where 'f(t)' is defined by the following expressions:

$$G(\omega) = \frac{lim}{\omega_0 \to \infty} \int_{-\infty}^{\infty} f(t) \left\{ \frac{e^{-2\pi i \omega t}}{2\pi i \tau} - \frac{e^{-2\pi i \omega_0 t}}{-2\pi i t} \right\} dt \qquad [30]$$

where, $f(t_n) = f_n$, and $0 \leq n \leq N - 1$

where the DFT is defined as,

$$F_m = \frac{1}{N} \sum_{N=0}^{N-1} f_n e^{\frac{-2\pi i n m}{N}} \qquad [31]$$

The DFT methodology defined by F_m is a complex expression which avoids convergence problems that other methodologies cannot avoid. G (ω) applies to all values $-\infty \leq m \leq \infty$, and is episodic in m with period N. Further, $f(t_n)$ is valid for all values $-\infty \leq m \leq \infty$, and provides an extension ($N\Delta t = T + \Delta t$) of episodic events beyond the restrictions of (0, T), even if the original data are not cyclic.

Importantly, DFT allows for the analysis of temporal frequency (spectral density) which are described by the following expressions:

lowest non–zero frequency

$$\omega_1 = \Delta\omega = \frac{1}{N\Delta t} = \frac{1}{T + \Delta t} \text{ as } \Delta t \to 0, T \to \infty; \text{ and} \qquad [32]$$

highest (Nyquist) detectable frequency

$$\omega_{\frac{N}{2}} = \frac{1}{2\Delta t} \to \infty \; as \; \Delta t \longrightarrow 0; \; where \qquad [33]$$

$t_n = n\Delta t$ is time;, and $\omega_m = \frac{m}{n\Delta t}$ is frequency.

One disadvantage with DFT is that the data set represents a finite ($T < \infty, \Delta\omega > 0$) temporal period ($t_n$). When the sample data do not sufficiently represent the actual long–term record characteristics, leakage can occur due to the limited temporal scale.

2.2.2.3 Filtering

There are several reasons why a filter would be applied to a data series. Some of the filter samples include smoothing, isolating or removing certain frequencies. Smoothing a time series is achieved by applying a running average to reduce the high frequencies to focus the analysis on low-frequency events, and is provided as (considering 2L +1):

$$f_n = \frac{1}{2L+1}\sum_{l=n-L}^{N+l} f_L \qquad [34]$$

Pre–whitening can be achieved by applying a high pass filter to reduce the distortion resulting from the low-frequency spectrum expressed as:

$$\hat{f}_n = -\frac{1}{4}f_{n-1} + \frac{1}{2}f_n - \frac{1}{4}f_{n+1} \qquad [35]$$

Testing the resulting spectral periods for statistical significance is achieved through the utilisation of the red–noise spectrum (Lau & Sheu, 1988). The red–noise spectrum is defined by the data series with one month lagged correlation (r_1), and expressed as:

$$S_k = S^*\left\{(1 - r_1^2) / \left[1 + r_1^2 - 2r_1 \cos\left(\frac{\pi k}{m}\right)\right]\right\} \qquad [36]$$

where, s^* is the mean of all spectral estimates (S_k), defined by:

$$S^* = \frac{1}{m+1}\sum_{k=0}^{m} S_k \qquad [37]$$

There are known risks using spectral analysis as a statistical methodology to identify frequencies, and periods. In the case of climatic data, actual periods may result due to high-frequency relationships or due to non–linear data. In some cases, filtering was known to induce statistical periods, which in reality are not present in the data (Burroughs, 1986). Even considering these known risks, spectral analysis is still a widely accepted methodology applied to climatic data.

2.2.3 Covariance, and correlation

Covariance is frequently determined between two data sets to identify the direction of the linear relationship between variables. In addition, correlation is a function of covariance, and applied to quantify both strength, and direction of the linear symmetric dependency between two variables. In some cases, the relationship between the two meteorological data sets is delayed. In these cases, a lagged covariance, considering a finite sample data set of $x_{n,\text{ and }}y_n$ can be applied to determine potential relationships between time series of x(t), and y(t) through the formula:

$$C_{xy}(\tau) = \lim_{\tau \to \infty} \frac{1}{2\tau} \int_{-T}^{T} x(t-\tau)y(t)dt \text{ [38]}$$

2.2.4 Multivariate analysis

This section presents the multivariate statistical methods applied to datasets with multiple variables. Relationships between the variables are quantified with the possibility that these may be principal components (PC) or factors. The aim of a Principal Component Analysis (PCA) is to identify intercorrelated variables which can be grouped to reduce the quantum of variables being assessed. PCA is of specific interest when analysing multivariate climatic data, and has been extensively used by natural, and social scientists (Appendini, et al., 2018; Azzellino, et al., 2019; Millstein, et al., 2019; Zhang, et al., 2019).

PCA is an objective statistical approach which quantifies common variability between the data series. The method converts the multivariate data series into a linear grouping of Empirical Orthogonal Functions, also referred to as PC's. These PC's are calculated by using the correlation or covariance matrix of the data series. The approach has several benefits including describing patters of record variance, data–set compression, and highlighting dominant interrelationships (Wang & Du, 2000). The first step in a PCA is to calculate the correlation or covariance matrix while the methodology is driven by the format of raw data. In the case of this research, a correlation approach is superior as the data series units vary. The correlation matrix is a non–singular, and symmetric matrix which can be compressed to a single diagonal matrix through pre, and post multiplying each diagonal with a specific

orthogonal matrix by calculating the eigenvalues (characteristics roots), and vectors. The resulting component scores, and loadings are then used to interpret data relationships.

2.2.5 Software

WindPro[2] is used to identify gross data errors, clean the raw data, quantify mean monthly wind speed, and analyse station Weibull profile to ensure it is normally distributed. WindPro is an internationally recognised wind modelling software used extensively by manufacturers, utilities, consultants, and the scientific community (Çakmak, et al., 2019; Dabar, et al., 2019; Sharma, et al., 2019; Warudkar, et al., 2019).

Two software programmes were essential to generate the results, and figures used in this study. First one is the Microsoft excel with the use of the XLSTAT[3] add-in which is used to facilitate the required statistical methods, and generate graphical representations. XLSTAT is a powerful software add-in, and used extensively in scientific research across multiple disciplines (Babenko, et al., 2019; Guignard, et al., 2019; Tahir, et al., 2019; Zhai, et al., 2019). The second one is the PAleontological STatistics software package (PAST4.01[4]) for education, and data analysis. It was used to perform multiple numerical operations (Hammer, et al., 2001). Key functions such as standardisation, filtering, statistical significance, and spectral analysis are applied to quantify data statistics. Key operation is the ability for the PAST to perform wavelet analysis, and generate the associated transform plots to indicate power level, and statistical significance. PAST is an internationally recognised software which has been used extensively in the fields of earth science, life science, economics, engineering, and

[2] *https://www.emd.dk/windpro/*
[3] *https://www.xlstat.com/en/*
[4] *https://folk.uio.no/ohammer/past/*

wind speed analysis (Cai, et al., 2016; Nogueira Júnior, et al., 2018; Dani, et al., 2019; Lindhorst, et al., 2019).

2.3 Datasets

This section describes the data sources, scale, and preparation methods applied to the raw data files. These data include SAWS wind speed series, Eskom electricity load profile, ONI, IOD, AAO, solar sunspot cycle, and regional MLC activity. Specific attention was given to SAWS wind speed data in order to validate the data quality, reliability, and consistency.

2.3.1 Wind speed

Decadal wind speed data can be obtained from sources such as satellite, ship, or ground measurements; the scientific preference being the latter. Ground recorded wind speed data removes potential uncertainty associated with satellite data reanalysis, however, a detailed quality control procedure is essential to obtain scientifically valid findings. In South Africa, the SAWS monitors, and manages several thousand weather stations across South Africa (SAWS, 2015). The associated data series are available on request for research purposes. The broad geographical distribution, availability, and temporal length of these data series result in them being a primary choice for surface wind speed research in South Africa (Diab & Garstang, 1984; Hagermann, 2008; Kruger, 2011; McVicar, et al., 2012; Argent, 2015; Fant, et al., 2016).

Historically, the accuracy of wind speed data was of less priority to other climate variables such as rain, temperature, and pressure. In this respect, it is unfortunate that few of these stations are equipped with an anemometer, and most wind speed series pre–1994 were obtained using pressure–plate anemometers or wind totalisators. Based on the data review, these instruments are inherently inaccurate resulting in high data uncertainty, and reducing the precision of statistical results. Since 1992, the SAWS has been upgrading stations to automatic weather stations, which among other climatic variables, record mean wind speed at a 5–minute interval as well.

A minimum requirement applied for station inclusion in this study is a record length of at least 20 years with greater than 90% data capture rate. The temporal scale selected is motivated by two primary factors. The first is the current operational life span of a wind project (i.e. 20 years) while the second is to quantify multi-decadal climatic variability. Shorter periods may result in misleading conclusions compared to the actual wind climate of a region. It is recognised that even a 20–year temporal scale provides limited insight to long–term climatological variance. To meet this scientific expectation, 68 years of the Cape Agulhas wind speed series is assessed to quantify long-term multidecadal trends (1950–2018). The Cape Agulhas station series extends to the beginning of the last century. However, increased inhomogeneity, and decreased data capture reliability are identified for the pre–1950 period. Therefore, the data series before 1950 for the Cape Agulhas data set was disregarded as these are not deemed sufficiently accurate for any scientific investigative purposes.

2.3.1.1 Wind speed data description

There are approximately 4,350 SAWS stations in the NC, WC, and EC Provinces. Of these, metadata are available for 77 stations with a 5–minute time interval observation for a period of at least 10–years (Figure 2.1). After extensive assessment, and discussions with the SAWS technical team, it was established that only 34 of these station series extended at least 20 years, and of these, only 21 stations met the temporal, and quality requirements (Figure 2.2). These 21 stations underwent further screening (detailed at below, and 2.3.2) with only 16 passing, and ultimately being used in this study (Table 2.1). The data series of Struis Bay station[5] is also considered, even though it did not pass the initial screening due to <90% capture rate. The station serves as a reference station (5km proximity) for the Cape Agulhas data series, and is further detailed at Section 2.3.2.1.

[5] *Station data only used as a reference mast for Cape Agulhas wind speed record*

Wind speed data series for the weather stations which contained at least 20 years of data, and passed the initial screening, and Struts Bay station were provided by the SAWS in the form of a ".txt" file. The station calibration, and maintenance records were reviewed as an essential aspect of the quality control process. The maintenance record, and anemometer calibration ensure not only data consistency but further prevent measurement bias. Even though limited information is available for the Cape Agulhas station, the 68–year period between 1950, and 2018 offers a valuable opportunity to gain undocumented insight into South Africa's longer–term wind speed trends. Wind speed data series range 20–68 years, with all but one station (Cape Agulhas, eight–hourly) recording high (medium) frequency sample intervals of five–minutes. All wind speed data records (except Queenstown) are considered until December 2018 (December 2014).

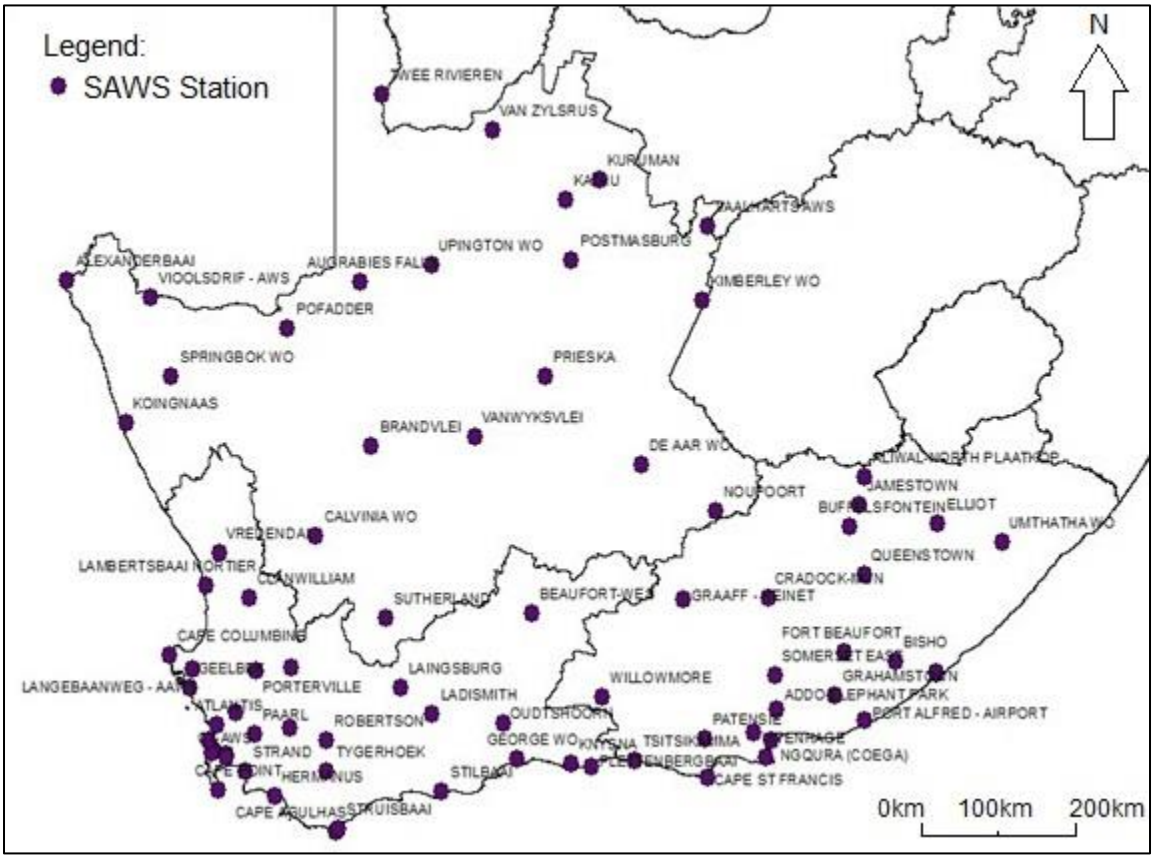


Figure 2.1: SAWS weather stations with at least 10 years of automatically recorded 5–minute wind speed data.

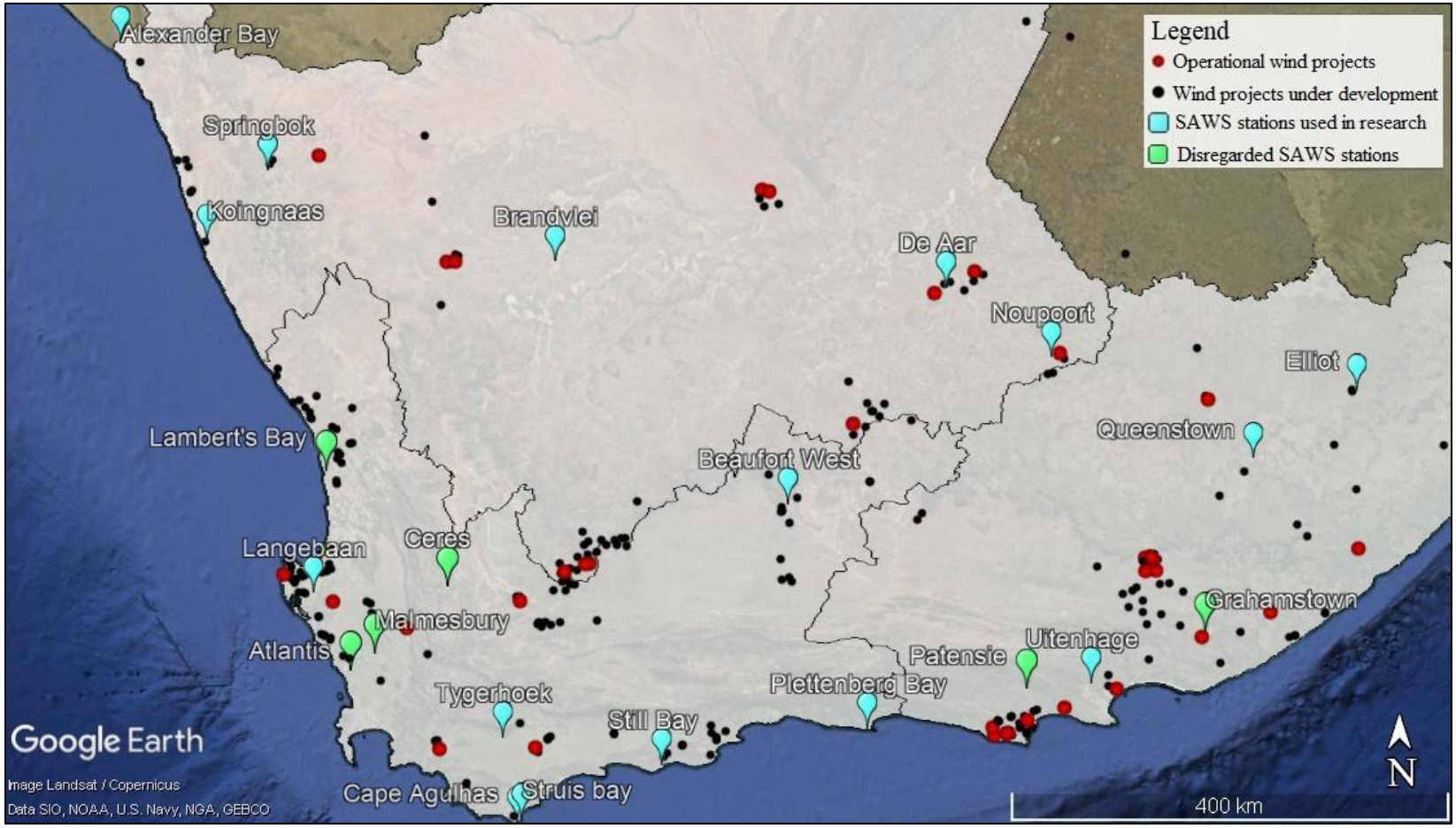


Figure 2.2: 21 SAWS weather stations with at least 20 years of wind speed data, and regional wind project developments.

Table 2.1: Meta–data for the 16 SAWS weather stations used in this thesis.

Station	Province	Region	Lat (S)	Long (E)	Elevation (amsl)	Record start	Monthly (m/s)				Capture rate
							Mean	Max	Min	Std Dev	
Alexander Bay	NC	Coastal	–28.57	16.53	24 m	1 Jan 1990	4.36	6.63	2.55	0.92	98.5%
Beaufort West	WC	Inland	–32.30	22.67	901 m	1 Sep 1993	4.14	5.47	2.87	0.49	99.4%
Brandvlei	NC	Inland	–30.46	20.48	924 m	1 Jul 1994	3.62	4.76	2.34	1.08	96.2%
Cape Agulhas	WC	Coastal	–34.85	20.01	9 m	1 Jan 1950	4.65	8.43	2.01	1.01	97.8%
De Aar	NC	Inland	–30.67	23.99	1,286 m	1 Aug 1993	4.66	6.29	3.28	0.70	99.8%
Elliot	EC	Inland	–31.34	27.84	1,463 m	1 Nov 1993	3.12	5.08	1.97	0.52	95.7%
Koingnaas	NC	Coastal	–30.20	17.29	95 m	1 Feb 1992	5.13	7.53	2.56	0.70	97.5%
Langebaan	WC	Hinterland	–32.98	18.16	34 m	1 Jan 1993	3.89	5.7	2.33	0.76	98.0%
Noupoort	NC	Inland	–31.19	24.96	1,495 m	1 Aug 1993	3.88	5.5	2.25	0.77	98.9%
Plettenberg Bay	WC	Coastal	–34.09	23.33	134 m	1 Jan 1990	3.23	4.11	2.1	0.34	99.2%
Queenstown	EC	Inland	–31.92	26.88	1,104 m	1 Jul 1991	3.24	4.52	2.09	0.65	96.5%
Springbok	NC	Inland	–29.67	17.88	1,006 m	1 Aug 1993	4.48	6.73	3.51	0.50	99.8%
Still Bay	WC	Coastal	–34.37	21.40	65 m	1 Sep 1993	3.67	4.56	2.85	0.39	99.4%
Struis Bay	WC	Coastal	–34.80	20.06	3 m	1 Jul 1996	4.64	6.04	3.32	0.48	86.7%
Tygerhoek	WC	Hinterland	–34.15	19.90	165 m	1 Jan 1990	2.51	3.53	1.62	0.49	97.8%
Uitenhage	EC	Hinterland	–33.71	25.44	158 m	1 Jan 1994	3.14	4.22	2.1	0.44	99.2%

The Queenstown station underwent substantial maintenance in January 2015, rendering subsequent data void due to anomalous records. Combined, these data accumulate more than 40 million data points over 438 years. These stations are equipped with automatic data loggers, and an RM Young 05130 propeller anemometer mounted at an elevation of 10m (Figure 2.2, Table 2.1, Table 2.3). It should be noted that this sensor has an associated accuracy error of 0.1 m/s. This error should be considered when interpreting the results of this thesis. Further, given the temporal period of data series, station maintenance is inevitable. When anemometer replacement has occurred, these change points have been assessed to ensure smooth data transition, and associated offsets, and alignment have been applied. It can also be noted that SAWS station data have inherent time domain stamp concerns. This is related to the alignment of data logger times to SAST. Minor deviations in this respect were identified, and corrected.

The only exception is the Cape Agulhas station which is mounted at 2m, and uses a Dines anemograph, for which limited information was available to define station specifications. It is accepted that this instrument is less accurate than the RM Young anemometers, and data correction was required, as detailed below in section 2.3.2.1. The mean annual wind speed differs between stations given complex regional, and synoptic influences. Based on the Beaufort wind scale (an empirical measure of observed wind speed), five stations are defined as a 'light breeze' (1.6–3.3 m/s) while 11 stations as a gentle breeze (3.4–5.4 m/s). Mean annual wind speed (1995–2018) is 3.9 m/s, which ranged between 2.51 m/s (Tygerhoek), and 5.13 m/s (Koingnaas). Mean data recovery rate for the 15 stations assessed is 98.25% with an SD of 1.3%. It should be noted that wind speed is not a primary concern or focus of this study. In this respect, all wind speed series were standardised, which by a process of mean centring, involving subtracting each data entry by the series mean, results in an empirical mean of zero. This approach was taken given that the primary research focus is on wind speed variability, as opposed to the energy contained therein. The data series was then filtered at a monthly, seasonal, annual, and daily scale in preparation for statistical analysis. Results are primarily presented as a percentage, and in certain cases, the associated wind speed value is provided for the reader's interest. Extended years above, and below the mean

are observed for the mean of all stations (Figure 2.3, 2.4, 2.5 & 2.6). The climatological drivers responsible for trends are identified, and presented in Chapter 5.

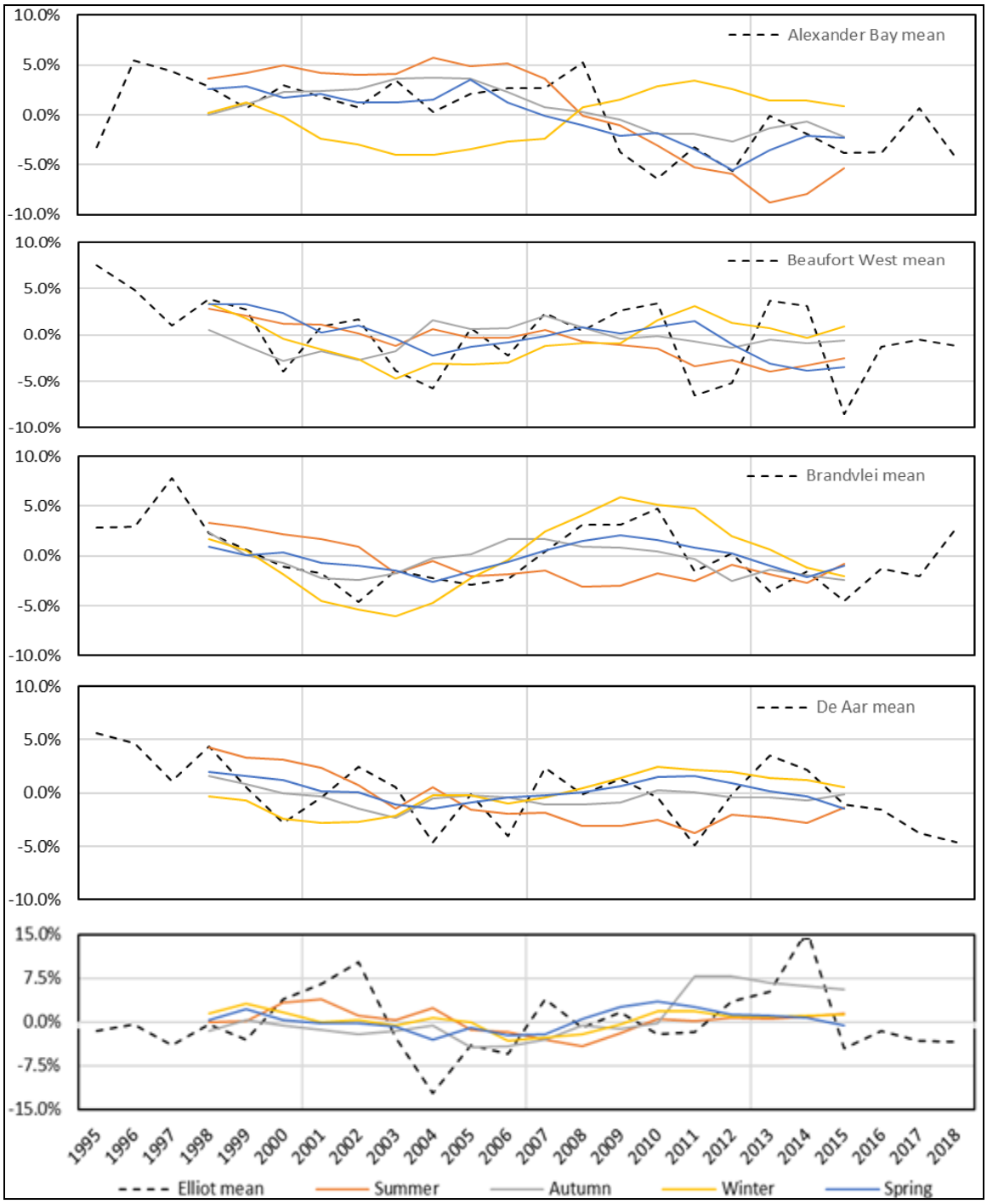


Figure 2.3: Standardised mean annual, and 6–year filtered seasonal wind speed for the period 1995 to 2018 (y-axis indicates deviation from the mean presented as a percentage)

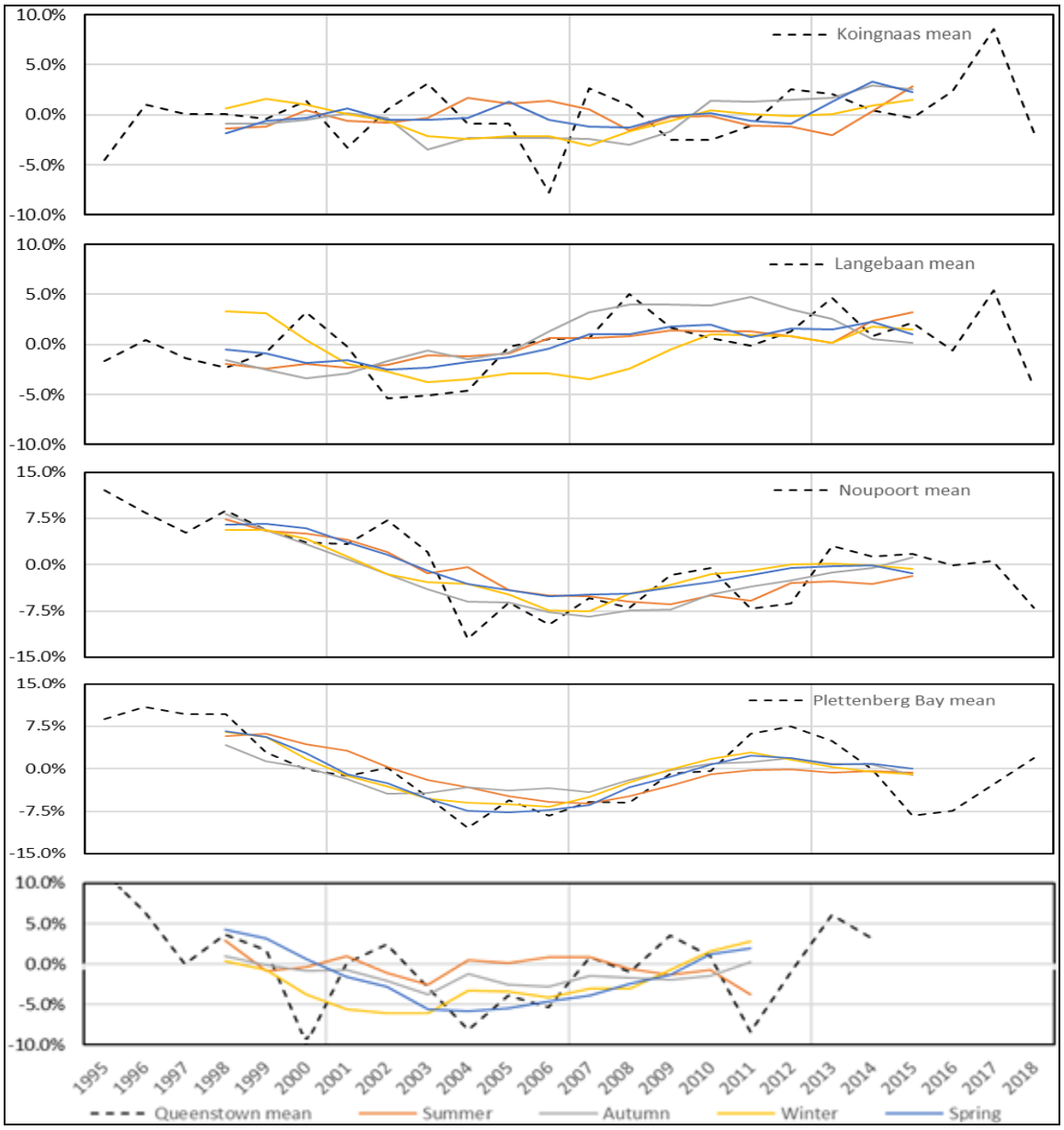


Figure 2.4: Standardised mean annual, and 6–year filtered seasonal wind speed for the period 1995 to 2018[6] (y-axis indicates deviation from the mean presented as a percentage)

6 Queenstown series (1995 – 2014)

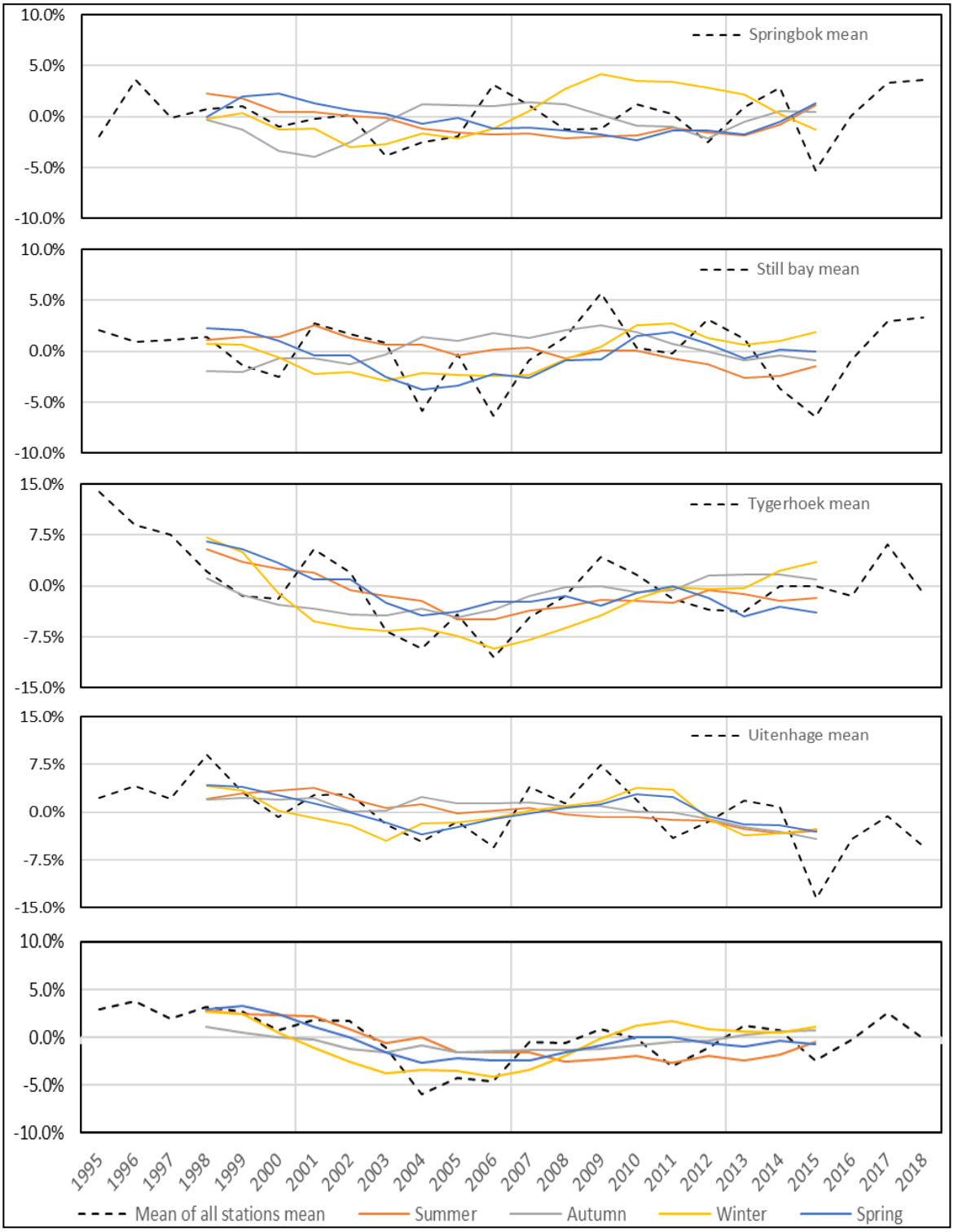


Figure 2.5: Standardised mean annual, and 6–year filtered seasonal wind speed for the period 1995 to 2018 (y-axis indicates deviation from the mean presented as a percentage)

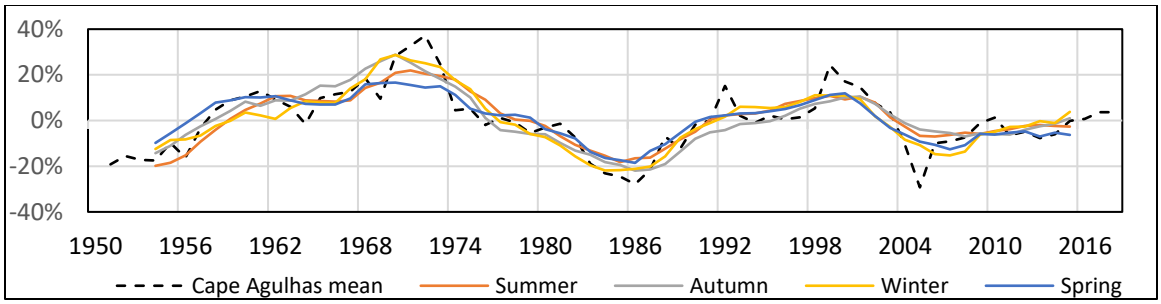


Figure 2.6: Standardised mean annual, and 6–year filtered seasonal wind speed for the Cape Agulhas station for the period 1950 to 2018 (y-axis indicates deviation from the mean as a percentage).

2.3.2 Quality assurance

Before performing any statistical analysis on wind speed data, uniformity checks were performed on these data. When applying quality control checks on wind speed data, it is essential to distinguish between natural wind effects, and invalid data which may be observed at a daily, monthly, or annual scale. Data anomalies result due to internal factors such as erratic data points due to technical failure or external factors such as station relocation, tree growth, or urbanization. In this regard, station calibration certificates, installation, and maintenance reports were reviewed to identify any documented change which may have resulted in specific data anomalies.

Several techniques were applied to validate data accuracies, such as spatial, and temporal coherency tests, tolerance tests, gross error checking, and internal record consistency checks (Aguilar, et al., 2003). Spatial, and temporal coherency tests were applied to determine if data series are consistent with other regional station series. Tolerance tests identify outlying values that are not consistent with the expected regional limits while gross checking identifies obvious errors such as negative wind speed. Additionally, manual screening was applied to ensure consistency. When specific events were identified, the associated data were removed from the data series.

It is worth noting that data from these stations have been previously used in several research initiatives by Botha et al. (2008), Hagermann (2008), Kruger et al. (2010), and Argent (2015). Each author has built on previous assessment results, and applied their unique methodology,

and processes to prepare the raw data for statistical assessment. Wind speed modelling is critically concerned with observed wind speed, in this respect aspects such as station exposure (generally too close to a building) can lead to underestimation of wind speed. Table 2.2 outlines each authors' station selection results as most stations pass each screening while several contrasting results stand out. Of specific interest are the most recent findings of Argent (2015). Five stations passed the screening procedure of the current PhD study, yet failed those applied by Argent (2015). Conversely, two stations which failed the screening of the current PhD study were passed by Argent (2015).

Table 2.2: Stations disregarded due to data anomalies not resulting from poor data capture.

Station	This Study	Botha et al. (2008)	Hagermann (2008)	Kruger et al. (2010)	Argent (2015)
Alexander Bay	Pass	Pass	Pass	Pass	Pass
Beaufort West	Pass	n/a	Pass	Pass	Fail (data)
Brandvlei	Pass	n/a	n/a	Pass	Pass
Cape Agulhas	Pass	n/a	n/a	n/a	Fail
De Aar	Pass	n/a	n/a	Pass	Pass
Elliot	Pass	n/a	n/a	Pass	Pass
Excelsior Ceres	Fail (data)	n/a	n/a	Pass	Fail (data)
Grahamstown	Fail (data)	n/a	n/a	Pass	Pass
Hermanus	Fail (data)	n/a	n/a	Pass	Fail
Koingnaas	Pass	Pass	n/a	Pass	Pass
Lamberts bay	Fail (data)	Pass	Pass	Pass	Fail (data)
Langebaan	Pass	n/a	Pass	Pass	Fail (data)
Malmesbury	Fail (data)	n/a	n/a	Pass	Fail
Noupoort	Pass	n/a	n/a	Pass	Pass
Patensie	Fail (data)	n/a	n/a	Pass	Pass
Plettenberg	Pass	n/a	n/a	Pass	Pass
Queenstown	Pass	n/a	n/a	Pass	Pass
Springbok	Pass	Pass	n/a	Pass	Fail
Still Bay	Pass	n/a	n/a	Pass	Pass
Struis Bay	Pass	n/a	n/a	Pass	Pass
Tygerhoek	Pass	n/a	n/a	Pass	Fail (exposure)
Uitenhage	Pass	n/a	n/a	Pass	Pass

Table 2.3: Stations disregarded due to data anomalies not resulting from poor data capture.

Station Name	Cause	Province	Lat	Long	Start Date	Years
Malmesbury	Tree growth	WC	–33.61	18.48	1 Oct 1979	39.3
Excelsior Ceres	Tree growth	WC	–32.96	19.43	1 Jul 1990	28.5
Grahamstown	Tree removal	EC	–33.29	26.50	1 Jul 1985	33.5
Hermanus	Urbanisation	WC	–34.43	19.22	1 Sep 1996	22.3
Lamberts bay	Relocation	WC	–32.04	18.33	1 Nov 1994	24.2
Patensie	Tree growth	EC	–33.77	24.82	1 Mar 1988	30.9

The quality assurance procedure of this study identified considerable inhomogeneity for data from six stations. An assessment was performed to quantify if any period could be valid, however, the anomalies are embedded in the data at a decadal scale, necessitating them to be completely disregarded. The anomalies resulted due to external factors which include tree growth/removal, station relocation, and urbanization (Table 2.3). As mentioned, five stations which passed data screening for the current study, failed Argent's (2015) screening. Three stations failed due to exposure (Cape Agulhas, Springbok, and Tygerhoek) while two failed due to poor data quality (Beaufort West, and Langebaan). The screening, and assessment methods applied in this study detected an non-significant influence in the wind speed series as a result of exposure with all data, and results within acceptable tolerance limits. The two stations concerned with data quality were extensively assessed at a 5–minute scale, and there is no indication of anomalous data. These differences could result due to different periods of assessment or as a result of notably different research applications.

Notably, even with extreme scrutiny, inaccurate station series can still unknowingly pass quality control procedures. Examples include the Grahamstown, Lamberts Bay, and Patensie wind speed series (Table 2.3). Lamberts Bay station has a high data capture (99.2%) but is affected by regional vegetation growth resulting in a consistent reduction of wind speed over the series (Figure 2.7). Where Argent (2015) correctly excluded the Lamberts Bay station series, both Botha et al. (2008), and Hagermann (2008) included these flawed data sets in their research (Table 2.2). Similarly, Grahamstown, and Patensie stations passed the stringent quality procedures applied by Argent (2015). At face value, the station data capture rates are a near-perfect record (99.4%, and 99.0%) respectively, while located at an

acceptable exposure, yet both series are fundamentally flawed. When assessed between 1995, and 2014, the Grahamstown data erroneously indicate a mean increasing wind speed (40.6% cumulative increase), and Patensie a mean decrease (–57.5% cumulative decrease). Such an outcome was owing to external factors of tree removal around the Grahamstown station, and tree growth around the Patensie station (Figure 2.7).

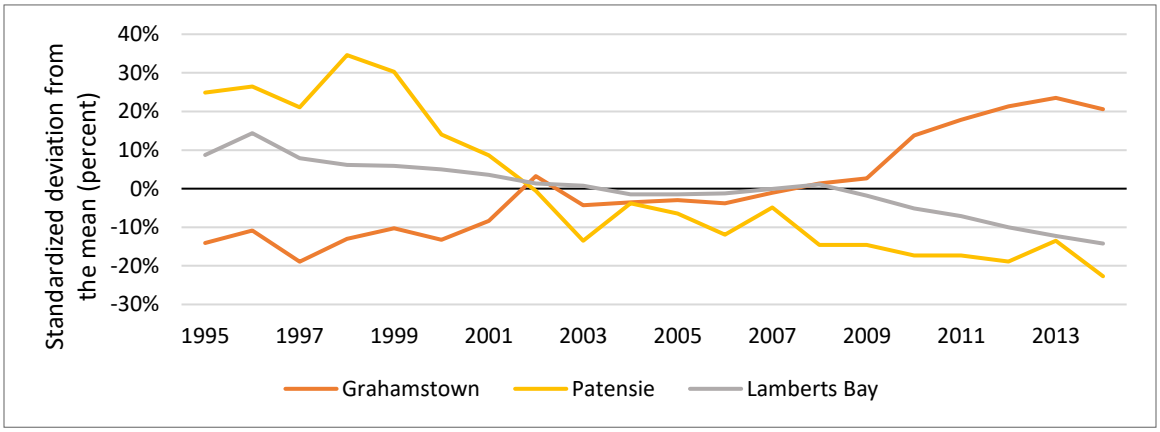


Figure 2.7: Example of erroneous wind speed series (standardised) for Grahamstown (tree removal), Patensie, and Lamberts Bay (tree growth) stations.

2.3.2.1 Processing

Importantly, two stations located in close proximity within a similar topography can be used to increase the temporal record for periods of missing or limited data series. The purpose of reconstruction is to increase the associated statistical accuracy by applying a single correlation approach between the available data points of the two data series, and using the result to reconstruct the missing data series of the incomplete data series. Data reconstruction is common practice, and extensive literature is available on the subject, with specific reference to wind data (Vaas & Kim, 2008; Schlipf, et al., 2012; Ni & Li, 2016; Borraccino, et al., 2017; Casella, 2019). In extreme cases, the extent of data removal or anomalies can render the entire data series void. Anomalous wind speed data are likely to introduce heterogeneity in the data series, leading to a misinterpretation of data trends, which may be caused due to internal or external variables opposed to actual wind speed variability. Similarly, as examined in section 2.3.1.1, the station anemometers have a coupled recording accuracy of 0.1 m/s which needs to be considered when interpreting results. This

is of limited concern given the temporal period considered, and the fact that the extent of datapoints would compensate for any data point uncertainties. These measurement uncertainties are accepted as embedded in all wind measurement data series globally.

No data processing has been applied to align wind speed measurement height. This is with respect to the observation that most stations are installed at 15m, while the Cape Agulhas station is mounted at 2m. Given that this PhD is not directly concerned with wind speed, but rather trends, profile, and correlation to climate drivers, this deviation is not of concern. This is due to the fact that the wind characteristics being assessed are present, and generic at a height of 2m or 15m. Station height is of critical importance when performing wind farm siting, calculating energy yield or mesoscale .

In this respect, only the Cape Agulhas station series required statistical intervention due to the medium frequency series, and was not applied to any other stations, ensuring no statistically generated trends were introduced to the data. The Struis Bay station is located 5km northeast of the Cape Agulhas station, having a similar in–situ topography. Further, a statistically significant ($P<0.01$) correlation ($r = 0.901$) at the two stations adds a level of statistical confidence. It is, however, noted that the process carries some level of uncertainty. Notwithstanding this, no other long–term record was available as an alternative for the southern African region, and is thus used with some measure of caution.

2.3.3 Electricity demand profile

Eskom is South Africa's primary electricity generator, and is also solely responsible for its distribution. Monthly electricity generation, demand, and source reports are published by Eskom, and Statistics South Africa (Eskom, 2019a; 2019c; StatsSA, 2019). These data were downloaded, and filtered into mean annual, seasonal, and monthly series in preparation for statistical analysis. The diurnal demand profile for South Africa is published in the schedule of standard prices for Eskom tariffs (Eskom, 2017b). A detailed overview of the electricity demand profile is presented in Chapter 4, section 2 (Figure 2.8).

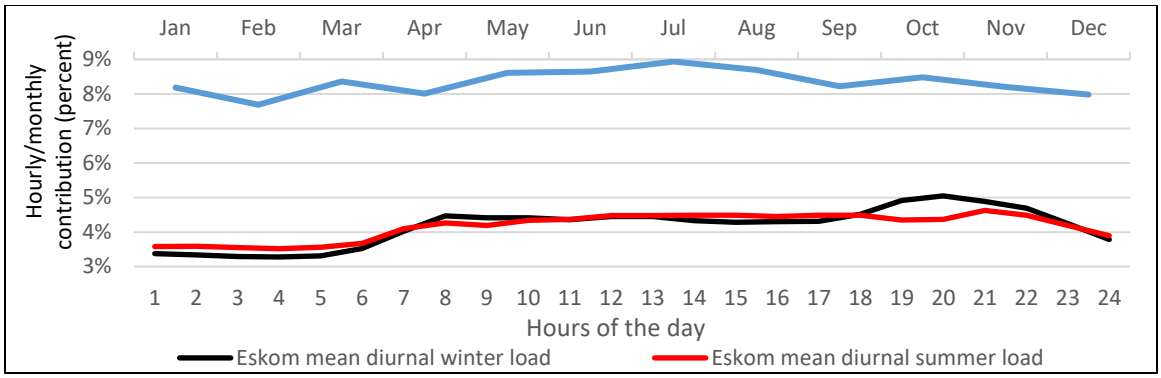


Figure 2.8: Eskom mean monthly, and diurnal load profile (Eskom, 2019c).

2.3.4 Climatic variables

The five climate mode series for the ONI, IOD, AAO, sunspot cycle, and regional MLC are considered ensuring a robust, unbiased analysis covering the 1950-2018 period (Figure 2.9). These pentad climate drivers are regarded as the most relevant to the climatic variability of South Africa, and have been extensively documented (Currie, 1993; Gray, et al., 2010; Weldon & Reason, 2014; Fant, et al., 2016; Dunning, et al., 2018; Sousa, et al., 2018; Pomposi, et al., 2018). Such climatic data are available online, with all but one (MLC activity, SAWS) available from NOAA. Below is an overview of these climate drivers which are detailed in Chapter 5 where the associated inter–variable, and wind speed connectivity results are presented.

Two of the indices assessed are SST linked but consider different regions. The first one is the ONI which measures the SST gradient between 5°N–5°S, and 120°W– 170°W, while the IOD considers the gradient between the western (50°E–70°E, and 10°S–10°N), and the south-eastern (90°E–110°E, and 10°S–0°N) equatorial the Indian Ocean. Both indices record negative, and positive phases which exert different effects on the global climate. The ONI is assessed based on the three–month running mean of the Niño 3.4 index (ERSSTv5 data), observed as the ONI between 1950, and 2018 (NOAA, 2019c). This filter was considered in the data assessment, ensuring alignment of temporal periods. The IOD is an aperiodic oscillation which is also assessed between 1950, and 2018 (NOAA, 2019b).

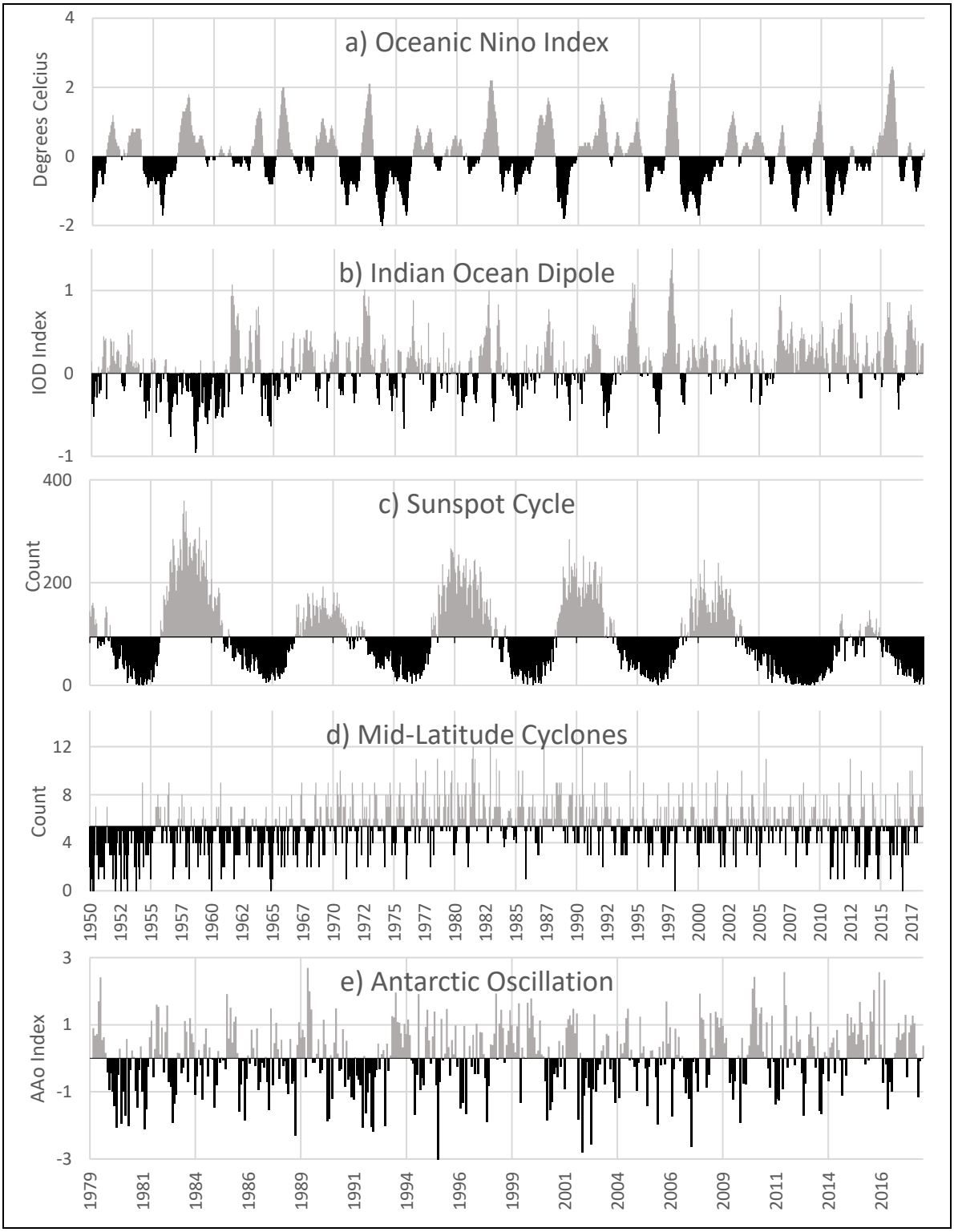


Figure 2.9: Climate indices used in this study.

Unlike the ONI, and IOD, the AAO is a pressure index which is calculated relative to the daily 700 millibar variance poleward of 20°S against the loading pattern of AAO. Daily AAO data series are standardised by the SD of the monthly AAO index of the complete record. Relative to the other variables, the AAO is a relatively recent discovery with data series extending since 1979 (NOAA, 2019a). Differing from the aforementioned indices, sunspot, and regional MLC data series are based on the number of events. Sunspot data, assessed between 1950, and 2018, are freely available as data series (NOAA, 2019d). Regional MLC activity was obtained through the analysis of historical synoptic charts between January 1950, and December 2018. The number of monthly MLC events are not automatically recorded. To obtain these data, the author manually reviewed 25, 201 daily synoptic charts to identify MLC events which passed over any portion of the Cape provinces, South Africa (SAWS, 2019).

2.4 Data limitations

To perform an unbiased, valid, and comprehensive study it is essential to recognise potential limitations inherent to the data assessed. Working with observed data always contains an element of inaccuracy due to the characteristic variability contained within the variables, and the measurement processes themselves. Thus, the recorded wind speed data contain both random, and systematic errors. For the stations which passed the quality control procedures, these errors are assumed to be nominal and, therefore, non-significant. The data series of the ONI, AAO, IOD, sunspot cycle, and electricity consumption are critically assessed, and verified prior to publication, and the potential measurements contained therein are also assumed non-significant. Considering the MLC data are obtained by visual inspection, there is a potential for human error. However, the process was performed on three separate occasions to reduce the likelihood of accidental oversight.

Best efforts have been made to contemplate multi-decadal climate cycles by considering 68 years of climate mode, and wind speed data series between 1950, and 2018. Noting, however, all but one station series are below 28 years, inherent statistical limitations are presently attempting to quantify relationships with large scale atmospheric, and ocean cycles which are

known to contain decadal variance. In this respect, there is a potential for statistically inferred bias.

Wind speed data obtained from each SAWS station are assumed to be a fair representation of the surrounding conditions, noting there is no intention to extrapolate results beyond the immediate station locale. Any level of extrapolation should proceed with caution as regional topography, flora, and anthropogenic influences can significantly impact ground wind speed. Noting there are many factors which affect wind speed, however, some may not yet be known. Therefore, despite the best efforts to consider multiple forcing factors, unknown variables could have unknowingly been overlooked. This results in the possibility of additional factors contributing to observed variability which should be considered in future research.

Despite the effectiveness of the statistical methods applied, it is worth noting that some methods applied may have resulted due to certain data assumptions. A primary example is the application of correlation which assumes two independent variables as in some cases it is not a reality resulting in misleading results. The correlation analysis also considers variables are normally distributed, and possess a linear relationship. Further, it is possible for two variables to record a coincidental correlation. To reduce this possibility, only coefficients with at least $P<0.1$ (90% confidence) are considered statistically significant. Where significance exceeds 90%, the actual confidence level is presented. Importantly, correlation does not indicate interconnection, and therefore results were carefully assessed for feasibility, and applied appropriately in the study.

3 SPATIO–TEMPORAL TRENDS OF NEAR–SURFACE WIND SPEED IN THE NORTHERN, WESTERN, AND EASTERN CAPE PROVINCES OF SOUTH AFRICA

3.1 Introduction

As discussed in Chapter 1, this chapter presents the spatio–temporal dynamics of near-surface wind speed at 15 stations in the study area for the period 1950-2018. The value of the long term (>50 years) climatological data are of utmost importance to validate trends in the context of multi-decadal change. Recent research has largely focused on rainfall, temperature, and SST variance in the context of a globally changing climate (Appendini, et al., 2018; Bonan & Doney, 2018; Routson, et al., 2019; Scott, et al., 2019). However, there is also increasing concern on global wind speed trends as other climate variables change. To this end, wind speed trends are quantified for the following time periods:

- 3.4.1 Annual wind speed trends
- 3.4.2 Monthly, and seasonal wind speed trends
- 3.4.3 Multi-temporal wind speed trends

It is brought to the reader's attention that a portion of this chapter was published as a peer reviewed research article in the South African Journal of Science. The paper is the first published analysis which quantifies long–term wind speed trends for the Cape provinces of South Africa in the context of wind power generation (Wright & Grab, 2017).

Considering all available literature, a knowledge gap exists in understanding annual, seasonal, and monthly wind speed trends with consideration of wind energy generation in the Cape provinces of South Africa. This chapter thus aims to address this gap by presenting a comprehensive assessment of the annual, seasonal, and monthly wind speed trends in this region.

Quantifying temporal wind speed trends are of importance across a multitude of spheres, including science, and engineering. Of specific interest to this chapter are near-surface wind speed trends in the context of wind power generation. Decadal wind speed trends are an essential variable to consider in South Africa as the other countries turn to wind power as a source of renewable electricity. Wind speed is an important indicator of atmospheric circulation, hence the considerable published work analysing its trends, and variance globally (de Lucena, et al., 2010; Wan, et al., 2010; McVicar, et al., 2012; Watson, et al., 2015; Efthimiou, et al., 2019; Arslan, et al., 2020).

A comprehensive assessment of available literature is fundamental to frame the results of this study in the context of global wind speed trends. Based on 12 years of personal experience in the wind power industry, it is worth mentioning that wind speed trends are poorly understood, and are not a factor considered when developing a wind power project. There is currently no international guideline for performing energy yield assessments for wind power projects. The IEC is one of the most respected international bodies providing globally accepted industry standards. The commission is proposing the IEC 61400–15 for the assessment of site-specific wind conditions for wind power stations (IEC, 2020). The standard will provide various loss, and uncertainty assumptions which need to be considered as one of which is the inter–annual variability of wind speed. Wind speed trends, however, are not considered. In this context, quantifying wind speed trends are of specific importance.

3.2 Review of wind speed trend studies

Globally, there are widespread observations of decreasing terrestrial near–surface wind speed. Recent findings over a similar (1979–2008) temporal period to this research, reports decreasing wind speed trends in Europe (–0.01 m/s/year), North America (–0.007 m/s/year), Central Asia (–0.016 m/s/year), Australia (–0.009 m/s/year), South Asia (–0.008 m/s/year), and East Asia (–0.012 m/s/year) (McVicar, et al., 2008; Ke, et al., 2014; van Vuuren & Vermeulen, 2019). Decreasing mean wind speed trends have also been identified in other countries such as Turkey (1975–2006), Brazil (1986–2011), China (1969–2005), and Canada (1940–2006) (Enloe, et al., 2004; Pryor, et al., 2005; Takatama, et al., 2015; Kramm,

et al., 2019). It should be noted that while global wind speed stilling is predominant, it is not ubiquitous. Increasing wind speed trends have also been documented in several regions including Spain (1980–2001), and Guyana (1968–1974; albeit not for the most recent decades in this case) (Pryor, et al., 2005; Wents, et al., 2007; Young, et al., 2011; McVicar, et al., 2012; Young & Ribal, 2019).

On the African continent, Mauritania, and Senegal (1951–1994), Egypt (1995–2003), and Tanzania (2001–2005) have likewise recorded increasing wind speed trends, while Libya (1979–1988), Ghana (2001–2005), and Cameroon (1991–1995) have reported strongest decreasing trends (McVicar, et al., 2012; Arreyndip, et al., 2016; Azeroual, et al., 2018). Mahowald et al. (2007) performed the most comprehensive research to date comprising 150 stations across North Africa. Their primary objective was to specifically quantify dust variability, which they identified to be directly correlated to wind speed in the case of North Africa. Their results show that the strongest trends are predominantly decreasing across North Africa, where few stations observed weak increasing wind speed trends (Table 3.1, Table 3.2).

The exact causes of a global wind speed stilling trend are still uncertain. Several authors have concluded that in many cases, the observed trends are strongly linked to fluctuations in synoptic, and global scale circulation (Roderick, et al., 2007; Azorin-Molina, et al., 2014; Azorin-Molina, et al., 2017; Kramm, et al., 2019; Zhang, et al., 2019). Chapter 5 of this thesis quantifies these teleconnections between wind speed, and key climatological variables.

Stutton (1905; 1908; 1910) published the earliest research on South African wind climatology by assessing wind speed availability to drive windmills for the extraction of water in Kimberley, and East London. The extensive international uptake of wind power generation has inspired South African research on wind resource distribution, by specifically focusing on such power for electricity generation (Jury, 1988; Jury & Diab, 1989). Until recently, the primary research goals were to quantify seasonal variance, distribution, and frequency of wind speed in South Africa (Bryukhan & Diab, 1993; Ayodele, et al., 2012; Fant & Gunturu, 2013; Fant, et al., 2016). For example, Nchaba (2013) assessed the modelling

accuracy of seasonal wind speed forecasts across three gridded regions of South Africa. The research found it difficult to obtain quality forecasts, and applied similar characteristics to each region but required the use of both model accuracy, and interpretation skill as a verification of quality. Nchaba further demonstrated that in some cases the model forecast may be accurate, but the inherent climatology is more useful than the wind speed forecast, depending on the temporal period, and geographical location.

Recent literature has shifted objectives from resource assessment to wind characteristics, trends, teleconnections, and resulting power generated from wind farms (Wright & Grab, 2017; Aliyu, 2018; Manyeredzi & Makaka, 2018; Sorensen, et al., 2018; Kekana & Landwehr, 2019; Jung, et al., 2019). Additionally, there is extensive literature which assesses wind speed, and its associated impacts on the built environment, rainfall bearing systems, evaporation, and meso–scale circulation (Hoffman, et al., 2011; Dyson, et al., 2015; Munday & Washington, 2018). Publications which are of specific interest to this study in the context of South Africa include those by Hoffman et al. (2011), Kruger (2011), McVicar et al. (2012), Argent (2015), Fant et al. (2016), and Jury (2018); these are summarized.

Hoffman et al. (2011) aimed to quantify the key drivers of pan evaporation in the Cape floristic region between 1974, and 2005. This research was primarily concerned with the quantum of wind movement. In this respect, these researchers calculated the mean daily wind run in kilometres. Data on this temporal scale provide limited insight to wind speed characteristics, and temporal profile in the context of wind energy generation. A notable finding, however, is that the mean annual wind running in the Cape floristic region reduced by more 25% at all stations over their research period. This observation is further assessed in section 3.4 of this chapter.

Kruger (2011) considered the impact of wind speed from an engineering design perspective, and suggested that the strong wind climate of South Africa is similar to that of southern South America, and Australia, considering the primary, and strong wind– producing mechanisms being thunderstorms, and extratropical cyclones. The findings defined six primary drivers of extreme winds in South Africa which result from thunderstorms, cold fronts, ridging ocean

high-pressure systems, troughs, ridging scenarios, system convergence, and western coastal lows. The current PhD study utilized much of the same data considered by Kruger (2011) who quantified extreme regional wind speeds using high-resolution SAWS data since 1995. The findings are specifically associated with the maximum of three-second gust wind speed but did not contemplate the association with renewable energy.

The study by McVicar et al. (2012) is particularly relevant as it quantifies a wind speed trend statistic for South Africa based on the studies of Kruger (2011), and Hoffman et al. (2011), with a focus on the environment, and evaporation. A primary variable contemplated is wind speed, and associated correlation with recorded evaporation trends. McVicar et al. (2012) obtained mean Sen's slope wind speed trend statistics for South Africa from Kruger (2011), and Hoffman et al. (2011) through personal communication. McVicar et al. (2012) do not provide any insight into the wind climate of South Africa or station data as these are not their primary research objectives.

Argent's PhD research (2015) assessed the wind climate across South Africa using seven years (1994–2010) of station, and reanalysis satellite data. The methodology considered a minimum of 3 years of wind speed data per station, and utilized reanalysis wind speed data to extend station series. The thesis documents the coupling of recorded wind speed with synoptic circulation, specifically defined by the 850hPa Climate Forecast System Reanalysis (CFSR) wind speeds with the specific intention of developing a classification scheme to define wind climate zones of South Africa. Wind speed trends (min three years of data) are used as one of the indicators to compare the accuracy between the CFSR, and wind speed data from SAWS stations. Little detail is provided on regional or individual wind speed trends as these are not a primary objective. However, the author does note that for the 7–years considered, recorded SAWS station wind speed trends ranged between +/– 2% per year while CFSR showed no discernible trend.

Fant et al. (2016) assessed wind power reliability in southern Africa using reanalysis wind data. The research applied wind power density as an indicator of reliability. Trends are not a

factor assessed, and the relevance of this paper are discussed in Chapter 4 where wind speed profile is presented considering South Africa's power demand profile.

Jury (2018) presents a comprehensive assessment of climate trends across South Africa for the period 1980-2017. The reanalysis, satellite, and modelled data are used for all climatic variables while specifically focused on temperature, SST, pressure, rainfall, and vegetation. Wind speed data are obtained from Modern-Era Retrospective for Research, and Analysis (MERRA) as it is presented as a secondary variable. Jury further identified a trend of upper airflow with a tendency of increased easterly winds, and increasing south-western Cape, and EC ocean margin surface wind speed trends (0.02 m/s/year). Jury additionally detected nominal surface trends in the Cape provinces, except for identifying a decreasing (–0.008 m/s/year) wind speed trend in the region of Koingnaas, and increasing wind speed trends around Queenstown (0.004 m/s/year), and west of Upington (0.008 m/s/year) (Figure 3.1).

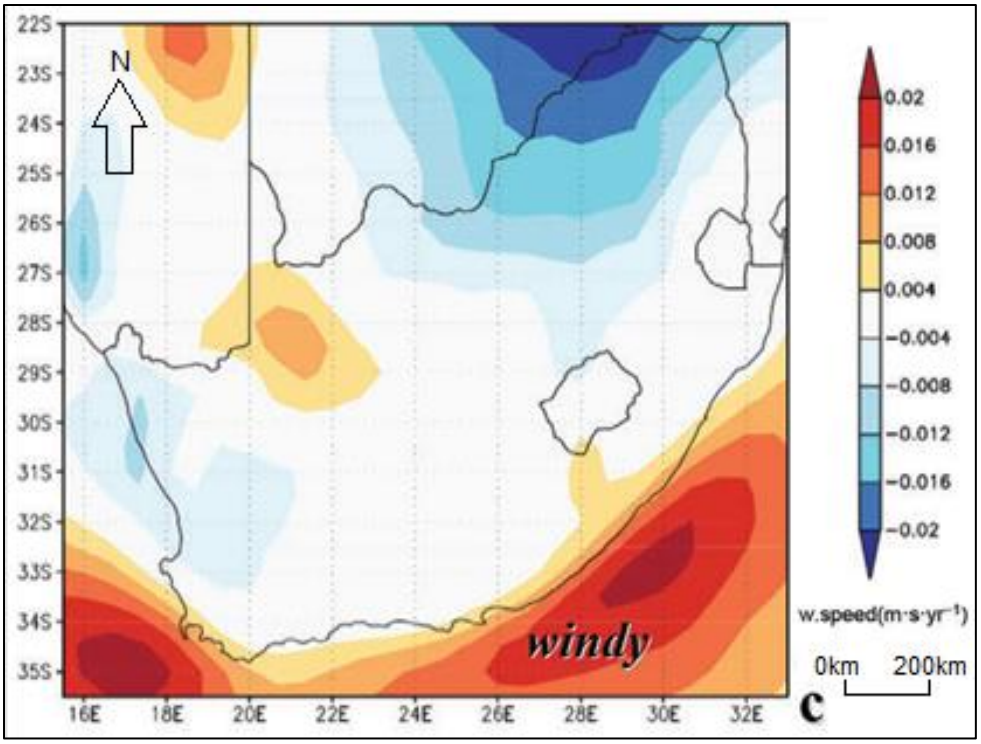


Figure 3.1: MERRA wind speed trends across South Africa between 1980–2014 (Jury, 2018).

3.2.1 Global wind speed trends

Based on the literature assessment in section 3.2, wind speed trend data were identified from over 160 publications across 60 countries considering 9,935 ground-mounted weather stations (Table 3.1, Table 3.2). While every effort was made to identify, and represent the most relevant research, it is acknowledged that there are likely several additional studies that are not included here. Little information is available on the specifications or maintenance of measurement equipment, resulting in a level of uncertainty which needs to be considered when interpreting the findings. The wind speed series range 4–127 years, referring to a weighted mean time-period of 36 years per station. Based on these data, a mean stilling of –0.013 meters per second per year (m/s/year) is indicated globally based on assessed literature since 1880. Observed wind speed trends per country were collected, and calculated based on a weighted mean trend.

Table 3.1: Recent wind speed trends across Africa.

Country/region	Number of sites	Coordinates	Period	Trend m/s/year	Reference
Tanzania	1	9°S, 35°E	2001–2005	0.063	(Kainkwa, 2010)
Egypt	1	24°N, 33°E	1995–2003	0.043	(Elsawwaf, et al., 2010)
Canary Islands	8	28–29°N, 15–17°W	1989–2014	0.032	(Azorin-Molina, et al., 2018)
Canary Islands	8	24°N, 33°E	1981–2014	0.023	(Azorin-Molina, et al., 2018)
Algeria	22	28–29°N, 15–17°W	1973–2003	0.005	(Mahowald, et al., 2007)
Atlantic Coast	24	15°S–21°N, 23°W–14°E	1955–1985	0.005	(Bigg, 1993)
Nigeria	20	4°–13°N, 4°–13°E	1970–2000	0.005	(Ogolo, 2011)
Mauritania & Senegal	4	14°– 21°N, 15°–17°W	1951–1994	0.001	(Ozer, 1996)
Kenya	1	1°S, 37°E	1979–2008	–0.002	(Vautard, et al., 2010)
South Africa	14	28°–35°S, 16°–28°E	1995–2014	–0.002	(Wright & Grab, 2017)
South Africa	1	34.83°S, 20.01°E	1950–2018	–0.003	This study

South Africa	15	28°–35°S, 16°–28°E	1995–2018	–0.005	This study
Nigeria	1	7°N, 4°E	1973–2008	–0.008	(Oguntunde, et al., 2011)
North Africa	150	10°–37°N, 15°W–55°E	1973–2003	–0.014	(Mahowald, et al., 2007)
South Africa	20	32°–34°S, 18°–22°E	1974–2005	–0.019	(McVicar, et al., 2012)
South Africa	29	24°–33°S, 20°–32°E	1993–2010	–0.021	(McVicar, et al., 2012)
Ethiopia	1	7°N, 39°E	1973–2003	–0.022	(Gebreegziabher, 2004)
Cameroon	2	7°–9°N, 13°E	1990–1999	–0.029	(Tchinda & Kaptouom, 2003)
Nigeria	2	11°–12°N, 11°–13°E	1969–1982	–0.046	(Hess, 1998)
Niger	1	13°N, 2°E	1984–1994	–0.064	(Michels, et al., 1999)
Libya	1	33°N, 13°E	1993–2002	–0.087	(Mohamed & Elmabrouk, 2009)
Algeria	8	24°–37°N, 0°–8°E	2002–2006	–0.091	(Himri, et al., 2009)
Libya	1	33°N, 12°E	1979–1988	–0.116	(El-Osta, et al., 1995)
Ghana	1	11°N, 0°E	2001–2005	–0.200	(O'Higgins, 2007)
Cameroon	1	10°N, 14°E	1991–1995	–0.200	(Nfah & Ngundam, 2008)
Cameroon	1	10°N, 14°E	1991–1995	–0.240	(Tchinda, et al., 2000)

Table 3.2: Recent global wind speed trends (excluding Africa).

Country / State	Number of sites	Coordinates	Period	Trend m/s/year	Reference
Guyana	1	7°N, 58°W	1968–1974	0.166	(Persaud, et al., 1999)
Spain	1	36°N, 4°W	1991–2006	0.118	(Recio, et al., 2009)
Netherlands	1	53°N, 5°E	1985–1992	0.043	(McVicar, et al., 2012)
Spain	1	42°N, 8°W	1995–2005	0.040	(Recio, et al., 2009)
Iran	5	30°–36°N, 53°– 57°E	1994–2005	0.036	(Mostafaeipour & Abarghooei, 2008)
Australia	14	20°–45°S, 112°–155°E	1975–2006	0.035	(McVicar, et al., 2012)
Iran	1	36°N, 51°E	1995–2005	0.035	(Keyhani, et al., 2010)
Australia	22	20°–45°S,	1989–2006	0.027	(McVicar, et al., 2012)

		112°–155°E			
USA, California	1	38°N, 122°W	1990–2010	0.022	(McVicar, et al., 2012)
Canada	3	60°–62°N, 134°–137°W	1956–2005	0.020	(McVicar, et al., 2012)
Iran	4	29°–39°N, 46°–61°E	1996–2005	0.018	(Sabziparvar, et al., 2011)
México	5	18°–21°N, 94°–97°W	2001–2006	0.017	(Cancino-Solórzano & Xiberta-Bernat, 2009)
Spain	8	40°–43°N, 1°– 7°W	1980–2009	0.017	(Moratiel, et al., 2011)
USA, Alaska	1	71°N, 157°W	1951–2001	0.015	(Hartmann & Wendler, 2005)
Israel	1	32°N, 35°E	1964–1997	0.014	(McVicar, et al., 2012)
Turkey	1	39°N, 39°E	1998–2002	0.013	(Akpinar & Akpinar, 2004)
Piarco	1	11°N, 61°W	1950–1999	0.009	(McVicar, et al., 2012)
USA, Alaska	1	71°N, 157°W	1921–2001	0.005	(Lynch, et al., 2004)
Saudi Arabia	1	30°N, 44°E	1970–2004	0.004	(Rehman, et al., 2007)
Canada	8	59°–83°N, 62°–105°W	1953–2006	0.003	(Wan, et al., 2010)
Iran	22	25°–38°N, 46°–61°E	1966–2005	0	(McVicar, et al., 2012)
Germany	73–113	47°–55°N, 6°–15°E	1951–2001	–0.001	(Rehman, et al., 2007)
Greece	20	35°–41°N, 20°–28°E	1959–2001	–0.001	(Papaioannou, et al., 2011)
Oman	6	17°–26°N, 54°–59°E	1986–1998	–0.001	(Dorvlo & Ampratwum, 2002)
USA, Idaho	2	43°N, 117°W	1984–2007	–0.001	(Reba, et al., 2011)
Australia	15	16°–45°S, 112°–155°E	1975–2006	–0.002	(McVicar, et al., 2012)
Germany	6	47°–55°N, 6°–15°E	1888–2006	–0.002	(Bormann, 2011)
Australia	14	18°–32°S, 115°–150°E	1973–2003	–0.003	(Mahowald, et al., 2007)
Germany	1	52°N, 7°E	1951–2000	–0.003	(Gerstengarbe, et al., 2004)
Belgium	1	51°N, 4°E	1880–2007	–0.004	(McVicar, et al., 2012)
USA, lower 48 states	176	25°–49°N, 65°–125°W	1961–1990	–0.004	(Klink, 1999)
Canada	109	42°–71°N, 53°–136°W	1953–2006	–0.005	(Mekis, et al., 2015)
France	51	43°–51°N, 5°W–8°E	1984–2003	–0.005	(Najac, et al., 2011)

Spain	8	37°–39°N, 1°–7°W	1967–2005	–0.005	(McVicar, et al., 2012)
USA, Alaska	18	55°–67°N, 132°–179°W	1951–2001	–0.005	(Hartmann & Wendler, 2005)
USA, California	2	34°–36°N, 117°–119°W	1979–2000	–0.005	(Rasmussen, et al., 2011)
USA, lower 48 states	207	25°–49°N, 65°–125°W	1962–1990	–0.005	(Hobbins, 2004)
USA, Minnesota	7	44°–49°N, 92°–98°W	1962–1993	–0.005	(Klink, 2002)
Australia	30	11°–45°S, 112°–155°E	1989–2006	–0.006	(McVicar, et al., 2012)
China	518	18°–54°N, 73°–135°E	1992–2007	–0.007	(Liu, et al., 2014)
China	119	21°–29°N, 98°–106°E	1961–2004	–0.007	(McVicar, et al., 2012)
China	77	37°–54°N, 108°–127°E	1982–2016	–0.007	(Zhang, et al., 2019)
North America	170	30°–75°N, 50°–170°W	1979–2008	–0.007	(Vautard, et al., 2010)
USA, Mid–West	3	34°–39°N, 84°–92°W	1948–2008	–0.007	(Abhishek, et al., 2010)
China	202	17°–42°N,	1956–2005	–0.008	(Cong, et al., 2010)
Czech Republic	23	48°–51°N, 12°–19°E	1961–2005	–0.008	(Brázdil, et al., 2009)
East Asia	8	23°–40°N, 91°–141°E	1979–1995	–0.008	(Xu, et al., 2006)
Southern USA, and México	20	25°–35°N, 95°–115°W	1973–2003	–0.008	(Mahowald, et al., 2007)
USA, Alaska, and Canada	14	55°–75°N, 68°–156°W	1953–1993	–0.008	(Keimig & Bradley, 2002)
USA, Massachusetts	1	42°N, 71°W	1885–2009	–0.008	(Iacono, 2009)
Australia	112–194	10°–45°S, 112°–155°E	1975–2006	–0.009	(McVicar, et al., 2008)
Canada	6	49°–51°N, 101°–114°W	1953–2006	–0.009	(McVicar, et al., 2012)
China	89	32°–42°N, 96°–119°E	1961–2006	–0.009	(Liu, et al., 2014)
China	18	32°–42°N, 113°–122°E	1961–2006	–0.009	(Song, et al., 2010)
China	652	18°–54°N, 73°–135°E	1961–2008	–0.009	(Yin, et al., 2010)
Spain	14	42°–43°N, 1°–2°W	1992–2005	–0.009	(Jiménez, et al., 2010)
Switzerland	25	46°–48°N, 6°–10°E	1983–2006	–0.009	(McVicar, et al., 2010)
Netherlands	5	51°–53°N, 4°–7°E	1970–2010	–0.009	(Cusack, 2013)

Australia	41	10°–45°S, 112°–155°E	1975–2004	–0.01	(Roderick, et al., 2007)
Australia	112–194	10°–45°S, 112°–155°E	1980–2006	–0.01	(Donohue, et al., 2010)
China	34	35°–43°N, 112°–120°E	1950–2007	–0.01	(Tang, et al., 2011)
China	150	24°–36°N, 92°– 122°E	1960–2000	–0.01	(Xu, et al., 2006)
Europe	276	30°–75°N, 20°W–40°E	1979–2008	–0.01	(Vautard, et al., 2010)
China	317	18°–54°N, 73°–135°E	1956–2005	–0.011	(Cong, et al., 2009)
New Zealand	5	36°–47°S, 168°–175°E	1975–2002	–0.011	(Roderick, et al., 2007)
South East Asia	32	0°–30°N, 99°–125°E	1979–2008	–0.011	(Vautard, et al., 2010)
South Korea	3	33°–34°N, 126°–127°E	1978–2007	–0.011	(Ko, et al., 2010)
China	190	30°–75°N, 100°–160°E	1979–2008	–0.012	(Vautard, et al., 2010)
China	535	18°–54°N, 73°–135°E	1956–2004	–0.012	(Jiang, et al., 2010)
China	603	18°–54°N, 73°–135°E	1971–2008	–0.012	(Yin, et al., 2010)
China	518	18°–54°N, 73°–135°E	1960–1991	–0.012	(Liu, et al., 2014)
Atlantic Coast, and Caribbean	25	23°S–22°N, 34°W–98°W	1955–1985	–0.013	(Bigg, 1993)
China	597	18°–54°N, 73°–135°E	1961–2007	–0.013	(Fu, et al., 2010)
China	101	26°–41°N, 74°–104°E	1961–2000	–0.013	(Shenbin, et al., 2006)
Italy	17	35°–45°N, 9°–18°E	1955–1996	–0.013	(Pirazzoli & Tomasin, 2003)
Kazakhstan, and Uzbekistan	15	36°–43°N, 55°–73°E	1973–2003	–0.013	(Mahowald, et al., 2007)
China	12	38°–40°N, 111°–115°E	1960–2000	–0.014	(Yang, et al., 2011)
China	45	35°–42°N, 111°–120°E	1957–2001	–0.014	(Zheng, et al., 2009)
China	69	33°–42°N, 100°–115°E	1960–2006	–0.014	(McVicar, et al., 2008)
China	62	18°–54°N, 73°–135°E	1961–2000	–0.015	(Zuo, et al., 2005)
Iran	32	25°–38°N, 45°–61°E	1960–2005	–0.016	(Rahimzadeh, et al., 2011)
Russia	64	40°–74°N, 30°–180°E	1936–2006	–0.016	(Gruza, 2008)
Russia	96	30°–75°N,	1979–2008	–0.016	(Vautard, et al., 2010)

		40°–100°E			
Belgium	1	51°N, 4°E	1965–2007	–0.017	(da Silva & Hesp, 2010)
Brazil	2	9°S, 40°W	1975–2009	–0.017	(da Silva & Hesp, 2010)
Canada	4	48°–52°N, 123°–131°W	1950–1995	–0.017	(Tuller, 2004)
China	75	26°–39°N, 80°–104°E	1966–2003	–0.017	(Zhang, et al., 2007)
Russia	23	60°–74°N, 31°–180°E	1936–2000	–0.017	(Mescherskaya, et al., 2006)
China	652	18°–54°N, 73°–135°E	1969–2005	–0.018	(Guo, et al., 2011)
China	75	26°–39°N, 73°–104°E	1970–2005	–0.018	(Liu, et al., 2014)
China	23	37°–42°N, 114°–120°E	2004–2014	–0.019	(Shi, et al., 2019)
USA, lower 48 states	336	25°–49°N, 65°–125°W	1973–2003	–0.019	(Pryor & Ledolter, 2010)
Kazakhstan	1	43°N, 77°E	1972–2007	–0.02	(McVicar, et al., 2012)
Ireland	12	51°–56°N, 6°–11°W	1961–1978	–0.021	(Haslett & Raftery, 1989)
China	305	18°–54°N, 73°–135°E	1969–2000	–0.022	(Xu, et al., 2006)
China	22	41°–25°N, 117°–124°E	1960–2012	–0.022	(Gao, et al., 2017)
Greece	4	39°N, 26–27°E	2003–2009	–0.022	(Palaiologou, et al., 2011)
India	11	27°N, 88°E	1979–2000	–0.022	(Jhajharia, et al., 2009)
Argentina	8	26°–35°S, 56°–69°W	1979–2008	–0.023	(Vautard, et al., 2010)
China	71	26°–37°N, 85°–101°E	1980–2005	–0.024	(You, et al., 2010)
Kazakhstan	7	43°–53°N, 51°–80°E	1936–2000	–0.024	(McVicar, et al., 2012)
Middle East	130	10°–45°N, 28°–75°E	1973–2003	–0.024	(Mahowald, et al., 2007)
Germany	1	52°N, 8°E	1982–2005	–0.025	(Böwer, 2006)
Pacific North West	53	45°–52°N, 121°–129°W	1950–2008	–0.025	(Griffin, et al., 2010)
Russia	17	46°–59°N, 37°–58°E	1936–2000	–0.025	(Meshcherskaya, et al., 2004)
USA, Nevada	3	38°–39°N, 117°–118°W	2003–2008	–0.025	(Belu & Koracin, 2009)
China	12	39°–41°N, 115°– 117°E	1960–2008	–0.026	(Li & Wang, 2003)
USA, Massachusetts	1	42°N, 71°W	1960–2009	–0.026	(Iacono, 2009)

Argentina, and Chile	6	17°–46°S, 60°–75°W	1973–2003	–0.027	(Mahowald, et al., 2007)
India	133	9°–34°N, 69°–95°E	1971–2002	–0.027	(Bandyopadhyay, et al., 2009)
India	35	16°–23°N, 73°–83°E	1961–2004	–0.027	(McVicar, et al., 2012)
China	25	36°–44°N, 80°–110°E	1973–2003	–0.029	(Mahowald, et al., 2007)
Saudi Arabia	16	17°–33°N, 37°–50°E	1977–2006	–0.03	(McVicar, et al., 2012)
Italy	1	45°N, 14°E	1951–1996	–0.031	(Pirazzoli & Tomasin, 1999)
México	33	15°–38°N, 87°–117°W	2000–2008	–0.031	(Hernández-Escobedo, et al., 2010)
Russia	22	46°–59°N, 37°–58°E	1961–1990	–0.031	(Meshcherskaya, et al., 2004)
Estonia	1	59°N, 24°E	1970–1991	–0.038	(Keevallik & Soomere, 2009)
India	10	25°–30°N, 70°–76°E	1951–2007	–0.038	(Choudhary, et al., 2009)
Cyprus	5	34°–35°N, 32°–34°E	1982–2002	–0.04	(Jacovides, et al., 2002)
Japan	327	31°–46°N, 129°–146°E	1979–2008	–0.042	(McVicar, et al., 2012)
USA, Wisconsin	1	46°N, 90°W	1989–1998	–0.051	(Lenters, et al., 2005)
México	9	18°–22°N, 87°–92°W	2000–2007	–0.053	(Soler-Bientz, et al., 2010)
Nepal	3	28°N, 87°E	2001–2006	–0.073	(Vuillermoz, et al., 2006)
Turkey	1	37°N, 39°E	1979–2001	–0.077	(Ozdogan & Salvucci, 2004)
India	1	18°N, 74°E	1983–2005	–0.079	(Jacob & Rajvanshi, 2006)
Cuba	4	22°–23°N, 79°–80°W	1979–2009	–0.085	(McVicar, et al., 2012)
Jordan	1	30°N, 35°E	1990–2001	–0.087	(Hrayshat, 2007)
Finland	33	60°–69°N, 20°–30°E	1959–2015	–0.090	(Laapas & Venäläinen, 2017)
Saudi Arabia	1	24°N, 38°E	1970–1983	–0.222	(Rehman, 2004)

3.3 Data, and trend tests

Wind speed data from the 15 stations presented in Chapter 2 are statistically assessed to quantify monthly, seasonal, annual, and multi-temporal wind speed trends. A trend analysis aims to identify, and quantify inherent patterns in data noise over an extended temporal

period. Trends can be downward or upward quantified for monthly, seasonal, annual or specific periods. Wind speed periodic trends are quantified when at least two distinct periods continue in a downward or upward tendency. The change points are of specific interest when assessing underlying climatic drivers, as will be discussed in Chapter 5. The wind speed series SD is calculated, and used as a descriptive statistic to quantify local variation. Several methods may be used to identify trends. In this study, Sen's slope is applied to estimate the trend strength (Sen, 1968). These trends are assessed for statistical significance by applying the non–parametric Mann–Kendall test, and the accompanying p– statistic (Mann, 1945; Kendall, 1975).

Local wind speed data are assessed between 1950, and 2018 at a concurrent, and Gaussian filtered scale. The filter period was identified from the spectral density analysis results of wind speed data series. Spectral density relates to the transform of a continuous-time series. By applying DFT methodology, periodograms were generated for wind speed data, and through a smoothing function, the spectral density estimate (discrete spectral average estimator) was obtained for the time series. A strong 12–month frequency is present in all series at a monthly scale, proving statistically significant ($P<0.001$) outcomes.

3.4 Results

3.4.1 Annual wind speed trends

Stations record a statistically significant ($P<0.05$) decreasing mean annual (1995–2018) wind speed trend of –0.14% per year (–0.005 m/s/year) with an associated mean SD of 2.52% (0.096 m/s). This trend strengthens to –0.24% per year (–0.009 m/s/year) when excluding the eight non-significant wind speed trends ($P>0.1$). While some stations record a high mean SD, including Noupoort (6.28%, 0.238 m/s), and Plettenberg Bay (6.28%, 0.201 m/s), others such as Springbok (2.3%, 0.102 m/s), and Langebaan (2.92%, 0.112 m/s) record a low mean inter-annual SD.

The Noupoort station recorded the strongest statistically significant ($p<0.01$) decreasing mean annual wind speed trend –0.49% per year (–0.019 m/s/year), cumulating –9.78% (–0.371 m/s) over a 20–year wind farm operational period. The Cape Agulhas station recorded a statistically non-significant ($P>0.1$) decreasing mean annual wind speed trend of –0.06% per year between 1950, and 2018 (–0.003 m/s/year), which increased to –0.24% per year between 1995, and 2018 (–0.011 m/s/year). Neither period proved significant when applying a 6–year Gaussian filter. The stilling is not ubiquitous; three stations indicate increasing mean annual wind speed trends, including Koingnaas, Langebaan, and Springbok. Langebaan, however, is the only station to record a statistically significant ($P<0.05$) increasing mean annual wind speed trend of 0.16% per year (0.006 m/s/year), increasing to 0.24% per year (0.009 m/s/year), when applying a 6–year filter ($P<0.01$) (Table 3.3, Figure 3.2).

Decreasing mean annual wind speed trends are recorded for regions. The NC (–0.15% per year, –0.006 m/s/year), and WC (–0.22% per year, –0.008 m/s/year) provinces indicate statistically significant ($P<0.1$) decreasing mean annual wind speed trends, where trends are statistically non-significant ($P>0.1$) in the EC (–0.22% per year, –0.007 m/s/year). Coastal stations indicate a statistically significant ($P<0.1$) decreasing mean annual wind speed trend (–0.21% per year, –0.009 m/s/year), where the mean wind speed of hinterland, and inland stations proved statistically non-significant ($P>0.1$). At a finer spatial scale, the three sub-regions indicate statistically significant ($P<0.1$) decreasing mean annual wind speed trends.

The EC hinterland region presented the strongest decreasing mean annual wind speed trend (–0.28% per year; –0.009 m/s/year), followed by the inland regions of the WC (–0.21% per year; –0.009 m/s/year), and NC (–0.19% per year; –0.008 m/s/year) provinces. Applying a 6–year Gaussian filter, the NC coastal region indicates a statistically significant ($P<0.01$) trend (–0.16% per year, –0.007 m/s/year), which was not identified at an inter-annual temporal scale (Table 3.3). Considering the spatial distribution of the stations, the strongest mean seasonal wind speed trends are indicated by those located in coastal regions. These coastal regions indicate statistically significant ($P<0.1$) trends in summer (–0.28% per year, –0.013 m/s/year), and winter (–0.31% per year, 0.012 m/s/year) (Table 3.3).

3.4.2 Monthly, and seasonal wind speed trends

Increasing, and decreasing statistically significant (P<0.1) monthly, and seasonal wind speed trends are identified between wind speed series. April, and June are the only two months which depict mean increasing wind speed trends (and consequently low mean wind speed months), proving statistically non-significant (P>0.1). Decreasing mean wind speed trends are observed in all other periods, although only October (–0.32%, –0.013 m/s/year), and Spring (–0.18% per year, –0.007 m/s/year) are statistically significant (P<0.1). Every month indicates at least one statistically significant (P<0.1) decreasing trend, where positive statistically significant (p<0.1) trends are only present in January (Langebaan), April (Alexander Bay, Koingnaas), June (Still Bay), September (Koingnaas), and November (Springbok) (Table 3.4).

The strongest statistically significant (P<0.05) monthly trends are recorded by the stations of Koingnaas (increasing) in April (0.67%, 0.031 m/s/year), and Uitenhage (decreasing) in May (–0.98%, –0.025 m/s/year). Plettenberg Bay is the only station which recorded mean ubiquitous decreasing trends, statistically significant (P<0.1) during May (–0.71% per year, –0.021 m/s/year), July (–0.61% per year, –0.020 m/s/year), October (–0.53% per year, –0.018 m/s/year), and summer (–0.31% per year, –0.010 m/s/year). The 68–year Cape Agulhas series portrays increasing, and decreasing mean monthly wind speed trends, although only statistically significant (P<0.1) in October (–0.18% per year, –0.010 m/s/year). The identified polarization of wind speed trends is of scientific importance as it indicates the variability of driving forces (Figure 3.3, Figure 3.4, Figure 3.5).

Table 3.3: Annual, and seasonal Sen's slope wind speed trend (%) per station, and region (1995–2018).

Station / Region	Annual	Annual 6–year filter	Summer	Autumn	Winter	Spring
Alexander Bay	**–0.32%**	**–0.39%**	**–0.50%**	–0.15%	0.19%	–0.32%
Beaufort West	–0.21%	**–0.11%**	–0.37%	–0.15%	–0.32%	**–0.32%**
Brandvlei	–0.15%	–0.06%	**–0.31%**	–0.31%	–0.14%	–0.03%
Cape Agulhas[7]	–0.06%	–0.12%	0.01%	–0.03%	0.03%	–0.14%
Cape Agulhas	–0.24%	–0.74%	–0.28%	–0.02%	–0.53%	–0.71%
De Aar	**–0.24%**	–0.06%	**–0.34%**	–0.21%	–0.02%	**–0.20%**
Elliot	–0.02%	0.07%	0.13%	0.23%	–0.29%	0.00%
Koingnaas	0.09%	0.07%	0.20%	0.09%	0.08%	0.21%
Langebaan	**0.16%**	**0.24%**	**0.31%**	0.17%	–0.10%	0.20%
Noupoort	**–0.49%**	–0.44%	**–0.56%**	–0.42%	–0.29%	**–0.39%**
Plettenberg Bay	–0.31%	–0.15%	–0.31%	–0.27%	–0.36%	–0.29%
Queenstown[8]	–0.16%	0.05%	–0.48%	0.05%	0.04%	–0.21%
Springbok	0.07%	0.04%	–0.06%	0.04%	0.08%	0.04%
Still bay	–0.01%	–0.01%	–0.10%	0.05%	0.05%	–0.09%
Tygerhoek	–0.27%	0.02%	–0.42%	0.16%	–0.05%	**–0.60%**
Uitenhage	**–0.28%**	**–0.19%**	–0.20%	**–0.40%**	–0.31%	–0.26%
Mean of stations	**–0.14%**	–0.08%	–0.17%	–0.03%	–0.09%	–0.18%
Eastern Cape	–0.22%	–0.08%	–0.25%	–0.20%	–0.26%	–0.31%
Northern Cape	**–0.15%**	–0.10%	–0.23%	–0.17%	0.00%	–0.12%
Western Cape	–0.22%	–0.15%	–0.16%	–0.06%	–0.19%	**–0.33%**
Coastal	–0.21%	–0.24%	–0.28%	–0.10%	–0.05%	–0.26%
Hinterland	–0.16%	0.00%	–0.01%	–0.05%	–0.17%	**–0.23%**
Inland	–0.07%	0.06%	–0.15%	–0.03%	–0.04%	–0.11%
EC Hinterland	**–0.28%**	**–0.27%**	–0.20%	**–0.40%**	–0.31%	–0.26%
EC Inland	–0.21%	0.00%	–0.38%	–0.12%	–0.21%	–0.25%
NC Coastal	–0.11%	**–0.16%**	–0.11%	–0.01%	0.10%	–0.06%
NC Inland	**–0.19%**	–0.07%	**–0.29%**	–0.20%	–0.11%	–0.15%
WC Coastal	–0.16%	–0.02%	–0.22%	–0.14%	–0.14%	–0.21%
WC Hinterland	–0.14%	–0.23%	–0.03%	0.01%	–0.24%	–0.38%
WC Inland	–0.21%	**–0.11%**	–0.37%	–0.15%	–0.32%	**–0.32%**

Bold underline denotes a MK statistical significance of 99% (P<0.01)
Bold denotes a MK statistical significance of 95% (P<0.05)
Underline denotes a MK statistical significance of 90% (P<0.1)

[7] *Cape Agulhas series (1950 – 2018)*
[8] *Queenstown series (1995 – 2014)*

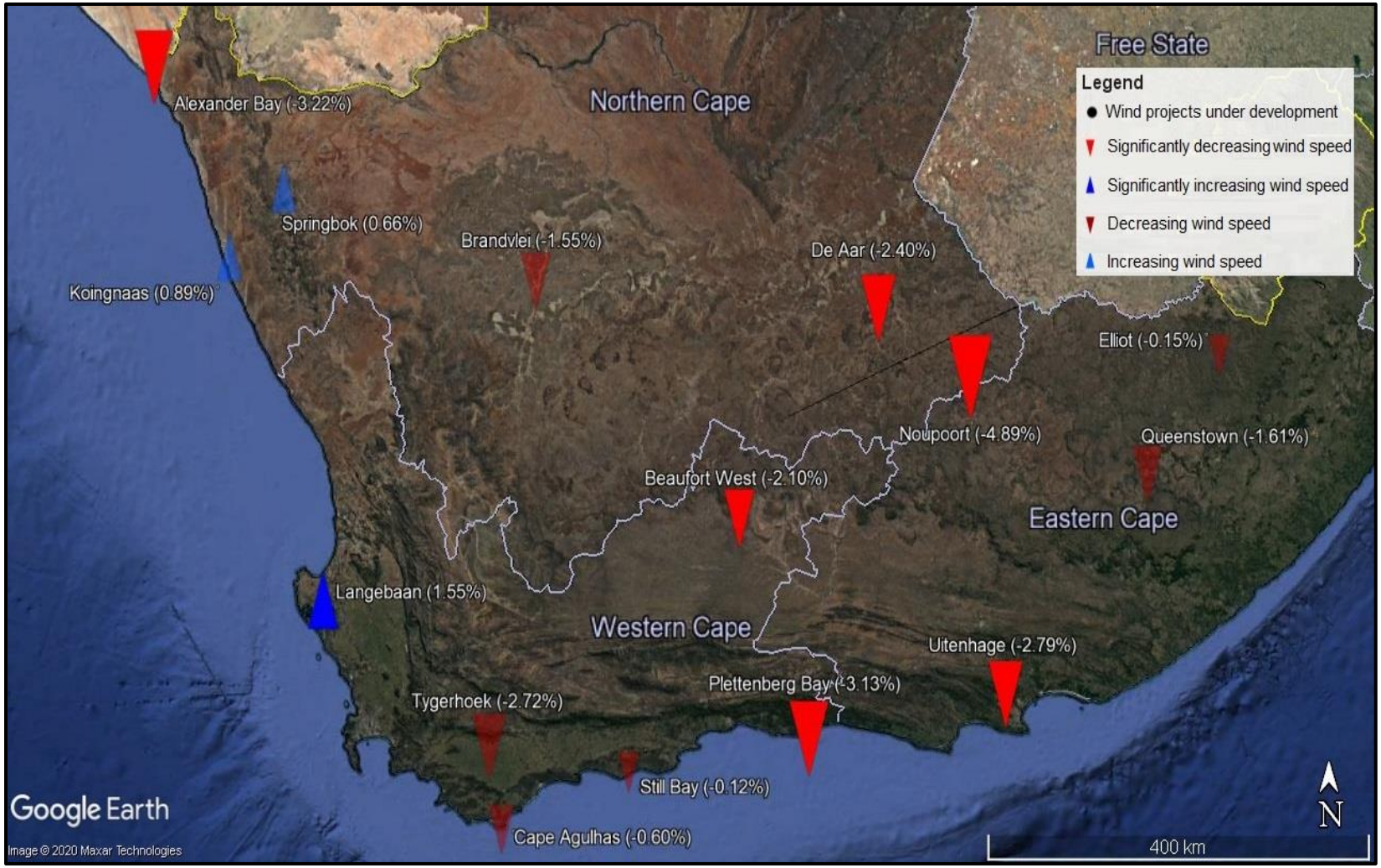


Figure 3.2: Mean decadal wind speed trends (1995–2018) & Cape Agulhas series (1950–2018), statistical significance is considered at a threshold of P<0.1.

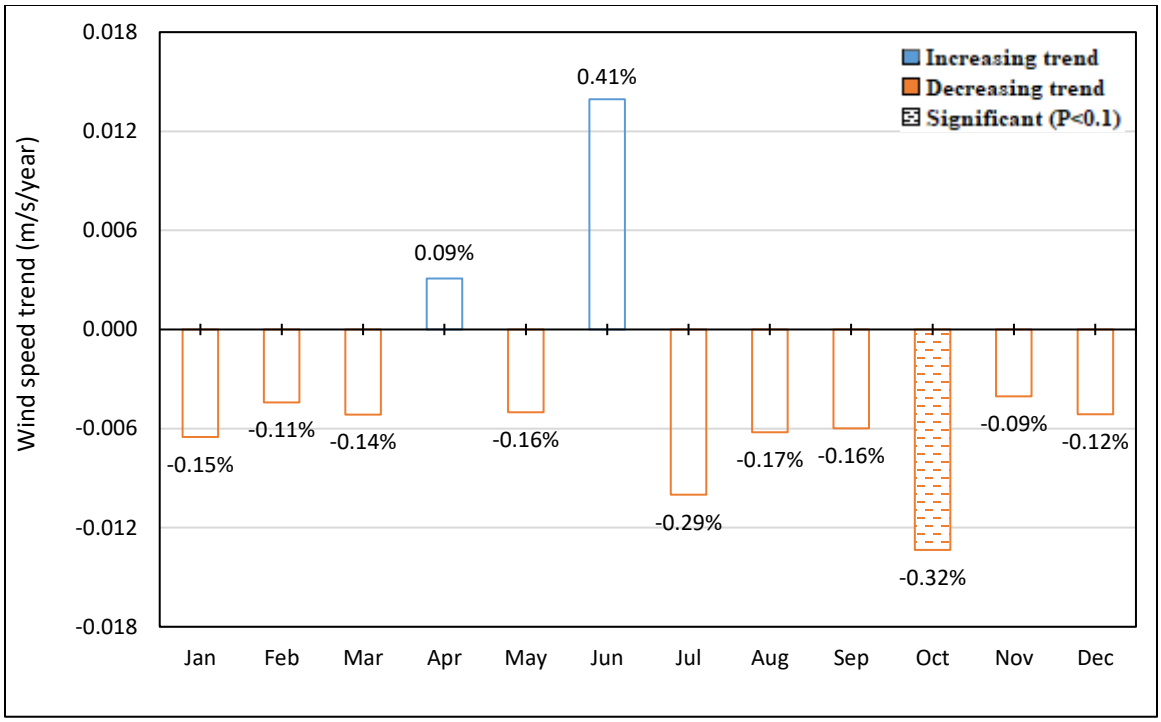


Figure 3.3: Mean monthly Sen's slope wind speed trend of all stations considering 1995–2018 period.

Statistically significant (P<0.1) mean monthly wind speed trends are present at a provincial scale in January, July, August, October, and November. The months of October, and November are the only two months where more than one province (EC, and WC) indicate significant wind speed trends. At a provincial scale, no statistically significant (P>0.1) increasing wind speed trends are observed. The strongest mean monthly decreasing wind speed trend from stations located in the EC province is for July (–0.90% per year, –0.026 m/s/year). Similarly, at a monthly scale, all statistically significant (P<0.1) trends are decreasing in coastal, hinterland, and inland regions. In addition to the months identified at a provincial scale, December also indicates statistically significant (P<0.1) mean monthly wind speed trends in coastal regions.

Four consecutive months (October, November, December, and January) indicates statistically significant (P<0.1) trends in the coastal region (spring, and summer), whereas July, August, and October (winter, and spring) are significant in the hinterland region. Notably, no statistically significant (P>0.1) wind speed trends are recorded when assessing the inland region at a mean monthly scale. At an increased spatial scale, the EC hinterland region recorded the strongest statistically significant decreasing wind speed trend (P<0.05; –0.98%, –0.025 m/s/year) in May. The NC coastal region (0.60%, 0.025 m/s/year) is the only region to record a statistically significant mean monthly increasing wind speed trend in April (P<0.05) (Figure 3.4).

At the mean seasonal scale, fewest statistically significant (P<0.1) wind speed trends are observed in winter (one station), and the most in summer (nine stations). The strongest decreasing mean seasonal wind speed is recorded by Tygerhoek in spring (–0.60% per year, –0.015 m/s/year), while the same station recorded mean increasing wind speed in autumn, also statistically non-significant (P>0.1). Langebaan is the only station to record a statistically significant (P<0.05) mean increasing seasonal trend present in summer (0.31% per year, 0.015 m/s/year). Noupoort station records statistically significant (P<0.1) negative trends in three seasons: summer, autumn, and spring. The 68–year Cape Agulhas station recorded increasing mean seasonal wind speed trends in summer, and winter, where decreasing wind speed trends are indicated in autumn, and spring, but none of which are statistically significant (P>0.1). Similarly, no statistically significant (P>0.1) mean seasonal wind speed trends are identified in the Elliot, Koingnaas, Springbok or Still Bay station series (Figure 3.4, Figure 3.5).

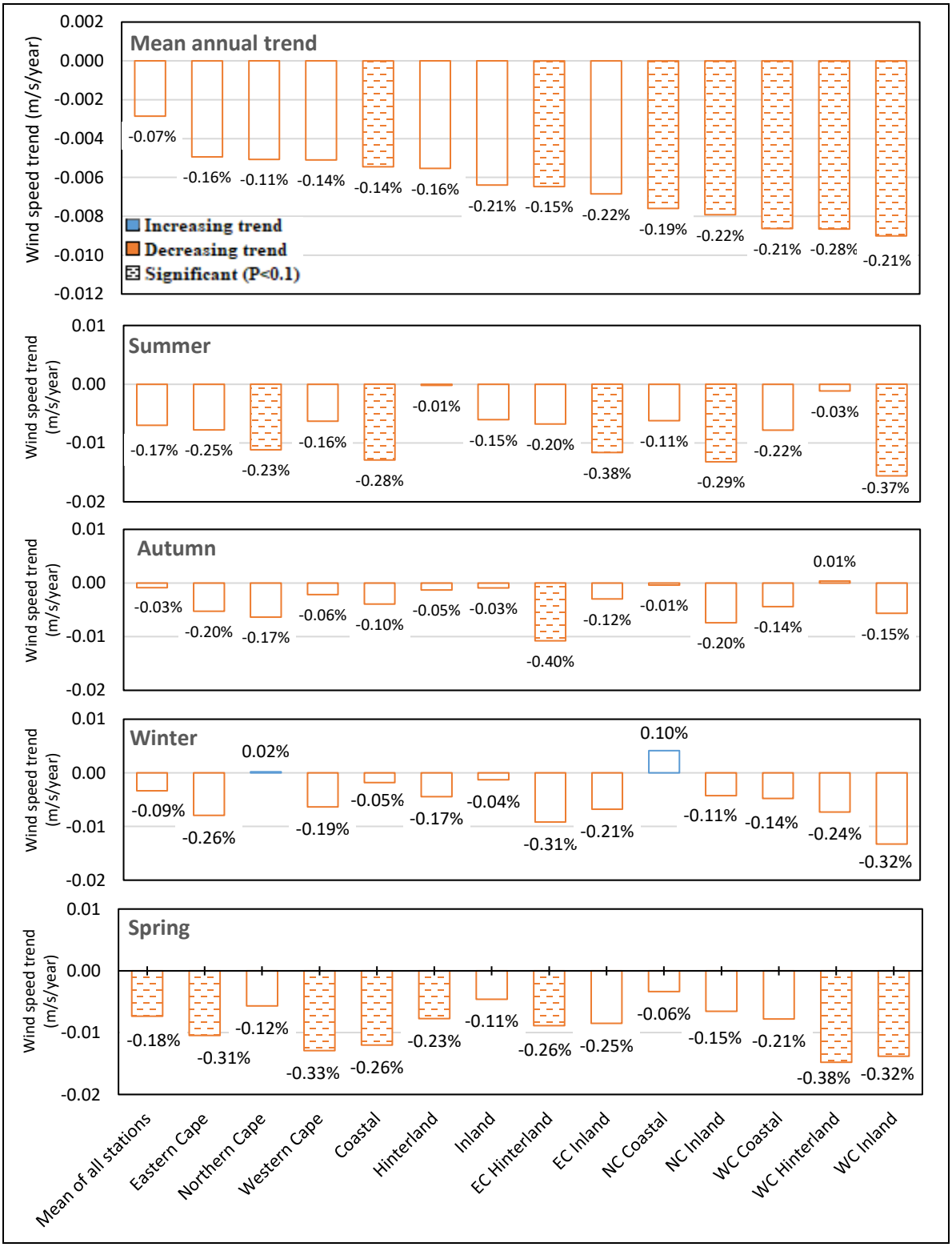


Figure 3.4: Mean annual, and seasonal Sen's slope wind speed trends presented for each region in m/s, and percentage per year (1995–2018).

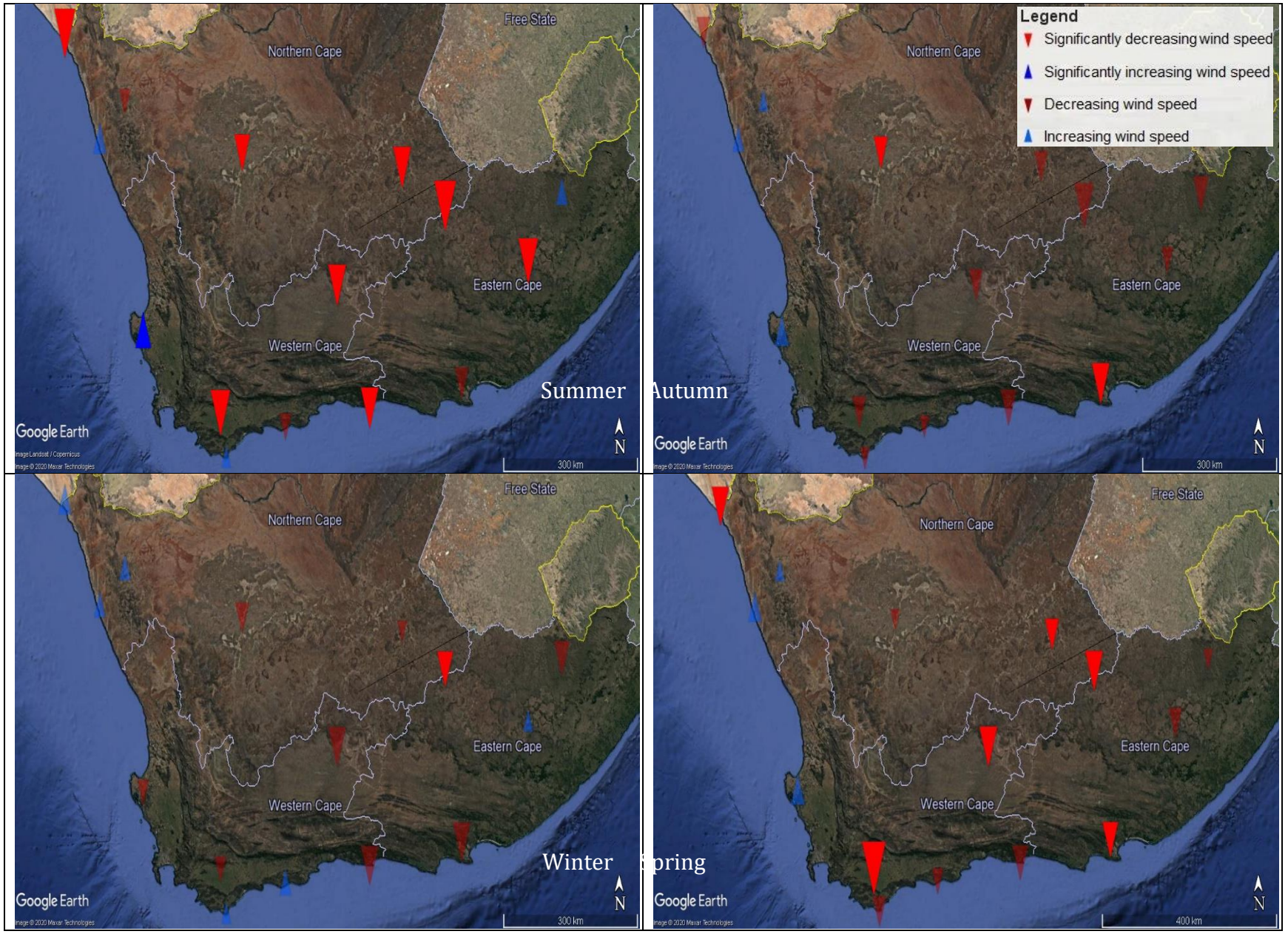


Figure 3.5: Mean seasonal wind speed trends per year (1995–2018) & Cape Agulhas series (1950–2018), statistical significance is considered at a threshold of P<0.1.

Table 3.4: Monthly station Sen's slope wind speed trend (%) per year (1995–2018).

	Jan	Feb	Mar	Apr	May	Jun	Jul	Aug	Sep	Oct	Nov	Dec
Alexander Bay	**–0.73%**	–0.40%	–0.56%	**0.55%**	–0.19%	0.29%	0.08%	–0.01%	0.07%	–0.44%	**–0.49%**	–0.73%
Beaufort West	–0.30%	–0.29%	–0.19%	–0.24%	–0.10%	0.61%	–0.76%	–0.51%	–0.21%	–0.50%	–0.12%	–0.18%
Brandvlei	–0.29%	–0.29%	–0.18%	–0.60%	–0.09%	0.28%	–0.35%	–0.36%	–0.44%	0.25%	0.00%	0.03%
Cape Agulhas[9]	0.00%	0.11%	0.02%	–0.01%	0.00%	–0.09%	0.04%	0.12%	–0.13%	–0.18%	–0.06%	–0.04%
Cape Agulhas	**–0.40%**	–0.22%	–0.55%	0.16%	0.13%	0.12%	–0.55%	–0.43%	–0.61%	–0.75%	–0.87%	**–0.89%**
De Aar	–0.43%	**–0.53%**	–0.27%	–0.24%	–0.21%	0.18%	–0.30%	0.02%	–0.25%	**–0.36%**	–0.03%	–0.06%
Elliot	0.00%	0.43%	0.61%	0.19%	–0.01%	0.50%	–0.83%	–0.37%	0.01%	–0.31%	0.01%	0.00%
Koingnaas	–0.05%	0.24%	–0.11%	**0.67%**	–0.26%	–0.11%	–0.06%	0.29%	0.46%	–0.08%	0.16%	0.14%
Langebaan	0.33%	0.23%	0.27%	0.35%	–0.25%	0.39%	–0.46%	0.22%	0.04%	0.05%	0.35%	0.36%
Noupoort	**–0.73%**	**–0.78%**	–0.64%	–0.52%	–0.41%	0.06%	–0.87%	–0.08%	–0.66%	–0.57%	–0.22%	–0.08%
Plettenberg Bay	–0.16%	–0.33%	–0.27%	–0.20%	**–0.71%**	–0.07%	**–0.61%**	–0.47%	–0.21%	**–0.53%**	–0.13%	–0.42%
Queenstown[10]	–0.76%	–0.55%	–0.44%	–0.29%	0.56%	1.37%	–0.65%	0.54%	–0.36%	–0.41%	0.07%	–0.16%
Springbok	0.11%	0.09%	–0.02%	0.33%	–0.33%	0.27%	–0.29%	0.24%	–0.03%	–0.09%	0.34%	–0.04%
Still bay	0.08%	–0.16%	–0.11%	0.47%	–0.05%	0.55%	–0.12%	–0.23%	–0.16%	–0.04%	–0.13%	–0.15%
Tygerhoek	–0.10%	–0.39%	–0.16%	0.25%	0.13%	1.05%	–0.63%	–0.50%	–0.61%	–0.54%	–0.42%	–0.41%
Uitenhage	–0.05%	–0.16%	–0.20%	–0.22%	**–0.98%**	0.36%	–0.61%	**–0.74%**	–0.15%	–0.19%	**–0.56%**	**–0.50%**
Mean of stations	–0.15%	–0.11%	–0.14%	0.09%	–0.16%	0.41%	–0.29%	–0.17%	–0.16%	–0.32%	–0.09%	–0.12%
Eastern Cape	–0.30%	–0.18%	0.06%	–0.12%	–0.40%	0.45%	–0.90%	–0.40%	–0.18%	**–0.44%**	–0.32%	–0.34%
Northern Cape	**–0.34%**	–0.28%	–0.28%	0.17%	–0.31%	0.14%	–0.33%	–0.02%	–0.14%	–0.19%	–0.10%	–0.17%
Western Cape	–0.06%	–0.14%	–0.22%	0.15%	–0.14%	0.49%	–0.50%	–0.31%	–0.25%	–0.42%	–0.30%	–0.27%
Coastal	–0.32%	–0.17%	–0.32%	0.27%	–0.18%	0.34%	–0.25%	–0.14%	–0.01%	**–0.38%**	**–0.32%**	–0.33%
Hinterland	0.13%	–0.04%	–0.03%	0.15%	–0.32%	0.43%	–0.62%	–0.38%	–0.19%	–0.32%	–0.13%	–0.13%
Inland	–0.21%	–0.18%	–0.03%	0.00%	–0.12%	0.46%	–0.34%	–0.12%	–0.22%	–0.18%	0.09%	0.04%
EC Hinterland	–0.05%	–0.16%	–0.20%	–0.22%	**–0.98%**	0.36%	–0.61%	**–0.74%**	–0.15%	–0.19%	**–0.56%**	–0.50%
EC Inland	**–0.45%**	–0.26%	0.14%	–0.10%	–0.28%	0.70%	–0.76%	–0.28%	–0.31%	**–0.55%**	–0.15%	–0.19%
NC Coastal	–0.35%	–0.07%	–0.24%	**0.60%**	–0.26%	0.07%	0.04%	0.15%	0.31%	–0.26%	–0.19%	**–0.30%**
NC Inland	–0.34%	**–0.34%**	–0.25%	–0.22%	–0.28%	0.24%	–0.39%	–0.08%	–0.35%	–0.16%	–0.03%	–0.04%
WC Coastal	–0.04%	–0.28%	–0.17%	0.00%	–0.43%	0.26%	–0.36%	–0.36%	–0.12%	–0.28%	–0.11%	–0.18%
WC Hinterland	0.00%	0.00%	–0.17%	0.25%	0.07%	0.39%	–0.47%	–0.32%	–0.35%	–0.43%	–0.36%	–0.42%
WC Inland	–0.30%	–0.29%	–0.19%	–0.24%	–0.10%	0.61%	–0.76%	–0.51%	–0.21%	–0.50%	–0.12%	–0.18%

Bold underline denotes a statistical MK significance of 99% (P<0.01)
Bold denotes a statistical MK significance of 95% (P<0.05)
Underline denotes a statistical MK significance of 90% (P<0.1)

[9] *Cape Agulhas series (1950 – 2018)*
[10] *Queenstown series (1995 – 2014)*

3.4.3 Multi-temporal wind speed trends

Annual wind speed series demonstrate multiple inter–annual, and decadal trends. It is thus essential to assess, and quantify the time–series at varying timeframes. A CWT is applied to identify dominant wind speed cycles since the wavelet plots (scalogram) visually present wind speed frequency, and strength over time. The cycles identified are of further importance to Chapter 5 where the climatic drivers are identified, and strength connection are quantified.

The scalograms generated by a CWT are a powerful representation of a data series harmonics which allow for a multi-temporal analysis. They are comprised of a vertical logarithmic axis indicating the cycle duration (years) while the horizontal axis identifies the temporal domain when the cycle occurred (year). Importantly, the signal observed at the top of the graphic is a detailed high–resolution scale considering two consecutive data points while a decadal view at the bottom is based at a scale of one-fourth of the complete series.

The cone of influence (U–shaped area) indicates the temporal boundary where the effects of frequencies are present. The colour shading indicates the signal strength quantified as the squared correlation with the mother wavelet. In the case of this study, the mother wavelet is based on Morlet (wavenumber 6) as it most accurately interprets wind speed data frequencies (Grossman & Morlet, 1984). Periods which record strong wavelet power are of most interest given that they indicate how long, and when cyclic behaviour occurred. These periods were then subjected to Sen's slope, and MK statistical methods to quantify the strength, and statistical significance of trends.

The resulting wind speed series wavelet plots, and Sen's slope trend statistics are presented, and further discussed in the sections to follow (Figure 3.6, Figure 3.7, and Figure 3.8). In Figure 3.8, where two dashed blue or two dashed red lines exist, both the upper, and lower 95th percentile indicate the same station trend direction (increasing or decreasing). While most stations upper, and lower 95th percentiles indicate a probability of increasing or decreasing trends, Alexander Bay, Beaufort West, and Uitenhage all indicate ubiquitously decreasing wind speed trends, and Langebaan is the only station indicating ubiquitously increasing wind speed trends.

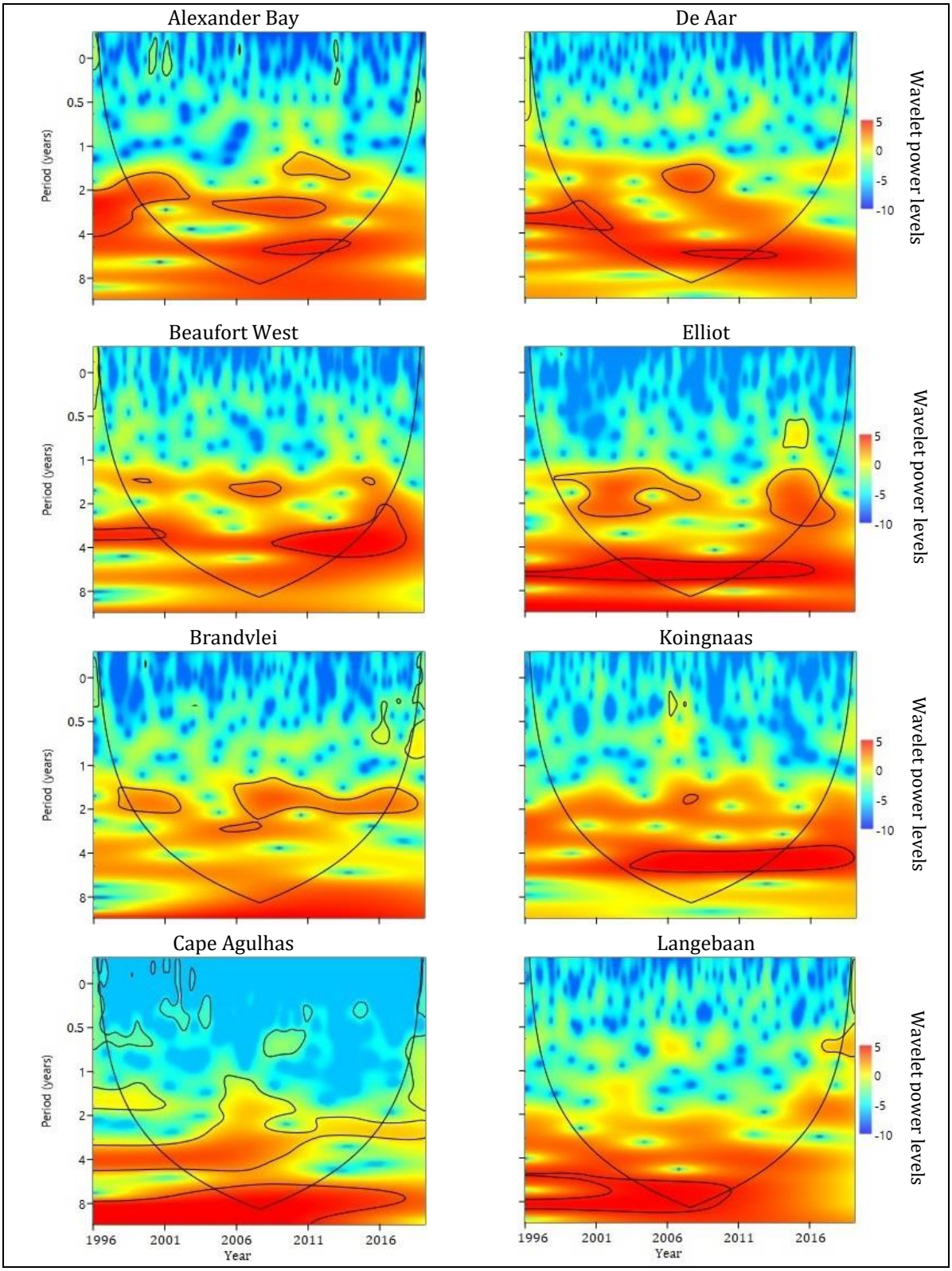


Figure 3.6: Station continuous wavelet transform plots (lag–1) applying a 12–month Gaussian filter to the wind speed series between 1995–2018. The shaded scale indicates the wavelet power scaled from lowest to highest. The black boundary defines periods of statistical significance (P<0.05), and the cone of influence is within the U–shaped area.

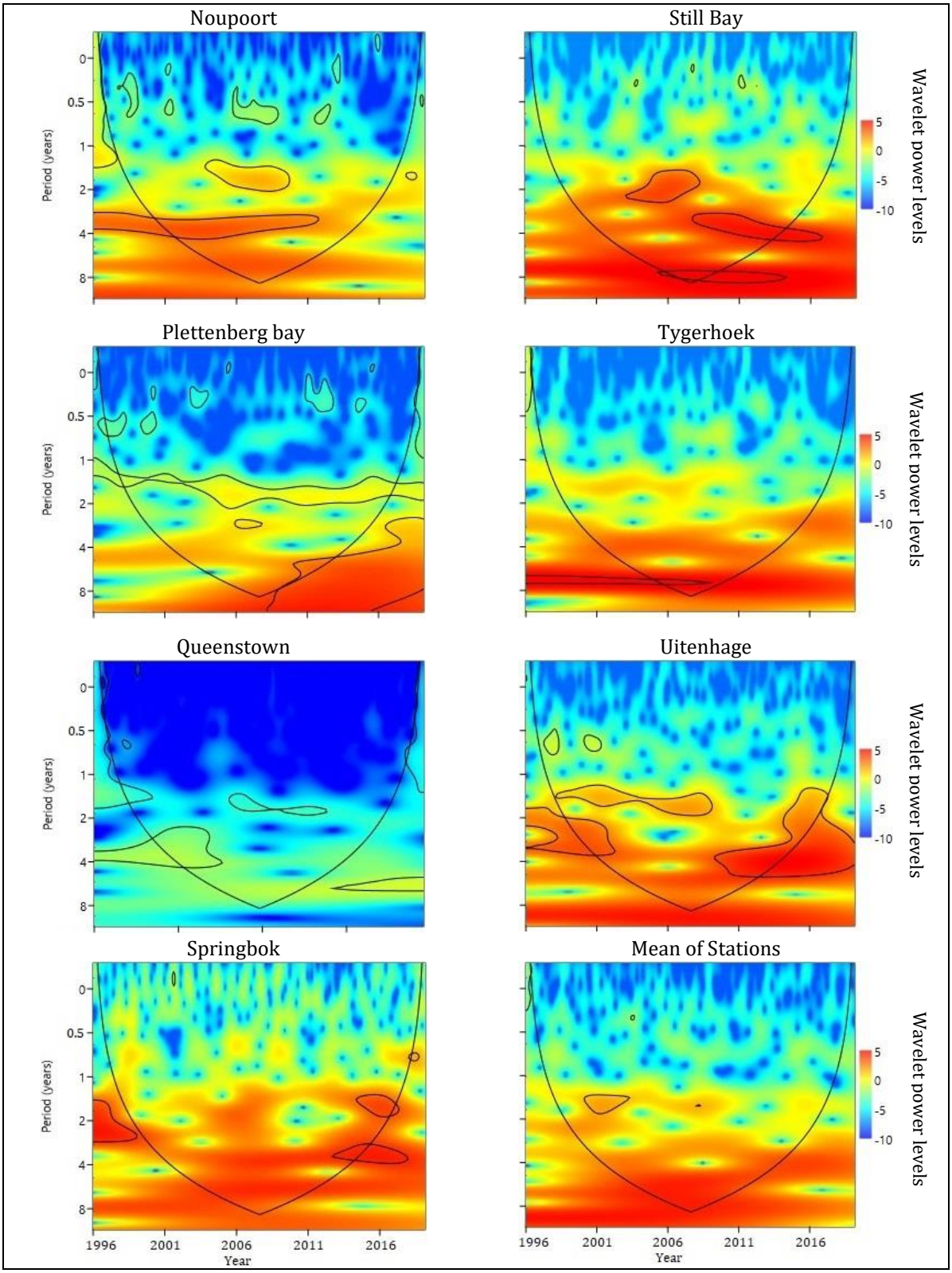


Figure 3.7: Station continuous wavelet transform plots (lag–1) applying a 12–month Gaussian filter to the wind speed series between 1995–2018. The shaded scale indicates the wavelet power scaled from lowest to highest. The black boundary defines periods of statistical significance (P<0.05), and the cone of influence is within the U–shaped area.

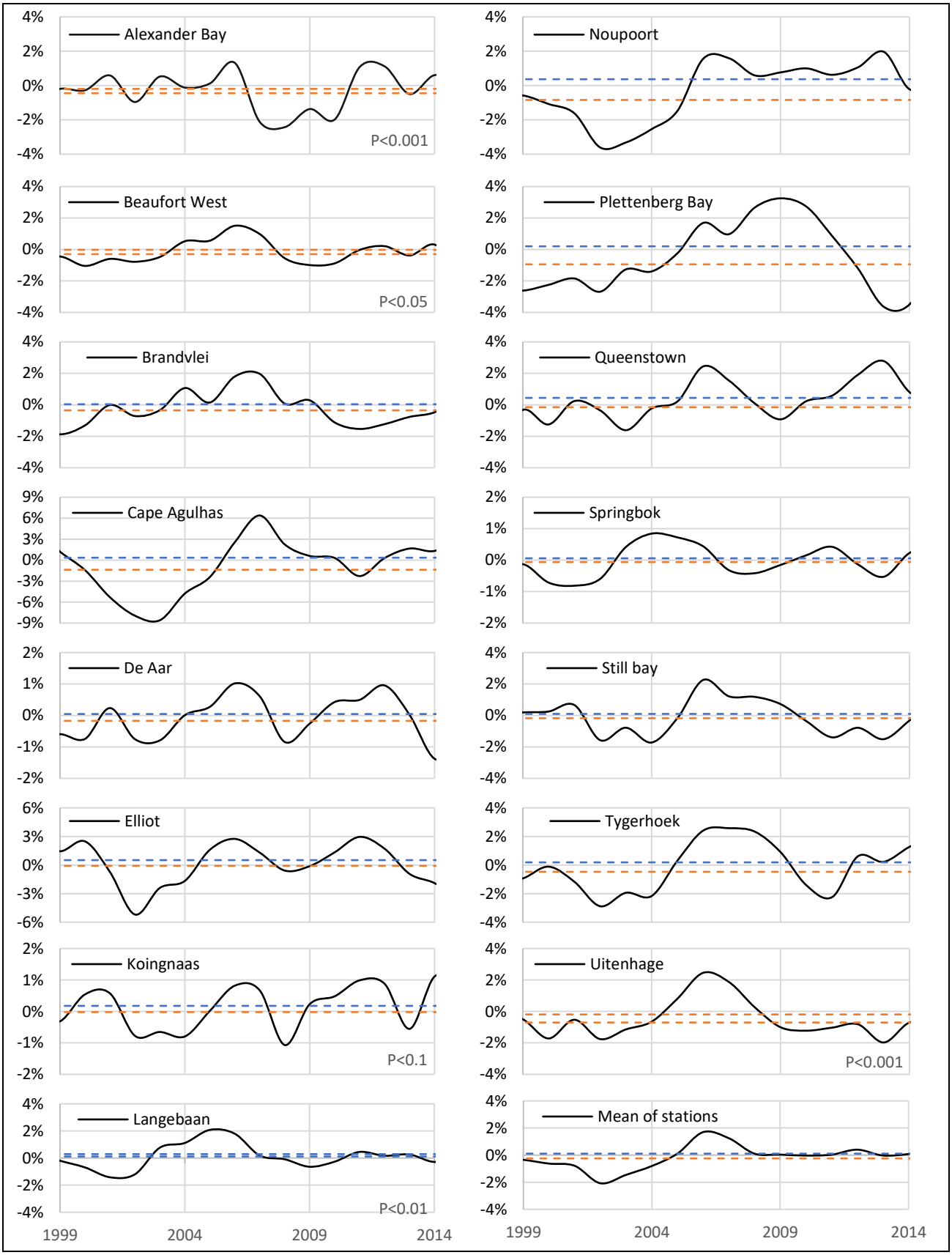


Figure 3.8: Inter–annual 48 month Gaussian filtered wind speed trends (1995–2018). Y-axis presents observed Sen's slope statistic as a percent (%) per year. The MK test was performed on each series with the dashed lines indicating the upper, and lower 95% statistical significance levels (red: decreasing trend; blue: increasing trend).

3.4.3.1 Station periodicities 1995–2018

Mean monthly wind speed data were standardised, and tested for serial correlation (SC). All results indicate a white noise series while none indicate the presence of SC. Applying a CWT to the unfiltered monthly wind series result in a dominant annual frequency. Considering the spectral density results, this would be expected. Notably, the mean annual data series period of 24 records is insufficient to apply a CWT. To overcome this limitation, and observe longer-term frequencies, mean monthly wind data were smoothed by applying a 12–month Gaussian filter to generate a red–noise series (lag 1). The resulting filtered monthly station series all indicate strong SC (mean r of 0.931). A CWT was performed on the 12-month filtered wind speed series, and MK testing applied to verify statistical significant ($P<0.1$) trend cycles present within the series (Figure 3.6a, b). Several multi-temporal trends are identified with cycles ranging 1–2 years, 2–4 years, and 4–8 years, as drawn from CWT plots provided in Table 3.5.

The mean wind speed series demonstrates a statistically significant ($P<0.05$) negative inter–annual wind speed trend (–0.19% per year, –0.006 m/s/year) between 1996, and 2017, however, this is only significant until 2010 considering a 2–4-year cycle. Langebaan is the only station with a statistically significant ($P<0.1$) increasing (0.13% per year, 0.007 m/s/year) inter–annual wind speed cycle, present throughout the series. Additionally, Langebaan is the only station where increasing wind speeds are present at all three temporal periods examined. Inversely, ubiquitous decreasing trends are identified in the series of Alexander Bay, Cape Agulhas, and Uitenhage (Table 3.5). Notably, 89% of statistically significant ($P<0,1$) 1–2-year wind speed cycle trends are decreasing but 77% of 4–8-year cycles are increasing. When applying an 8–year cycle, the mean annual series exhibits a statistically significant ($P<0.1$) increasing wind speed trend (0.36% per year, 0.011 m/s/year) between 2006, and 2013. Contributing to the mean are ten stations where statistically significant ($P<0.1$) increasing (mean 0.33% per year, 0.012 m/s/year) wind speed cycles are observed over time windows of 4–8 years between 1999, and 2014. During the same cycle time windows, three stations (Alexander Bay, Cape Agulhas, and Uitenhage) indicate statistically significant ($P<0.1$) decreasing (mean –0.33% per year, –0.022 m/s/year) wind speed cycles (Table 3.5).

Table 3.5: Station inter-annual cycle period lengths, and dates (at 10% statistical significance level) for continuous cycles lasting at least two periods when applying a continuous wavelet analysis between 1995–2018 (red: decreasing trend; blue: increasing trend).

Station	Period: Years (p<0.1)		
	1–2	2–4	4–8
Alexander Bay	1996–2017	1997–2016	1999–2014
Beaufort West	1996–2017	1997–2016	2002–2011
Brandvlei	2007–2017		2001–2012
Cape Agulhas	1997 –2014	1997–2009	1999–2014
De Aar	1996–2017	–	–
Elliot	–	–	–
Koingnaas	–	1997–2016	2007–2014
Langebaan	1996–2017	1997–2016	1999–2014
Noupoort	1996–2017	–	2007–2014
Plettenberg Bay	1996–2017	–	2005–2014
Queenstown	–	–	1999–2014
Springbok	–	–	1999–2014
Still bay	–	–	2002–2013
Tygerhoek	–	–	2002–2014
Uitenhage	1996–2017	1997–2016	1999–2014
Mean of stations	1996–2017	1997–2010	2006–2013

3.4.3.2 Cape Agulhas periodicities 1950–2018

The standardised Cape Agulhas mean annual, seasonal, and monthly wind speed series were tested for SC. The resulting statistics indicate a weak mean annual SC of 0.387, ranging from SC = 0.192 (November) to SC = 0.706. Considering this, it was concluded the absence of SC justified the application of a lag–0 white noise model. A CWT was performed on each series based on the identified cycles, and MK testing applied to quantify significance (P<0.1). The resulting wind speed series wavelet plots, and Sen's slope trend statistic are presented in Figure 3.11, Figure 3.9, and Figure 3.10. Several multi-temporal trends are identified from each series of CWT plots with cycles ranging 4–8 years, 8–16 years, and 16–32 years as detailed in Table 3.6. Assessing 4–8-year cycles of the annual, seasonal, and monthly wind speed series, July (2.15% per year, 0.059 m/s/year), and November (–3.34% per year, –0.182 m/s/year) are the only two months with statistically significant (P<0.001) trends. July indicates an increasing trend between 1959, and 1972, while a decreasing trend is observed for the November series between 1973, and 1984. These two monthly records are the strongest increasing, and decreasing trends recorded at all temporal scales. At a scale of 8–

16 years, February, and March are the only two monthly series where no statistically significant (P>0.1) wind speed trends are present, while 25% of monthly series portray statistically significant (p<0.01) increasing trends (0.78% per year, 0.034 m/s/year), and 58% are decreasing trends (–0.83% per year, –0.039 m/s/year). When the scale is increased to 16–32 years, July is the only series where no statistically significant (P>0.1) wind speed trends are observed, while significantly (P<0.05) increasing trends are identified in 50% of the monthly series (0.8% per year, 0.039 m/s/year), and 42% are decreasing (–0.81% per year, –0.036 m/s/year).

At an 8–16 year scale, the mean annual Cape Agulhas wind speed series presents evidence of an 8–12-year cycle between 1978, and 2008. MK trend tests for this period proved statistically significant (P<0.001), indicating an increasing mean wind speed (0.47% per year, 0.017 m/s/year). Similarly, the Autumn series also presents a statistically significant (P<0.01) increasing trend (1.76% per year, 0.076 m/s/year) between 1983, and 1999. Statistically significant (P<0.001) decreasing wind speed trends are present for summer (–0.96% per year, –0.048 m/s/year), and winter (–1.71% per year, –0.071 m/s/year) series. Spring is the only season where all trends are statistically non-significant (P>0.1), even though statistically significant (P<0.05) cycles are present in the wavelet plots (Figure 3.9, Figure 3.11). At a 16–32-year scale, significant (P<0.05) cycles are present for annual, summer, autumn, winter, and spring series, although only autumn (–0.83% per year, –0.036 m/s/year), and winter (–0.58% per year, –0.024 m/s/year) indicates statistically significant (P<0.001) wind speed trends (Figure 3.9, Figure 3.11). The mean annual Cape Agulhas series (1950–2018) underwent a multi-decadal (10–60 years) assessment, and data were subjected to the same statistical methodology (Sen's slope, and MK) as described earlier (Figure 3.12). All six decadal scales proved statistically significant (P<0.05). The 10–year (–0.18% per year, –0.009 m/s/year), 20–year (–0.23% per year, –0.011 m/s/year), 30–year (–0.28% per year, –0.013 m/s/year), 40–year, and 50–year (–0.17% per year, –0.008 m/s/year) series all portray decreasing wind speed trends. In contrast, the 60–year decadal scale is the only series which portrays a statistically significant (P<0.001) increasing (0.18% per year, 0.009 m/s/year) wind speed trend (Figure 3.12).

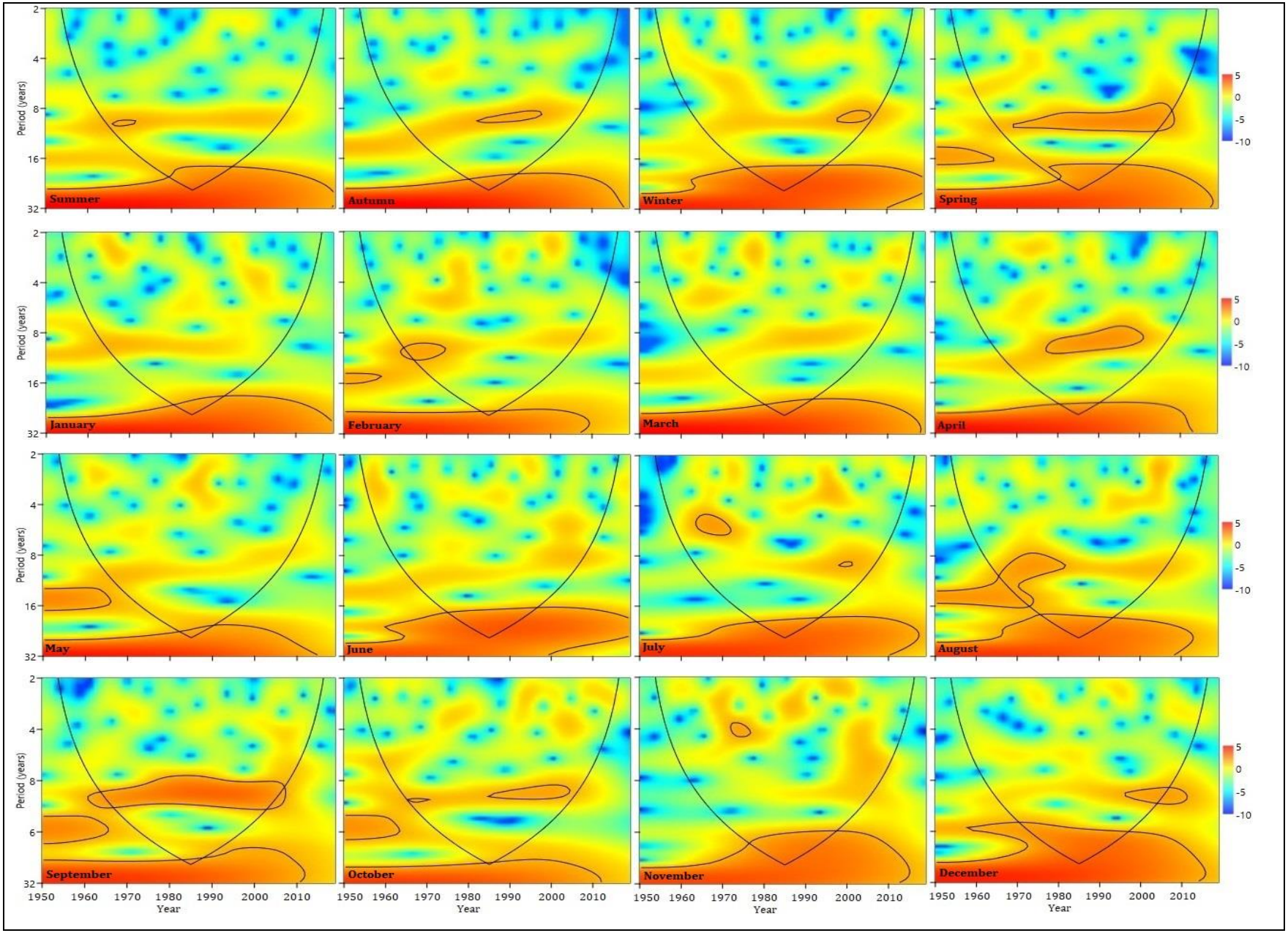


Figure 3.9: Monthly, and seasonal continuous wavelet transform plots (lag–0) for the Cape Agulhas station applying a mean annual filter to the wind speed series between 1950–2018. The shaded scale indicates the wavelet power scaled from lowest to highest. The black boundary defines periods of statistical significance (P<0.05), and the cone of influence is within the U–shaped area.

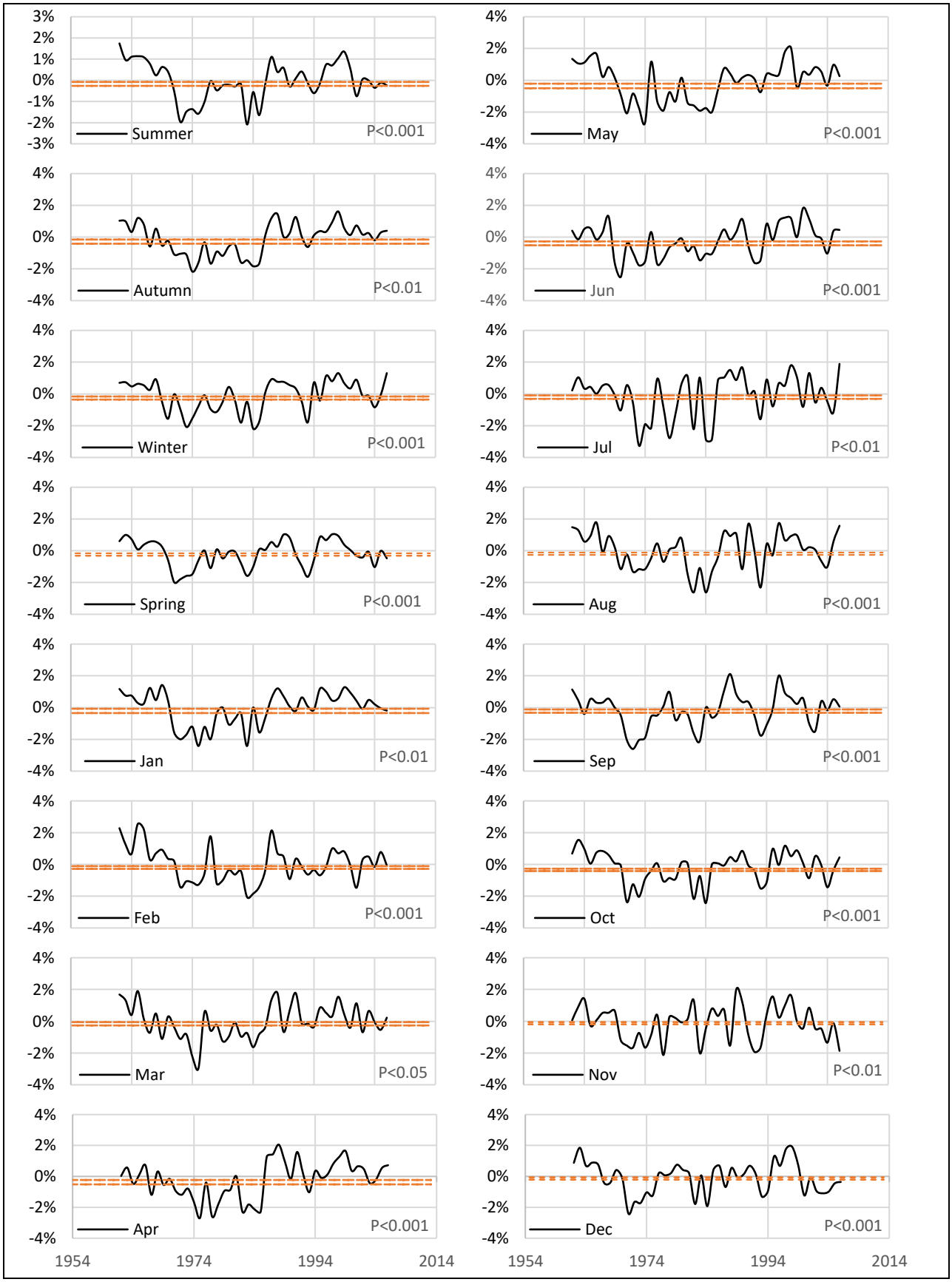


Figure 3.10: Monthly, and seasonal wind speed trend (24–year Gaussian filtered) of the Cape Agulhas station between 1950–2018. Y-axis presents observed Sen's slope statistic as a percent (%) per year. The MK test was performed on each series with the dashed lines indicating the upper, and lower 95% statistical significance levels (red: decreasing trend; blue: increasing trend).

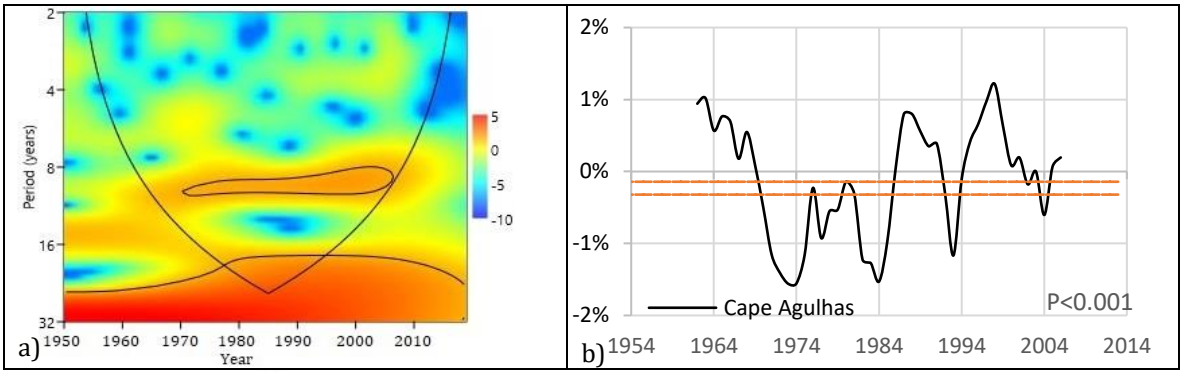


Figure 3.11: Cape Agulhas station mean annual a) CWT plot (lag–0) for the period 1950–2018. The shaded scale indicates the wavelet power scaled from lowest to highest. The black boundary defines periods of statistical significance (P<0.05), and the cone of influence is within the U–shaped area. b) 24–year Gaussian filtered wind speed trend between 1950–2018. Y-axis presents observed Sen's slope statistic as a percent (%) per year. The MK test was performed with the dashed lines indicating the upper, and lower 95% statistical significance levels (red: decreasing trend; blue: increasing trend).

Table 3.6: Seasonal, and monthly Cape Agulhas cycle period lengths, and dates (at 10% statistical significance level) for continuous cycles lasting at least two periods when applying a continuous wavelet analysis between 1950–2018 (red: decreasing trend; blue: increasing trend).

Period	**Period: Years (p<0.05)**		
	4–8	8–16	16–32
Annual		1978–2008	
Summer		1993–2011	
Autumn		1984–1999	1963–1998
Winter		1997–2009	1963–1998
Spring			
January		1978–2009	1963–1998
February			1980–1996
March			1967–1996
April		1984–2009	1961–1998
May		1987–2008	1964–1998
June		1971–2009	1962–1998
July	1958– 1972	1992–2011	
August		1964–1991	1981–2004
September		1966–2009	1977–1996
October		1963–2002	1980–1996
November	1973–1984	1990–2012	1974–1997
December		1990–2010	1974–2000

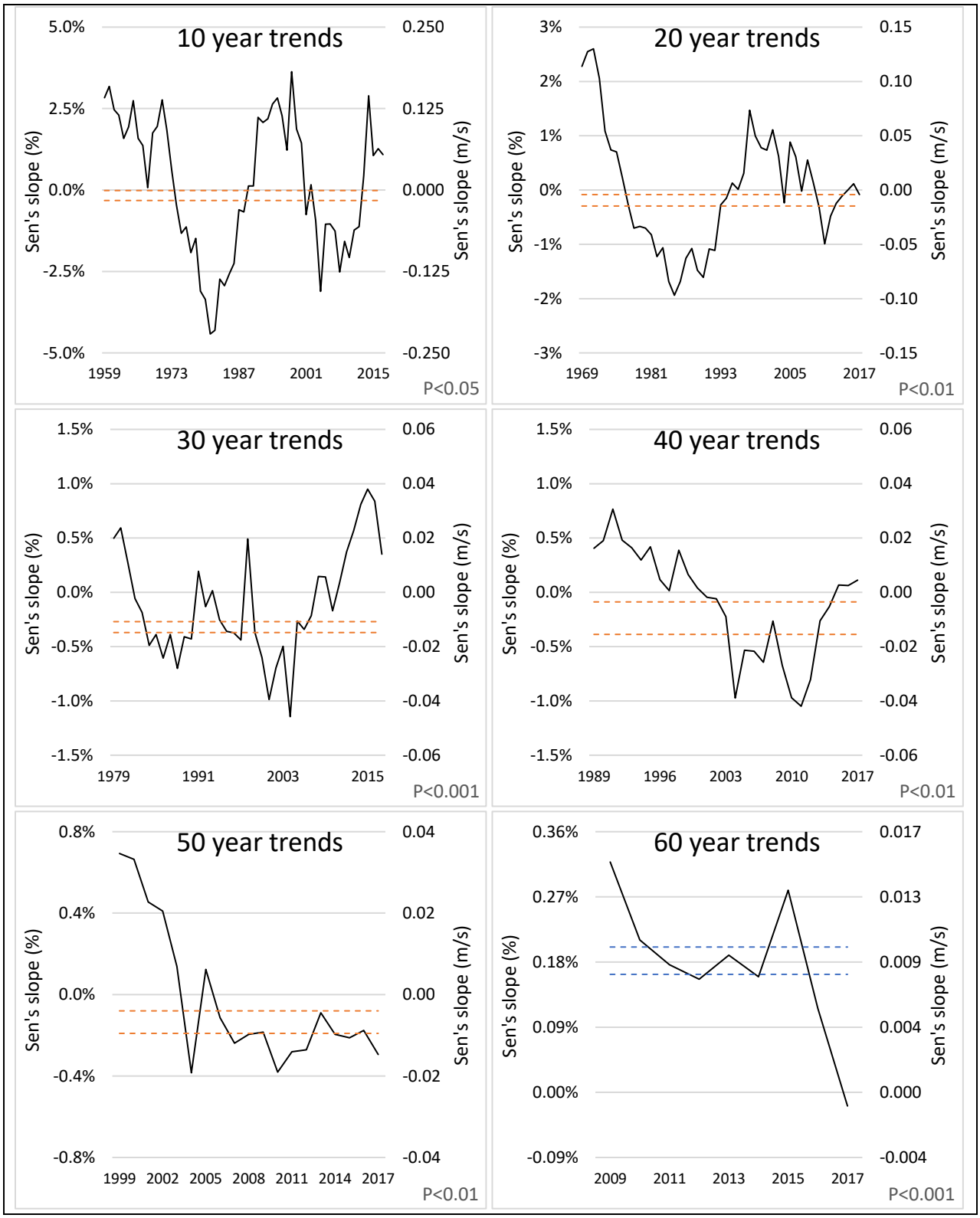


Figure 3.12: Multi–decadal trend analysis for annual wind speed at the Cape Agulhas station, ranging 1–6 decades over the period 1950–2018. Y-axis presents observed Sen's slope statistic in percent (%) per year, and m/s/year. The MK test was performed on each decadal record with the dashed lines indicating the upper, and lower 95% statistical significance level (red-dashed line: decreasing trend; blue-dashed line: increasing trend).

3.5 Discussion

This section addresses the first objective of this thesis, which is to quantify observed wind speed trends within the study region. Station series required a minimum period of 20 years, and trends were assessed on several temporal scales, as listed below:

- Annual (mean annual);
- Seasonal (summer, autumn, winter, and spring mean seasonal);
- Monthly (January to December monthly means);
- Multi–temporal (periodic trends); and
- Multi–decadal (10–year periods).

This chapter presents the most comprehensive wind speed trend analysis for South Africa to date by considering 15 stations, one of which has the longest wind speed record for Africa. The advantage of using 15 multi-decadal anemometer recorded wind speed series (20–68 years) is that it permits a more robust assessment of wind speed trends, and cycles. Several authors have previously attempted to quantify wind speed trends in South Africa on shorter time series of generally below a decade (Hoffman, et al., 2011; Kruger, 2011; McVicar, et al., 2012; Argent, 2015; Fant, et al., 2016). The temporal periods were previously insufficient to provide reliable insight to wind speed trends in South Africa.

It is necessary to differentiate these chapter findings from those objectives of the WASA programme, which is the primary catalysis of wind climatology research in South Africa over the past decade. The project consists of several work packages with the primary aims, and objectives to model wind speed for the purpose of wind power generation. A key differentiator is that the WASA programme, only being a decade long, is unable to assess multi-decadal scale wind speed trends. To date, the work group focus has been concerned with the assessment of macro, and micro scale wind speed. The macro–scale WASA wind modelling project utilized reanalysis wind data to extrapolate measured data, and create the verified numeric wind atlas. Where the micro–scale wind modelling objective quantifies wind speed to determine the mean annual wind speed for wind power feasibility assessment. The programme presents the station recorded wind speeds on mean daily, monthly, and seasonal

temporal scales. WASA is also concerned with extreme wind speeds, and the associated mapping of the extreme wind climate of South Africa (WASA, 2015).

Methodologies applied to the wind speed series in this research chapter include nonparametric (Sen's slope, and MK), and spectral density techniques (CWT). It can be pointed out that all previous attempts to quantify wind speed trends have applied linear trend methodologies. There is an inherent flaw in this approach which may result in the presentation of significant trends which are statistically induced. This is the first-time wind speed trends of South Africa are being assessed by applying the above-defined methodologies, which greatly improves the statistical accuracy of results. Additionally, multi-temporal trends have never previously been considered, and the application of the advanced statistical CWT methodology is similarly presented for the first time in the case of South African wind speed cyclic trends.

Long term (1950 - 2018) wind speed trends proved statistically non-significant, while more recent (1995 - 2018) mean wind speed trends proved statistically significant ($P<0.05$). The magnitude of observed decreasing wind speed trends are marginal, and such variance is of limited concern. This adds confidence to the justification by the South African government to procure additional electricity generated by wind power. This section identified some works which utilised below 10 years of wind data. These statistics should be interpreted with caution given the temporal period is insufficient to obtain scientifically sound results.

3.5.1 Annual wind speed trends

This research confirms that long term mean annual near-surface wind speed trends (Sen's slope) are non-significantly ($P>0.1$) declining by -0.06% per annum (–0.003 m/s/year) between 1950, and 2018. Where recent (1995 - 2018) wind speed trends are significantly ($P<0.05$) decreasing (-0.14% per year; -0.005 m/s/year). This result is in close agreement to regionally reported stilling trends as presented in section 3.1, specifically those located in other subtropical latitudes post-1980. Both increasing, and decreasing wind speed trends have been recorded across Africa in the last 65 years. For instance, Tanzania records the

largest increasing trend of 0.065 m/s/year, while Cameroon records the largest decreasing trend of -0.2 m/s/ year (Tchinda, et al., 2000; Kainkwa, 2010).

The strongest wind speed percentage decrease is identified in the EC Hinterland region (–0.28% per year; –0.009 m/s/year), followed by the Western Cape (–0.22% per year,–0.008 m/s/year), and coastal region (-0.21% per year; -0.009 m/s/year). These decreases equate to a reduction in available energy over a 20-year PPA period of 2.12%, 1.06%, and 0.93%, respectively. Considering wind energy forecasts typically apply a 6% long term wind forecast uncertainty, the decreases do not pose a significant risk to wind power generation in the study region.

Extensive international literature has been published, which seeks to elucidate wind speed trends, and reasoning for recent stilling. Recent global circulation trends have recorded a poleward expansion of the Hadley cell which has been linked to this global wind speed stilling phenomenon, mostly present in the mid–latitudes (Azorin-Molina, et al., 2018). In the case of South Africa, located between the latitudes of 28°–35°S, it has been specifically influenced due to its location between tropical, and subtropical regions which are dominated by subtropical high–pressure trade winds (Lu, et al., 2007; Roderick, et al., 2007; Vautard, et al., 2010; McVicar, et al., 2012; Azorin-Molina, et al., 2018). In the context of South African wind speed trends, Hoffman (2011) reported a mean decrease of more than 25% (-0.8% p.a.) of wind run over 31 years (1974 to 2005) in the WC. Based on this study, a decrease of -6.82% (-0.22% p.a) is indicated over the same 31–year period. Hoffman's research is based on station data series at a 2m elevation. Due to the magnitude of decrease, global climate modes are unlikely to be primary drivers of such wind speed decrease. It is hypothesised that the wind speed decrease is a result of increased regional surface roughness from vegetation growth in the vicinity of the stations over the study period.

3.5.2 Monthly, and seasonal wind speed trends

Similar to the annual wind speed trends, both positive, and negative significant trends are identified in the seasonal, and monthly wind speeds over the study area. The application of Sen's slope analysis indicates a mean decreasing wind speed tendency for all seasons during

the study period. At a mean monthly scale, April, and June are the only months which indicate increasing mean wind speed trends, and ubiquitously decreasing mean wind speeds prevail for all other months. It can be noted that only spring (-0.18% per year; -0.007 m/s/year), and October (–0.32%, –0.013 m/s/year) proved significant ($P<0.05$). Over the same study period, significant ($P<0.1$) increasing wind speed trends are identified during certain periods in the Langebaan (January, and summer), Koingnaas (April, and September), and Springbok (September) wind speed series.

Winter (June - August) is the only season which does not indicate any significant wind speed trends assessed at a regional scale. All regions (coastal, hinterland, and inland) indicate significantly ($P<0.1$) decreasing mean wind speed trends of -0.26%, -0.23%, and -0.11% per year respectively. It should be noted that strongest trends occur at coastal stations. The strongest decreasing wind speed trend (-0.40% per year) is identified in the EC hinterland series. The coastal regions of the NC, and WC are the only areas which did not record any significant ($P>0.1$) mean seasonal wind speed trends, with only April (0.6%), and August (-0.36%) respectively indicating significant ($P<0.05$, and $P<0.1$) trends. Similar seasonality is identified at stations in the northern hemisphere subtropics, with weakening wind speed trends in autumn, and winter (September to February), and increasing in spring, and summer (March to August) (Rauthe & Paeth, 2004).

3.5.3 Multi-temporal wind speed trends

Although not all annual series exhibit significant annual trends over the full recording period, a multi-temporal trend assessment identifies some statistically significant ($P<0.1$) trends which are not identified if the cyclic nature of wind were not considered. This extended trend analysis required at least two consecutive periods to be considered valid, and identified several significant trends. The majority (89.89%) of statistically significant ($p<0.1$) inter-annual (1–2 year) trends between 1996, and 2017 are decreasing, while inversely, at a 4–8-year scale, 76.92% of station trends are increasing between 1999, and 2014.

The Cape Agulhas station also indicates an increasing multi-temporal wind speed trend at an 8–16-year scale between 1978, and 1998. The long–term monthly trends of the Cape Agulhas

station indicats decreasing wind speed trends in the latter half of the year (June–December) at an 8–16-year scale, approximately between 1970, and 2010. The same months indicate statistically significant ($P<0.1$) increasing wind speed trends when assessed at a 16–32-year scale. The Cape Agulhas station was also filtered at a decadal scale (1–6 decades), all proving statistically significant ($P<0.05$). All trends are decreasing except the 60–year wind speed trend with a significantly ($P<0.001$) increasing wind speed. These findings highlight the importance to consider wind speed trends at a multi-temporal scale as periods of extreme high/low wind speed strongly influence trend results.

3.5.4 Limitations

The identification, and assessment of uncertainty is an essential aspect to consider. In this respect, it cannot be discounted that the observed wind speed trends are indeed a misrepresentation of the actual climate trends. Factors such as instrument type, anemometer degradation, anthropogenic obstructions, and tree growth may be affecting near-surface wind speed series at the stations considered.

The reader is further referred to section 2.4 where additional data limitations have been identified. These include the fact that there are inherent uncertainty, and accuracy concerns related to the SAWS wind speed series which are unavoidable. Further, given the temporal span of the series, instrument, and station changes are inevitable. Changes in this regard have been considered as far as possible by reviewing the documented maintenance records. However, it cannot be discounted that undocumented maintenance events have been overlooked.

3.6 Recommendation for future research

In light of the findings, and assessment presented in this chapter, there are several spheres which warrant further research. There is extensive ongoing research concerning the WASA programme, and once long-term (20+ years) data are available, it is highly recommended that verification of the identified regional wind speed trends be undertaken, specifically at hub height. This will eliminate current uncertainty which cannot be eliminated based on the

existing station data series. The WASA project has been performed according to international best practice, and the Masts importantly comply to IEC 64-100. This results in a lower measurement uncertainty, and higher accuracy. The incorporation of these data should continue to be included in future macro-scale wind models as longer-term time series become available.

During the past several years, there has been an extensive increase of South Africa's operational wind power fleet. To this end, an assessment of these operational wind power projects, and their associated long-term contribution to South Africa's power grid is warranted, so as to identify, and verify trends. These results can be paired with the findings of this PhD project, which may then further support the development of wind power in South Africa. Finally, to expand this study, it is recommended that future assessments include additional SAWS station data when data periods exceeding 20 years become available.

4 CHARACTERISING NEAR–SURFACE WIND SPEED, AND ELECTRICITY DEMAND PROFILE IN THE NORTHERN, WESTERN,, AND EASTERN CAPE PROVINCES OF SOUTH AFRICA

4.1 Introduction

As noted in Chapter 1, Section 1.2, this chapter builds on the previous seeking to quantify the diurnal, monthly, and seasonal wind speed profile at each of the 15 stations in the study regions. Of specific interest is the wind speed profile concerning electricity demand. Findings are presented in the sub–sections of:

- 4.3.1 Seasonal, and monthly wind speed profiles
- 4.3.2 Diurnal wind speed profiles

Reducing air pollution, and addressing global warming where adding sustainable electricity sources, requires a paradigm shift of current electricity generation methodologies. Wind energy is one of the leading renewable energy technologies, which fulfils this obligation due to its cost-effectiveness, and quick deployment. A recognized downside, however, is wind speed intermittency causing instantaneous electricity fluctuations (Archer & Jacobson, 2007; Collins, et al., 2018; Ren, et al., 2018). This unpredictability is the largest barrier to widespread integration of wind electricity generation (Awad, et al., 2017). One method of reducing wind-generated electricity intermittency is incorporating several wind facilities across a diverse geographical location. This chapter intends to evaluate the wind speed profiles recorded within the study area to detail observed diversity, and if certain regions should be prioritised for wind power generation.

In the context of South Africa, electricity supply security is an ongoing concern. The country is experiencing an electricity crisis given that the national electricity generator (Eskom) is unable to meet electricity demand (Eygelaar, et al., 2018). Extensive load shedding was implemented for the first time in 2008, and over a decade later, in 2020, this had become exponentially more frequent. This crisis developed over an extended period with reduced

electricity reserve margins, which resulted in the utility paying its high load customers to reduce their consumption during peak demand periods. The urgent need to deploy additional generation capacity resulted in wind-generated electricity procured through the REIPPP programme. The quick deployment, and ability to generate electricity during both day, and night served as an advantage over other technologies as recognized by the highest capacity (MW) allocation in the programme. The uptake of wind-generated electricity resulted in a renewed scientific interest in the country's wind speed, and electricity demand profiles. Several authors have sought to model the country's long–term security in electricity supply, with increased uptake of wind-generated electricity (Wright, et al., 2017; Sorensen, et al., 2018; Thopil, et al., 2018; Adefarati & Obikoya, 2019).

The value of this chapter is by providing the results which correlate station wind speed to Eskom's demand profile. These are of great value to identify which stations wind speed profiles may be better suited to support the power supply profile of Eskom. Unlike Eskom's traditional power generation fleet of nuclear, coal, and hydro power facilities which have highly predictable (and controllable) power output profiles, wind power facilities only generate power when the wind is blowing sufficiently (>3 m/s) to turn the blades. Currently, wind power is only procured on price, opposed to time of generation. While wind power may be the most cost-effective power source, if most of the power is generated during off-peak periods this creates two issues for Eskom. First, the need to store excess power generated when demand is low (or decrease generation from the Eskom fleet), and second, to source additional power during peak demand period if wind power is unable to generate sufficient power during these periods. It is in this respect that the siting of wind power projects should not only consider mean wind speed, but also power generation profile, and the ability to provide power when Eskom demand peaks.

This is not a new concept. For instance, Kahn (1979) published one of the first reports contemplating the benefits of dispersed wind-generated electricity generation by analysing availability, reliability, and generation profile. The theory is that the correlation of wind speed profile decreases with increasing horizontal distance due to terrain variability. Authors such as Archer, and Jacobson (2007) have extended research in this domain, demonstrating a

mean (max) wind-generated electricity reliability of 33% (47%) across 19 sites in the mid–western United States. Similarly, in an earlier paper across eight wind project locations in the central United States, they calculated a frequency of below 2% when none of the locations recorded sufficient wind speed (3 m/s) to generate electricity (Archer & Jacobson, 2003; 2004). Simonsen, and Stevens (2004) assessed an array of 28 wind farms in the central United States, and concluded that electricity reliability increased by a factor of between 175%, and 340%, depending on the number of facilities considered. Ernst, and Czisch (2001) modelled a hypothetical array of wind farms across northern Africa, and Europe, which could consistently support 70% of the entire European electricity demand. More recently, Shaner et al. (2018) quantified that distributed wind-generated electricity could, in principle, provide up to 80% of the United States' electricity requirements.

Diurnal, monthly, and seasonal wind speed profiles are an important variable which should be quantified, specifically with consideration of geographical dispersion (Mentis, et al., 2015; Fant, et al., 2016). There is extensive literature presenting regional wind characteristics, such as Ouammi et al. (2010) who assessed the wind speed profile of four sites in Liguria, Italy, to quantify mean monthly profile, and seasonality. The main finding is that the highest wind speeds occur during winter months, peaking in December. Li & Li (2005) investigated wind speed characteristic in Waterloo, Canada, and identified that the high wind season was during winter between November, and April, peaking in February. Additionally, stronger wind speeds are observed during the day, peaking at 2 pm, when the diurnal wind speed profile is considered. Al–Abbai (2005) assessed seven years of wind data from five sites in Saudi Arabia, and similarly identified that wind speeds peak in the afternoon. Boudia et al. (2012) assessed five years of wind data for Mecharia, Algeria, to determine the seasonal, and mean monthly wind speed profiles. They identified that Spring indicates the highest mean seasonal wind speed while the highest mean monthly wind speed occurs in April.

Aside from the international efforts to quantify wind speed profile, there are ongoing efforts to develop advanced modelling techniques. These include mean monthly, and diurnal wind speed variance when quantifying wind energy potential by considering electricity demand

(Xie, et al., 2017; Katinas, et al., 2018; MacLeod, et al., 2018; de Queiroz, et al., 2019; Liu, et al., 2019; Lledó, et al., 2019).

The literature review identified similar published research, which supports the aims of this chapter. Olaofe (2017) modelled the sensitivity of ocean winds, and local effects along the south, and west coasts of South Africa, considering five years of wind data in the context of load dispatch reliability. The methodology applied the Monin Obukhov similarity theory, and main findings revealed that highest nearshore wind speeds are observed in summer, and spring along the west coast, while it varied for the south coast (winter). Fant et al. (2016) examined wind resource reliability in southern Africa using MERRA satellite wind data. The source data are of a low resolution (1/2° by 2/3°) as the authors acknowledged where the results presented mean conditions but could misrepresent small–scale variability. An important finding is that there is poor potential to resolve the diurnal peak demand requirement by interconnecting facilities due to wind speed profile similarity. A primary recommendation of this research is further to perform the analysis by applying station recorded high–resolution wind speed data to quantify wind speed characteristics.

A further important point of investigation would be to improve knowledge on maximum gusts, changes in the patterns associated with cut-in, and cut-out speeds, analysis of the patterns, and temporal, and spatial structure, and changes of ramp events. To support this request additional text has been added to section 4.4.2 (Diurnal wind speed profile anomalies) assessing sub-daily wind speed ramp events, and the impact on the Eskom grid network. Further, the text below identifies supporting literature to complete the identified research gaps.

With respect to maximum gusts, and cut-in, and cut-out speeds, there is extensive published, and ongoing research assessing these wind speed characteristics. Such examples include Dalton et al. (2019; 2020a; 2020b) who investigate wind power variability during the passage of cold fronts across South Africa, and the associated implication on wind power generation. The authors investigate the passage of frontal activity at a 10-minute resolution, and the associated power generation variance, and maximum gusts. These authors generated a historic wind power time-series by applying variations to numeric weather prediction

reanalysis wind speed data. Ramp events were identified within the time-series, and the temporal, and spatial ramp statistics assessed. In addition, the driving forces of the ramp events were established, linking events to a set of atmospheric circulation archetypes. These studies conclude that mean power, and associated variability differ significantly, identifying that atmospheric circulation is the primary driving force of ramp events, specifically the phenomena of thermally propelled land-sea breeze interaction.

However, critical work in this sphere is the pioneering literature of Kruger (2010; 2011) who mapped high wind zones of South Africa as well as assessed the maximum 10-minute gusts. It is important to note that Kruger used the same SAWS wind station data set applied in this PhD thesis. Kruger et.al. (2013a; 2013b) further published an update of Kruger's original works, using updated SAWS station wind speed data. These authors revised the strong wind statistics, and refined the zones originally identified in the 2010 works, and further assessed the maximum gusts observed at stations at a three second-, and one-hour temporal scale identifying that most extreme wind events resulted from synoptic disturbance, and meso-scale climatic systems.

More recently Kruger et al. (2016), defined the national wind hazard profile of South Africa. The authors primary aims were to identify, and update the strong wind gust, and zones across the country using wind data of at least 10 years from 124 South African Weather Service stations. The results are presented on a municipal scale, considering 220 municipalities across South Africa. The results indicate a highly variable wind hazard both seasonally, and spatially across South Africa. The highest wind gusts occur in the southwestern Cape, extending to the eastern, and central Northern Cape, eastern coast of the Western Cape as well as the eastern interior of the Eastern Cape. The southern parts of the country indicate low wind gust variability at a seasonal scale, while the northern areas indicate a strong seasonal variance, with the highest risk during summer, and spring coinciding with increased convective activity. The gusting is assessed in m/s, and uses the same wind data assessed in this PhD.

Building from these earlier studies which were primarily only concerned with wind gusting, recent research has included the impact on wind power generation, and the Eskom grid

(Joubert, 2017; Sorensen, et al., 2018; Mararakanye & Bekker, 2019b; Mararakanye & Bekker, 2019a). Joubert (2017) completed a PhD assessing the geographical dispersion of wind, and solar power in South Africa considering time series clustering, and applying a mean variance portfolio theory. The investigation simulated wind, and power time series for South Africa, and identified optimal development cluster regions. The research presents four case studies which clearly indicate the benefit of distributed power generation, and quantification of the adverse grid ramp affects associated with a high penetration of renewables. Sorensen et al. (2018) further assesses the impact of wind variance on power system reserves in South Africa. The study is based on information provided by the DoE, and Eskom, presenting a scenario of 5% penetration of wind power generation by 2025. The authors modelled the impact, and duration of wind power ramp rates on the grid network of South Africa, and identified that power reserves would need to increase by 2% in the short-term to support the modelled scenario.

More recently, Mararakanye & Bekker (2019a; 2019b) assessed the impacts of renewable energy penetration level on grid characteristics, and modelled renewable energy as a flexible power resource by applying curtailment. Their 2019a work is not specific to South Africa, but identifies valuable associations between wind power ramp events, and grid characteristics. The paper broadly presents renewable energy integration, and the associate impact on grid networks considering penetration level, generator type, and grid characteristics, noting that system penetration is a localised concern but affects the broader power system. A specific concern are scenarios where penetration exceeds 20%, driving such grid networks to implement a proactive strategy to maintain grid stability during ramp events. When penetration exceeds 50%, frequency, and transient grid stability is affected, and additional measures need to be implemented to prevent grid faults. Mararakanye & Bekker 2019b specifically focused on South Africa, and assess the scenario of flexible renewable energy in the grid. A feasibility assessment is performed by applying curtailment as a method of inducing system flexibility. Results indicate that implementing curtailment of renewable energy during isolated extreme ramping events may be a least cost option opposed to adding additional support generators. Findings suggest that accurate short-term wind speed forecasting, paired with automated curtailment is required to successfully achieve the modelled results.

To date, research has not published diurnal, monthly or seasonal wind speed profiles for the study area using ground recorded wind speed, in context of the national electricity demand profile. This research fills an important scientific gap of the wind-generated electricity profile at 15 stations located in the NC, WC, and EC provinces to aid in the planning of wind farm developments to increase wind-generated electricity reliability.

4.2 Data

The 15 stations as presented in Chapter 2, section 2.2.1, are statistically evaluated using station recorded wind speed data between 1950, and 2018, in consideration of the national electricity demand profile. Electricity generation, and supply data are published in Eskom's mean monthly integrated report. In 2018, Eskom observed a nominal installed capacity of 49.1GW, and delivered 234.4GWh of electricity from multiple sources (Table 4.1). Independent electricity producers (IPP's) generated 11.4GWh (4.86%) of electricity of which 50% is generated by wind facilities (Eskom, 2019b). The portion of IPP electricity distributed increased by a factor of 2.3 between 2017, and 2018 (Eskom, 2018; 2019b). The Eskom electricity load records distinct seasonality which is reflected in the associated demand profile (Figure 4.1). This seasonality is governed by summer, and winter (high season) as well as spring, and autumn (low season) (Eskom, 2017a). The load is defined by three periods, namely: peak (17:00 –19:59; 06:00–09:59), standard (10:00–16:59; 20:00–21:59), and off-peak (22:00–05:59) (Eskom, 2017a).

The diurnal, monthly, and seasonal wind speed, and electricity demand anomalies were calculated for each data series, for which results are provided in Table 4.2, and 4.3. The data anomalies quantify the percentage of wind resource (electricity demand) recorded during each month (hour), which when summed, quantify 100% of the monthly (diurnal) wind speed (electricity demand) profile while seasonal anomalies correspond to the sum of associated months. All correlations are tested for statistical significance by considering $P<0.05$.

Wind speed anomalies record similar diurnal, monthly, and seasonal fluctuations. The highest (lowest) mean percentage of annual wind resource of 9.5% (7.2%) is recorded in November

(May). Langebaan (Alexander Bay) station records the highest (lowest) mean wind speed anomaly of 10.55% (6.22%) in January (May). Electricity demand peaks in winter (26.27%), followed by autumn (24.98%), and is the lowest in summer (23.85%). In contrast, the highest mean wind speed anomalies are observed in summer (27.12%), followed by spring (26.99%), and winter (23.53%). Langebaan (Springbok) indicates the highest mean summer (winter) wind resource anomaly of 30.55% (27.38%) (Figure 4.2a). The mean diurnal wind speed profile follows a normally distribution, and is positively skewed, observing the highest wind speed during the afternoon, and peaking between 15:00–16:00, while the lowest is before sunrise between 05:00, and 06:00 (Figure 4.2b).

Table 4.1: Eskom 2018 electricity source by technology (Eskom, 2019b).

Generator	**Classification**	**Technology**		**Installed capacity (MW)**
Eskom	Baseload stations	Coal–fired stations		36,479
		Nuclear electricity		1,860
	Mid–merit/peaking stations	Pumped storage stations		2,724
		Hydro stations		600
		Open–cycle gas turbines		2,409
	Self–dispatching	Wind		100
		Total		45,561
IPP	**Classification**	**Technology**	**Contracted (MW)**	**Installed capacity (MW)**
	Self–dispatching	Wind	1,995	1,980
		Solar Photo Voltaic	1,478	1,474
		Gas turbines	1,005	1,005
		Concentrating solar electricity	500	500
		Hydro, biomass, and landfill	27	22
		Total	5,005	4,779

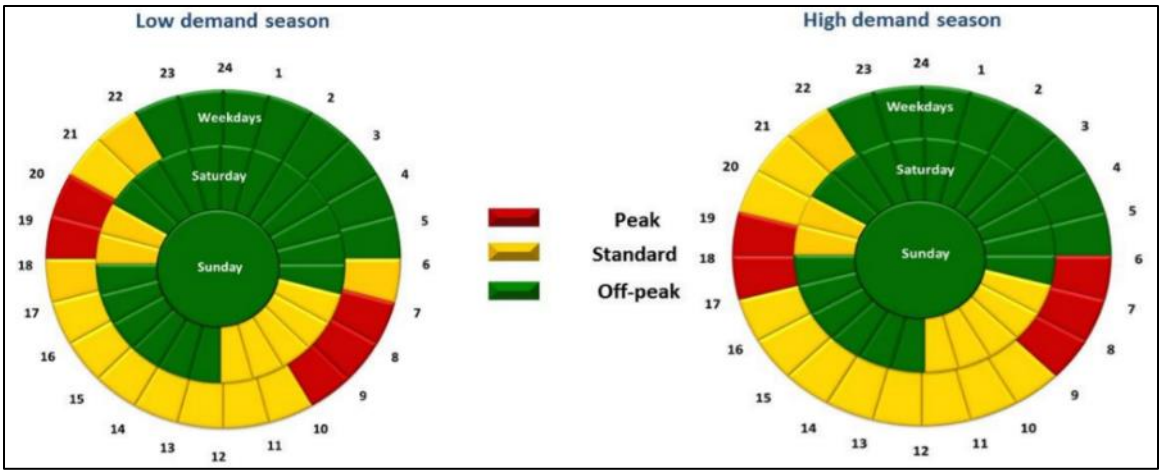


Figure 4.1: Eskom diurnal electricity demand profile (Eskom, 2017b).

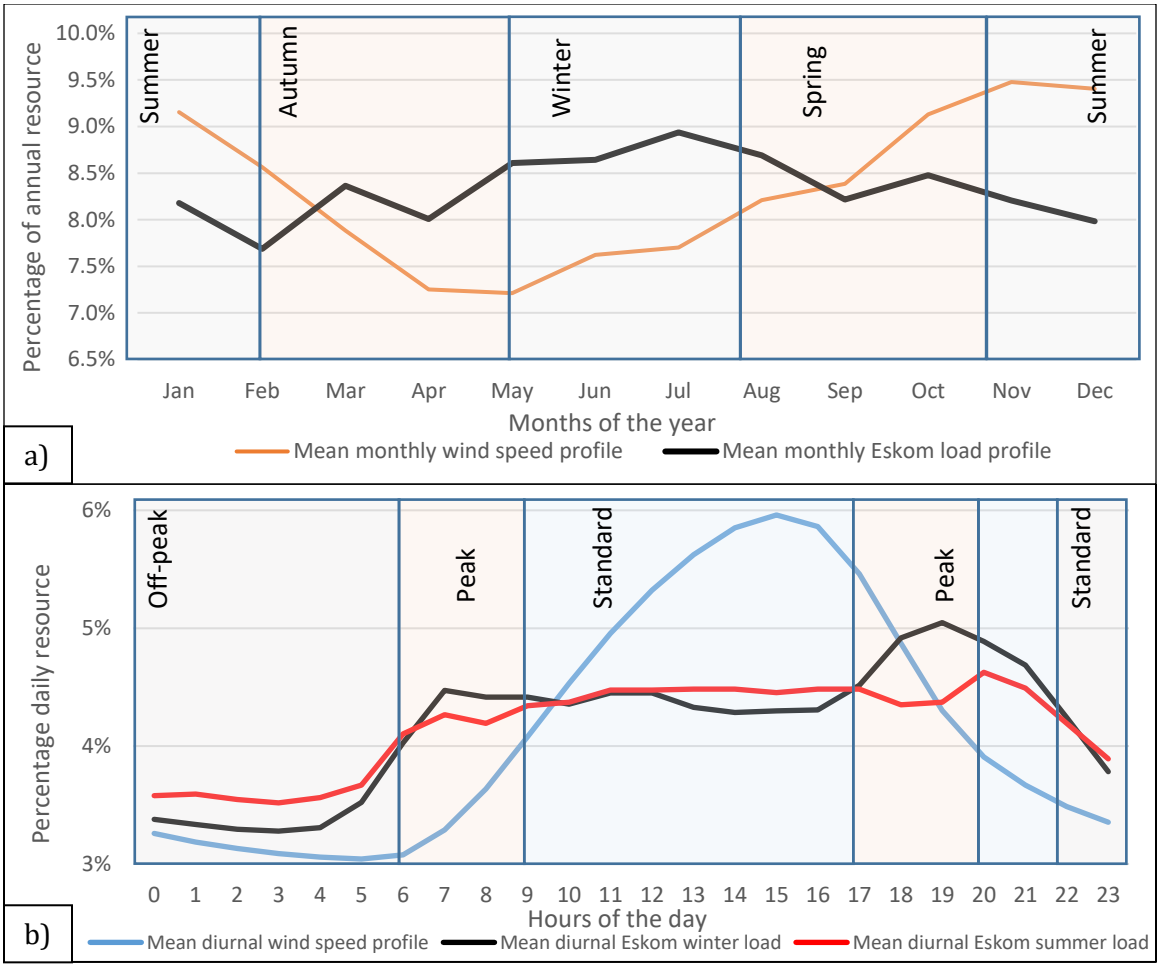


Figure 4.2: Mean a) Monthly;, and b) Diurnal wind speed, and electricity load anomalies.



Figure 4.3: Mean monthly wind speed anomalies a) Province b) Region c) Sub-region.

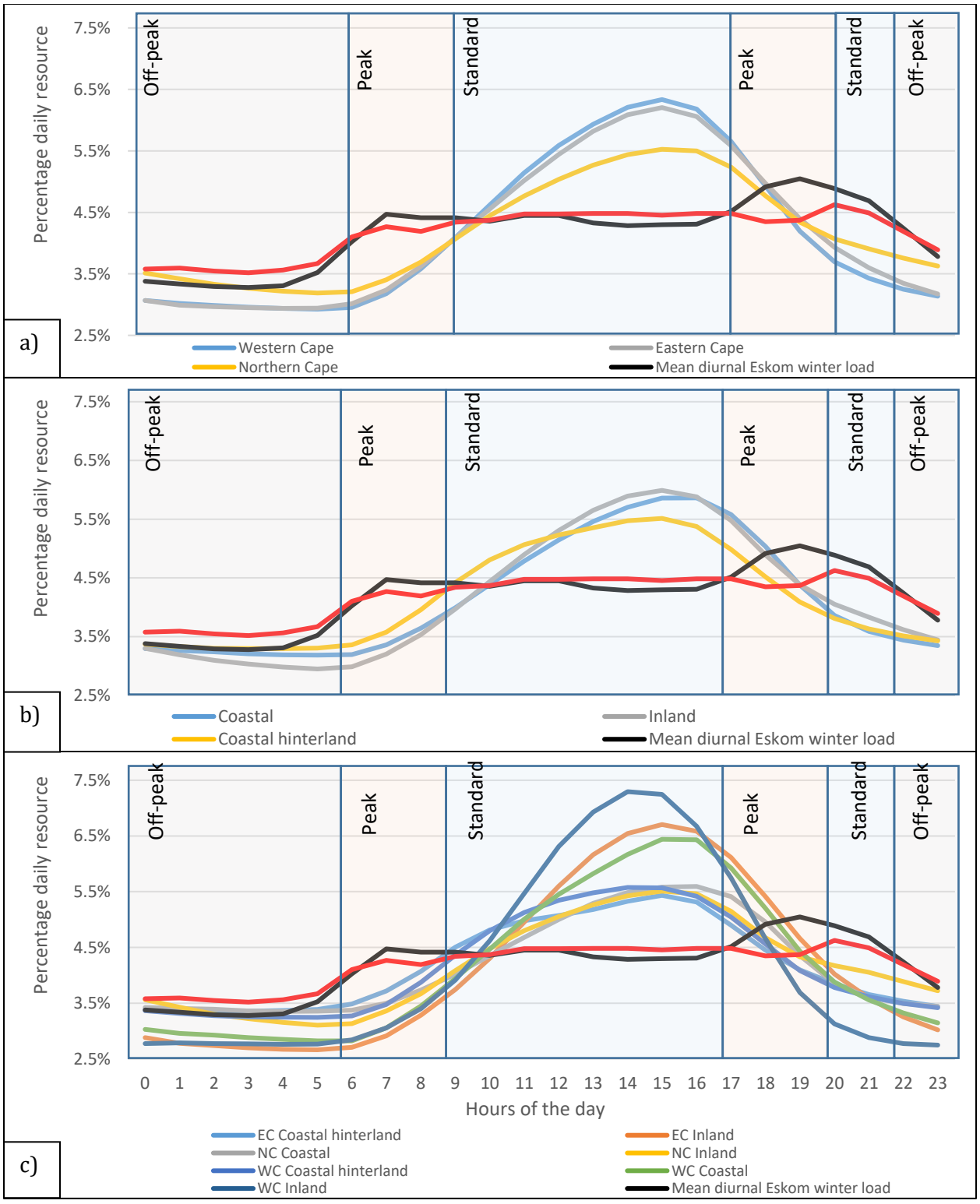


Figure 4.4: Mean diurnal wind speed, and Eskom load anomalies a) Province b) Region c) Sub-region.

Table 4.2: Diurnal, monthly, and seasonal wind resource correlation (r) with Eskom load profile.

Station / Region	Eskom load profile			
	Seasonal	Monthly	Diurnal	
			High demand	Low demand
Alexander Bay	**-0.842**	**-0.622**	**0.531**	**0.712**
Beaufort West	0.097	0.217	0.404	**0.648**
Brandvlei	**-0.782**	**-0.554**	**0.532**	**0.733**
Cape Agulhas	0.710	0.463	0.404	**0.648**
De Aar	-0.694	-0.487	0.484	**0.727**
Elliot	0.486	0.448	**0.557**	**0.699**
Koingnaas	**-0.810**	**-0.585**	0.497	**0.669**
Langebaan	**-0.965**	**-0.718**	**0.583**	**0.742**
Noupoort	**-0.742**	**-0.521**	**0.568**	**0.736**
Plettenberg Bay	-0.103	0.076	**0.557**	**0.738**
Queenstown	-0.059	0.053	**0.497**	**0.732**
Springbok	**0.833**	**0.739**	**0.683**	**0.823**
Still bay	-0.444	-0.244	**0.521**	**0.713**
Tygerhoek	**-0.858**	**-0.648**	0.385	**0.645**
Uitenhage	-0.455	-0.298	**0.546**	**0.757**
Mean of all stations	0.627	-0.408	**0.545**	**0.742**
Eastern Cape	-0.032	0.064	**0.560**	**0.753**
Northern Cape	-0.725	**-0.506**	**0.571**	**0.759**
Western Cape	-0.738	-0.492	**0.511**	**0.719**
Coastal	-0.865	**-0.632**	**0.530**	**0.744**
Hinterland	-0.372	-0.195	**0.561**	**0.753**
Inland	-0.740	**-0.518**	**0.534**	**0.717**
EC Hinterland	-0.455	-0.298	**0.546**	**0.757**
EC Inland	0.196	0.249	**0.562**	**0.739**
NC Coastal	-0.831	**-0.610**	**0.525**	**0.705**
NC Inland	-0.634	-0.418	**0.587**	**0.777**
WC Coastal	-0.315	-0.120	**0.544**	**0.731**
WC Hinterland	**-0.931**	**-0.697**	**0.519**	**0.735**
WC Inland	0.097	0.217	0.404	**0.648**

Bold underline denotes a MK statistical significance of 99% (P<0.01)
Bold denotes a MK statistical significance of 95% (P<0.05)
Underline denotes a MK statistical significance of 90% (P<0.1)

Table 4.3: Mean seasonal, and monthly wind speed, and Eskom electricity load anomalies.

Data Source	Month												Season			
	Jan	Feb	Mar	Apr	May	Jun	Jul	Au	Sep	Oct	Nov	Dec	Sum	Aut	Win	Spr
Alexander Bay	10.4%	9.5%	8.4%	6.9%	6.2%	6.4%	6.6%	7.2%	8.3%	9.6%	10.3%	10.3%	30.2%	21.5%	20.2%	28.2%
Beaufort West	8.6%	8.1%	7.6%	7.3%	7.9%	8.3%	8.5%	9.0%	8.2%	8.8%	9.0%	8.8%	25.5%	22.7%	25.8%	26.0%
Brandvlei	9.7%	8.9%	7.9%	7.2%	6.8%	6.8%	7.2%	8.0%	8.3%	9.2%	9.9%	10.1%	28.7%	21.9%	22.0%	27.4%
Cape Agulhas	9.0%	8.4%	8.3%	7.6%	7.1%	7.3%	7.5%	7.3%	8.3%	9.8%	9.8%	9.3%	26.8%	23.1%	22.2%	27.9%
De Aar	9.3%	8.6%	7.9%	7.2%	6.9%	7.0%	7.3%	8.1%	8.6%	9.5%	9.9%	9.8%	27.7%	22.0%	22.3%	27.9%
Elliot	7.9%	7.4%	6.9%	7.2%	8.0%	8.9%	8.6%	9.4%	9.1%	9.2%	8.8%	8.6%	24.0%	22.1%	26.9%	27.1%
Koingnaas	9.6%	8.9%	8.3%	7.5%	7.0%	7.4%	7.6%	7.6%	8.3%	9.0%	9.5%	9.4%	27.9%	22.8%	22.6%	26.7%
Langebaan	10.5%	9.8%	8.8%	7.6%	7.0%	6.7%	6.5%	7.1%	7.3%	8.7%	9.8%	10.2%	30.6%	23.4%	20.2%	25.9%
Noupoort	9.9%	8.8%	7.8%	7.1%	6.5%	6.8%	7.1%	7.8%	8.3%	9.7%	10.1%	10.1%	28.9%	21.4%	21.7%	28.1%
Plettenberg Bay	8.4%	8.1%	7.9%	7.6%	7.9%	8.2%	8.3%	8.5%	8.6%	9.0%	8.7%	8.8%	25.3%	23.4%	25.0%	26.3%
Queenstown	8.7%	8.0%	7.3%	6.5%	7.2%	8.2%	8.1%	9.1%	9.1%	9.5%	9.5%	9.0%	25.6%	21.0%	25.3%	28.0%
Springbok	8.1%	7.7%	7.4%	7.9%	8.3%	9.2%	9.5%	8.8%	8.2%	8.4%	8.5%	8.2%	24.0%	23.6%	27.4%	25.1%
Still Bay	8.8%	8.4%	7.8%	7.3%	7.5%	7.9%	8.0%	8.4%	8.4%	9.0%	9.2%	9.2%	26.4%	22.6%	24.4%	26.6%
Tygerhoek	9.5%	9.2%	8.5%	7.4%	6.9%	7.1%	7.0%	7.7%	8.1%	9.0%	9.8%	9.8%	28.5%	22.8%	21.8%	26.9%
Uitenhage	8.9%	8.5%	7.8%	6.9%	7.0%	7.8%	7.8%	8.3%	8.6%	9.4%	9.7%	9.3%	26.7%	21.8%	23.8%	27.7%
Eastern Cape	8.5%	8.0%	7.3%	6.9%	7.4%	8.3%	8.1%	8.9%	8.9%	9.3%	9.3%	9.0%	25.4%	21.6%	25.3%	27.6%
Northern Cape	9.5%	8.7%	8.0%	7.3%	6.9%	7.3%	7.5%	7.9%	8.3%	9.2%	9.7%	9.7%	27.9%	22.2%	22.7%	27.2%
Western Cape	9.2%	8.7%	8.1%	7.4%	7.4%	7.7%	7.7%	8.1%	8.1%	8.9%	9.3%	9.4%	27.2%	23.0%	23.5%	26.3%
Coastal	9.4%	8.8%	8.1%	7.3%	7.1%	7.4%	7.6%	7.9%	8.4%	9.1%	9.5%	9.5%	27.6%	22.5%	22.8%	27.0%
Hinterland	9.7%	9.2%	8.4%	7.3%	7.0%	7.1%	7.0%	7.6%	8.0%	9.0%	9.8%	9.8%	28.8%	22.7%	21.8%	26.8%
Inland	8.9%	8.2%	7.6%	7.2%	7.4%	7.9%	8.0%	8.5%	8.5%	9.2%	9.4%	9.2%	26.4%	22.2%	24.4%	27.0%
Eskom load	8.2%	7.7%	8.4%	8.0%	8.6%	8.6%	8.9%	8.7%	8.2%	8.5%	8.2%	8.0%	23.8%	25.0%	26.3%	24.9%

4.3 Results

The observed wind speed profile in the Cape provinces of South Africa is considered in light of national electricity demand.

Statistically significant inter-station correlation is present at all stations at a diurnal ($r = 0.927$), seasonal ($r = 0.706$), and monthly ($r = 0.641$) temporal scale. Notably, the inter-station diurnal hourly wind speed profile indicates a remarkably nominal mean-variance (0.002%). No statistically significant regression statistics were obtained when assessing inter-station distance with associated diurnal, monthly, and seasonal wind speed profile. Despite the geographical dispersion, a statistically significant positive correlation between every station's diurnal wind speed series, and the Eskom summer, and winter diurnal load profile. Springbok is the only station to record a statistically significant positive correlation with the Eskom seasonal, and monthly load profile, which is unique, and scientifically important.

Two primary factors to consider when integrating power into an electricity grid are the location, and stability of generation. Traditional sources of power, such as coal, generate a constant power output as it is controllable, predictable, and consistent. The same cannot be said for renewable energy sources, and is especially variable in the case of wind power generation. The concept of distributed renewable generation was raised in the introduction of Chapter 4. This concept hypothesises that increasing the geographical dispersion of renewable energy increases the stability of output. In the case of wind power, the assumption is that if wind is not present in one region, then it could be in another as it increases the likelihood for power generation. A key assumption is a variable wind speed profile at a diurnal, monthly, and seasonal temporal scale. This assumption on wind speed variability is of particular concern in consideration of electricity generation potential.

Stations exhibit a statistically significant increase in wind speed profile diversity when regressing station geographical distribution to mean inter-annual wind speed. Stations within 200km of each other indicate a mean statistical correlation of $r = 0.42$ ($P<0.001$), which reduces to $r = 0.07$ for stations located 800 – 1000km apart. This finding is positive, indicating that while the diurnal wind power generation profile cannot be diversified, wind

power reliability increases with geographical distribution (Figure 4.5). Additionally, given wind speed is not a constant, the associated correlation between stations varies. This association is well presented when applying an autocorrelation function as presented by Davis & Sampson (1986). As presented in Figure 4.6, the graphical representation shows the autocorrelation of station series which is symmetrical at zero, and the predominant annual wind speed periodicities can be identified by the observed peaks. The x-axis identifies the temporal period (year), and the y-axis the associated autocorrelation between all of the stations. Correlation at most stations fluctuate over time, resulting in the observed "waves", where y=0 indicates no correlation between the assessed station series, and the other station series. Fluctuations where y>0 indicates positive correlation periods, while y<0 indicates negative correlation periods. It is observed that Beaufort West indicates the weakest correlation to all other stations, which is identified by the fact the series predominantly fluctuates around zero. Inversely, Alexander Bay, and Langebaan indicate the strongest similarity between stations, fluctuating between a correlation of r = 0.14, and r = 0.4 (significance of 90%).

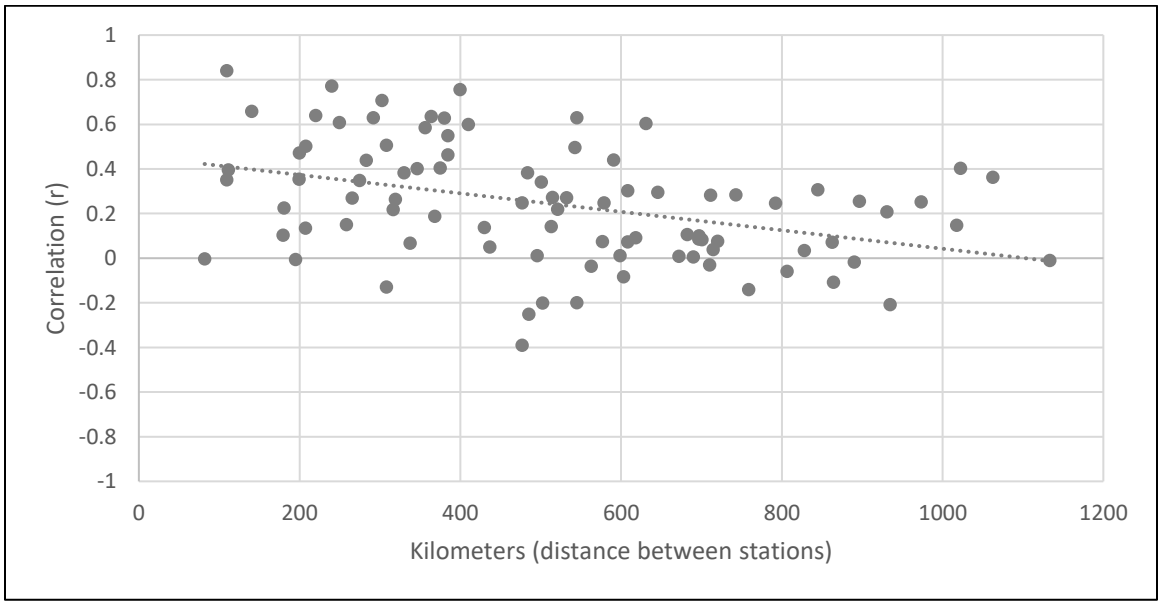


Figure 4.5: Mean inter-annual wind speed correlation (r) as a function of the distance between stations.

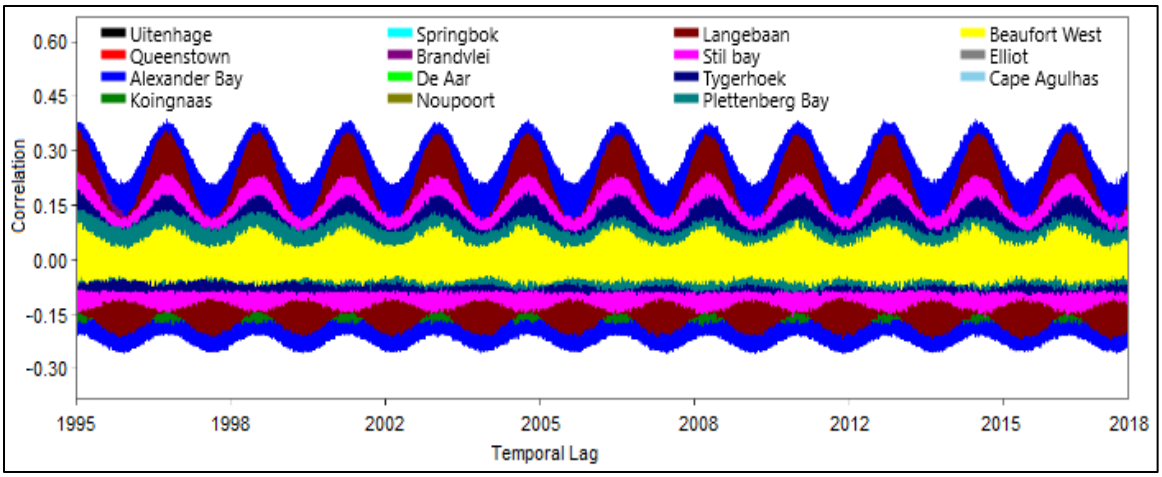


Figure 4.6: Mean hourly wind speed autocorrelation as a function of temporal lag.

4.3.1 Seasonal, and monthly wind speed profile anomalies

A strong statistically significant (P<0.1) inter-station seasonal (r = 0.650), and monthly (r = 0.642) correlation is present (Figure 4.7a, b). Considering the geographical dispersion, some stations record a strong profile correlation such as Uitenhage/Alexander Bay (1022km, r = 0.888), Alexander Bay/Noupoort (864km, r = 0.991), Uitenhage/Koingnaas (863km, r = 0.904), and Alexander Bay/De Aar (759km, r = 0.980). A statistically non-significant (P>0.1) correlation is indicated between the mean Eskom seasonal (r = -0.381), and monthly (r = –0.408) demand profile. Langebaan is the only station to record a statistically significant seasonal correlation (r = –0.961) with the Eskom profile. A statistically significant correlation is present between seven stations, and the Eskom monthly demand profile, including Springbok (r = 0.793), Langebaan (r = –0.718), Tygerhoek (r = –0.648), Alexander Bay (r = –0.622), Koingnaas (r = –0.585), Brandvlei (r = –0.554), and Noupoort (r = –0.521). The most important of these is Springbok, which is the only station to record a statistically significant positive correlation between wind speed, and the Eskom load profile on both seasonal (r = 0.776), and monthly (r = 0.635) scales. Positive correlations are also observed between Queenstown, Elliot, Plettenberg Bay, and Beaufort West, and the Eskom monthly load profile, all proving statistically non-significant (Table 4.2). The strategic importance of the monthly wind speed profiles at Springbok, and Elliot are detailed in the discussions of this chapter.

All three Cape provinces record a statistically significant mean inter-station seasonal (r = 0.797), and monthly (r = 0.792) wind speed profile correlation. The strongest monthly correlation (r = 0.996) is identified between the NC, and WC, followed by the NC, and EC (r = 0.710), and EC, and WC (r = 0.686) provinces. The lowest (highest) mean inter-province seasonal variance is identified in spring (winter) due to the low SD of 0.68% (1.3%), and sample variance of 0.004% (0.019%). Similarly, the mean provincial wind speed anomalies indicate a low seasonal SD (1.03%) with sample variance (0.0006%), and range (0.5%). Even though the seasonal, and monthly profiles are strongly correlated, only the NC indicates a statistically significant correlation (r = –0.506) with the Eskom monthly load profile (Table 4.2; Figure 4.3a). The coastal, hinterland, and inland regions all record a similar monthly wind speed profile, resulting in a statistically significant mean seasonal (r = 0.887), and monthly (r = 0.881) correlation. The hinterland, and coastal region record the strongest monthly profile correlation (r = 0.976). The WC hinterland is the only region which indicates a statistically significant correlation with the Eskom seasonal (r = –0.931), and monthly (–0.697) load demand. Statistically significant correlations are present between the mean monthly wind speed in the coastal (r = –0.518), hinterland (r = –0.632), and NC coastal (r = –0.610) regions, and Eskom monthly demand profile. A positive correlation is identified between the EC, and WC inland regions, and Eskom seasonal, and monthly load profile, although being statistically non-significant (Table 4.2, Figure 4.3).

4.3.2 Diurnal profile anomalies

Stations record a strong statistically significant diurnal inter-station correlation (r = 0.927) (Figure 4.7c). Notably, all correlations in this section indicate statistical significance (P<0.01). The lowest mean inter-station diurnal wind speed profile correlation is identified at Tygerhoek (r = 0.847). A statistically significant positive correlation is present between every station's diurnal wind speed profile, and the Eskom diurnal high (r = 0.545), and low (r = 0.742) season demand profiles. The Springbok wind speed series portrays the strongest diurnal correlation with the Eskom high (r = 0.683), and low (r = 0.823) demand periods. In contrast, the Tygerhoek station recorded the weakest correlations during high (r = 0.385), and low (r = 0.645) periods. Stations on average record more wind resource during the day–time (62.51%) compared to night–time (37.53%). The peak wind resource anomaly is

identified between 15:00–15:59 (5.96%), while the lowest is between 05:00, and 05:59 (3.04%). Considering the Eskom diurnal load periods, a similar mean wind resource is present during standard (42.91%), and off-peak (42.62%) periods with the least wind speed indicated during peak (14.47%) periods. The highest mean peak, standard, and off-peak wind resources are recorded by Langebaan (15.35%), Beaufort West (46.01%), and Noupoort (45.08%), respectively (Table 4.2).

An almost identical mean diurnal profile is present between provinces, confirmed by the statistically significant strong mean correlation (r = 0.994), and low hourly wind speed anomaly SD (1.11%). The mean diurnal wind speed anomalies of all three Cape provinces indicate a statistically significant correlation with the Eskom low (r = 0.744), and high season (r = 0.548) diurnal load profile. This is expected based on the individual station correlations presented above. The NC indicates the strongest mean correlation with the Eskom diurnal high (r = 0.571), and low (r = 0.759) season profile (Table 4.2). Considering the Eskom diurnal load periods, the NC (43.88%) indicates the largest percentage of available resource during off-peak periods, while it was during standard demand periods for the EC (43.73%), and WC (43.11%) provinces. The three Cape provinces indicate similar wind resource anomalies during peak periods, with a mean of 14.48%, and range of 0.17% (Figure 4.4a).

As with the provincial analysis, marginal diurnal variance was present between the coastal, hinterland, and inland regions, with all statistically significant correlations (r = 0.973). The wind resource anomalies during off-peak (SD = 0.47%), standard (SD = 0.93%), and peak (SD = 0.46%) periods indicate less variability than those obtained in the assessment at a provincial spatial scale. When considering both the provincial, and regional location, a stronger wind resource anomaly variation is present during off-peak (3.64%), standard (3.33), and peak (1.14%) periods. Even though a higher variance is indicated, the statistically significant strong correlation (r = 0.970) between sub-regions remain strong. All sub-regions indicate a statistically significant correlation with the high, and low period Eskom diurnal demand. The NC inland region indicate the strongest high (r = 0.587), and low (r = 0.777) period correlation with the Eskom diurnal demand, noting Springbok is located in this region. The highest off-peak, standard, and peak wind speed anomalies are observed at stations

located at inland regions of the NC (43.91%), WC (46.01%), and EC coastal (14.86%) regions. Where the WC inland region indicates the highest wind speed anomalies during the Eskom standard period, it inversely also indicates the lowest off-peak (40.27%), and peak (13.72%) anomalies. Similarly, the NC coastal region indicates the lowest wind speed anomalies during standard (41.34%) periods (Table 4.2, Figure 4.4b, c).

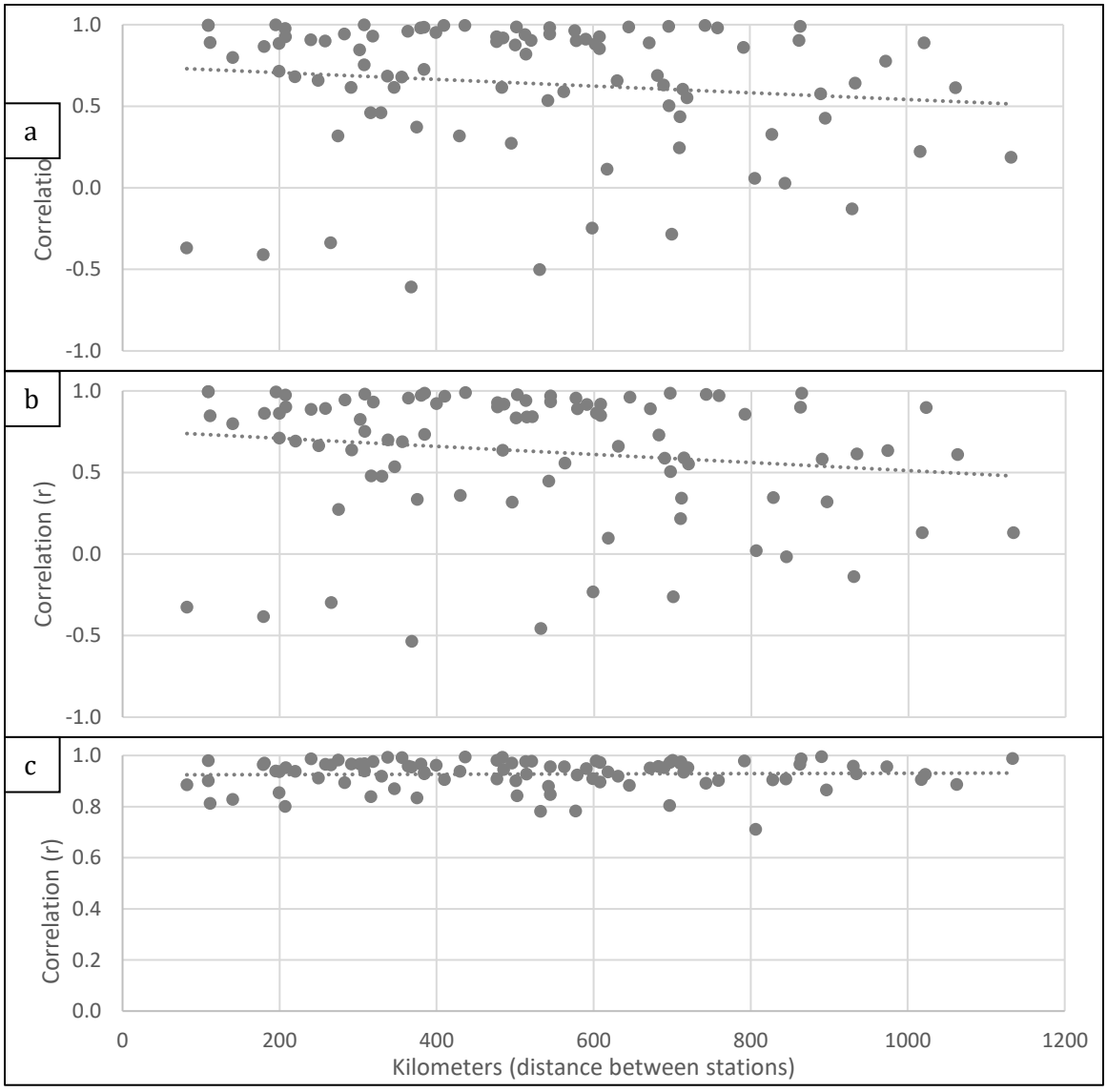


Figure 4.7: Mean inter-station a) monthly b) seasonal, and c) diurnal wind speed profile correlation as a function of the distance between stations.

4.4 Discussion

The ideal electricity source is available instantaneously, and able to produce electricity consistently. Wind speed forecasting is predictable at a low-frequency scale, however, geographical location needs are considered ahead of project implementation. The importance of both temporal, and spatial location for wind farms was substantiated in the research of King (2006) who assessed wind farm location in relation to electricity load demand in Minnesota, United States. The findings include the fact that certain regions (north, and south of Dakota) provided significant 'smoothing' of electricity generated by regional facilities. Inversely, Pei et al. (2015) highlighted the ongoing curtailment dilemma in China as a pertinent example of regional wind farm clustering oversupply. Eskom (2019b) has already acknowledged that renewable energy generation, supplied mainly by wind IPPs, continued to support the electricity system, with a pattern of high wind generation over evening peak periods in summer. This reinforces the importance of understanding wind speed profile to enable strategic development at locations that generate a larger percentage of power during periods of highest electricity demand.

This chapter has presented wind speed profiles considering high-frequency wind speed data. The relationship between the Eskom load profile, and station diurnal, seasonal, and monthly wind speed profiles were quantified, and statistically assessed. Considering the limited published research assessing wind speed profiles for the Cape provinces of South Africa, the observations are of considerable scientific value. Wind power in South Africa is currently procured based on two primary variables, namely price, and economic development. These aspects are weighted 70%, and 30% respectively under the REIPPPP evaluation methodology. The associated wind power PPA awarded to successful bidders applies the tariff tendered by the project per kWh, irrespective of diurnal period generated. Some renewable energy PPA's in South Africa, such as that for concentrated solar power, contemplate a premium tariff of up to 270% of the base tariff tendered if electricity can be generated during periods of high demand. A dynamic, such as this, could be used to incentivize the development of wind projects in specific regions that historically record increased wind speed during peak demand periods. Ren et al. (2017) identified that globally, site-specific diurnal, seasonal, and monthly wind speed profiles should be of importance

when developing a wind energy facility. In this regard, there is particular interest in the findings of the Springbok wind data series, given that the mean diurnal, monthly, and seasonal wind speed profile is positively correlated ($P<0.05$) to the Eskom load profile. The Springbok region can serve as a strategic development region to balance South Africa's generic annual wind speed profile. Springbok's wind climate is of great strategic importance in the context of wind-generated electricity generation in South Africa.

4.4.1 Monthly, and seasonal wind speed profile anomalies

The strongest mean monthly, and seasonal wind speeds are observed in December, and summer respectively. Similar findings are identified in the northern hemisphere, such as for peak wind speeds during the winter months of December across four sites in Italy (Ouammi et al., 2010). Similar observations have been documented in Canada where above average wind speeds between November, and April peaking in February (Li & Li, 2005). Distinct seasonality is identified across all stations in the study area with above average wind speed anomalies (54.16%) recorded during spring, and summer, where below average anomalies (45.84%) are recorded during winter, and autumn. Fant et al. (2016) published an overview of wind speed seasonality in southern Africa based on MERRA satellite wind speed data. These authors identified a stronger wind resource during summer than winter but noted that their meso-scale data source contained potential errors due to micro-scale wind speed variability in South Africa. The current PhD work verifies their observation that the largest (27.10%) mean wind speed anomalies are present during summer, closely followed by spring (27.06%).

The statistical assessment between Eskom, and station monthly data anomalies identified that Springbok recorded the strongest positive correlation while Langebaan recorded the strongest negative correlation. The monthly profile for Springbok is well suited to deliver a higher percentage of power during the months when the grid is most constrained. Additionally, Springbok also recorded the strongest diurnal correlation with Eskom's high, and low demand periods. Springbok is unique in that it is the only station to record a statistically significant positive correlation with both the monthly, and diurnal Eskom load demand (Figure 4.8). The author was concerned about the results of the Springbok station,

and contacted SAWS to discuss the findings. There are no known time stamp issues or data logging offsets that could explain the unique findings. The monthly, and diurnal results differ from the mean of other stations, and the result could be due to local influence, and topography. This remains an important finding, and additional wind masts should be erected in the area to establish the geographic extent of the identified wind speed profile.

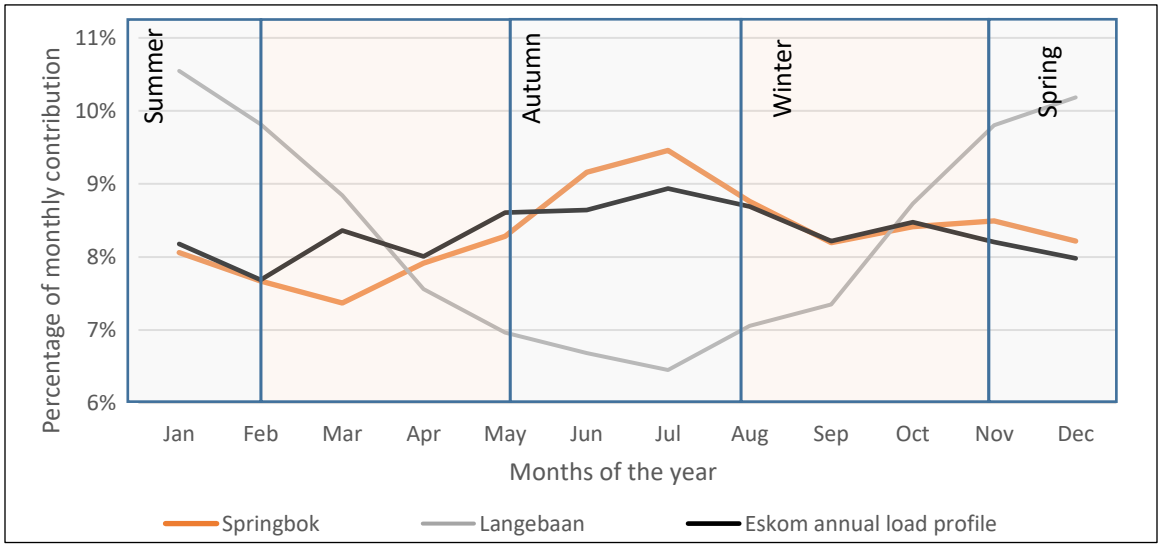


Figure 4.8: Springbok, Langebaan, and Eskom load to the monthly data anomalies.

Stations indicate statistically significant mean inter-station seasonal (r = 0.706), and monthly (r = 0.641) correlations. When assessing the seasonal, and monthly inter-station correlations at provincial (r = 0.797, 0.792), and regional (r = 0.887, 0.881) scales, correlations increased resulting in almost identical mean monthly profiles. While a strong similarity is present between stations at a mean monthly scale, inter-monthly correlation reduced significantly. Similar results are also documented in northern Europe, Bolivia, and north-central United States (Robeson & Shein, 1997; Giebel, 2000; Cisneros-Saldana & Hosseinian, 2018). Such examples include the findings across 11 sites spanning 650km in Minnesota, USA (Klink, 2007). The work identified statistically significant correlations between mean monthly wind speed, and inter-station distance, observing weaker correlation with increased distance between stations.

Considering all stations, a mean inter-monthly correlation of r = 0.49 is present. This similarity increases when only considering stations within 200 km of each other (r = 0.57), further increasing (r = 0.73) when excluding the two stations which record an inverse correlation. Considering sites in excess of 800 km range, mean correlation reduces to r = 0.29 (Figure 4.9). This confirms the benefit of dispersed wind power generation in the study area, even at a mean inter-monthly scale.

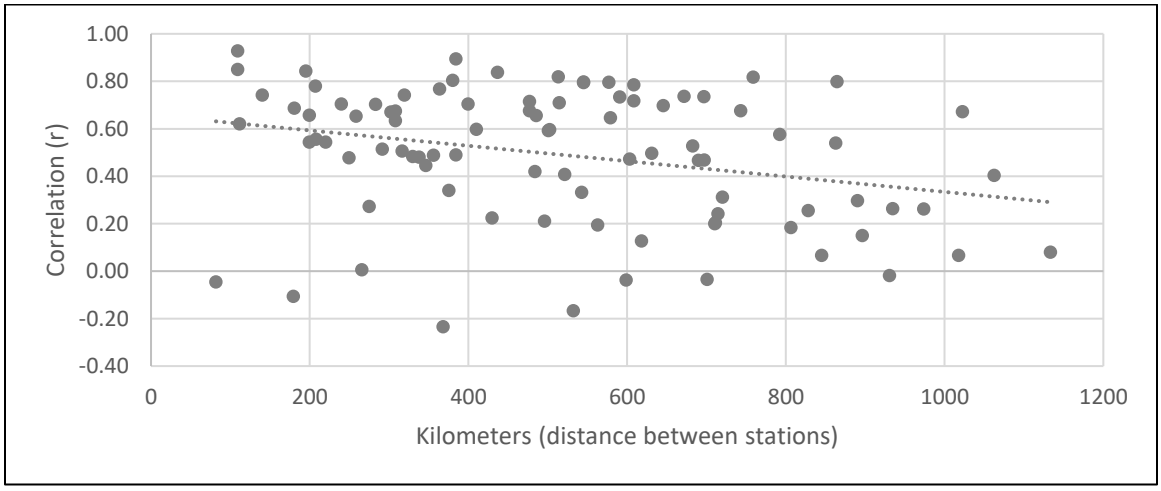


Figure 4.9: Inter-monthly wind speed correlation (r) of stations in the study area ranging 50km - 1100km apart.

4.4.2 Diurnal wind speed profile anomalies

The diurnal cycle is a fundamental variation of global climate systems, for atmosphere, ocean, and land (Keevallik & Soomere, 2009; Resmi, et al., 2019). This study quantifies station diurnal wind speed profile at 10 m (tower height). The wind speeds peak during the day, and are lowest at night at all stations. At a mean annual, seasonal, and monthly scale, maxima, and minima wind speed anomalies are present between 14:00, and 16:00 SAST (South African Standard Time), and 04:00, and 06:00 SAST respectively. These diurnal wind speed phases result from solar heating identified by a convection system during the day (06:00 – 17:59), and a stable nocturnal air flow. Wind speed profiles gradually start to increase from 07:00 SAST, peaks at 15:00, with 43.37% of resource available in the afternoon between 12:00, and 18:00. The indicative downward flow of atmospheric momentum during the day drives the development of the near surface wind speeds.

Mean daily wind speeds indicate an almost identical diurnal wind speed profile between the 15 stations, and is confirmed by the strong significant ($P<0.01$) mean inter-station correlation ($r = 0.927$). Fant, et al. (2016) identified that day–time periods across South Africa yield higher wind resource in comparison to those at night. The findings noted uncertainty associated with their MERRA meso–scale data. This research confirms all stations record higher mean wind speed anomalies during the day (62.0% of observed resource) between 06:00 – 17:59, as opposed to nocturnal hours (38.0% of observed resource) between 18:00 – 05:59. The wind speed transition feature present in the near surface boundary layer, specifically late afternoon, during the hours before sunset indicate surface layer wind speed variance clearly capture the signature of this transition. It is due to this association that both diurnal, and seasonal wind speed variation are clearly identified at stations in the study area. The primary driver of this phenomena is related local boundary layer heat transfer, related to the varied land heating, and dominant convection systems.

The diurnal mean hourly, and inter-hourly wind speed profiles provide the most valuable insight for wind power in the study area. Unlike the identified weak or inverse seasonal, and monthly correlation to the Eskom load profile, every station recorded a statistically significant ($P<0.1$) positive correlation to the mean Eskom diurnal load profile. A stronger mean correlation ($P<0.05$) is present between Eskom load profile, and station wind speed profiles during low electricity demand periods ($r = 0.742$) compared to periods of high demand ($r = 0.545$). The strongest similarity between wind speed, and Eskom load in the Springbok series indicates a correlation of $r = 0.683$ ($P<0.05$) during high demand, and $r = 0.823$ ($P<0.01$) during low demand periods, which is an important finding. Noting Springbok similarly recorded the strongest positive mean monthly correlation to the Eskom load profile, the location is ideally suited to provide wind power during the months, seasons, and time of day Eskom observes its load. This observation is unique, and not identified in any other station assessed.

Assessment of sub-daily patterns is indeed an important sphere which provides intriguing insight to the regional wind climate. Wind speed variance at an hourly scale is the primary factor hindering its widespread implementation, and restricts the reliance on wind power as

a sole electricity source. During times of high wind speed Eskom needs to reduce generation from traditional coal facilities, while ramping up generation during low wind speed periods. The hourly wind speed deviation is of interest to quantify the amount of instantaneously available supplementary power required to support the grid network during reduced wind speed periods. While, earlier in this chapter the diurnal wind speed profile has been presented, the rate of change was not investigated. Wind speed varies instantaneously, however, even at a long-term average hourly scale, significant inter-hourly daily variations are observed (Figure 4.10).

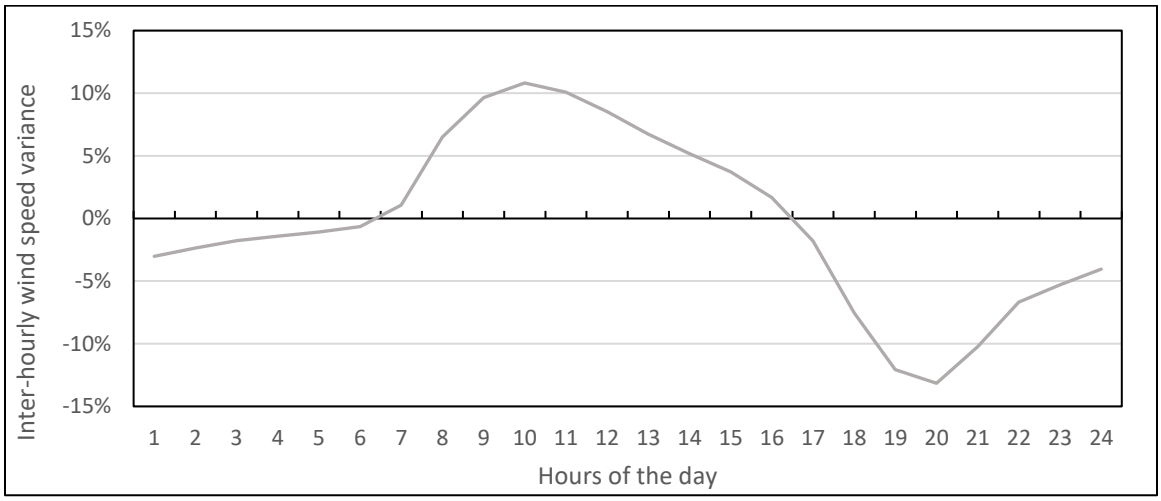


Figure 4.10: Mean inter-hourly station wind speed variance.

Two periods (each of four hours) indicate extreme inter-hourly variance, namely mid-morning (07:00 – 11:00), and early evening (16:00 – 20:00). These two periods quantify a mean inter-hourly wind speed variance of 9.77%, and -10.75% respectively. Considering the cubic relationship between power, and wind, this equates to a 30% increase/decrease in wind power generation per hour during these periods. This variance presents a challenge to Eskom in balancing the power demand on the grid network to prevent a fault resulting in a power outage. The Elliot station recorded the highest positive mean inter-hourly wind speed variance between 10:00, and 11:00 (18.8%), where Beaufort West station recorded the highest negative between 18:00, and 19:00 (-26.2%). These equate to a power generation variance of 53%, and 201% respectively. There is extensive ongoing research to incorporate wind power generation to power networks, and the challenge is not unique to South Africa.

The reader is referred to, among others Adedeji et al. (2020), Apata et al. (2020), Ncwane & Folly (2020), and Ntsadu (2019) who assess the incorporation of wind power generation into the Eskom grid network, with a specific focus on South African wind speed variance.

Considering all stations, a mean inter-hourly correlation of r = 0.28 is present. This similarity increases to r = 0.39 only considering stations within 200 km of each other, but decreases to r = 0.24 considering sites in excess of 800 km of one another (Figure 4.10). This again confirms the benefit of dispersed wind power generation in the study area, indicating a significant increase in wind power availability given the statistically weak correlation between hourly wind speed profiles. This observation is not unique to the study area, and is also observed elsewhere globally. One example includes an assessment of the hourly mean wind speed across multiple sites in the Nordic countries ranging 10km to 2000km. While the decrease in mean hourly correlation between stations in the study area is not as prominent, the exponential decrease is clearly observed in the Nordic assessment (Figure 4.11, Figure 4.12).

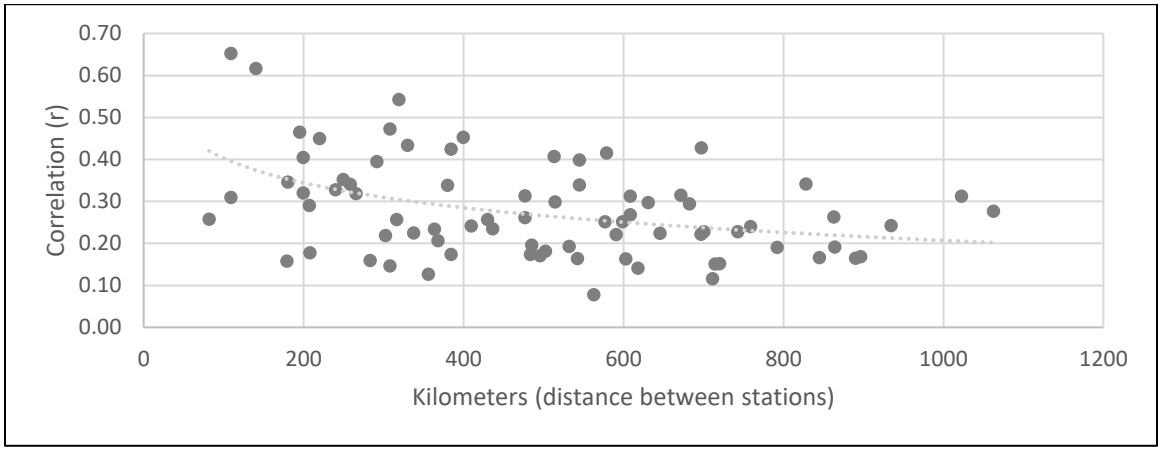


Figure 4.11: Inter-hourly wind speed correlation (r) of stations in the study area ranging 80km - 1100km apart.

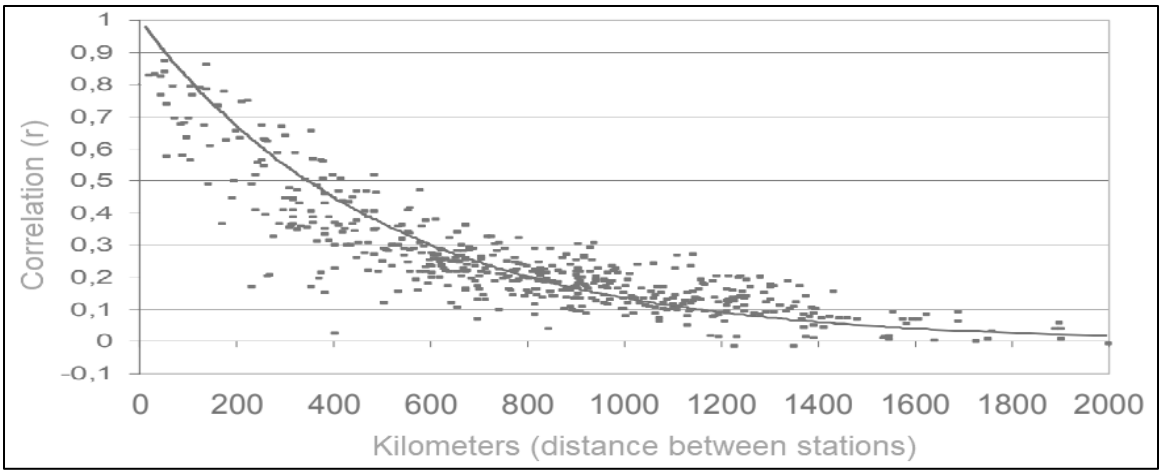


Figure 4.12: Hourly power correlation of sites in the Nordic countries ranging 10km - 2000km apart (Holttinen, 2004).

4.5 Recommendation for future research

The recent call for additional wind power generation to be tendered under the REIPPPP reinforces the importance of understanding the impact of wind power variability, and its associated impact on the Eskom grid. This PhD has assessed all available data, while there are inherent flaws, no better data sets currently exist. An observed gap is the association of observed near ground wind speeds with those at hub height. While it is assumed that a similar impact is present, further research should verify South Africa's wind speed profiles, specifically at hub height using WASA data once 10+ years of data are available. In addition, all newly constructed wind farms have ongoing wind measurement campaigns. These data sets should be made available for scientific research which would reduce extrapolation uncertainty. Some of these operational projects have wind data sets extending from the mid-2000's, which could be used for further assessment of wind power project locations, and their wind power generation profiles to the power grid. The intention would be to identify strategic development zones which help balance the Eskom demand load.

An important factor identified in the wind speed, and power dynamic's section is that of wind shear. This is the rate of wind speed increase with increased altitude. Locations of high wind shear are of strategic importance in that higher yields are obtained, offering more power, at the same location. The identification of these high wind shear areas would justify the

implementation of increased hub height to optimise power generation. Of further interest is the ongoing assessment of the impact of the wind power profile on operational performance, and maintenance requirements of a wind farm. Sites with high extreme wind speeds may demand more maintenance, and an associated higher unavailability. Research assessing the forecast compared to actual power generation would be of great importance to further understand, and optimise wind power generation in South Africa.

5 TELECONNECTIONS, AND NEAR–SURFACE WIND SPEED VARIABILITY IN THE NORTHERN, WESTERN, AND EASTERN CAPE PROVINCES OF SOUTH AFRICA

As discussed in Chapter 1, section 1.2, this chapter presents the mean monthly wind speed teleconnection to large scale atmospheric circulation modes at the 15 stations. The climate influencing factors considered, include:

- 5.2.1: El Niño Southern Oscillation (ONI)
- 5.2.2: Indian Ocean Dipole (IOD)
- 5.2.3: Antarctic Oscillation (AAO)
- 5.2.4: Regional Mid–Latitude Cyclones (MLC)
- 5.2.5: Solar cycle

5.1 Introduction

The implementation of wind energy as a power source is steadily increasing in South Africa. One of the highest uncertainties with electricity generated from wind is the associated temporal uncertainty of wind energy availability (Pryor, et al., 2006; Klink, 2007; Pryor & Barthelmie, 2013). Building on the findings of Chapter 3 (wind speed trends), and Chapter 4 (wind speed profiles), Chapter 5 investigates global, and synoptic-scale climate events, and their associated impact on near-surface wind speed in the study area. The objective is to evaluate if there is an impact on wind speed at specific localities associated with the ONI, IOD, AAO, regional MLC, and solar activity at monthly, annual, and multi–cyclic scales. Global climate events cause inter-annual variation in wind strength, resulting in large uncertainty when predicting future wind energy outputs (Bossanyi, et al., 2001; Carslaw, et al., 2002; Foukal, et al., 2006; Solomom, et al., 2011; Kobashi, et al., 2015; Gonzalez, et al., 2019; Sniderman, et al., 2019). The temporal, and spatial teleconnections between large–scale atmospheric circulation modes, and local South African climate are broadly examined in several publications (Goddard & Graham, 1999; Reason, 2001; Weldon & Reason, 2014; Fant,

et al., 2016; Sousa, et al., 2018). Climatic variability is extremely complex with infinite interactions, teleconnections, and probabilities.

However, wind speed variability is still poorly understood in southern Africa, specifically why, and how wind speed varies inter–annually. Information of this nature is important, particularly for the renewable (wind) energy generation sector, and specifically to anticipate wind turbine power generation typically considering a time span between 20–30 years. This chapter considers wind speed data from 15 stations located across the study region. Stations are analysed to identify spatial, and temporal relationships considering each climate event. A climatological analysis should consider data over a period of at least 30–years (Colette & Ancellet, 2005; Spinoni, et al., 2015; Fischer, et al., 2019). Data are derived from 15 stations with wind speed records between 1995, and 2018 (Cape Agulhas 1950, and 2018), which provide the longest reliable series available for the southern African region.

5.2 Review of teleconnection studies

The first step to assess the relationships between regional near-surface wind speed, and climate variables is to identify the weather producing systems which define South Africa's climate (located between 22°S–35°S, and 16°S to 33°E). The four broad scales of 'micro', 'meso', 'synoptic', and 'global' are used to define regional impacts of an event (Figure 5.1). Global-scale forcing is the most extensive mode, which in turn affects micro–, meso–, and synoptic-scale events that are also affected by local features such as orography, land use, and elevation. Four main global scale climatic modes, including ENSO, IOD, AAO, and the solar irradiance cycle, impact South African weather, and climate (Currie, 1993; Gray, et al., 2010; Fant, et al., 2016; Dunning, et al., 2018; Pomposi, et al., 2018; Sousa, et al., 2018; Lennard, 2019). Mid-latitude cyclonic events play an important role on regional–scale synoptic climatic conditions but are not expected to be a primary driver of wind speed due to its restricted scale, and frequency (Berry, et al., 2011; Weldon & Reason, 2014). Many micro-scale factors influence wind variability, including topography, land use, and surface roughness. These features exert a nominal impact on regional wind variability, and are thus not the focus of this thesis (Papadopoulos & Helmis, 1999; Landberg, et al., 2003; Fedorovich & Shapiro, 2009; Huang, et al., 2015).

There is ongoing research quantifying the potential impact of climate change on global wind speed variability (Davy, et al., 2018; Karnauskas, et al., 2018; Clarke, et al., 2019; Gonzalez, et al., 2019; Tian, et al., 2019). Several authors forecast that the continental US, and China will record a significant climate change-induced wind speed reduction between 1%, and 3.2% over the next 50 years. In contrast, over the same period, the impact on southern Africa is expected to be negligible with a median change close to 0% (Breslow & Sailor, 2002; Hart, et al., 2008; Pryor, et al., 2009; Ke, et al., 2014; Zhou, et al., 2015; Fant, et al., 2016). Climate change-induced variability considers a broad range of forcing, and is not a subject of this thesis.

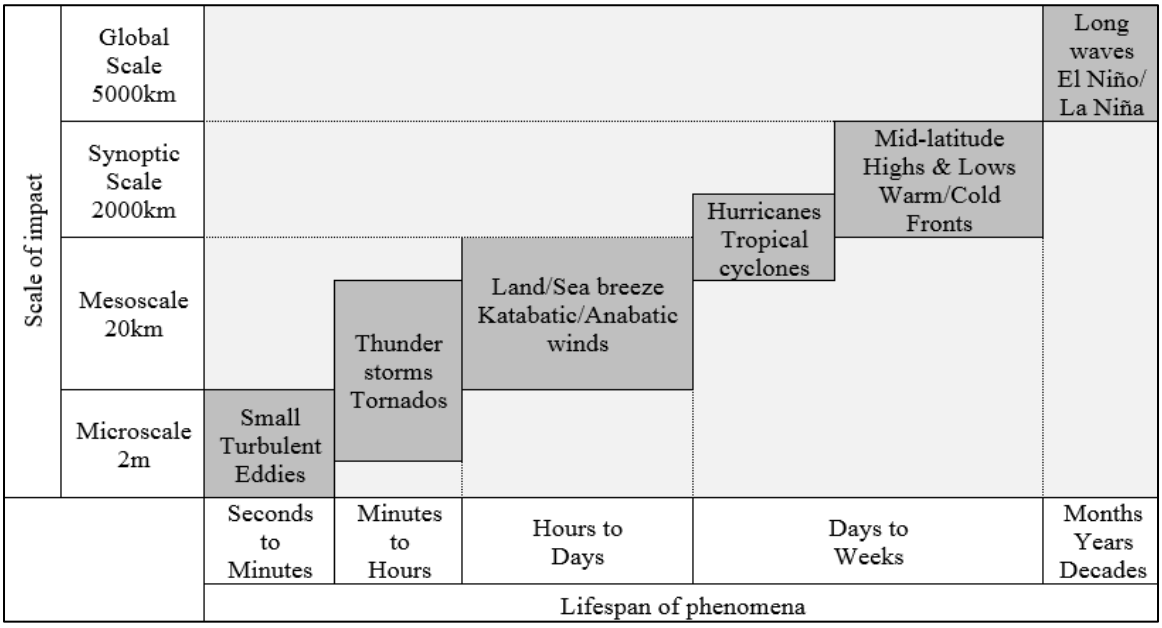


Figure 5.1: Drivers of regional climate (EMD, 2015).

5.2.1 El Niño Southern Oscillation

The ENSO refers to an oscillation with two centres situated over the western Pacific/eastern IO, and southeastern tropical Pacific Ocean, and is widely acknowledged as the most significant driver of global climate (Carpenter & Rasmusson, 1982; Halpert & Ropelewski, 1987; Anderson, et al., 2002; Bianchi, et al., 2017; Maoyi, et al., 2018). The ENSO is recorded as the ONI, consisting of an irregular cycle (4–7 years) of both positive (El Niño), and negative (La Niña) phases (Cane, 2005; Moon, et al., 2015; Sun, et al., 2015; Herold & Santoso, 2018).

Monthly series of the ONI is presented in the form of a 3–month rolling mean of recorded SST. An El Niño event is associated with an increase of SST in the central/eastern tropical Pacific Ocean. This results from a low–pressure cell in the eastern pacific, and a high–pressure cell in the west pacific; inverse forces occur during a La Niña event (Hoerling, et al., 1997; Glantz, 2001; Collins, 2005; Claar, et al., 2018). An El Niño, La Niña or neutral phase is defined by a period of at least three consecutive months of above, below or near mean SST records (NOAA, 2019c).

Extensive scientific literature documents the relationship between ENSO events, and global ecosystems, climate, fisheries, marine ecology, and weather (Wang, et al., 2000; Alexander & Scott, 2002; Yu & Zwiers, 2007; Chen & Song, 2018). Notably, the past two decades observed two very strong El Niño events (VSE) (1997/98–2015/16), stimulating considerable recent research attention (Bianchi, et al., 2017; Lindergren, et al., 2017; An, 2018; Herold & Santoso, 2018; Maoyi, et al., 2018). The 1997/98 VSE event resulted in global climatic impacts, and is considered by some as the climactic event of the century (Jiménez-Muñoz, et al., 2016). Several studies document ENSO, and wind speed interactions across the USA. For instance, Mohammadi & Goudarzi (2018) evaluated eight stations across California between 1961, and 2010, from which they identified the impact of ENSO events on station recorded wind speed. Some stations are complemented by above-average wind speeds, while others record below-average wind speed. A stronger influence is identified during very strong El Niño events. Enloe et al. (2004) assessed wind data between 1948, and 1998 across the United States, identifying a mean increase in wind speed during El Niño events, and to a lesser magnitude, an inverse during La Niña events. Similar results are observed across southern South America when assessing MERRA reanalysis wind data between 1979, and 2015 (Bianchi, et al., 2017). Several publications have confirmed the presence of a 5–month lagged teleconnection between mean monthly wind speed, and ONI, which is contemplated in the results of this PhD (Diaz, et al., 2001; Klink, 2007).

Early research by Schumann (1992) assessed the correlation between ENSO events, and 38–years of wind speed data from three stations in Durban, Port Elizabeth, and Cape Town, however, no relationships were identified, but the work acknowledged a need for future

research to consider additional, and longer series. To date, there has been no published work quantifying the impact of ENSO events on ground recorded wind speed in southern Africa. Extensive literature assesses ENSO events in relation to other climatic aspects of South Africa, including rainfall, temperature, and SST (Rouault, et al., 2010; Philippon, et al., 2011; Meque & Abiodun, 2015; Fant, et al., 2016). For instance, Philippon (2011) assessed data from 682 rain gauges in Cape Town between 1950, and 1999, and identified a strong correlation between ENSO events (ONI), and rainfall. During El Niño events, longer, more frequent, and larger rain-bearing events are identified where the inverse is observed in a La Niña event. Philippon (2011) similarly investigated the correlation between the WC coastal SST variance, and ENSO events. Wind speed was identified as a primary source of coastal upwelling, with a strong correlation against ENSO events. Weaker mean coastal wind speeds are observed during El Niño events, and stronger during La Niña events. Further work has identified that ENSO events record a strong correlation with temperature, rainfall, and the frequency of tropical cyclones across some regions of southern Africa (Fitchett & Grab, 2014; Weldon & Reason, 2014; Meque & Abiodun, 2015; Lakhraj-Govender & Grab, 2018; Pomposi, et al., 2018).

5.2.2 Indian Ocean dipole

The IOD is a primary source of inter–annual variability in the IO (Cai, et al., 2014). The extreme simultaneous IOD, and El Niño events of 1997 stimulated considerable scientific research, resulting in the IOD being identified as a global scale forcing factor in 1999 (Saji, et al., 1999; Webster, et al., 1999). It is known that SST variability alters the tropical IO atmospheric circulation impacting surrounding countries (Ashok, et al., 2003; Behera, et al., 2005; Ng, et al., 2018). Climate modes such as the IOD affect global climate, but given its dynamical complexity, is only broadly understood by current scientific knowledge (Bonan & Doney, 2018; Cox, et al., 2018; Gillingham, et al., 2018). Recently, Hui & Zheng (2018) assessed the correlation between the IOD, and global warming trends through climate model projections (community earth system model large ensemble). They identified a weak correlation between inter–annual IOD variance, and mean modelled warming change, while strong correlations are observed between IOD, and ONI amplitude change events.

The IOD exhibits both positive, and negative phases; during the positive phase, above average (warmer) SSTs are observed in the western IO, while the inverse (cooler) SSTs are observed in the eastern IO (NOAA, 2019b). During the negative phase, the opposite anomalies occur with cooler SSTs observed in the western IO as well as warmer temperatures observed in the eastern IO (Saji & Yamagata, 2003). IOD variance tends to be more extreme during the positive phase, resulting in wetter than usual conditions across East Africa, while drier than usual conditions prevail over Australia, and Indonesia, primarily because positive events tend to record higher amplitudes (Ummenhofer, et al., 2009; Saji, et al., 2005). The extreme positive event of 1997 resulted in wide-scale flooding across East Africa. However, bushfires, and drought were observed across Indonesia, and Australia (Black, et al., 2003). Further, the recent strong negative event of 2016 resulted in extensive drought over East Africa (Lu, et al., 2018). The IOD consistently presents a strong correlation with the East African climate, and is used as a short–term climatic predictor (Behera, et al., 2005; Marchant, et al., 2006).

Extensive literature documents the teleconnection between the IOD, and regional rainfall, circulation, climate variance, as well as sea, and land surface air temperatures (Dunning, et al., 2018; Lazenby, et al., 2018; Maoyi, et al., 2018; Pomposi, et al., 2018; Verdon-kidd, 2018). However, no literature to date has attempted to identify a teleconnection between the IOD, and ground recorded mean annual wind speeds in South Africa. Several authors have quantified IOD relationships to the intensity, and duration of South African rain-bearing months during both positive, and negative ENSO phases (Goddard & Graham, 1999; Black, et al., 2003; Ummenhofer, et al., 2009). During the positive phase, an abnormal low–pressure cell is generated in the warm south–western Indian Ocean. This results in increased evaporation due to the strengthened onshore flow, driving moist air toward the east coast of South Africa, and Mozambique (Reason, 2001; Slingo, et al., 2004; Zinke, et al., 2004; Black, 2005). Surface wind speeds are analysed during these phases to identify variance due to altered climate.

There is limited literature considering the tele–connectivity between IOD variance, and wind, with only several authors publishing related findings, as further presented in this paragraph. Behera et al. (1999) identified that the IOD was a primary influence driving strong Indian,

and East Asian shoreline surface wind speeds, directly resulting in below average regional SST's during 1994. The reduced SST induced a positive feedback convection which in turn-maintained surface wind speed anomalies. Similarly, Saji & Yamagata (2003) identified that the IOD variance exerted a strong effect on IO SST variability, in turn affecting regional wind speed. Vinayachandran et al. (2002) examined IOD variance between 1975, and 1998, and found that strong positive events were present in 1982, 1994, and 1997, resulting in above average SST, and strong easterly wind speed anomalies. During the strong negative events of 1984/1985, and 1996, central IO wind forcing was observed, as were increased westerly winds. Li & Wang (2003), and Liu et al. (2018) also identified wind direction reversal during the polar phases of the IOD, and related wind speed teleconnection. Recently, Lu et al. (2018) investigated the strong negative event of 2016, also confirming that the wind speed-evaporation SST feedback led to increased strength in summer IOD indicies. Finally, Nigam et al. (2018) assessed IOD/wind speed linkages between 1982, and 2010, identifying a strong wind stress teleconnection to IOD variability.

No literature was identified which statistically quantifies the relationship between wind speed, and IOD variance.

5.2.3 Antarctic Oscillation

The AAO also referred to as Southern Annular Mode, is an important source of atmospheric circulation variance in the southern hemisphere, southwards of 20˚S (Ferster, et al., 2018; Scott, et al., 2019; Lennard, 2019; Sniderman, et al., 2019). Hemispheric pressure gradient is identified as the primary driver of AAO variance, as teleconnections between mid-latitude climate events, and AAO variance are demonstrated (Thomson & Wallace, 2000). The AAO is defined by sea level pressure differentials between 40˚S, and 60˚S, and is recorded as the Antarctic Oscillation Index (AOI), which presents both positive, and negative phases (Gong & Wang, 1999). Positive phases of the AOI are dominated by a low–pressure cell at high latitudes. This results in the intensification of the westerly wind belt, and the Antarctic Circumpolar Current which is drawn towards Antarctica. The opposite occurs during the negative AOI phase when there is a high-pressure cell at mid-latitudes, resulting in the Antarctic Circumpolar Current shifting equatorward (Thomson, et al., 2011).

AAO teleconnection to climate variables such as cloud cover, wave height, temperature, and rainfall are well documented (Davis, et al., 2018; Vaideanu, et al., 2018). Marshall, et al. (2018) assessed 30–years of AAO data, and identified a statistically significant correlation between global ocean wind speed, and associated wave height. The seasonal analysis resulted in stronger correlations, and these authors concluded that local wind speed variations are directly related to the positive, and negative AAO phases. The AAO impacts the timing, and inter–annual variability of vegetation growing months in Africa, and South America, driven by the associated impact on rainfall (Zambrano, et al., 2016).

The work by Bianchi, et al. (2017), is the only to date, identifying tele–connectivity between near-surface wind speed, and AAO variance. These authors assessed MERRA wind speed data at a daily, monthly, seasonal, and annual scale across southern South America, considering AAO index variance. Results indicate that the AAO exerts a significant impact on mean seasonal, and inter-annual wind speed series. This impact is more prominent during summer, and spring, with negative correlations over Paraguay, Argentina, and northern Patagonia. They further concluded that the connections between wind speed, and AAO variance are scientifically important in the context of projecting climate change in the study area for the coming decades. Additionally, they highlighted the ability of the AAO index to be applied as a predictor of seasonal, and monthly wind energy generation variance in Argentina, Southern Patagonia, and central Chile.

To date, there is no literature documenting teleconnections between the AAO, and ground recorded wind speeds in South Africa. Sousa, et al. (2018) investigated the AAO impact on South African rainfall patterns during the 2015–2017 extreme drought over the WC. They concluded that the strong positive AAO phase was responsible for this drought. The intensified poleward shift during this period further resulted in record warm temperatures at a global scale (Sousa, et al., 2018). Earlier literature investigating the correlation between the AAO, and rainfall over the WC of South Africa, identified a strong correlation between the wettest/driest winters (JJA), and negative/positive AAO phases respectively (Reason, et al., 2002; Reason & Rouault, 2005; Pohl, 2010). A similar correlation between rainfall, and AAO was identified for the South Coast region of South Africa, resulting from the increased

(decreased) frequency of MLC systems related to the positive (negative) AAO phase (Weldon & Reason, 2014).

5.2.4 Mid–latitude cyclones

MLCs typically develop, and impact regions between latitudes 23°, and 66° north, and south of the equator (Eddy, 1965). They are short-lived events with a usual lifespan between three to ten days. They are generally associated with precipitation bearing systems (depending on location), and high wind speeds (Reason, 2019). Frequency, and strength of MLCs are primarily governed by SSTs, and the strength of the polar jet stream, resulting in inter–annual variability (Trouet, et al., 2018; Routson, et al., 2019). In this regard, it is well documented that MLCs are generally more frequent during winter–months, resulting from strengthened polar jet streams (Sato, et al., 2018; Verdon-kidd, 2018; Crétat, et al., 2019; Lennard, 2019).

Extensive literature is published investigating MLC activity, and climate tele–connectivity. Prikryl et al. (2009a; 2009b) assessed the correlation between high–speed solar wind streams, and MLC activity. They also identified that an increase of extreme cyclones occurs in months after solar stream events. These results are concurrent with previous literature confirming an important connection between solar events, and MLC activity (Tinsley, 1991). Several authors have investigated the relationship between MLC activity, and surface-level ozone, and collectively postulate that airstreams of MLC events are responsible for increased ozone measurements at monitoring stations (Shen, et al., 2015; Jing, et al., 2016; Knowland, et al., 2017; Ordóñez, et al., 2017). Westra et al. (2016) identified that south-east Australia observed an increased frequency of MLCs during winter–months of an El Niño event during the past decade. Similar results are documented evaluating ONI variance to inter–annual record of MLCs in Pacific (Pepler, et al., 2018). Kim et al. (2017) investigated MLC activity with specific interest on the variation of surface particulate matter (PM) concentration, and surface wind speed in the Seoul metropolitan area of Korea. They identified that years of below-average mean annual wind speed are paired with increased PM concentrations, and a strong positive correlation exists between recorded mean annual wind speed, and MLC activity. Their findings are further supported by several authors who have published similar findings globally (Agee, 1991; Key & Chan, 1999; McCabe, et al., 2001; Zhang, et al., 2015).

However, Key & Chan (1999) did not identify any statistically significant correlation (over 40–years (1958–1997) between ENSO activity, and MLC activity in the southern, and northern hemisphere tropics.

MLCs frequently pass over South Africa, and are often associated with winter rainfall over the southwestern Cape. Notably, ~70% of MLCs passing over the region are not rain-bearing (Berry, et al., 2011). The Cape provinces of South Africa record substantial inter–annual rainfall variability, driven to a large extent by ENSO events (Reason & Rouault, 2005; Philippon, et al., 2011; Engelbrecht & Landman, 2016; Crétat, et al., 2019; Mahlalela, et al., 2019). During La Niña (El Niño) periods, local climatic conditions are affected due to a poleward (equatorward) shift of the subtropical jet, resulting in dryer (wetter) years, anticyclonic (cyclonic) conditions over South Africa, and a decreased (increased) density of MLC events (Reason, et al., 2002; Weldon & Reason, 2014). Grab & Simson (2000) assessed 45–years of cold front activity between 1950, and 2000 over KwaZulu–Natal, intending to quantify the relationship between temperature, precipitation, and airflow during pre–, current– and, post-frontal phases as well as the associated relationship to air pollution levels in Msunduzi, Pietermaritzburg (South Africa). Findings concluded that during winter cold front events the strongest impact on regional pollution, and climate is observed, were the increased regional circulation resulted in decreased regional air pollution. Their objectives did not consider any connection between the MLC activity, and recorded wind speed.

Despite the regular incidence of MLC activity over southern African, the connection between these cyclonic event frequencies, and long-term wind speed have not been documented. To this end, this research presents the first documented connection (1950 to 2018) between MLC activity, and recorded wind speed in the study area.

5.2.5 Solar sunspot cycle

The sun is the ultimate source of energy for earth so that extensive literature available investigating its impact on earth's climate cycles (Beer, et al., 2000; Foukal, et al., 2006; Schulze-Makuch & Irwin, 2018). Several phases are well known, including the Schwabe cycle (8–16 years), Bruckner cycle (30–40 years), Gleissberg cycle (65–110 years), Suess cycle

(150–210 years), and Link cycle (380–420 years) (Nagovitsyn & Kuleshova, 2015). Sunspot data are available since 1750, with the number of sunspots ranging between near zero to over 100 per year (Haigh & Roy, 2010; Bianchi, et al., 2017). This 11–year cycle generates a one W/m^2 variance between trough, and peaks as it is a small percentage of total energy reaching the earth (Fröhlich, 2006; Gray, et al., 2010). Climate observations, however, indicate much more significant variations resulting from a complex solar–climate relationship (Gray, et al., 2010). Multiple studies investigate the solar cycle, and its impact on global climate, including variance in stratospheric ozone, temperature, winds, tropical circulations, clouds, and precipitation. The most distinctive, and documented sunspot cycle is ~11–year cycle (Meehl, et al., 2007; Misios, 2012; Mohammadi & Goudarzi, 2018).

Gray et al. (2010) noted the tropospheric region interacts most directly with particles, magnetic fields, and radiation emitted by the sun. They documented statistically significant relationships between mean tropospheric wind, and temperature, and the 11–year solar cycle, with stronger correlations during peak solar forcing periods. Their findings are supported by identifying the 11–year solar cycle's impact on the tropospheric wind being more predominant during winter (Crooks & Gray, 2005; Frame & Gray, 2008; Gray, et al., 2010). Ma et al. (2018) assessed solar data series between 1751–2016, from which they identified relationships between surface weather patterns across Europe, and the 11–year sunspot cycle. Labitzke & van Loon (1995) assessed a location near Hawaii, and demonstrated that mean mid-stratospheric temperatures, below 24km in altitude, are warmer during sunspot cycle peaks, and cooler during troughs. Several authors have assessed the relationship between the 11–year solar cycle, and midlatitude wind jets by documenting a weakening, and poleward shift during peak solar forcing periods (Haigh, 2002; Haigh, et al., 2005; Haigh & Blackburn, 2006). Multiple authors also indicate the relationship between the 11–year solar cycle, and satellite obtained ozone data, as well as a positive ozone response of 2–4% in the upper, and mid stratosphere during peak solar forcing (Soukharev & Hood, 2006; Randel & Wu, 2007; Gray, et al., 2010; Ma, et al., 2018).

Correlations are identified between rainfall across southern Africa, and solar activity, with significant 'Zero', and '3–month' time lags, explains by variations of SST anomalies in the

southwest Indian, and South Atlantic oceans (Mason & Tyson, 1992). Alexander & Emeritus (2005) identified a statistically significant 21–year periodicity in solar cycle variance, and assessed the relationship to river flow, annual rainfall, groundwater levels, and dam levels of South Africa. The authors concluded that during the first solar cycle (below-average solar activity), reduced river flow, and rainfall is observed, with widespread drought. They further demonstrate that the second cycle (above average solar activity) is associated with increased rainfall, and flood frequency. On the other hand, no literature is available assessing the relationship between the 11–year solar cycle, and near-surface wind speed over South Africa. The influence of solar forcing on South African climate is primarily mediated by SSTs, in turn driving regional circulation modes such as the IOD or AAO (Kodera, et al., 2007; Meehl, et al., 2007; Gray, et al., 2010).

5.3 Dataset description

This work assesses the climatological relationship of ONI, IOD, Sunspot cycle, MLC activity, and AAO on wind speed series at 15 stations located across the study region. As detailed in section 2.3, the Cape Agulhas wind speed series is the longest wind speed series (1950–2018), while the remaining 14 stations range between 1995, and 2018 (all series > 20–years). Anomalies are calculated for each data series by subtracting the total mean monthly from the mean of the month considered. The ONI is assessed for influence on station recorded wind anomalies at a concurrent, and 5–month temporal lag. Concurrent values for IOD, AAO, Sunspot, and MLC activity are used in the statistical analysis as there is little evidence of any lagged relationship to wind speed based on available literature (Angel & Isard, 1998; Thompson & Wallace, 1998; Rauthe & Paeth, 2004; Liu & Alexander, 2007; Rodrigues, 2015; Jasmine, et al., 2018). IOD, MLC, and solar cycle data are available for the continuous period 1950–2018, while AAO data are available for the period 1979–2018. The inter–climate teleconnections are considered in isolation, and inclusion considering primary, and secondary variables.

5.3.1 Spectral analysis

A spectral density analysis (Fourier transform) was performed to determine the dominant frequency of each data set. Further, the climate mode, and wind speed series underwent a white noise analysis at annual, seasonal, and monthly temporal scales. Applying Bartlett's methodology, every station indicats statistical significance ($p<0.01$) at a monthly, and seasonal scale, indicating that data series statistically differ from white noise. Similar statistical results ($p<0.01$) are obtained using Fisher's method, apart for the AAO record (non-significant $P>0.1$). At an annual scale, six data series (wind speed series of Cape Agulhas, Elliot, Noupoort Plettenberg, and climate series of MLC, and sunspot activity) passed the white noise tests of Bartlett's, and Fisher's methodology. At an inter–annual scale, the AAO, IOD, and ONI series failed both white noise tests as several strong monthly frequencies stand out over the observed white noise. The ONI, sunspot cycle, MLC, and all 15 wind data series exhibit a "red noise" data spectrum, defined by higher spectral density with decreasing frequency (Figure 5.2). Cyclic harmonics are assessed on the spectral analysis frequencies (Table 5.1).

The ONI observed multiple inter–annual frequencies (18, 42, 68, and 135.6 month) observed at monthly, and annual data scales (Figure 5.2a). Given that the ENSO is an atmospheric–ocean coupled oscillation, the presence of multi-temporal frequencies is expected given a slow response time to atmospheric change. Similarly, the IOD also indicates inter-annual (18, 25, 37, 62 months), and decadal (34–year) harmonics (Figure 5.2b). The sunspot cycle only indicates decadal oscillations, the strongest being an 11.3–year harmonic, and two less prominent (22–34 year) (Figure 5.2c). Strong 9.7, and 34–year harmonics are identified in the annual, and decadal MLC, and wind speed data series (Figure 5.2d, e). The following sections characterise the results between each climate mode, and wind speed anomalies (Figure 5.3, Figure 5.4).

Table 5.1: Primary harmonic, and period observed in each data series.

Climate mode	ONI	AAO	IOD	MLC activity	Sunspot activity	Wind speed
Harmonic	68–month	16–month	62–month	12–month	11.3–year	12–month
Period	34–month	8–month	31–month	6–month	67–month	6–month

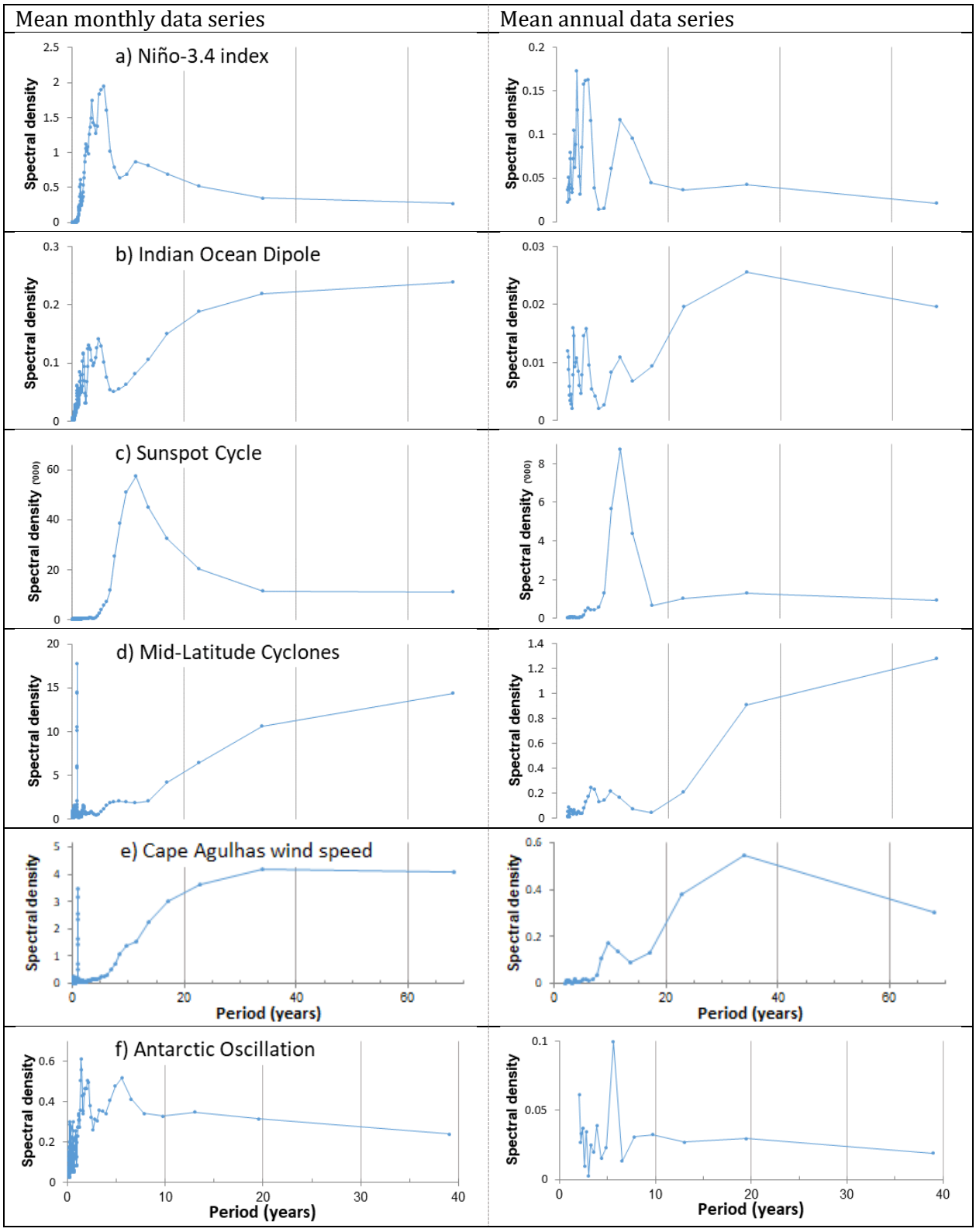


Figure 5.2: Monthly (left), and annual (right) data spectral density for all available data series.

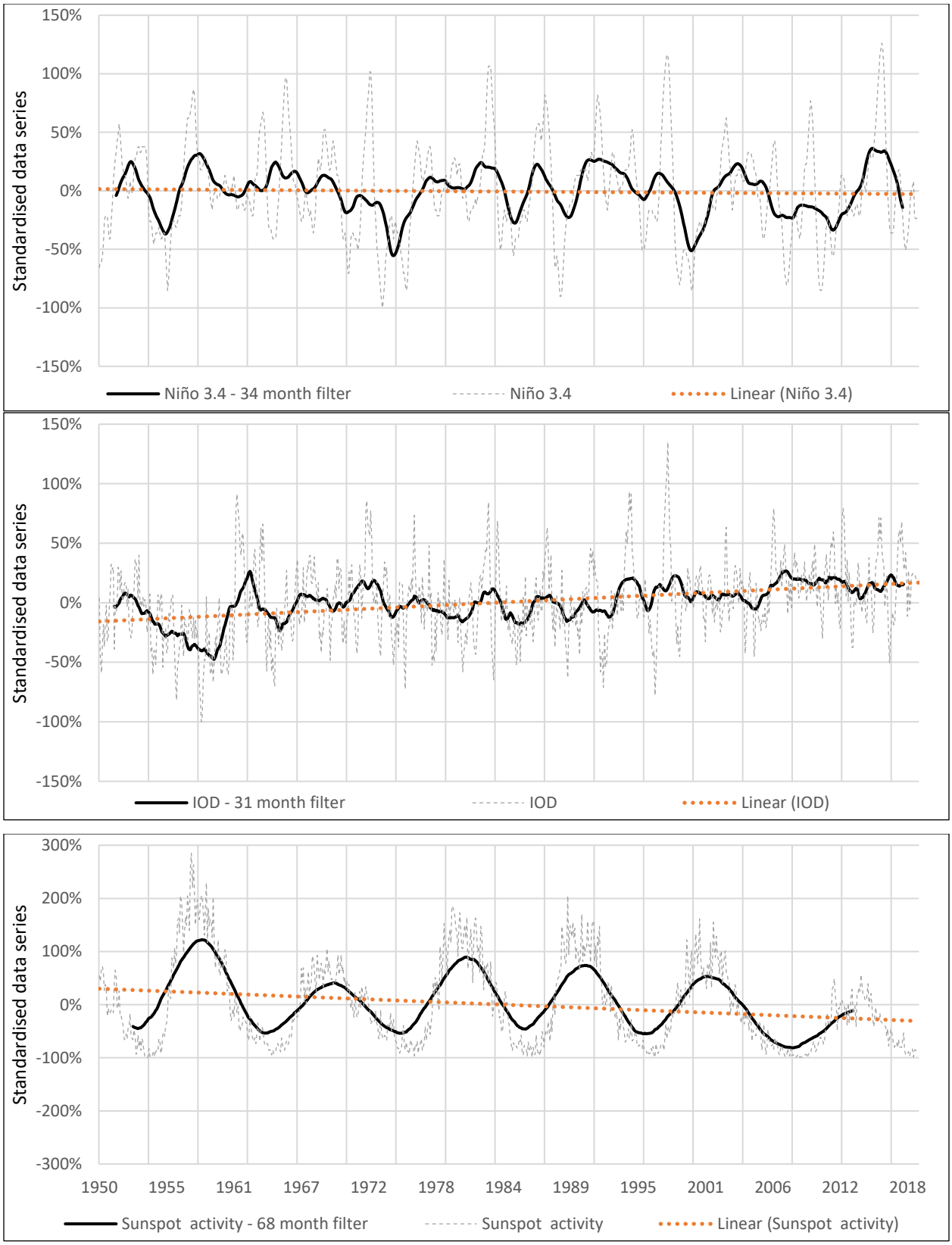


Figure 5.3: ONI, IOD,, and Sunspot activity Gaussian filtered monthly data anomalies (1950 –2018).

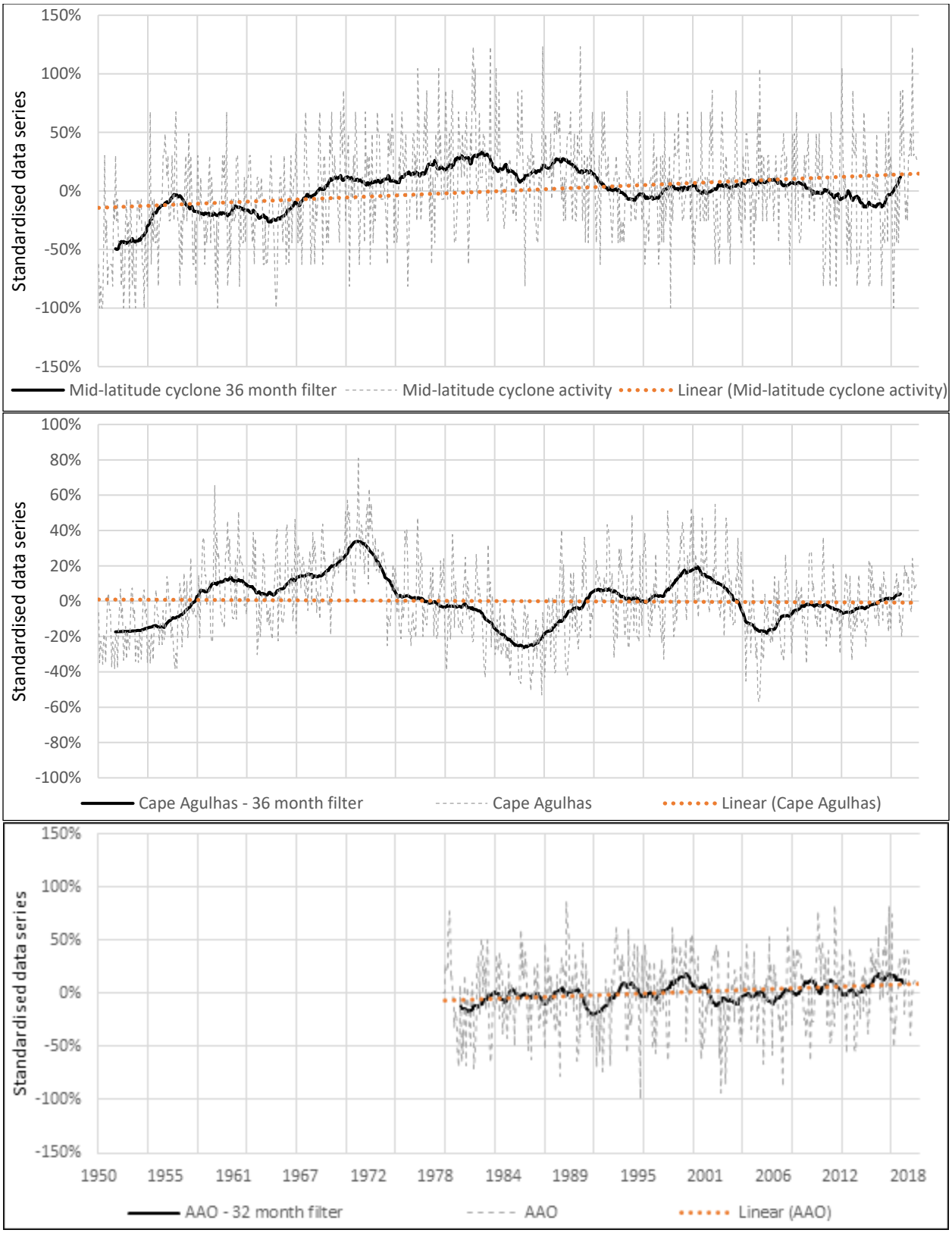


Figure 5.4: Mid–latitude cyclone activity, Cape Agulhas wind station, and AAO Gaussian filtered monthly data anomalies (1950–2018).

5.4 Results

Results demonstrate variable associations between wind speed anomalies across 15 stations, and five climate variables (ONI, AAO, IOD, MLCs, and sunspot activity) for the period 1995 – 2018 (Cape Agulhas 1950–2018). Spectral density analysis is used to identify each climate mode harmonic while white noise is checked by using both Fisher's kappa (Fisher's), and Bartlett's Kolmogorov–Smirnov (Bartlett's) statistical methodologies. Thereafter, wind speed anomalies are regressed, and correlated to the five climate variables at a monthly, seasonal, annual, and periodic scale. The results are tested for statistical significance ($P<0.1$).

5.4.1 Multi–decadal association of station observed wind speed characteristics with key climate indices

All climate variables showed weak, and statistically non-significant inter–mode relationships at an inter–month, –seasonal, and –annual scale between 1995 – 2018 (Cape Agulhas 1950–2018). This result is not surprising as the spectral analysis only identifies a dominant annual harmonic in the MLC data series. The 5–month lagged ONI proved statistically non-significant at a concurrent, and 5–month lagged scale to all wind speed anomalies.

5.4.1.1 Inter–annual, and inter-seasonal

The multiple regression statistics of all climate variables proved statistically significant ($P<0.1$), except for the 5–month lagged ONI, and AAO series (Table 5.2). The most notable observation is the inter–annual result between sunspot activity, and secondary climatic variables. The statistically significant ($P<0.01$) multiple regression statistics (multiple $R = 0.475$), and adjusted R statistic (22.16%) indicate a moderate teleconnection. Similarly, the statistically significant ($P<0.01$) inter–annual multiple regression statistics (multiple $R = 0.419$) between the ONI record, and associated secondary climate variables (AAO, IOD, and MLCs) explains 13.67% of inter–annual mode variance. A statistically significant ($P<0.1$) inter–annual multiple regression statistic (multiple $R = 0.313$) is identified between the IOD, and MLC activity, and the AAO index.

This result is expected as MLC activity is the only variable which indicates an annual harmonic, identified by the spectral analysis. All correlations between individual climate variables are weak, with only two statistically significant ($P<0.05$) results observed between the IOD data series, and the ONI, and AAO. Correlation strength increased between climate variables when assessed at a mean annual scale (detailed information is provided in Section 5.4.3)

Elliot, Langebaan, and Queenstown are the only stations which indicate statistically significant ($P<0.01$) results to the climate variables when performing a multiple regression analysis. Few statistically significant ($P<0.1$) correlations are present between wind speed (Cape Agulhas, De Aar, Noupoort, Queenstown, and Tygerhoek), and inter–annual climate mode variance (Table 5.2). Stations were further assessed seasonally to quantify the climate mode impact on seasonal variance. Weak results are identified between seasonal wind speed, and climate mode variance, but varying considerably between stations. Significant ($P<0.05$) multiple regression statistics are present for autumn (8.4%), and spring (6.1%) between the Cape Agulhas wind speed, and climate mode data series. Similarly, Plettenberg Bay (22.1%), and Springbok (21%) indicate statistically significant ($P<0.1$) multiple regression climate mode statistics in Autumn, while Uitenhage (26.1%) records the only statistically significant ($P<0.1$) multiple regression statistic in winter. The ONI is the only climate mode which does not record any statistically significant ($P<0.1$) seasonal relationship to wind speed variance, even though inter–month, and inter-annual statistical significance are observed.

Considering spatial clustering at a provincial scale on an inter-annual resolution, stations located in the Eastern Cape province returned the strongest multiple regression statistic of 0.555. This indicates that when combined, climate drivers exert a moderate impact on observed wind speed, explaining 30.84% (multiple R^2) of recorded variability. This decreases for the Northern, and Western Cape explaining only 16.12%, and 18.32% of recorded variability (multiple R^2) respectively. Climate driver variance explains the least observed variance for stations located in coastal areas (11.76%), but increase for inland (23.91%), and hinterland (25.17%) regions (Table 5.2).

The Eastern Cape inland region indicats the strongest association to climate drivers, which explains 34.81% (multiple R^2) of inter-annual wind speed variance, followed by the Western Cape hinterland (25.96%), and Eastern Cape hinterland (23.62%) regions. The lowest multiple regression result is obtained from stations located in the Northern Cape coastal region, explaining a nominal 7.34% (multiple R^2) of observed wind speed variance. Similar to results obtained from the assessment of individual stations, non-significant correlations are obtained when clustering stations regionally. There are only three regions which observe double digit impacts, all located in the Eastern Cape province. These include the association between stations located in the Eastern Cape hinterland, and a concurrent ONI record, Eastern Cape inland, and AAO record, and Eastern Cape inland, and sunspot activity, explaining 15.68%, 13.91%, and 14.75% (multiple R^2) of recorded variability, respectively (Table 5.2).

Further, non-significant results are obtained performing a similar clustering assessment at a mean seasonal resolution. At a provincial scale, the strongest multiple regression statistic is obtained between climate variables, and the Eastern Cape during summer, explaining 9.59% (multiple R^2) of observed wind speed variance. The only notable multiple regression statistics from the regional assessment are observed in summer, and winter for stations located in the Eastern Cape hinterland region, where climate mode variance explains 20.98%, and 33.64% (multiple R^2) of observed wind speed variability respectively. Additionally, the EC hinterland is the only region to record a statistically significant ($P<0.05$) relationship to climate mode variance observed during winter (Table 5.3).

Table 5.2: Inter–annual wind speed correlation (r), and multiple regression (multiple R) for each climatic mode.

Station / Region/Mode	Multiple regression	5–month lagged ONI	ONI	AAO	IOD	MLC activity	Sunspot activity
ONI	**0.419**	**-**	**n/a**	**-**	**-**	**-**	**-**
AAO	0.436	**-**	-0.117	**n/a**	**-**	**-**	**-**
IOD	**0.509**	**-**	**0.269**	0.197	**n/a**	**-**	**-**
MLC activity	*0.313*	**-**	-0.136	0.179	0.101	**n/a**	**-**
Sunspot activity	**0.475**	**-**	0.133	0.238	**-0.341**	0.148	**n/a**
Alexander Bay	0.383	-0.061	-0.086	-0.331	-0.105	-0.017	0.117
Beaufort West	0.376	0.128	-0.193	-0.042	-0.221	-0.106	-0.129
Brandvlei	0.510	0.033	-0.214	0.129	0.111	-0.165	-0.281
Cape Agulhas	0.349	-0.043	*-0.072*	0.099	**0.103**	0.031	**0.221**
De Aar	0.468	*0.241*	*0.092*	0.034	-0.273	-0.364	*0.063*
Elliot	*0.604*	-0.137	-0.073	-0.286	-0.182	-0.357	0.485
Koingnaas	0.159	0.040	-0.054	0.021	0.065	-0.114	0.052
Langebaan	**0.640**	-0.274	-0.212	0.209	0.184	*-0.378*	-0.131
Noupoort	0.479	0.221	0.112	0.108	-0.191	-0.383	**0.266**
Plettenberg Bay	0.324	-0.024	-0.024	-0.242	-0.108	-0.056	0.240
Queenstown	*0.576*	0.052	-0.124	-0.46	-0.298	-0.046	*0.283*
Springbok	0.410	-0.239	-0.324	-0.034	0.031	0.065	-0.165
Still bay	0.500	-0.130	-0.229	-0.265	0.114	0.325	-0.100
Tygerhoek	0.379	-0.053	**-0.029**	0.031	0.311	-0.103	-0.233
Uitenhage	0.486	-0.066	-0.396	-0.187	-0.279	0.020	0.080
Mean of stations[11]	0.426	-0.097	-0.257	-0.117	-0.088	-0.232	0.226

Bold underline denotes a MK statistical significance of 99% (P<0.01)
Bold denotes a MK statistical significance of 95% (P<0.05)
Underline denotes a MK statistical significance of 90% (P<0.1)

[11] *Mean all stations (1995 – 2018)*

Table 5.3: Seasonal multiple regression statistics to all climatic modes per station, and region.

Station / Region	Summer	Autumn	Winter	Spring
Alexander Bay	-0.151	-0.218	0.298	-0.193
Beaufort West	0.127	0.018	0.233	-0.278
Brandvlei	-0.364	0.133	0.222	0.320
Cape Agulhas	0.109	**0.187**	0.069	**0.136**
De Aar	0.356	0.300	0.000	-0.171
Elliot	**0.604**	0.164	0.138	0.036
Koingnaas	0.069	-0.318	-0.271	0.009
Langebaan	-0.120	0.244	-0.129	0.113
Noupoort	0.264	0.387	-0.227	-0.109
Plettenberg Bay	0.364	*0.491*	-0.340	-0.109
Queenstown	-0.133	0.056	-0.331	-0.082
Springbok	0.267	*0.467*	0.313	0.338
Still bay	-0.289	-0.018	0.247	-0.264
Tygerhoek	-0.318	0.291	-0.004	-0.391
Uitenhage	*0.458*	-0.318	*0.580*	-0.089
Mean of stations[12]	-0.167	-0.251	-0.233	-0.176
Eastern Cape	0.324	-0.167	0.156	-0.002
Northern Cape	0.162	**0.664**	-0.011	-0.142
Western Cape	-0.162	-0.269	-0.344	-0.191
Coastal	0.164	0.087	-0.242	0.064
Hinterland	0.189	-0.193	-0.144	-0.338
Inland	0.202	0.007	-0.336	-0.293
EC Hinterland	0.311	-0.353	**0.624**	-0.131
EC Inland	0.176	-0.040	0.009	0.013
NC Coastal	0.242	-0.142	-0.238	-0.173
NC Inland	0.118	*0.569*	0.009	-0.047
WC Coastal	0.140	-0.013	-0.107	-0.089
WC Hinterland	-0.240	**0.638**	-0.502	-0.120
WC Inland	0.282	-0.002	0.371	-0.320

Bold underline denotes a MK statistical significance of 99% (P<0.01)
Bold denotes a MK statistical significance of 95% (P<0.05)
Underline denotes a MK statistical significance of 90% (P<0.1)

[12] *Mean all stations (1995 – 2018)*

5.4.1.2 Inter–month

The inter–climate multiple regression statistics of all climate variables proved statistically significant (P<0.1), except for 5–month lagged ONI, and MLC data series. The inter–month multiple R between sunspot activity, and secondary climatic variables decreased at monthly scale. On the other hand, unlike the inter–annual result, statistically significant (P<0.10) results are identified against every climate mode assessed concurrently. A similar increase in statistical significance is present between other climate variables. All correlations between climate variables on an inter-monthly scale are weak (Table 5.4). The most notable observation is that a statistically significant (P<0.1) inter–month multiple regression statistic is observed between every station, and the climate modes. The statistically significant (P<0.01) multiple regression results (adjusted R) confirmed that climate mode variance drives 6.9% of inter–month Cape Agulhas wind speed variance between 1950, and 2018. All results are weak, but the scientific importance of statistical significance across all recorded wind speed values indicates that a more intricate system exists. These findings are presented in section 5.4.2, and 5.4.3 (Table 5.4).

The most statistically significant (P<0.01; n = 13 station records) correlations between MLC activity, and wind speed anomalies are identified at a monthly scale. Positive (four stations), and negative (nine stations) correlations are present which explain a mean 9% of wind speed variance. The AAO indicates a statistically significant P<0.01 (P<0.1) results with five (six) stations. All statistically significant (P<0.1) AAO results are negative, explaining ~ 3.5% of wind speed variance. Four Stations record weak inter–month statistically significant (p<0.03) results with sunspot activity. Considering the limited scientific knowledge documenting the solar–climate teleconnection, this observation is of interest, and further assessed at a cyclic, and 34–year harmonic. Cape Agulhas is the only station to record a statistically significant (P<0.01) correlation with IOD variance, explaining r^2 = 1.51% of wind speed variance. Uitenhage (r^2 = 2.04%), and Queenstown (r^2 = 0.94%) are the only stations which record a statistically significant (P<0.01) correlation with a concurrent ONI record, explaining a small percentage of wind speed variance (Table 5.4).

At an inter-month resolution, all regions recorded a significant ($P<0.01$) multiple regression statistic when assessed against the climate modes. At a provincial scale, the assessed climate modes exert most impact on the Northern Cape, explaining 12.64% (multiple R^2) of observed wind speed variance, followed by the Eastern Cape (multiple $R^2 = 12.13\%$), and Western Cape (multiple $R^2 = 8.8\%$). The hinterland region observed the strongest impact from climate mode variance explaining 13.86% (multiple R^2), while the coastal region indicates the weakest impact, explaining just 8.15% (multiple R^2) of recorded wind speed variance. At a finer scale, the Western Cape hinterland region indicates these stations are the most affected, with a moderate multiple regression statistic of $r = 0.409$ ($P<0.01$) explaining 16.69% (multiple R^2) of recorded wind speed variance. The weakest impact is also observed in the Western Cape, in the coastal region where climate mode variance only explains 4.8% (multiple R^2) of recorded wind speed variance. When assessing the correlation between the regions, and each individual climate mode, non-significant results are observed for the ONI, AAO, and sunspot activity scenarios. The AAO indicates a significant ($P<0.05$) correlation between the Eastern Cape ($r = 0.210$), and Eastern Cape inland ($r = 0.22$) regions which explains a nominal 4.41%, and 4.82% (multiple R^2) of observed variance.

All regions indicate a significant ($P<0.05$) association to MLC activity, however, the correlations are weak. The Northern Cape indicates the strongest provincial correlation ($r = -229$) explaining 5.25% (multiple R^2) of observed wind speed variance. This was followed by the Eastern ($r = 0.176$), and Western ($r = -0.096$) Cape provinces, explaining 3.1%, and 0.91% (multiple R^2) of observed variance respectively. The hinterland region indicates stations located in this area are impacted the most ($r = -0.256$) by the climate mode variance compared to stations located in coastal ($r = 0.151$), and inland ($r = 0.015$) regions. The sub-region of the Western Cape hinterland ($r = -0.368$) recorded the strongest correlation, followed by the Northern Cape coastal ($r = -0.342$), and Eastern Cape inland ($r = 0.281$) regions. The observed climate mode variance explains 13.51%, 11.70%, and 7.87% (multiple R^2) of recorded wind speed variance respectively.

Table 5.4: Inter–month wind speed correlation (r), and multiple regression (multiple R) statistics for each climate mode.

Station / Region / Mode	Multiple regression	5–month lagged ONI	ONI	AAO	IOD	MLC activity	Sunspot activity
ONI	**0.321**	-	**n/a**	-	-	-	-
AAO	**0.239**	-	**-0.134**	**n/a**	-	-	-
IOD	**0.368**	-	**0.275**	0.047	**n/a**	-	-
MLC activity	0.072	-	-0.025	**-0.169**	-0.003	**n/a**	-
Sunspot activity	**0.278**	-	**0.100**	**-0.089**	**-0.214**	*0.061*	**n/a**
Alexander Bay	**0.404**	-0.014	-0.058	0.016	-0.024	**-0.372**	0.013
Beaufort West	**0.306**	0.088	-0.044	**-0.187**	-0.027	**0.233**	-0.047
Brandvlei	**0.404**	0.035	-0.063	-0.017	0.023	**-0.325**	-0.083
Cape Agulhas	**0.263**	0.007	-0.022	0.011	**0.123**	**-0.126**	**0.131**
De Aar	**0.335**	0.093	-0.001	-0.071	-0.012	**-0.264**	-0.023
Elliot	**0.469**	-0.017	-0.004	**-0.254**	0.059	**0.403**	**0.149**
Koingnaas	**0.366**	0.016	-0.041	-0.060	0.032	**-0.312**	-0.001
Langebaan	**0.473**	-0.046	-0.061	0.009	-0.064	**-0.447**	-0.058
Noupoort	**0.369**	0.092	0.017	0.005	-0.011	**-0.319**	0.068
Plettenberg Bay	**0.202**	0.021	-0.072	-0.080	-0.016	0.057	**0.115**
Queenstown	**0.276**	0.010	-0.097	**-0.185**	-0.068	**0.158**	0.099
Springbok	**0.255**	-0.036	-0.068	*-0.098*	0.015	**0.218**	-0.034
Still bay	*0.192*	-0.017	-0.063	**-0.155**	0.012	-0.002	-0.040
Tygerhoek	**0.344**	-0.007	-0.009	-0.030	0.079	**-0.288**	**-0.121**
Uitenhage	**0.300**	0.012	**-0.143**	**-0.191**	-0.042	-0.033	-0.001
Mean of stations	**0.369**	0.027	-0.016	*-0.106*	0.032	**-0.198**	0.072

Bold underline denotes a MK statistical significance of 99% (P<0.01)
Bold denotes a MK statistical significance of 95% (P<0.05)
Underline denotes a MK statistical significance of 90% (P<0.1)

5.4.1.3 Assessment of anomalous wind years

Anomalous high, and low wind speed years are identified for all wind speed series used to investigate climate mode anomalies that may have influenced wind speed at a seasonal, and mean annual scale. ENSO variability is identified as the primary mode influencing regional wind speed. Periods which record very strong (VSE), strong (SE), moderate (ME), and weak (WE) El Niño as well as strong (SL), moderate (ML), and weak (WL) La Niña events are identified. Anomalous years vary, however, but distinct ENSO impacts are observed at all stations.

Periods following VSE, and SE events are generally associated with high wind speed anomalies. The highest mean annual wind speed anomalies for every season result from the 1997–1998 VSE event. Inversely, the lowest wind speed anomalies are observed during post-ENSO transition periods in 2004, 2006, 2015–2016. Fewer observations are associated with SL events while low wind speed anomalies generally occur post SL events. The only two exceptions are the SL in 2011, resulting in high winter wind anomalies (Alexander Bay, and Springbok). In contrast, the VSE in 2016 resulted in low spring wind speed anomalies (Beaufort West, Queenstown & Uitenhage). Interestingly, the IOD, and AAO indicates strong positive indexes prior, and during 2011–2015. Additionally, in 2011, the AAO recorded its highest peak since 1989. It is expected that a combination of the strong IOD, and AAO indexes during 2011 (SL), and 2015 (VSE), in combination with the associated ONI anomalies, likely resulted in these unexpected outcomes for the five stations mentioned above.

The strongest positive mean annual wind speed variance (4.23%, 0.161 m/s) is present between 2006, and 2007. During the same period, De Aar (6.37%), Elliot (9.26%), Koingnaas (10.38%), and Uitenhage (9.48%) recorded strong positive inter–annual wind speed change points (Figure 5.5). The strongest decreasing mean annual wind speed variance (–4.93%, –0.187 m/s) is identified between 2003, and 2004, and followed by 2014–2015 (–3.15%, –0.120 m/s). During the 2003/4 period, the Cape Agulhas (–14.15%), Elliot (–9.51%), Noupoort (–14.04%), and Still Bay (–6.69%) stations recorded strong decreasing inter–annual wind speed change points.

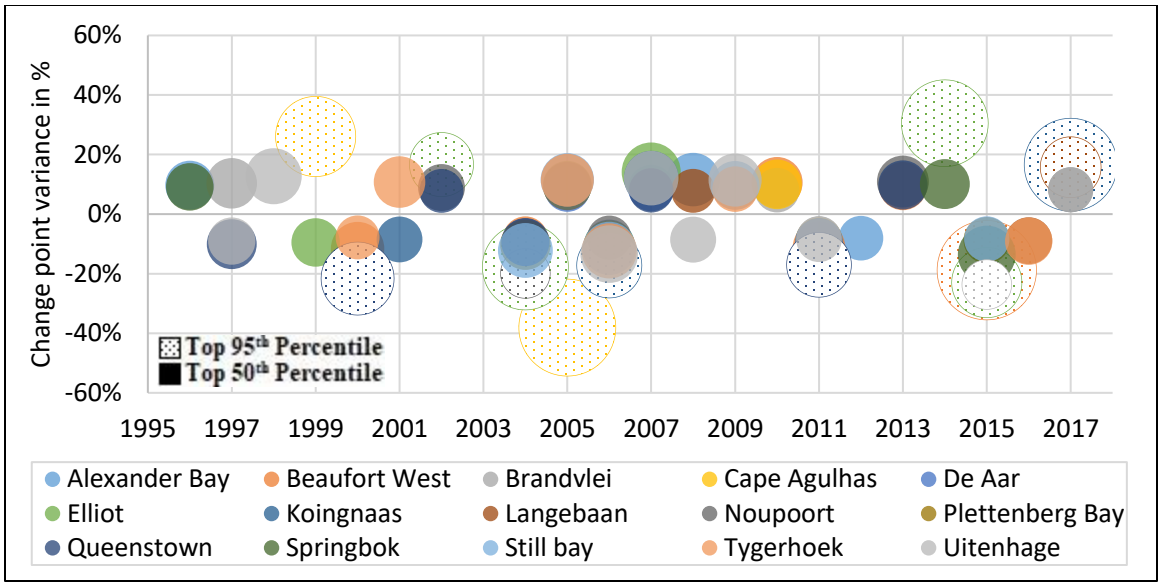


Figure 5.5: Anomalous high, and low wind speed change points (larger circles indicate stronger anomalies relative to station mean wind speed).

5.4.2 Periodic association of observed wind speed characteristics with key climate indices

The spectral analysis result identified the period of each climate mode, each of which was in turn applied as a Gaussian filter to the data series. The resulting data are correlated, and tested for statistical significance ($P<0.1$). A multiple regression analysis quantifies the relationship between primary, and secondary climate variables (Table 5.5). The multiple regression, and individual station results are presented after the tables, split into subsections per climatic mode.

Table 5.5: Periodic climatic mode correlation (r) with wind speed series.

Station	5 month lagged ONI	ONI	AAO	IOD	MLC activity	Sunspot activity
Gaussian filter	34–month	34–month	8–month	31–month	6–month	67–month
ONI	**-**	**-**	**-0.201**	**-0.093**	-0.055	**0.387**
AAO	**-0.169**	**-0.286**	**-**	**0.540**	**-0.238**	**-0.505**
IOD	**-0.131**	**-0.136**	**0.187**	**-**	0.050	**-0.626**
MLC activity	**-0.147**	**-0.151**	**-0.229**	**0.120**	**-**	**0.122**
Sunspot activity	**0.154**	**0.224**	**-0.208**	**-0.501**	**0.134**	**-**
Alexander Bay	**-0.130**	**-0.134**	*-0.104*	**-0.149**	0.070	-0.053
Beaufort West	**-0.181**	**-0.179**	**-0.214**	0.030	**0.160**	-0.004
Brandvlei	0.111	0.075	-0.046	*0.112*	-0.076	**-0.137**
Cape Agulhas	**-0.068**	**-0.085**	0.068	**0.137**	*0.059*	**0.146**
De Aar	-0.041	0.002	*-0.106*	0.049	0.026	**0.363**
Elliot	**-0.303**	-0.083	**-0.426**	0.073	0.066	**0.148**
Koingnaas	**0.200**	**0.208**	-0.041	**0.210**	0.022	-0.009
Langebaan	**-0.272**	**-0.263**	*0.099*	**0.365**	-0.037	**-0.375**
Noupoort	0.041	0.074	0.013	-0.130	-0.056	**0.535**
Plettenberg Bay	-0.052	-0.060	**-0.139**	**-0.114**	-0.020	**0.335**
Queenstown	**-0.336**	**-0.316**	**-0.341**	*-0.113*	**0.120**	**0.349**
Springbok	**-0.289**	**-0.372**	-0.066	**0.247**	0.048	-0.081
Still bay	**-0.393**	**-0.332**	**-0.233**	**0.224**	**0.157**	**-0.382**
Tygerhoek	**-0.165**	**-0.150**	0.037	**0.370**	-0.003	**-0.370**
Uitenhage	**-0.516**	**-0.521**	**-0.224**	0.099	**0.170**	**-0.224**
Mean of stations	**-0.264**	**-0.209**	0.080	0.043	**-0.209**	**0.182**

Bold underline denotes a MK statistical significance of 99% (P<0.01)
Bold denotes a MK statistical significance of 95% (P<0.05)
Underline denotes a MK statistical significance of 90% (P<0.1)

5.4.2.1 ONI periodicity (34–month)

ENSO oscillations are well documented with several inter-annual harmonics. Based on the spectral analysis result, a Gaussian 34–month filter was applied to all data. The ONI results are regressed at a concurrent, and 5 month lagged scale. All climate mode results are statistically significant (P<0.01), and in every case, a stronger correlation is present concurrently. Negative correlations are indicated for all climatic modes apart for sunspot activity, for which there is a positive correlation (Table 5.5).

Eleven stations (73%) indicate a statistically significant ($p<0.02$) correlation with the lagged ONI data series, but this is reduced to ten stations at a concurrent temporal scale of investigation. The Uitenhage series portrays the strongest correlation with the ONI ($r = -0.521$) while the only significant ($P<0.1$) positive correlation is identified between Koingnaas, and ONI ($r = 0.208$). Considering the correlation between Uitenhage, and ONI data series, the lagged ONI explains 26.6% of wind speed variance but increases to 27.2% at a concurrent temporal scale of investigation. When removing statistically non-significant stations, concurrent ONI explains 8.1% of wind speed variance, and increases marginally to 8.2% at a 5–month lagged period (Table 5.5)

Further, the stations have been grouped by province, and region. Considering the multiple regression statistics results of the ONI at a concurrent, and five month lagged scale the association is stronger in all cases at a five-month lagged scale. In this regard, results are presented for a five-month lagged ONI. It is noted that the five-month lagged ONI assessment indicates this to be the strongest driver of regional wind speed at a periodic scale compared to the weaker results obtained for other climate modes. At a provincial scale the Eastern Cape indicates the strongest (multiple $R = -0.385$) association with a five-month lagged ONI when assessed at a periodic scale which, explains 14.82% (multiple R^2) of observed wind speed variance. Results for the Northern, and Western Cape are non-significant, and extremely weak explaining 0.83%, and 3.55% (multiple R^2) of observed wind speed variance respectively. At a regional scale, stations located in the hinterland region indicate the periodic variance of a five-month lagged ONI, explaining 10.09% (multiple R^2) of observed wind speed variance. The multiple regression result for stations located in the coastal, and inland regions are inconsequential. The Eastern Cape hinterland indicates the strongest connection between stations located in this region, and a five-month lagged ONI, explaining 26.63% (multiple R^2) of observed wind speed variance. The only other region indicating a significant ($P<0.05$) association to a five-month lagged ONI is the Eastern Cape inland area, explaining 10.21% (multiple R^2) of recorded wind speed variance.

5.4.2.2 AAO periodicity (8–month)

The spectral density analysis identified a strong 16–month AAO harmonic. Considering this, an 8–month Gaussian filter (one phase) was applied to all data. A weak but statistically significant (P<01) correlation is present between AAO, and all climate variables, but for which none are of scientific importance.

Six stations record statistically significant (p<0.05) correlations with AAO variance, increasing to nine when considering P<0.1. All statistically significant (P<0.1) results are weak, and record a negative mean correlation (r = –0.263), explaining 2–18% of wind speed variance. Langebaan is the only station to record a statistically significant (P<0.1) positive correlation (r = 0.099) to AAO period variance. The mean negative correlation between recorded wind speeds, and the 8–month AAO period, indicates that AAO peaks (troughs) record below (above) average wind speed anomalies. The NC did not record any statistically significant (p<0.1) correlations but data from every station in the EC indicate a statistically significant (P<0.01) correlation with the 8–month AAO period. Further, the EC stations record the strongest (r = –0.330) correlation with the AAO periodicity, explaining 10.9% of wind speed variance (Table 5.5).

When assessed regionally, the periodic variance of the AAO explains a nominal amount of observed wind speed variance. There are only two significant (P<0.05) results which include stations located in the Eastern Cape province, and more specifically the Eastern Cape inland regions. An assessment based on the periodic variance of the AAO, and other climate modes explains 10.91%, and 14.71% (multiple R^2) of observed wind speed variance respectively. No other regions indicate noteworthy results.

5.4.2.3 IOD periodicity (31–month)

The spectral density analysis identified a dominantly 62–month harmonic. A 31–month Gaussian filter was applied to all data, and then regressed the IOD 31–month filtered data anomalies. All recorded climate variables indicate statistically significant (P<0.01) results. The strongest 31–month IOD period tele–connection is present between the ONI (r = 0.540), and sunspot (r = –0.501) activity. Weak, non-significant correlations are identified between

IOD, and ONI as well as MLC activity. The most notable teleconnection is with solar sunspot activity as it explains 25.1% of IOD variance. Statistically significant ($p<0.05$) positive, and negative relationships are present between eight of the station wind speed anomalies, and the IOD periodicity variance. All statistically significant ($P<0.05$) relationships are determined to be weak, explaining 5.5% of observed wind variance at a 31–month periodicity. The EC did not record any statistically significant ($P<0.1$) relationships. In contrast, three stations in the NC, and five stations in the WC indicate statistically significant ($P<0.05$) relationships with 31–month IOD periodicity (Table 5.5).

When assessed regionally, the periodic variance of the IOD explains a nominal amount of observed wind speed variance. There are only two significant ($P<0.05$) results which include stations located in the hinterland, and at a higher spatial scale the Western Cape hinterland regions. An assessment based on the periodic variance of the IOD, and other climate modes explains 7.73%, and 13.51% (multiple R^2) of observed wind speed variance respectively. No other regions indicate noteworthy results.

5.4.2.4 MLC periodicity (12–month)

A 6–month (one phase) Gaussian filter was applied to all data, and the resulting data anomalies were regressed to the MLC 6–month filtered data anomalies. Weak significant connections are observed between cyclone activity, and AAO along with sunspot activity, but are of no scientific importance. MLC activity was not expected to be a primary driver of wind speed variance as it is confirmed by only four stations which record a statistically significant ($P<0.01$) correlation with a 6–month MLC periodicity. These stations record a mean weak ($r = 0.2$) correlation with the MLC periodicity while explaining a nominal 2.3% of wind speed variance (Table 5.5).

When assessed regionally, the periodic variance of MLC activity explains the least of observed wind speed variance. All results are non-significant ($P>0.05$), and none are noteworthy results.

5.4.2.5 Sunspot periodicity (67–month)

Results obtained from the 67–month sunspot periodicity analysis are scientifically important. Every climate mode indicates a statistically significant ($P<0.01$) correlation with sunspot periodicity. The strongest correlations are observed with the IOD ($r = –0.626$), and AAO ($r = –0.505$), and it is followed by the ONI. Sunspot periodicity explains a moderate percent of IOD (39.2%), AAO (25.5%), and ONI (15.0%) variance. A multiple regression analysis was applied to quantify the connectivity of the 67–month sunspot periodicity across all other anomalies, and all records indicate statistically significant ($P<0.05$) relationships. The ONI, IOD, MLC, sunspot, Cape Agulhas wind speed, and AAO data series were regressed to the sunspot periodicity for the period 1950–2018 (1979–2018). The regression confirmed a strong ($r = 0.771$) relationship for the period 1950–2018, which increases even further to $r = 0.843$ when the AAO is included from 1979. Considering this result, the sunspot 67–month periodicity explains 59.3% of climate mode variable between 1950, and 2018 as it increased to 70.8% for the period 1979–2018. This finding further confirms the complexity of teleconnections between global climate variables, which has not previously been quantified.

Positive, and negative statistically significant ($p<0.02$) relationships are identified between eleven stations, and the 67–month sunspot period. The strongest correlation ($r = 0.535$) is measured with the Noupoort wind speed series. However, the remaining stations record weak correlations to a 67–month sunspot periodicity. The sunspot cycle explains, on average, 10.8% of wind speed variance at statistically significant ($P<0.05$) stations, ranging between Cape Agulhas (1.9%), and Noupoort (28.6%) (Table 5.5).

When assessed regionally, the periodic variance of sunspot activity mostly explains non-significant ($P<0.05$) amount of observed wind speed variance. Similar to the periodic IOD assessment, there are surprisingly two significant ($P<0.05$) results which include stations located in the hinterland, and at a higher spatial scale the Western Cape hinterland regions. An assessment based on the periodic variance of sunspot activity, and other climate modes explains 10.43%, and 13.88% (multiple R^2) of observed wind speed variance respectively. No other regions indicate noteworthy results.

5.4.2.6 Thirty–four–year harmonic

The 34–year harmonic analysis yielded the most scientifically important results of all climate mode periodicities. The spectral assessment identified 34–year frequencies in all data records with at least 34 years of data. The harmonic is prominent in a MLC, Cape Agulhas, and IOD data series as well as to a lesser extent in ONI, and solar–cycle data series. The short term 20-year station series is insufficient in length for any assessment. A 17-year Gaussian filter would result in too few data points to present any statistically significant outcome. This multidecadal periodicity aligns the Bruckner solar sunspot cycle (34–35–year harmonic) which several authors consider a likely source of climatic forcing (Raspopov, et al., 2004; Moore, et al., 2006; Kasatkina, et al., 2007; Kobashi, et al., 2015; Nagovitsyn & Kuleshova, 2015; Prestes, et al., 2018). A 17–year period (half of the identified 34–year harmonic) is applied as a Gaussian filter, and data anomalies are presented graphically, and statistically to quantify relationships. Statistical significance is considered where $P<0.01$ (Figure 5.6, Table 5.6). Considering the period, a 5–month lagged ONI resulted in similar results to the concurrent assessment. In this respect, a lagged ONI is not deemed scientifically important at a 34–year harmonic scale.

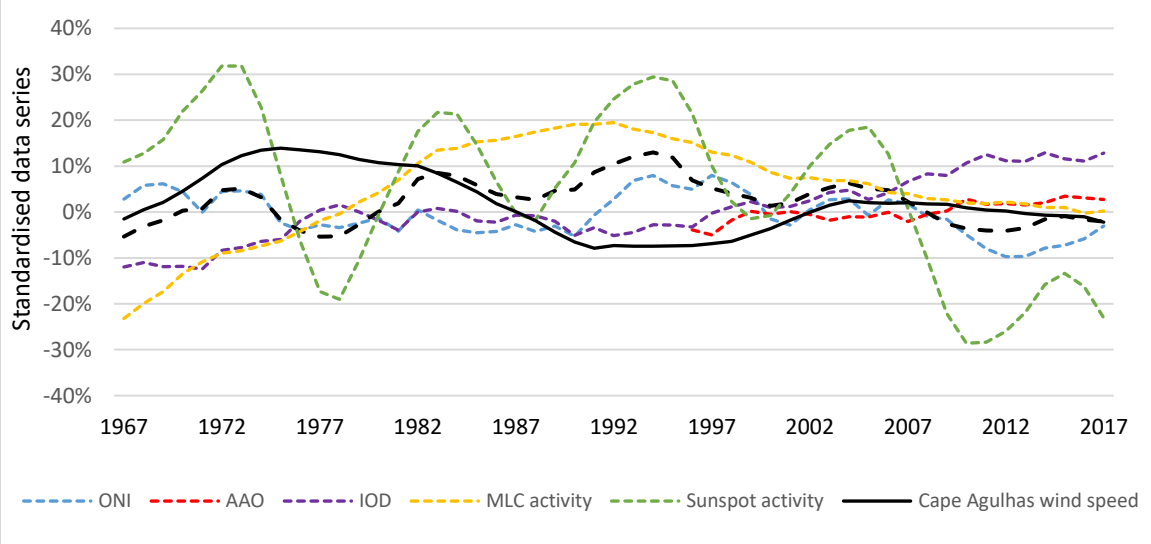


Figure 5.6: Seventeen–year mean monthly filter for climatic variables, and Cape Agulhas wind speed series (black dashed line presenting the combined influence of all climatic variables).

Table 5.6: Seventeen–year periodic climatic mode correlation (r), and multiple regression (multiple R) statistics.

Station / Region / Mode	Multiple regression	ONI	AAO	IOD	MLC activity	Sunspot activity
Adjusted R^2	-	**58.54%**	**80.37%**	**66.94%**	**45.86%**	**75.06%**
ONI	**0.767**	1				
AAO	**0.899**	**-0.834**	1%			
IOD	**0.820**	**-0.572**	**0.840**	1		
MLC activity	**0.680**	-0.061	**-0.821**	**0.192**	1	
Sunspot activity	**0.867**	**0.689**	**-0.754**	**-0.765**	**0.121**	1
Cape Agulhas	**0.649**	**-0.193**	**0.325**	**-0.186**	**-0.530**	-0.020

Bold underline denotes a MK statistical significance of 99% (P<0.01)
Bold denotes a MK statistical significance of 95% (P<0.05)
Underline denotes a MK statistical significance of 90% (P<0.1)

Every climate mode assessed records a statistically significant (P<0.01) multiple regression result to the Cape Agulhas wind speed series when applying a 17–year Gaussian filter. The multiple regression statistics (adjusted R^2) of the AAO indicates the strongest (R^2 = 80.37%) relationship to other climate variables at a 17–year periodic filter. The most scientifically significant relationship is the regression statistic (R^2 = 0.867) between sunspot activity, and other climate variables explaining 75.06% (adjusted R^2) of secondary climate mode variance. Further, the mean of all climate variables (presented as the black dashed line in (Figure 5.6) resulted in a statistically significant (P<0.001) influence on the Cape Agulhas wind speed, explaining 14.65% of observed variance.

Several strong relationships also exist when assessing each mode individually. The ONI record explains r^2 = 70.56% of AAO variance where the strongest driver of regional MLC activity is AAO variance, explaining r^2 = 69.56% of MLC activity (r = –0.821). The AAO is also strongly correlated (r = 0.840) to IOD variance, which explains 67.40% of the observed variance. The AAO, and IOD both indicate strong negative relationships to sunspot activity, and ONI variance, indicating periods of subdued (increased) AAO, and IOD indices identified during periods of increased (subdued) sunspot activity, and ONI. The Cape Agulhas station recorded a moderate multiple regression statistic (r = 0.649) to the 17–year climate mode periods, explaining 41.68% of wind speed variance. Statistically significant results ($p<0.03$) are present between the Cape Agulhas wind speed series, and a 17–year Gaussian filtered ONI, AAO, IOD,, and MLC anomaly variance. The Cape Agulhas station recorded the strongest relationship to MLC anomalies (r = –0.530), explaining 28.1% of 17–year Gaussian filtered wind speed variance (Table 5.6).

5.4.3 Mean monthly association of station observed wind speed characteristics with key climate indices

The objective of this section is to identify the mean monthly relationship between wind speed, and the pentad climate variables. A mean monthly assessment is justified by the spectral scale, which confirmed wind speed series to have a strong annual harmonic. In order to quantify potential teleconnections, the mean monthly value for each data series was quantified for all available data. Standardised data for each series were obtained, and to allow for statistical analysis of the data anomalies. Stations are geographically assessed, and grouped per province, and region. Mean monthly wind speed is calculated for each region, and resultant anomalies are correlated, and multiple regression analysis performed (Table 5.7, Table 5.8).

Table 5.7: Mean monthly correlation, and multiple regression (multiple R) for all series.

Station / Region / Mode	Multiple regression analysis results	5–month ONI lag	ONI	AAO	IOD	MLC	Sunspot Activity
Five month lagged ONI	**0.004**	**1**	-	-	-	-	-
ONI	**0.001**	-	**1**	-	-	-	-
AAO	0.648	-0.198	-0.182	**1**	-	-	-
IOD	0.159	**0.524**	-0.270	0.085	**1**	-	-
MLC activity	**0.003**	**-0.888**	**0.917**	-0.007	-0.251	**1**	-
Sunspot activity	**0.019**	-0.269	**0.684**	0.095	0.305	**0.692**	**1**
Alexander Bay	**0.942**	**0.890**	**-0.744**	-0.033	**0.626**	**-0.824**	-0.243
Beaufort West	0.642	0.369	-0.07	-0.169	*0.504*	0.004	0.305
Brandvlei	**0.926**	**0.867**	**-0.704**	-0.037	**0.654**	**-0.783**	-0.169
Cape Agulhas	**0.850**	**0.781**	**-0.598**	-0.136	**0.578**	**-0.734**	-0.227
De Aar	**0.910**	**0.843**	**-0.584**	-0.107	**0.695**	**-0.702**	-0.063
Elliot	0.744	-0.012	0.465	-0.213	0.339	0.400	**0.665**
Koingnaas	**0.927**	**0.846**	**-0.748**	-0.021	**0.643**	**-0.800**	-0.266
Langebaan	**0.968**	**0.860**	**-0.898**	0.066	0.424	**-0.939**	-0.450
Noupoort	**0.913**	**0.853**	**-0.651**	-0.073	**0.666**	**-0.739**	-0.128
Plettenberg Bay	0.687	0.385	0.021	-0.159	**0.607**	-0.024	0.382
Queenstown	0.752	0.446	-0.004	-0.206	**0.652**	-0.062	0.402
Springbok	0.828	**-0.587**	**0.577**	-0.159	-0.002	**0.843**	0.371
Still bay	0.768	**0.650**	-0.412	-0.076	**0.666**	-0.428	0.088
Tygerhoek	**0.944**	**0.880**	**-0.804**	0.000	*0.531*	**-0.886**	-0.350
Uitenhage	0.792	**0.725**	-0.430	-0.158	**0.654**	*-0.475*	0.020
Mean of stations	**0.809**	**0.794**	*-0.565*	-0.095	**0.666**	**-0.611**	-0.064

Bold underline denotes a MK statistical significance of 99% (P<0.01)
Bold denotes a MK statistical significance of 95% (P<0.05)
Underline denotes a MK statistical significance of 90% (P<0.1)

Table 5.8: Mean regional monthly correlation, and multiple regression (multiple R).

Station / Region / Mode	Multiple regression analysis results	5 month lagged ONI	ONI	AAO	IOD	MLC activity	Sunspot activity
Eastern Cape	0.716	0.419	0.016	-0.210	**0.601**	-0.027	0.400
Northern Cape	**0.902**	**0.835**	**-0.654**	-0.071	**0.675**	**-0.698**	-0.144
Western Cape	**0.849**	**0.837**	**-0.695**	-0.047	**0.592**	**-0.738**	-0.214
Coastal	**0.887**	**0.826**	**-0.636**	-0.073	**0.658**	**-0.699**	-0.153
Hinterland	**0.928**	**0.874**	**-0.788**	-0.011	*0.541*	**-0.830**	-0.316
Inland	0.784	**0.643**	-0.315	-0.155	**0.687**	-0.346	0.170
EC Hinterland	0.792	**0.725**	-0.430	-0.158	**0.654**	-0.491	0.020
EC Inland	0.728	0.244	0.221	-0.218	*0.528*	0.190	*0.544*
NC Coastal	**0.937**	**0.876**	**-0.747**	-0.029	**0.633**	**-0.798**	-0.252
NC Inland	**0.831**	**0.793**	**-0.582**	-0.098	**0.692**	**-0.620**	-0.070
WC Coastal	0.730	*0.567*	-0.253	-0.112	**0.666**	-0.272	0.209
WC Hinterland	**0.945**	**0.874**	**-0.815**	-0.008	*0.515*	**-0.872**	-0.370
WC Inland	0.642	0.369	-0.070	-0.169	*0.504*	-0.017	0.305

Bold underline denotes a MK statistical significance of 99% (P<0.01)
Bold denotes a MK statistical significance of 95% (P<0.05)
Underline denotes a MK statistical significance of 90% (P<0.1)

5.4.3.1 Multiple regression statistics

Weak multiple regression statistics are obtained for all climate variables at a mean monthly scale. This result is expected as the frequency of climate variables vary at different periods, and not defined by a calendar year. The strongest statistically significant (P<0.01) mean monthly climatic relationship (r = 0.917) is present between the concurrent ONI, and MLC activity. This positive relationship confirms that stronger El Niño events (warmer ONI) contribute to more frequent MLCs, while stronger La Niña events (colder ONI) are associated with reduced MLC activity. The ONI explains 84.1% of observed mean monthly cyclonic variability. Moderate correlations (P<0.01) are observed in the ONI (r = 0.684), and MLC data series (r = 0.692) for the sunspot activity where it explains 46.79%, and 47.89% of the variance, respectively. This finding indicates that increased sunspot activity coincides with

increasing SST. This relationship is scientifically important considering the ongoing efforts to document solar–climate teleconnection (Table 5.7).

The multiple regression analysis yielded the most scientifically important results, quantifying the primary drivers of wind speed. Eight stations indicate statistically significant ($P<0.01$) multiple regression statistics between recorded wind speed, and monthly climate mode variance, resulting in a strong mean correlation ($r = 0.809$). Considering only statistically significant stations, a near-perfect mean multiple regression statistic ($r = 0.924$) is obtained between mean monthly climate mode variance, and wind speed, explaining 74.5% of the observed variance (adjusted R^2). Stations which did not indicate statistically significant ($P<0.1$) results were reassessed removing non-significant variables, however, results remain unchanged (Table 5.7).

At a provincial scale, statistically significant ($P<0.01$) multiple regression statistics are obtained between climate mode, and wind speed variance for stations located in the NC (multiple $R = 0.902$), and WC (multiple $R = 0.849$) provinces, explaining 81.36%, and 72.08% (multiple R^2) of observed variance respectively. Only the coastal (multiple $R = 0.887$), and hinterland (multiple $R = 0.928$) regions obtained statistically significant ($P<0.01$) results, explaining a significant 78.62%, and 86.12% (multiple R^2) of observed wind speed variance respectively. At a finer resolution, stations located in the sub-regions of the NC coastal (multiple $R = 0.937$), NC inland (multiple $R = 0.831$), and WC hinterland (multiple $R = 0.945$) all indicate that a significant ($P<0.05$) correlation exists between observed wind speed, and climate mode variance. Considering this result, climate mode variance explains 87.8%, 69.06%, and 89.3% (multiple R^2) of observed mean monthly wind speed. Further assessment was undertaken of the sub–regions where statistically non-significant ($P>0.1$) results were observed. Recalculation was done removing non-significant variables, however, results remained unchanged (Table 5.8).

5.4.3.2 ONI

Wind speed series were regressed at a concurrent, and 5–month lagged scale for the ONI identifying a negative, and positive correlation respectively. As identified in the literature

review, others such as Diaz et al. (2001), Enloe et al. (2004), and Klink (2007) have confirmed the existence of a 5–month lagged relationship between wind speed, and ONI variance. Considering this, alternative lags are not considered. Eleven Stations indicate statistically significant ($P<0.01$) regression statistics with a 5–month lagged ONI. Springbok is the only station which indicates a statistically significant ($P<0.01$) negative relationship. All other statistically significant ($P<0.1$) correlations are positive, indicating above (below) average wind speed associated with five month post-El Niño (La Niña) events. Considering the statistically significant correlations, a 5–month lagged ONI explains 63.7% of observed wind speed variance (Table 5.7).

Considering the mean monthly results of a 5-month lagged ONI, statistically significant ($P<0.05$) correlations are observed at a provincial scale in the NC ($r = 0.835$), and WC ($r = 0.837$. The 5-month lagged ONI variance explains 69.72%, and 70.06% (r^2) of observed NC, and EC wind speed variance respectively. A non-significant ($P>0.1$) correlation is observed for stations located in the EC. Similarly, statistically significant ($P<0.05$) positive correlations are indicated for stations located in the coastal ($r = 0.826$), hinterland ($r = 0.874$), and inland ($r = 0.643$) regions, explaining 68.23%, 76.39%, and 41.34% (r^2) of observed wind speed variance respectively. The weaker result obtained from stations located in the inland region is explains through the ocean-climate dominated characteristics of the ONI, resulting in those regions located closest (coastal, and hinterland) to the ocean indicating a stronger relationship. The strongest correlation ($r = 0.876$) is observed between a 5-month lagged ONI, and stations located in the NC coastal region, explaining 76.7% of observed wind speed variance. The NC coastal region was followed by the WC hinterland where a 5-month lagged ONI explains 76.39% (r^2) of observed wind speed variance. Stations located in the sub-regions of the EC, and WC inland indicate statistically non-significant ($P>0.1$) correlation results when compared to a 5-month lagged ONI data set. (Table 5.8).

5.4.3.3 AAO

No statistically significant ($P>0.1$) results are obtained between the AAO, and observed wind speed variance when considered on an individual station, provincial or regional scale. Most correlations are negative, however, are of limited scientific importance (Table 5.7, Table 5.8)

5.4.3.4 IOD

The IOD yielded the second strongest mean correlation (r = 0.666) to wind speed after the ONI, explaining 44.4% of mean monthly wind speed. Most stations recorded statistically significant (P<0.1) positive correlations, indicating stronger (weaker) wind speed associated with periods of warmer (cooler) IOD SSTs. Additionally, the range of statistically significant (P<0.1) correlations is low (r = 0.191), indicating that the IOD affects wind speed fairly uniformly. This is scientifically important as the IOD has not previously been linked to regional wind speed (Table 5.7).

When assessing the impact of IOD variance on stations clustered at a provincial scale, statistically significant (P<0.05) correlations are present for the NC (r = 0.675), WC (r = 0.592), and EC (r = 0.601) provinces, explaining 45.56%, 35.05%, and 36.12% (r^2) of observed wind speed variance respectively. Notably, the IOD data set is the only climate mode record for which all provinces indicate a statistically significant (P<0.1) correlation to observed wind speed variance. Similarly, statistically significant (P<0.05) correlations are identified between AAO variance, and mean wind speed in coastal (r = 0.658), inland (r = 0.687), and hinterland (r = 0.541) regions, further explaining 43.3%, 47.2%, and 29.27% (r^2) of observed wind speed variance respectively. At a finer spatial scale, every sub-region indicates a statistically significant (P<0.1) correlation between the IOD, and clustered station wind speed data. The strongest correlations are observed between IOD variance, and stations located in the NC inland (r = 0.692), WC coastal (r = 0.666), EC hinterland (r = 0.654), and NC coastal (r = 0.633) regions, explaining 47.89%, 44.36%, 42.77%, and 40.07% (r^2) of observed wind speed variance respectively (Table 5.8).

5.4.3.5 MLC activity

A negative correlation (p<0.1) is present between MLC activity, and all wind speed series, except for Springbok. Considering statistically significant results, the strong inverse result (r = –0.771) indicates that MLC activity is not a primary driver of wind speed variance in the study region. In fact, the assessed data series indicate South Africa records increased (decreased) MLC activity during winter (summer), inversely correlating to mean monthly wind speed profiles, which generally record increased (decreased) wind speed anomalies

during summer (winter). The only two exceptions are the wind speed series of Springbok, and Elliot, where a positive correlation is observed (Table 5.7).

Assessing the impact of MLC activity on stations clustered at a provincial scale, statistically significant ($P<0.05$) correlations are observed in the NC ($r = -0.698$), and WC ($r = 0.738$) provinces, explaining 48.72%, and 54.46% (r^2) of observed wind speed variance respectively. Statistically significant ($P<0.05$) correlations are identified between MLC variance, and mean wind speed in the coastal ($r = 0.699$), and hinterland ($r = 0.83$) regions, explaining 48.86%, and 68.89% (r^2) of observed wind speed variance respectively. At a finer spatial scale, only the sub-regions of the WC hinterland ($r = -0.872$), NC coastal ($r = -0.798$), and NC inland ($r = -0.62$) indicate a statistically significant ($P<0.05$) correlations between MLC activity, and clustered station wind speed data explaining 76.04%, 63.68%, and 38.44% (r^2) of observed wind speed variance respectively (Table 5.8).

While a strong inverse correlation presides between MLC activity, and observed wind speed profile, the impact, and importance of MLC activity on the climate of South Africa should not be discounted. Considering in excess of 60 events occur annually these are a predominant feature of the regional climate. It is acknowledged that MLC events are intricately associated with rainfall, and extreme weather events. In this respect, specifically relating to wind speed, the work already presented by Kruger (2010; 2011) is primarily concerned with classifying, and assessing high wind gust zones, and the impact on the built environment. Kruger assessed the local wind speed pre-, during-, and post- MLC events. A notable difference between the objectives of Kruger, and this PhD is the temporal scale assessed, and the concept of instantaneous, opposed to mean wind speed. Given the strong wind zones of South Africa have already been delineated, there was limited value in reassessing the findings of Kruger, especially considering he used the same dataset as this PhD.

5.4.3.6 Sunspot activity

Elliot is the only station where a weak statistically significant ($P<0.05$) correlation to mean monthly sunspot activity is recorded. Similar non-significant results are obtained for station clusters at provincial, and regional geographic spaces. Considering the weak correlation ($r =$

0.665) result from Elliot, and the fact that the influence of solar activity is a macro-scale forcing phenomena, it is assumed that this result is a mere coincidence based on the stations' wind speed profile. Given sunspot activity is a multi-decadal phenomena, the observed monthly relationships are scientifically unimportant (Table 5.7, Table 5.8).

5.5 Discussion

Given the current uptake of wind energy globally, and in South Africa, it is of increasing importance to further identify, and quantify regional drivers of wind speed variance. Few regions, such as Europe, and North America, have received the necessary attention quantifying teleconnections between climate mode, and wind speed. This chapter statistically addressed the teleconnection between wind speed, and five climate indices (ONI, IOD, AAO, MLC, and sunspot activity) at several time-scales between 1950, and 2018.

The observed climatic variability appears to synergistically influence recorded wind speed in the study area. Station data record significant correlations between 1995 – 2018 (Cape Agulhas 1950, and 2018) across the 15 investigated stations of the NC, WC, and EC provinces. However, results reflect that certain regions, and stations correlate poorly, which confirms the complexity of climatic forces driving regional wind speed, as there is no single primary driver as summarised in Table 5.9. Statistically non-significant ($P>0.1$) correlations are mostly identified between climate mode, and wind speed variance at an annual, and monthly time-scale where the harmonic analysis identified several weak correlations ($P<0.1$). A strong multiple regression statistic ($r = 0.678$) is observed in the 34–year harmonic series, explaining 42.1% of observed wind speed. Mean-monthly, and -seasonal scale series are given priority in the discussion, as limited value was identified at a multi-decadal scale, as presented in section 5.5.3.

Table 5.9: Mean wind speed variance explains by climate mode data series at different periods (statistical significance P<0.1).

Period		Wind speed driver					
		Multiple Regression	5–month Lagged ONI	AAO	IOD	MLC	Sunspot
Inter–annual		–	–	–	–	–	–
Inter–month		13.6%	–	–	1.1%	–	–
Climate mode period		n/a	7.0%	–	–	–	3.3%
34–year harmonic		42.1%	3.7%	10.6%	3.5%	–	–
Mean Monthly		65.4%	63.04%	–	44.4%	–	–
Mean Seasonal	Summer	–	–	–	18.9%	–	–
	Autumn	–	97.4%	–	16.9%	–	–
	Winter	–	94.9%	–	–	–	–
	Spring	–	99.9%	–	20.3%	–	

5.5.1 Multi–decadal association between station wind speed characteristics, and key climate indices

All stations were assessed on an annual, and monthly temporal-scale to quantify the relationship between wind speed, and climate variables. An non-significant regression statistic was obtained on an inter-annual scale, whereas inter-monthly variance indicates that the assessed climate mode explains 13.6% of recorded wind speed. All climate variables except the AAO at an inter-annual scale, and MLC activity qt an inter-monthly scale, yield statistically significant (P<0.1) multiple regression statistics. The presence of inter–climate relationships confirms the complexity of forces driving regional wind speed. The synoptic relationships identified are similar to those described by Kruger (1999), Fant et al. (2016), and Lennard (2019), which capture the macro-scale drivers of regional wind speed.

Even though significant correlations are indicated between the climate variables at an inter–annual, and inter-seasonal scale, few statistically significant (P<0.1) correlations are identified with station wind speed series. This observation is further explains by the spectral density results which did not identify any significant climate mode frequencies on an annual temporal scale. Notably, where statistically significant (P<0.1) correlations are observed, all are positive, indicating that above average climate mode indices are paired with periods of higher wind speed. This is explains by the fact that several indices are SST linked. Warmer SSTs result in an increase in climatic energy, and in turn drive an increased strength of

regional wind speed. Every station indicates statistically significant ($p<0.1$) inter–month multiple regression statistics to climate mode variance, confirming that these climate variables are responsible for driving regional wind speed. An assessment of anomalously high, and low wind speed seasons, and years identified that although not ubiquitous, periods following VSE, and SE events record relatively high wind speed anomalies.

This observation is important in the context of future ENSO variance climate models are forecasting. In a scenario where future El Niño events strengthen, this PhD study indicates an associated increase in wind speed strength could be observed, and inversely for La Niña events. Chand et al. (2017) forecast that by the late twenty-first century, global climate change could observe a strengthening of El Niño, and a weakening of La Niña, resulting in an increase in tropical cyclone events of between 20–40%. This scenario would result in more extreme wind speeds, and an increased interannual variability, which would pose a complication to operational wind energy facilities designed to withstand historically weak windstorm events. Conversely, Perry et al. (2020), based on their assessed of historical (1950 - 1999), and future (2040 - 2089) ENSO events, found largely non-significant climate teleconnections. Exceptions include East Africa, and South America where strong, significant teleconnections are identified between La Niña events, and climate variability (rainfall, and temperature). Despite this observation, findings were inconclusive regarding the extent to which ENSO variance will affect climatic teleconnections, noting changes in ENSO teleconnections are relatively non-significant when compared to historically (1950 - 1999) observed regional climatic variability.

5.5.2 Periodic association between station wind speed characteristics and key climate indices

The analysis of climate mode periodicity identified statistically significant relationships to wind speed variance. However, most correlations are weak, and not strong indicators of wind speed variance. Several authors (e.g. Jasmine et al. (2018), Mohammadi & Goudarzi (2018), and Trouet et al. (2018)) have assessed tele–connectivity between wind speed, and climate variability, considering annual, seasonal, and monthly variance. Very few, however, have considered this tele–connectivity by applying Gaussian filter, and climate mode harmonics

(Bianchi, et al., 2017; Naizghi & Ouarda, 2017). The strongest inter–climate linkages are to sunspot activity at a 67–month Gaussian period, which resulted in statistically significant ($P<0.01$) weak to moderate correlations. Several have documented strong solar-climate linkages (e.g. Beer et al. (2000), Fröhlich (2006), Owens et al. (2017), and Egorova et al. (2018)). The findings of the current PhD study are in agreement, namely that a statistically significant ($P<0.01$) correlation is present between a 67–year sunspot harmonic (11.3 year period), and other assessed climate variables.

Further, it is identified that sunspot activity is a statistically significant ($P<0.01$), but weak driver of wind speeds, explaining on average 3.3% of the observed variance when assessed at an 11.3 year period (67-month harmonic). Noupoort indicates the strongest association to the sunspot cycle, explaining 28.6% of wind speed variance. It is expected that the inland location of this station, and regional driving forces drive this moderate correlation, which is not identified at other stations. A 5-month lagged ONI explains a mean 7% of station wind speed variance. Interestingly, a mean negative correlation is seen at both a concurrent, and 5–month lagged scale. This result is explains by the 5–month lagged teleconnection between the ONI, and wind speed, and the fact that when assessed at a 34–month Gaussian filter, the period distorts the true positive relationship.

In addition, series with at least 35 years of data indicate a dominant 34–year harmonic (17–year period). This is present in the Cape Agulhas wind speed series, and climate mode variables. The climate mode multiple regression statistics are all statistically significant ($P<0.01$), and explain 42.1% of station wind speed variance. It is also of interest that sunspot activity explains a statistically significant ($P<0.01$) 75.1% of climate mode variance. This reinforces existing literature, confirming a strong solar-climate teleconnection (Meehl, et al., 2007; Misios, 2012; Mohammadi & Goudarzi, 2018).

The observed climate, and associated climate periodicities are further influenced by regional climatic oscillations. These include a predominant quasi 20-year oscillation, identified during summer over the north-eastern half of South Africa, and a 10 to 12-year oscillation which predominantly affects the southern coastal, and adjacent inland areas, as documented by Tyson & Preston-Whyte (2000). Further, Currie (1993) identified climatic periodicities

linked to the solar cycle across South Africa at scales of 6 to 7 years, 10 to 12 years, and 16–20 years.

5.5.3 Mean monthly association of wind speed characteristics with key climate indices

The objective this section was to quantify the relationship between the identified global teleconnections which may define monthly observed wind speed in the study area. Weak significant correlations identified from the inter-monthly, and inter-annual wind speed-climate mode characteristic analysis support the notion that climate mode variance is a key determinant of wind speed. At these scales, however, climate mode characteristic-wind speed correlations were unable to explain the wind speed variance. To resolve this, mean-monthly wind speed characteristics were investigated. These results are identified as the most scientifically important findings of this Chapter 5.

The mean monthly assessment identified several relationships between climate variables. The ONI dominated as the primary driver of regional MLC activity, IOD, and wind speed. MLCs recorded an almost perfect positive ($r = 0.917$) correlation with a concurrent ONI. The assessment further confirmed that a 5–month lagged ONI agrees with a significant amount of observed wind speed variance, and as such are an indicator of future wind speed. All seasons, except summer, indicate statistically significant ($P<0.01$) results to a 5–month lagged ONI. No significant relationship is identified between the wind speed series of Beaufort West, Elliot, Plettenberg Bay or Queenstown, to a lagged or concurrent ONI. All stations except Elliot, recorded statistically significant ($P<0.05$) positive correlations to the IOD.

Previous literature has identified significant teleconnections between climatic modes, and regional South African rainfall at a mean monthly scale (Reason & Rouault, 2005; Philippon, et al., 2011; Engelbrecht & Landman, 2016; Crétat, et al., 2019; Mahlalela, et al., 2019). It was assumed that the primary drivers of this association may similarly influence regional wind speed. The assumption is correct for most significant correlations, with the exception of ONI-wind speed correlation. The ONI correlations indicate a 5-month lagged association due to the temporal rate of ENSO variance impacting on regional climate. Notably, this observation

may also hold true for rainfall or wheat yield correlations in the study area. Kloppers (2014) for example, was perplexed by the inverse correlation obtained between ENSO variance, rainfall, and wheat production. Kloppers (2014, p91) remarked "Therefore, the ENSO indices-wheat yield correlations intimate that higher yields are associated with years of drier winters. This result, in isolation, is rather perplexing, and counterintuitive". This lagged observation is also present in other climate indices, such as the ONI, and IOD. When assessing the correlation between the IOD, and a concurrent ONI, an non-significant ($P>0.1$) negative ($r = -0.270$) result is obtained. Given that the IOD is connected to the SST index, a positive correlation would be expected. When re-assessed, considering a 5-month lagged ONI, a significant ($P<0.05$) positive correlation ($r = 0.524$) is identified. It would be expected that if the data used by Kloppers (2014) were reassessed based at a 5-month lagged ONI, a significant positive correlation would be obtained (as presented in this research).

Scientifically important results ($P<0.1$) are identified between mean monthly wind speed, and climate mode variance. The strongest is the climate mode multiple regression statistic ($r = 0.809$) describing a mean of 65.4% of observed wind speed variance, increasing to 74.5% when excluding statistically non-significant ($P>0.1$) results. The strongest mean monthly correlation is between wind speed, and a 5–month lagged ONI, describing a mean 63.0% of wind speed variance. The IOD variance further explains a mean of 44.4% of the wind speed variance. A widespread positive correlation is identified between the IOD, and 5–month lagged ONI. Further, a 5–month lagged ONI proved the most useful indicator for the forecasting of wind speed variance. The strongest impacts are present during winter, autumn, and spring (Table 5.9).

At a provincial, and regional scale, strong statistically significant ($P<0.05$) multiple regression statistics are obtained, indicating that the climatic variables explain a large amount of variance. The NC ($r = 0.902$), WC ($r = 0.849$), coastal ($r = 0.887$), and hinterland ($r = 0.928$) regions indicate the strongest association. The EC, and inland regions did not indicate a significant multiple regression static. It is expected that the inland region is not as obviously impacted due to the dilution of other topographic influences. The coastal, and hinterland regions are closest to the oceanic shoreline, hence given that the primary driver is ENSO, and

associated SST temperature variance, it is logical that the strongest association would be observed at stations located closest to the source of variation.

Of further interest is the statistically significant ($P<0.01$) relationship between IOD, and 5–month lagged ONI, as it indicates a positive correlation ($r = 0.524$). A positive correlation is identified between all stations except Elliot, and the IOD. A 5–month lagged ONI indicates stronger positive SST records (El Niño events) result in above-average wind speed anomalies (inverse to La Niña events). Considering this, a concurrent IOD, and 5–month lagged ONI explains an average of 44.4%, and 63% of wind speed variance, respectively. A multiple regression analysis of these two modes, and mean wind speed confirms a statistically significant ($P<0.01$) positive relationship, explaining 65.4% of observed wind speed variance. Considering this, the current ONI data series can be used to forecast the expected wind speed in the fifth succeeding month, with below (above) average wind speed anomalies being observed post cool (warm) La Niña (El Niño) events.

The identified correlation between wind speed, and climate modes provide invaluable information to the current state of atmospheric variance, and its probable influence on wind speed in the study region. These associations are strongest in the NC, WC, Coastal, and hinterland regions. The identified teleconnections associated with the observed wind speed variance have been previously identified in the assessment of other climatic characteristics (e.g. rain, temperature). The predominant wind speed variance originates from a 5-month lagged ONI which is significant at 73% of stations.

It is concluded that the ENSO phases exert a direct, 5-month lagged influence on wind speed over South Africa. Based on regional observations, the impact manifests as SST variance in the western Indian, and eastern Atlantic Oceans. This relationship has been examined in other climatic variables, and similar observations made by Mason & Tyson (1992), Kruger (1999), and Reason & Rouaul (2005). Given, at a seasonal resolution, that the 5-month lagged ONI explains over 99% of variance, applying this index as a tool for forecasting wind speed predictions are likely to prove accurate. Thus, a primary driver of wind speed is regional SST forcing, driven by the relationship to ENSO variance. This association is similarly identified in other climatic indices as reported by Philippon et al. (2011).

5.6 Recommendation for future research

This chapter has identified several significant teleconnections between climatic drivers, and observed wind speed. One limitation is the geographical distribution of stations, and the limited stations which quantify in excess of 20 years of wind speed data. Further research assessing South Africa's wind speed teleconnections, importantly on an increased spatial resolution is recommended by using WASA data once long-term data are available. Similar to the recommendations in earlier chapters, the inclusion of operational wind farm data would help provide additional data points. These wind measurement campaigns are generally at hub height (or at-least 2/3 of hub height), and compliant to international best practice measurement campaigns.

One significant finding in this chapter is the relationship between a 3-month lagged ONI, and observed wind speed variance. The ability to accurately forecast near term wind speed in excess of 7 days holds a high uncertainty. The statistically significant correlations indicate that the ONI could be a strong indicator, which should be incorporated to advanced wind speed forecasting models. It would also be of value to verify the identified ONI/ Wind speed relationship based on the operational performance of wind power projects connected to the South Africa power network. There is ongoing research into the impact of instantaneous wind speed changes on the grid network at minute, hourly, and daily resolutions. As additional operational wind farm reference data become available, these data need be assessed to further refine the distribution of renewable energy in the Eskom grid.

While every effort was made to include the most relevant, and strongest climate drivers in this PhD, there are indeed other climate indices which exist, and so this research could be expanded to include other climate variables. While it is assumed this research presents the most significant drivers, it is indeed possible that additional significant teleconnections exist. While this PhD has focused on the statistical assessment of observed wind speed data, additional research opportunities exist in performing advanced climatic system modelling to further understand long term wind speed variance. Wind speed teleconnections to global climate variables are complex, and no one model can comprehensively assess all potential linkages.

6 CONCLUSION

6.1 Introduction

This study has three distinct aims, all of which have been achieved through the assessment of 15 wind speed series obtained from different stations across the Cape provinces of South Africa. The assessed wind speed series were identified, and reviewed from the SAWS. Each station record was filtered to identify the respective daily, monthly, seasonal, and annual temporal scale wind speed series, prior to performing the statistical analysis required to achieve the objectives.

The first study aim is addressed in Chapter 3, and quantify wind speed trends on monthly, seasonal, annual, inter-annual, multi-temporal, and multi-decadal scales. Additionally, station wind speed trends are quantified over a 20-year PPA period of 20 years, for the determination of the hypothetical reduction of wind speed power over the study period. The second aim of the study is addressed in Chapter 4. The primary objective is to verify the station wind speed profiles in terms of station seasonal, diurnal, and monthly records. Further, these profiles are assessed in consideration of the South African power demand profile, and noting the differences between the stations when applying spatial dispersion of wind power generation is put into consideration. The third, and final aim of this study is addressed in Chapter 5. The primary objective is to identify, and quantify teleconnections between observed wind speed characteristics in the study area to large-scale climate modes. Additionally, the identification of climate indices which could be applied to forecast wind speed in the study area, concludes the study.

This conclusion section presents the achievement of each of the aims stated above, with a reflection on how the results have assisted to address these aims.

6.2 Achievement of study aims

6.2.1 Aim One: Wind speed trends

The first aim was to validate observed wind speed variability in the study area as presented in Chapter 3. A comprehensive assessment of available literature on global wind speed trends, and those in the study area was identified, and presented. Quantification of station wind speed variability were done through the applications of Sens's slope estimator for records available between 1995, and 2018 (Cape Agulhas 1950, and 2018). The first observation is the statistically significant ($P<0.05$) mean decreasing (-0.14% per year; -0.005 m/s/year) inter-annual wind speed trend in the study area. The strongest decreasing inter-annual trend is present in the Noupoort series (-0.49% per year, –0.019 m/s/year). Koingnaas, Langebaan, and Springbok all indicate increasing mean annual wind speed trends, however, only Langebaan (0.16% per year, 0.006 m/s/year) proved statistically significant ($P<0.05$).

The review notes that the mean annual provincial wind speeds all indicate a decreasing trend, while only the NC ($P<0.05$), and WC ($P<0.1$) proved statistically significant. The WC indicates the strongest significant trend, decreasing at a mean of -0.22% per year (–0.008 m/s/year). The mean monthly wind speeds are quantified, and presented for each station, and grouped per region. October is the only month to indicate a statistically significant ($P>0.1$) decreasing mean wind speed trend. The strongest decreasing monthly trend is identified in the mean May series for Uitenhage (-0.98%, -0.025 m/s/year), while the strongest increasing wind speed trend is observed in the April series for Koingnaas (–0.98%, –0.025 m/s/year). Station data further underwent a multi-temporal analysis through the application of a continuous wavelet analysis. Decreasing mean trends are identified over temporal periods of 1 to 2 years, and 2 to 4 years (ranging 1996 to 2017). Increasing trends dominate longer term temporal scales of 4 to 8 years (ranging 1996 to 2014).

Achievement of this aim is made through the statistical evaluation of each of the wind speed series in the study area. Despite the observed wind speed decreases identified, the trends

would not have posed a material risk to power generation from wind for the assessed stations, based on the period 1995, and 2018 (Cape Agulhas 1950, and 2018).

6.2.2 Aim two: Wind speed profiles

The second aim set to validate the observed wind speed profiles in the study area as presented in Chapter 4. This objective is achieved through the assessment of wind speed anomalies to quantify daily, monthly, and seasonal series profiles in relation to the south African electricity load profile. As presented in Figure 4.1, the diurnal electricity profile in South Africa is highest during weekdays, for both high, and low demand seasons, depending on the season peaking between 06:00 to 09:00, and 17:00 to 20:00 SAST. The diurnal wind speed profile in the Cape provinces, however, indicate that the wind speed resource is highest between 14:00, and 16:00, peaking at 15:00 hours.

Results indicate a statistically significant ($P<0.1$) positive correlation between all station diurnal wind speeds, and Eskom demand profiles. Moderate strength ($r = 0.545$) correlations are identified between mean diurnal wind speed profiles, and the Eskom load. The correlation significantly ($P<0.05$) increases ($r = 0.743$) during low demand periods. Similar wind speed profile are observed between stations at a seasonal ($r = 0.706$), and monthly ($r = 0.641$) scale. However, distinct seasonality is observed in station seasonal, and monthly wind speed profiles, with summer, and December recording the strongest anomalies respectively. The stations of Alexander Bay, Langebaan, and Still Bay recorded the strongest wind speed profile similarities, and inter-annual correlations.

Importantly, Springbok is the only station to indicate significant ($P<0.01$) correlations to the Eskom mean seasonal ($r = 0.833$), and monthly ($r = 0.739$) profiles. Given that Springbok also recorded the strongest diurnal correlation during both high ($r = 0.683$), and low ($r = 0.823$) demand periods, the location is uniquely suited to support the country's energy demand through wind power generation.

6.2.3 Aim three: Wind speed teleconnections

The third aim set to identify, and quantify the observed wind speed teleconnections in the study region, to climate indices (ONI, IOD, AAO, MLC, and sunspot activity) as presented in Chapter 5. Once these modes were identified, available literature on their regional, and global influence on wind speed is presented. This study notes several interconnected climatic events which drive wind speed throughout the study region. The inter-monthly multiple regression statistic of wind speed variability in the study area indicate weak, but statistically significant connections to the climate variables assessed, explaining 13.6% of wind speed variance. This result may be expected due to the fact that variables fluctuate according to periods of observation, for which impacts are not identified at an inter-annual or inter-monthly scale.

Each series was filtered based on their unique periods. The intention is to identify if certain modes exert a specific influence, considering the series harmonics. A 5-month lagged ONI, MLC, and Sunspot activity indicate a significant ($P<0.1$) impact on wind speed series, however, these associations are weak, explaining a mere 7.0%, 4.4%, and 3.3% of observed wind speed variance. Further, series were filtered over a 34-year period, which is based on the identified harmonic in the spectral analysis. A moderate multiple regression statistic indicates that the assessed climate modes explain 42.1% of long-term wind speed variance.

The mean monthly, and mean seasonal assessment yielded the most scientifically important results. The strongest multiple regression statistic is evident at a mean monthly temporal scale, indicating that climate variables explain 65.4% of observed mean monthly wind speed anomalies. Further, a 5-month lagged ONI, and concurrent IOD series explains a moderate 63.04%, and 44.4% of wind speed variance respectively. An exceptionally strong teleconnection is identified between a five month lagged ONI series, and wind speed variance. This association is present in all seasons except summer, and stands out from other results, indicating a near perfect correlation, explaining on average 97.4% of seasonal wind speed variance. Given the lagged relationship, a 5-month lagged ONI can be applied to forecast seasonal wind speed variance compared to the expected long-term mean.

The objectives of this chapter have been achieved through the statistical (spectral, correlation, and regression analysis) assessment of relationships between climate variables, and wind speed anomalies.

6.3 Application, and Importance of Findings

In the first instance, findings from this study can be used in the development, integration, and optimisation of wind power generation in the national grid of South Africa. The study highlights that there is an ongoing gross shortfall of power in South Africa. While Eskom, and IPP's produce 45,561MW, and 4,779MW respectively, there have been significant power shortages observed by the country's power grid, requiring "load shedding" in a bid to accommodate power demand, and safeguard the grid. Fitting the temporal, and spatial wind power contribution in consideration to such electricity shortfalls during specific times, requires the application of the findings such as those presented in this PhD study.

Both increasing, and decreasing wind speed trends are identified. While significantly ($P<0.1$) decreasing wind speed trends dominate the past 20 years of station records, the observed sen's statistics are not of concern to the long-term sustainability of wind power generation. Additionally, the multi-decadal assessment indicates increasing mean wind speeds, proving statistically significant ($P<0.01$).

An essential application of findings can be made through the derived diurnal, and monthly scale wind speed profiles. These can be used to determine the optimal temporal, and spatial periods when wind power is most available. A unique observation is the statistically significant ($P<0.1$) positive correlation between the Springbok mean hourly, diurnal, seasonal, and monthly wind speed profiles to the Eskom load profile. This is the only station to indicate a significant positive correlation on every scale, meaning the surrounding regional wind speed profiles are most likely ideally suited to support the power demands of South Africa at daily, and annual temporal-scales. This finding needs to be verified by the installation of additional stations to identify the geographic extent of the wind profile. This region should be assessed further, and considered for a strategic development zone for wind power generation.

Of key importance is the teleconnection between a 5-month lagged ONI, and wind speed anomalies. The 5-month lagged ONI exhibits a near perfect correlation ($P<0.01$) to observed mean autumn, winter, and spring station wind speeds. Thus, this index is ideally suited to forecast seasonal wind resource capacity relative to long-term expected mean wind speed.

The identification, and quantification of wind speed trends, profile, and teleconnections in the study region adds significant knowledge to an emerging topic of research which can be applied to ensure the sustainable development of wind power in South Africa. Additionally, the findings have regional importance due to their future application in wind power development, which is forecast to be an essential component of power generation.

6.4 Recommendation for future research

The below sections summarise the identified areas which warrant future research, considering the findings, and observations of this PhD.

6.4.1 Wind speed trends

- Further research into the verifying South Africa's wind speed trends, specifically at hub height is recommended using WASA data once long term (10+ years) data are available.
- Assessment of operational wind power project electricity contribution to the South African power grid to identify trends which can be paired to this research.
- Include additional wind speed data from SAWS stations as periods of 20+ years become available.

6.4.2 Wind speed profiles

- Further research into verifying South Africa's wind speed profiles, specifically at hub height is recommended using WASA data once long term (10+ years) data are available.
- Further assessment of operational wind power projects, and their profile contribution to the power grid, so as to identify preferable development zones.

- Identification of high wind shear areas which justify the implementation of increased hub height to optimise power generation.
- Assessment of the impact that the wind power profile has on the operational performance, and maintenance requirements of a wind farm.

6.4.3 Wind speed teleconnections

- Further research into assessing South Africa's wind speed teleconnections, importantly on an increased spatial resolution is recommended using WASA data once long term (10+ years) data are available.
- Verify the relationship between wind speed, and 3-month ONI forecasting based on the operational performance of wind power projects connected to the South African power network.
- Expansion of ongoing research to establish the impact of instantaneous wind speed changes to the grid network at a minute, hourly, and daily resolution.
- Inclusion of further climate variables to assess unidentified teleconnections.
- Perform advanced wind modelling to verify the accuracy of forecasting wind speed based on the 3-month lagged relationship between wind speed, and ONI, and create an industry tool to forecast wind speed three months in advance based on ONI variance.

7 REFERENCES

Abdraman, M. A., Tahir, A. M., Lissouc, D., Kazet, M. Y., & Mouangue, R. M. (2016). Wind resource assessment in the city of N'djamena in Chad. International Journal of Renewable Energy Resources, 6(3), pp. 1022 - 36.

Abhishek, A., Lee, J., Keener, T. C., & Yang, Y. J. (2010). Long-Term Wind Speed Variations for Three Midwestern U.S. Cities. Journal of The Air & Waste Management Association, 60(9), pp. 1057 - 64.

Adaramola, M. S., Agelin-Chaab, M. & Paul, S. S. (2014). Assessment of wind power generation along the coast of Ghana. Energy Conversion, and Management, 77(1), pp. 61 - 9.

Adedeji, P. A., Akinlabi, S., Madushele, N. & Olatunji, O. O. (2020). Latent Dynamics in Siting Onshore Wind Energy Farms: A Case of a Wind Farm in South Africa. Cape Town, American Society of Mechanical Engineers Digital Collection.

Adefarati, T. & Obikoya, G. D. (2019). Evaluation of Wind Resources Potential, and Economic Analysis of Wind Power Generation in South Africa. International Journal of Engineering Research in Africa, 44(08), pp. 150 - 81.

Afungchui, D. (2014). Rayleigh distribution-based model for prediction of wind energy potential of Cameroon. Asian Journal of Energy Conversion Management, 1(1), pp. 26 - 43.

Agee, E. M. (1991). Trends in Cyclone, and Anticyclone Frequency, and Comparison with Periods of Warming, and Cooling over the Northern Hemisphere. Journal of Climate, 4(2), pp. 263 - 7.

Aguilar, E., Auer, I., Brunet, M., Peterson, T. C., & Wieringa, J. (2003). Guidance on metadata, and homogenization. World Meteorological Organisation, 1186(01), pp. 1 - 53.

Akpinar, E. K. & Akpinar, S. (2004). Determination of the wind energy potential for Maden-Elazig, Turkey. Energy Conversion, and Management, 45(18 - 19), pp. 2901 - 14.

Al-Abbadi, N. M. (2005). Wind energy resource assessment for five locations in Saudi Arabia. Renewable Energy, 30(10), pp. 1489 - 99.

Alexander, M. & Scott, J. (2002). The influence of ENSO on air-sea interaction in the Atlantic. Geophysical research letters, 29(14), pp. 46-1.

Alexander, W. J. R. & Emeritus, W. J. R. (2005). Linkages between Solar Activity, and Climatic Responses. Energy & Environment, 16(2), pp. 239 - 253.

Aliyu, A. K., Modu, B., Tan, C. W. (2018). A review of renewable energy development in Africa: A focus in South Africa, Egypt, and Nigeria. Renewable, and Sustainable Energy Reviews, 81(2), pp. 2502 - 18.

An, S. (2018). Impact of Pacific Decadal Oscillation on Frequency Asymmetry of El Niño, and La Niña Events. Advances in Atmospheric Sciences, 35(5), pp. 493 - 4.

Anderson, D. M., Moy, C. M., Rodbell, D. T. & Seltzer, G. O. (2002). Variability of El Niño/Southern Oscillation activity at millennial timescales during the Holocene epoch. Letters to Nature, 420(6912), pp. 162 - 65.

Angel, J. R. & Isard, S. A. (1998). The frequency, and intensity of Great Lake cyclones. Journal of Climate, 11(1), pp. 61 - 71.

Angell, J. K. (1981). Comparison of variations in atmospheric quantities with sea surface temperature variations in the equatorial eastern Pacific. Monthly Weather Review, 109(2), pp. 230 - 43.

Apata, O., Adebayo, A. V. & Awodele, K. O. (2020). Grid Integration of Wind Energy: The South African Challenge. Kenya, IEEE PES/IAS PowerAfrica.

Appendini, C. M., Hernández-Lasheras, J., Meza-Padilla, R. & Kurczyn, J. A. (2018). Effect of climate change on wind waves generated by anticyclonic cold front intrusions in the Gulf of Mexico. Climate Dynamics, 51(9-10), pp. 3747 - 63.

Archer, C. L. & Jacobson, M. Z. (2003). Spatial, and temporal distribution of U.S. winds, and wind power at 80 m derived from measurements. Journal of Geophysical Research, 108(D9), pp. 1 - 20.

Archer, C. L. & Jacobson, M. Z. (2004). Corrections to "Spatial, and temporal distribution of US winds, and wind power at 80 m derived from measurements. Journal of Geophysical Research, 109(D20116), pp. 1 - 11.

Archer, C. L. & Jacobson, M. Z. (2005). Evaluation of global wind power. Journal of Geophysical Research, 110(D12), pp. 1 - 20.

Archer, C. L. & Jacobson, M. Z. (2007). Supplying baseload power, and reducing transmission requirements by interconnecting wind farms. Journal of Applied Meteorology, and Climatology, 46 (11), pp. 1701 - 17.

Argent, B. (2015). An exploration of South Africa's wind climate using station records, and reanalysis data, Cape Town: University of Cape Town.

Arreyndip, N. A., Ebobenow, J. & Afungchui, D. (2016). Wind energy potential assessment of Cameroon's coastal regions for the installation of an onshore wind farm. Heliyon, 2(11), p. e00187.

Arslan, H., Baltaci, H., Akkoyunlu, B. O., Karanfil, S., & Tayanc, M. (2020). Wind speed variability, and wind power potential over Turkey: Case studies for Çanakkale, and İstanbul. Renewable Energy, 145(15992), pp. 1020 - 32.

Ashok, K., Guan, Z. & Yamagata, T. (2003). Influence of the Indian Ocean Dipole on the Australian winter rainfall. Geophys. Res. Lett., 30(15), p. 1821.

Asumadu-Sarkodie, S. & Owusu, P. A. (2016). The potential, and economic viability of wind farms in Ghana. Energy Sources, 38(5), pp. 695 - 701.

Awad, A. S. A., Ahmed, M. H., El-Fouly, T. H. M. & Salama, M. M. A. (2017). The impact of wind farm location, and control strategy on wind generation penetration, and market prices. Renewable Energy, 106(06), pp. 254 - 64.

Ayodele, T. R., Jimoh, A. A., Munda, J. L. & Agee, J. T. (2012). Wind distribution, and capacity factor estimation for wind turbines in the coastal region of South Africa. Energy Conversion, and Management, 64(12), pp. 614-25.

Ayodele, T. R., Jimoh, A. A., Mundal, J. L. & Agee, J. T. (2012). Statistical analysis of wind speed, and wind power potential of Port Elizabeth using Weibull parameters. J. Energy South, 23(2), pp. 30 - 8.

Azeroual, M., Makrini, A. E., Moussaoui, H. E. & H, M. E. (2018). Renewable Energy Potential, and Available Capacity for Wind, and Solar Power in Morocco Towards 2030. Journal of Engineering Science, and Technology Review, 11(1), pp. 189 - 98.

Azorin-Molina, C., Menendez, M., McVicar, T. R., Acevedo, A., Vicente-Serrano, S. M., Cuevas, E., Chen, D. (2018). Wind speed variability over the Canary Islands, 1948–2014: focusing on trend differences at the land–ocean interface, and below–above the inversion layer. Climate Dynamics, 50(11-12), pp. 4061 - 81.

Azorin-Molina, C., Vicente-Serrano, S. M., McVicar, T. R., Jerez, S., Sanchez-Lorenzo, A., López-Moreno, J. I., Espírito-Santo, F. (2014). Homogenization, and assessment of observed near-surface wind speed trends over Spain, and Portugal, 1961–2011. Journal of Climate, 27(10), pp. 3692 - 3712.

Azorin-Molina, C., Vicente-Serrano, S. M., McVicar, T. R., Revuelto, J., Jerez, S., & López-Moreno, J. I. (2017). Assessing the impact of measurement time interval when calculating wind speed means, and trends under the stilling phenomenon. International Journal of Climatology, 37(1), pp. 480 - 92.

Azzellino, A., Lanfredi, C., Riefolo, L., Contestabile, P., & Vicinanza, D. (2019). Combined Exploitation of Offshore Wind, and Wave Energy in the Italian Seas: A Spatial Planning Approach. Fontiers in Energy Research, 7(42), pp. 1 - 15.

Babenko, V., Babenko, R., Gamieldien, J. & Markel, A. (2019). FTO haplotyping underlines high obesity risk for European populations. BMC Medical Genomics, 12(2), p. 46.

Bandyopadhyay, A., Bhadra, A., Raghuwanshi, N. S. & Singh, R. (2009). Temporal trends in estimates of reference evapotranspiration over India. Journal of Hydrologic Engineering, 14(5), pp. 508 - 15.

Barry, M., Steyn, H. & Brent, A. (2011). Selection of renewable energy technologies for Africa: Eight case studies in Rwanda, Tanzania, and Malawi. Renewable Energy, 36(11), pp. 2845 - 52.

Barthelmie, R. J., Pryor, S. C. & Schoof, J. T. (2006). Inter-annual Variability of Wind Indices across Europe. Wind Energy, 06 (9), pp. 27 - 38.

Bayer, B. (2018). Experience with auctions for wind power in Brazil. Renewable, and Sustainable Energy Reviews, 81(01), pp. 2644 - 58.

Beer, J., Cubasch, U., Fleitmann, D. & Geller, M. (2010). Solar influences on climate. Reviews of Geophysics, 48 (4), pp. 1 - 40.

Beer, J., Mende, W. & Stellmacher, R. (2000). The role of the sun in climate forcing. Quaternary Science Reviews, 19(1 - 5), pp. 403 - 15.

Behera, S. K. & Yamagata, T. (2001). Subtropical SST dipole events in the southern Indian Ocean. Geophysical Research Letters, 28(2), pp. 327 - 30.

Behera, S. K., Krishnan, R. & Yamagata, T. (1999). Unusual ocean-atmosphere conditions in the tropical Indian Ocean during 1994. Geophysical research letters, 26(19), pp. 3001 - 4.

Behera, S. K., Luo, j. & Masson, S. (2005). Paramount impact of the Indian Ocean Dipole on the East African short rains. Journal of Climate, 18(21), pp. 4514 - 30.

Bekele, G. & Palm, B. (2009). Wind energy potential assessment at four typical locations in Ethiopia. Applied Eenrgy, 86(3), pp. 388 - 96.

Belu, R. & Koracin, D. (2009). Wind characteristics, and wind energy potential in western Nevada. Renewable energy, 34(10), pp. 2246 - 51.

Benmemdejahed, M. & Mouhadjer, S. (2016). Evaluation of wind energy cost, and site selection for wind-farm in the south of Algeria. Algeria, AIP Publishing LLC.

Berry, G., Reeder, M. J. & Jakob, C. (2011). A global climatology of atmospheric fronts. Geophysical research letters, 38(4), pp. 1 - 5.

Betz, A. (1966). Introduction to the Theory of Flow Machines. Oxford: Pergamon press.

Bianchi, E., Solarte, A. & Guozden, T. M. (2017). Large scale climate drivers for wind resource in Southern South America. Rnewable Energy, 114(B), pp. 708 - 15.

Bigg, G. R. (1993). Comparison of coastal wind, and pressure trends over the tropical Atlantic: 1946–1987. Internationa; Journal of Climatology, 13(4), pp. 411 - 21.

Bjerknes, J. (1969). Atmospheric teleconnections from the equatorial Pacific. Monthly Weather Reviews, 97(3), pp. 163 - 72.

Black, E. (2005). The relationship between Indian Ocean sea–surface temperature, and East African rainfall. Philosophical Transactions of the Royal Society A, 363(1826), pp. 43 - 7.

Black, E., Slingo, J. & Sperber, K. R. (2003). An observational study of the relationship between excessively strong short rains in coastal East Africa, and Indian Ocean SST. Monthly Weather Rreview, 131(1), pp. 74 - 94.

Bloomfield, P. (1976). Fourier analysis of time series; An introduction. New York: Wiley, and Sons, Inc..

Bonan, G. B. & Doney, S. C. (2018). Climate, ecosystems, and planetary futures: The challenge to predict life in Earth system models. Science, 359(6375), pp. 1 - 11.

Bormann, H. (2011). Sensitivity analysis of 18 different potential evapotranspiration models to observed climatic change at German climate stations. Climatic Change, 104(3 - 4), pp. 729 - 53.

Borraccino, A., Schlipf, D., Haizmann, F. & Wagner, R. (2017). Wind Field Reconstruction from Nacelle-Mounted Lidars Short Range Measurements. Wind Energy Science Discussions, 2(1), pp. 269 - 83.

Bossanyi, E., Burton, T., Jenkins, N. & Sharpe, D. (2001). Wind energy handbook. 1 ed. West Sussex, England: John Whiley & Sons Ltd.

Botha, M. S., Carrick, P. J. & Allsopp, N. (2008). Capturing lessons from land-users to aid the development of ecological restoration guidelines for lowland Namaqualand. Biological Conservation, 141(4), pp. 885 - 95.

Boudia, S. M., Benmansour, A., Ghellai, N., Benmedjahed, M., & Tabet Hellal, M. A. (2012). Monthly, and seasonal assessment of wind energy potential in Mechria region, occidental highlands of Algeria. International Journal of Green Energy, 9(3), pp. 243 - 55.

Böwer, C. (2006). Die Entwicklung des Klimas in Münster/Westfalen, Germany: Westfälischen Wilhelms-Universität Münster.

Brázdil, R., Chromá, K., Dobrovolný, P. & Tolasz, R. (2009). Climate fluctuations in the Czech Republic during the period 1961–2005. International Journal of Climatology: A Journal of the Royal Meteorological Society, 29(2), pp. 223 - 42.

Breslow, P. B. & Sailor, D. J. (2002). Vulnerability of wind power resources to climate change in the continental United States. Renewable Energy, 02 (27), pp. 585 - 98.

Bryukhan, F. F. & Diab, R. D. (1993). A Wind Power Simulation Model for a System of Compound Wind Farms. Wind Engineering, 17(1), pp. 15 - 23.

Burroughs, W. (1986). Randomness rules the weather. New Scientist, 10(7), pp. 36 - 40.

Cai, W., Santoso, A., Wang, G., Weller, E., Wu, L., Ashok, K., Yamagata, T. (2014). Increased frequency of extreme Indian Ocean Dipole events due to greenhouse warming. Nature, 510(7504), pp. 254 - 58.

Cai, Y., Lu, Y., Liu, J., Dai, X., Xu, H., Lu, Y., & Gong, Z. (2016). Macrozoobenthic community structure in a large shallow lake: Disentangling the effect of eutrophication, and wind-wave disturbance. Limnologica, 59(07), pp. 1 - 9.

Çakmak, R. E., Akpinar, A. & Van Vledder, G. P. (2019). Comparative Performance Analysis of Different Wind Fields in Southern, and North-Western Coastal Areas of the Black Sea. Mediterranean Marine Science, 20(2), pp. 427 - 452.

Calitz, J. R. & Wright, J. G. (2019). Statistics of utility-scale solar PV, wind, and CSP in South Africa in 2018. [Online] Available at: http://researchspace.csir.co.za/dspace/handle/10204/10636. [Accessed 28 07 2019].

Cancino-Solórzano, Y. & Xiberta-Bernat, J. (2009). Statistical analysis of wind power in the region of Veracruz (Mexico). Renewable Energy, 34(6), pp. 1628 - 34.

Cane, M. A. (2005). The evolution of El Niño, past, and future. Earth, and Planetary Science Letters, 230 (3-4), pp. 227 - 40.

Carpenter, T. H. & Rasmusson, E. M. (1982). Variations in Tropical Sea Surface Temperature, and Surface Wind Fields Associated with the Southern Oscillation/El Niño. Monthly Weather Review, 110(5), pp. 354 - 84.

Carslaw, K. S., Harrison, R. G. & Kirkby, J. (2002). Cosmic rays, clouds, and climate. Science, 298 (5599), pp. 1732 - 37.

Casella, L. (2019). Wind speed reconstruction using a novel Multivariate Probabilistic method, and Multiple Linear Regression: advantages compared to the single correlation approach. Journal of Wind Engineering, and Industrial Aerodynamics, 191(8), pp. 252 - 65.

Cevallos-Sierra, J. & Ramos-Martin, J. (2018). Spatial assessment of the potential of renewable energy: The case of Ecuador. Reviews, Renewable, and Sustainable Energy, 81(1), pp. 1154 - 65.

Chand, S. S., Tory, K. J., Ye, H. & Walsh, K. J. (2017). Projected increase in El Niño-driven tropical cyclone frequency in the Pacific. Nature Climate Change, 7(2), pp. 123 - 27.

Chen, S. F. & Song, L. Y. (2018). The leading interannual variability modes of winter surface air temperature over Southeast Asia. Climate Dynamics, 51(327), pp. 1 - 20.

Choudhary, R. R., Jhajharia, D., Lal, M., Jain, J. K., Lunayach, A., & Choudhary, M. K. (2009). Climate, and its variations over Bikaner since 1951–2008. Journal, Indian Geological Congress, 1(2), pp. 76 - 86.

Cisneros-Saldana, J. I. & Hosseinian, S. B. S. (2018). Network-based optimization techniques for wind farm location decisions. Frontiers of Engineering Management, 5(4), pp. 533 - 40.

Claar, D. C., Szostek, L., McDevitt-Irwin, J. M., Schanze, J. J., & Baum, J. K. (2018). Global patterns, and impacts of El Niño events on coral reefs: A meta-analysis. PLoS ONE, 13(2), p. e0190957.

Clarke, H., Tran, B., Boer, M. M., Price, O., Kenny, B., & Bradstock, R. (2019). Climate change effects on the frequency, seasonality, and interannual variability of suitable prescribed burning weather conditions in south-eastern Australia. Agricultural, and Forest Meteorology, 271(6), pp. 148 - 57.

Clarke, H., Tran, B., Boer, M. M., Price, O., Kenny, B., & Bradstock, R. (2019). Climate of Inter-annual Wind, and Solar Variations on the European Power System. Joule, 2(10), pp. 2076 - 90.

Colette, A. & Ancellet, G. (2005). Impact of vertical transport processes on the tropospheric ozone layering above Europe.: Part II: climatological analysis of the past 30 years. Atmospheric environment, 39(29), pp. 5423 - 35.

Collins, M. (2005). El Niño- or La Niña-like climate change. Climate Dynamics, 24(1), pp. 89 - 104.

Cong, Z. T., Yang, D. W. & Ni, G. H. (2009). Does evaporation paradox exist in China?. Hydrology, and Earth System Sciences, 13(3), pp. 357 - 66.

Cong, Z., Zhao, J., Yang, D. & Ni, G. (2010). Understanding the hydrological trends of river basins in China. Journal of Hydrology, 388(3 - 4), pp. 350 - 6.

Cox, P. M., Huntingford, C. & Williamson, M. S. (2018). Emergent constraint on equilibrium climate sensitivity from global temperature variability. Nature, 553(7688), pp. 319 - 22.

Crétat, J., Pohl, B., Dieppois, B., Berthou, S., & Pergaud, J. (2019). The Angola Low: relationship with southern African rainfall, and ENSO. Climate Dynamics, 52(3 - 4), pp. 1783 - 803.

Crétat, J., Richard, Y., Phol, B. & Rouault, M. (2012). Recurrent daily rainfall patterns over South Africa, and associated dynamics during the core of the austral summer. International Journal of Climatology, 32 (2), pp. 261 - 73.

Crooks, S. A. & Gray, L. J. (2005). Characterisation of the 11-year solar signal using a multiple regression analysis of the ERA-40 dataset. Journal of climat, 18(7), pp. 996 - 1015.

CSIR, (2010). WASA (Wind Atlas for South Africa). [Online] Available at: http://www.wasa.csir.co.za/ [Accessed 09 April 2015].

Currie, R. G. (1993). Luni-solar 18.6-, and 10–11-year solar cycle signals in South African rainfall. Royal meteorological society, 13(3), pp. 237 - 56.

Cusack, S. (2013). A 101 year record of windstorms in the Netherlands. Climate Change, 116(3 - 4), pp. 693 - 704.

Czisch, G. & Ernst, B. (2001). High wind power penetration by the systematic use of smoothing effects within huge catchment areas shown in a European example. Windpower, 2001(6), pp. 1 - 10.

da Silva, G. M. & Hesp, P. (2010). Coastline orientation, aeolian sediment transport, and foredune, and dunefield dynamics of Moçambique Beach, Southern Brazil. Geomorphology, 120(3 - 4), pp. 258 - 78.

Dabar, O. A., Awaleh, M. O., Kirk-Davidoff, D., Olauson, J., Söder, L., & Awaleh, S. I. (2019). Wind resource assessment, and economic analysis for electricity generation in three locations of the Republic of Djibouti. Energy, 185(10), pp. 884 - 94.

Dadaser-Celik, F. & Cengiz, E. (2013). Wind speed trends over Turky from 1975 to 2006. International Journal of Climatology, 14(34), pp. 1913 - 27.

Dalton, A., Bekker, B. & Koivisto, M. J. (2020a). Atmospheric circulation archetypes as clustering criteria for wind power inputs into probabilistic power flow analysis. Belgium / Virtual, IEEE.

Dalton, A., Bekker, B. & Koivisto, M. J. (2020b). Simulation, and detection of wind power ramps, and identification of their causative atmospheric circulation patterns. Electric Power Systems Research, pp. 106936.

Dalton, A., Bekker, B. & Kruger, A. C. (2019). Wind power variability during the passage of cold fronts across South Africa. Journal of Energy in Southern Africa, 30(3), pp. 52 - 67.

Dani, T., Priyatikanto, R., Winarko, A., Putri, G. P., & Antariksa, P. S. (2019). Relationship, and periodicity of solar coronal hole area with the solar wind speed, and geomagnetic activities. Jurnal Sains Dirgantara, 16(2), pp. 27 - 38.

Davis, J. C. & Sampson, R. J. (1986). Statistics, and data analysis in geology. 646 ed. New York: Wiley.

Davis, J. C. (1973). Statistics, and data analysis in geology. 3rd ed. New York: John Wiley, and Sons.

Davis, W. J., Taylor, p. J. & Davies, W. B. (2018). The Antarctic Centennial Oscillation: A Natural Paleoclimate Cycle in the Southern Hemisphere That Influences Global Temperature. Climate, 6(1), p. 3.

Davy, R., Gnatiuk, N., Pettersson, L. & Bobylev, L. (2018). Climate change impacts on wind energy potential in the European domain with a focus on the Black Sea. Renewable, and Sustainable Energy Reviews, 81(2), pp. 1652 - 9.

de Lucena, A. F., Dutra, R. M., Schaeffer, R. & Szklo, A. S. (2010). The vulnerability of wind power to climate change in Brazil. Renewable Energy, 10 (35), pp. 904 - 12.

de Queiroz, A. R., Mulcahy, D., Sankarasubramanian, A., Deane, J. P., Mahinthakumar, G., Lu, N., & DeCarolis, J. F. (2019). Repurposing an energy system optimization model for seasonal power generation planning. Energy, 181(8), pp. 1321 - 30.

Diab, R. D. & Garstang, M. (1984). Assessment of wind power potential for two contrasting coastlines of South Africa using a numerical model. Journal of Climate, and Applied Meteorology, 84 (23), pp. 1645 - 59.

Diab, R. D. (1995). Wind atlas of South Africa, Johannesburg: Department of Mineral, and Energy Affairs.

Diaz, H. F., Hoerling, M. P. & Eischeid, J. K. (2001). ENSO variability, teleconnections, and climate change. International Journal of Climatology, 21(15), pp. 1845 - 1862.

Dincer, F. (2011). The analysis on wind energy electricity generation status, potential, and policies in the world. Renewable, and Sustainable Energy Reviews, 15(9), pp. 5135 - 42.

DoE. (2012). Government gazette No.36005, Pretoria: DOE.

DoE. (2013). IRP 2010-2030 UPDATE REPORT, Pretoria: DOE.

DoE. (2015a). IPP renewables Press Centre. [Online] Available at: http://www.ipprenewables.co.za/#page/304 [Accessed 30 April 2015].

DoE. (2015b). Press Center. [Online] Available at: http://www.ipprenewables.co.za/#page/304 [Accessed 16 March 2015].

Donohue, R. J., McVicarm, T., Li, L., Roderick, M. L. (2010). A data resource for analysing dynamics in Australian ecohydrological conditions. Austral Ecology, 35(5), pp. 593 - 4.

Dorvlo, A. S. S. & Ampratwum, D. B. (2002). Wind energy potential for Oman. Renewable Energy, 26(3), pp. 333 - 38.

Dunning, C. M., Black, E. & Allan, R. P. (2018). Later Wet Seasons with More Intense Rainfall over Africa under Future Climate Change. Journal of Climate, 31(23), pp. 9719 - 38.

Dyson, L. L., Van Heerden, J. & Sumner, P. D. (2015). A baseline climatology of sounding-derived parameters associated with heavy rainfall over Gauteng, South Africa. International Journal of Climatology, 35(1), pp. 114 - 27.

Eddy, A. (1965). Kinetic energy production in a mid-latitude storm. Journal of Applied Meteorology, 4(5), pp. 569 - 75.

Efthimiou, G. C., Kumar, P., Giannissi, S. G., Feiz, A. A., & Andronopoulos, S. (2019). Prediction of the wind speed probabilities in the atmospheric surface layer. Renewable Energy, 132(3), pp. 921 - 30.

Egorova, T., Schmutz, W., Rozanov, E., Shapiro, A. I., Usoskin, I., Beer, J., Peter, T. (2018). Revised historical solar irradiance forcing. Astronomy & Astrophysics, 615(7), pp. 1 - 10.

Elmabruk, A. M., Aleej, F. A. & Badii, M. M. (2014). Estimation of wind energy in Libya. In 2014 5th International Renewable Energy Congress (IREC). Tunisia, IEEE.

El-Osta, W., Belhag, M., Klat, M., Fallah, I., & Kalifa, Y. (1995). Wind farm pilot project in Libya. Renewable Energy, 6(5-6), pp. 639 - 42.

Elsawwaf, M., Willems, P. & Feyn, J. (2010). Assessment of the sensitivity, and prediction uncertainty of evaporation models applied to Nasser Lake, Egypt. Journal of Hydrology, 1-2(395), pp. 10 - 22.

Elsner, P. (2019). Continental-scale assessment of the African offshore wind energy potential: Spatial analysis of an under-appreciated renewable energy resource. Renewable, and Sustainable Energy Reviews, 104(4), pp. 394 - 407.

EMD. (2015). EMD International. [Online] Available at: http://www.emd.dk/ [Accessed 16 March 2015].

Emeis, S. (2018). Wind Regimes. In: Cham, ed. Wind Energy Meteorology. Garmisch-Partenkirchen, Germany: Springer, pp. 11 - 30.

Engelbrecht, C. J. & Landman, W. A. (2016). Interannual variability of seasonal rainfall over the Cape south coast of South Africa, and synoptic type association. Climate dynamics, 47(1 - 2), pp. 295 - 313.

Enloe, J., O'Brian, J. J. & Smith, S. R. (2004). ENSO impacts on peak wind gusts in the United States. Journal of Climate, 04 (17), pp. 1728 - 37.

Erik, P. L., Niels, M. G., Landberg, L. & Hojstrup, J. (1997). Wind Power Meteorology, Denmark: Riso National Laboratory.

Eskom. (2017a). Eskom 2018/19 Revenue Application. [Online] Available at: http://www.nersa.org.za/Admin/Document/Editor/file/Consultations/Electricity/Presentations/Eskom14-11-2017.pdf [Accessed 23 June 2018].

Eskom. (2017b). SCHEDULE OF STANDARD PRICES FOR ESKOM TARIFFS. [Online] Available at: http://www.eskom.co.za/CustomerCare/TariffsAndCharges/Documents/Eskom%2

0schedule%20of%20standard%20prices%202017_18%2015_02_2017%20%2800%29.pdf [Accessed 23 June 2018].

Eskom. (2018). Integrated report 2017. [Online] Available at: http://www.eskom.co.za/IR2018/Documents/Eskom2018IntegratedReport.pdf [Accessed 03 10 2018].

Eskom. (2019a). Eskom Weekly System Status Reports. [Online] Available at: www.eskom.co.za/Whatweredoing/SupplyStatus/Pages/AdequacyReports2018.aspx [Accessed 7 Sept 2019].

Eskom. (2019b). Intergrated Report 2018. [Online] Available at: http://www.eskom.co.za/IR2019/Documents/Eskom_2019_integrated_report.pdf [Accessed 20 10 2019].

Eskom. (2019c). System Adequacy Reports. [Online] Available at: www.eskom.co.za/Whatweredoing/SupplyStatus/Pages/SupplyStatusT.aspx [Accessed 7 Sept 2019].

European Commission. (2013). European Commission guidance for the design of renewables support schemes-Accompanying the document Communication from the Commission delivering the internal market in electricity, and making the most of public intervention, Brussels: European Commission.

Eygelaar, J., Lotter, D. P. & van Vuuren, J. H. (2018). Generator maintenance scheduling based on the risk of power generating unit failure. International Journal of Electrical Power & Energy Systems, 95(2), pp. 83 - 95.

Fant, C., Gunturu, B. & Schlosser, A. (2016). Characterizing wind power resource reliability in southern Africa. Applied Energy, 161(1), pp. 565-73.

Fant, C., Schlosser, A. C. & Strzepek, K. (2016). The impact of climate change on wind, and solar resources in Southern Africa. Applied Energy, 161 (16), pp. 556 - 64.

Fedorovich, E. & Shapiro, A. (2009). Structure of numerically simulated katabatic, and anabatic flows along steep slopes. Acta Geophysica, 57 (4), pp. 981 - 1010.

Ferster, B., Subrahmanyam, B. & Macdonald, A. (2018). Confirmation of ENSO-Southern Ocean teleconnections using satellite-derived SST. Remote Sensing, 10(2), p. 331.

Fischer, M. S., Tang, B. H. & Corbosiero, K. L. (2019). A Climatological Analysis of Tropical Cyclone Rapid Intensification in Environments of Upper-Tropospheric Troughs. Monthly Weather Review, 147(10), pp. 3693 - 719.

Fitchett, J. M. & Grab, S. W. (2014). A 66-year tropical cyclone record for south-east Africa: temporal trends in a global context. International Journal of Climatology, 34(13), pp. 3604 - 15.

Foukal, P., Frohlich, C., Spruit, H. & Wigley, T. M. L. (2006). Variations in solar luminosity, and their effect on the Earth's climate. Nature, 06 (443), pp. 161 - 66.

Frame, T. H. A. & Gray, L. J. (2008). The 11-year solar cycle in ERA-40 data: An update to 2008. Journal of Climate, 23(7), pp. 2213 - 22.

Fröhlich, C. (2006). Solar irradiance variability since 1978: Revision of the PMOD composite during solar cycle 21. Space science reviews, 125(1-4), pp. 53 - 65.

Fu, G., Yu, J., Zhang, Y., Hu, S., Ouyang, R., & Lui, W. (2010). Temporal variation of wind speed in China for 1961 - 2007. Theory of Applied Climatology, 10(104), pp. 313 - 24.

Gao, Z., He, J., Dong, K. & Li, X. (2017). Trends in reference evapotranspiration, and their causative factors in the West Liao River basin, China. Agricultural, and Forest Meteorology, 232(01), pp. 106 - 17.

Gebreegziabher, Y. (2004). Assessment of the Water Balance of Lake Awassa Catchment, Ethiopia. The Netherlands: ITC, Enschede.

Gerstengarbe, F. W., Werner, P. C. & Hauf, Y. (2004). Erstellung regionaler Klimaszenarien für Nordrhein-Westfalen. [Online] Available at:

http://klimastrategie.jensbemme.de/download/nrw_klimastudie2004.pdf [Accessed 22 02 2020].

Giannini, A., Biasutti, M., Held, I. M. & Sobel, A. H. (2008). A global perspective on African climate. Climatic Change, 90(4), pp. 359 - 83.

Giebel, G. (2000). Equalizing effects of the wind energy production in Northern Europe determined from reanalysis data, Denmark: DTU.

Gielen, D., Boshell, F., Saygin, D., Bazilian, M. D., Wagner, N., & Gorini, R. (2019). The role of renewable energy in the global energy transformation. Energy Strategy Reviews, 24(04), pp. 38 - 50.

Gillingham, K., Nordhaus, W., Anthoff, D., Blanford, G., Bosetti, V., Christensen, P., Reilly, J. (2018). Modeling Uncertainty in Integrated Assessment of Climate Change: A Multimodel Comparison. Journal of the Association of Environmental, and Resource Economists, 5(4), pp. 791 - 826.

Glantz, M. H. (2001). Currents of Change: Impacts of El Niño, and La Niña on Climate, and Society. Cambridge: Cambrige University Press.

Goddard, L. & Graham, N. E. (1999). Importance of the Indian Ocean for simulating rainfall anomalies over eastern, and southern Africa. Journal of Geo, 104(D16), pp. 19099 - 116.

Gong, D. & Wang, S. (1999). Definition of Antarctic oscillation index. Geophysical research letters, 26(4), pp. 459 - 62.

Gonzalez, P. L., Brayshaw, D. J. & Zappa, G. (2019). The contribution of North Atlantic atmospheric circulation shifts to future wind speed projections for wind power over Europe. Climate Dynamics, 53(7-8), pp. 4095 - 113.

Grab, S. W. & Simson, A. J. (2000). Climatic, and environmental impacts of cold fronts over KwaZulu-Natal, and the adjacent interior of southern Africa. South African Journal of Science, 96(11/12), pp. 602 - 8.

Gray, L. J., Beer, J., Geller, M., Haigh, J. D., Lockwood, M., Matthes, K., Hood, L. (2010). Solar influences on climate. Reviews of Geophysics, 48(4), p. RG4001.

Griffin, B. J., Kohfeld, K. E., Cooper, A. B. & Boenisch, G. (2010). Importance of location for describing typical, and extreme wind speed behavior. Geophysical research letters, 37(22), p. L22804.

Grossman, A. & Morlet, J. (1984). Decomposition of Hardy functions into square integrable wavelets of constant shape. SIAM Journal on Mathematical Analysis, 15(4), pp. 723 - 36.

Grundstrom, M., Tang, L., Hallquist, M. & Hung, N. (2015). Influence of atmospheric circulation patterns on urban air quality during the winter. Atmospheric Pollution Research, 6 (2), pp. 278 - 85.

Gruza, G. V. (2008). Assessment report on climate change, and their impact on the territory of the Russian Federation, Moscow: Federal service for hydrometerology, and environmental monitoring (Roshydromet).

Guignard, G., Yang, X. J. & Wang, Y. D. (2019). Cuticle ultrastructure of Baiera furcata from Northeast China, and its implication in taxonomy, and paleoenvironment. Review of Palaeobotany, and Palynology. Review of Palaeobotany, and Palynology, 268(9), pp. 95 - 108.

Guo, H., Xu, M. & Hu, Q. (2011). Changes in near-surface wind speed in China: 1969–2005. International Journal of Climatology, 31(3), p. 349 – 358.

Guyot, G. & Guyot, G. (1998). Physics of the Environment, and Climate. New York: Wiley.

Hagermann, K. (2008). Mesoscale Wind Atlas of South Africa, Thesis presented for the degree of Doctor of Philosophy, University of Cape Town.. [Online] Available at: https://open.uct.ac.za/handle/11427/5287 [Accessed 24 October 2015].

Hagermann, K. (2008). Mesoscale Wind Atlas of South Africa, Thesis presented for the degree of Doctor of Philosophy, University of Cape Town.. [Online] Available at: https://open.uct.ac.za/handle/11427/5287

Haigh, J. D. & Blackburn, M. (2006). Solar influences on dynamical coupling between the stratosphere, and troposphere. Space science reviews, 125(1 - 4), pp. 331 - 344.

Haigh, J. D. & Roy, I. (2010). Solar cycle signals in sea level pressure, and sea surface temperature. Atmosphere Chemistry, and Physics, 10(10), pp. 3147 - 53.

Haigh, J. D. (2002). The effects of solar variability on the Earth's climate. Philosophical Transactions of the Royal Society of London. Series A: Mathematical, Physical, and Engineering Sciences, 361(1802), pp. 95 - 111.

Haigh, J. D., Blackburn, M. & Day, R. (2005). The response of tropospheric circulation to perturbations in lower-stratospheric temperature. Journal of climate, 18(17), pp. 3672 - 3685.

Halpert, M. S. & Ropelewski, C. F. (1987). Global, and Regional Scale Precipitation Patterns Associated with the El Niño/Southern Oscillation. Monthly Weather Review, 115(8), pp. 1606 - 26.

Hammer, Ø., Harper, D. A. T. & Ryan, P. D. (2001). PAST: Paleontological Statistics Software Package for Education, and Data Analysis. Palaeontologia Electronica, 4(1), p. 9.

Hart, M., Sailor, D. J. & Smith, M. (2008). Climate change implications for wind power resources in the Northwest United States. Renewable Energy, 08 (33), pp. 2393 - 2406.

Hartmann, B. & Wendler, G. (2005). The significance of the 1976 Pacific climate shift in the climatology of Alaska. Journal of climate, 18(22), pp. 4824 - 39.

Haslett, J. & Raftery, A. E. (1989). Space-time modelling with long-memory dependence: Assessing Ireland's wind power resource. Journal of the Royal Statistical Society: Series C (Applied Statistics), 38(1), pp. 1- 21.

Herbst, L. & Lalk, J. (2014). A case study of climate variability effects on wind resources in South Africa. Journal of Energy in Southern Africa, 25(3), pp. 2 - 10.

Hernández-Escobedo, Q., Manzano-Agugliaro, F. & Zapata-Sierra, A. (2010). The wind power of Mexico. Renewable, and Sustainable Energy reviews, 14(9), p. 2830 – 40.

Herold, N. & Santoso, A. (2018). Indian Ocean warming during peak El Niño cools surrounding land masses. Climate Dynamics, 51(5-6), pp. 2097 - 2112.

Hess, T. M. (1998). Trends in reference evapo-transpiration in the North East Arid Zone of Nigeria, 1961–91. Journal of Arid Environments, 38(1), pp. 99 - 115.

Himri, Y., Himri, S. & Boudghene Stambouli, A. (2009). Assessing the wind energy potential projects in Algeria. Renewable, and Suustainable Energy, 13(8), pp. 2187 - 91.

Hobbins, M. (2004). Regional evapotranspiration, and pan evaporation: complementary interactions, and long-term trends across the conterminous United States. [Online] Available at: https://search.proquest.com/openview/21c91becbde3618d4501bf6b50d9a6c4/1?pq-origsite=gscholar&cbl=18750&diss=y [Accessed 22 Feb 2020].

Hoerling, M. P., Kumar, A. & Zhong, M. (1997). El Niño, La Niña, and the Nonlinearity of Their Teleconnections. Journal of Climate, 10(8), pp. 1769 - 86.

Hoffman, M. T., Cramer, M. D., Gillson, L. & Wallace, M. (2011). Pan evaporation, and wind run decline in the Cape Floristic Region of South Africa (1974–2005): implications for vegetation responses to climate change. Climatic Change, 109(3 - 4), pp. 437 - 52.

Holttinen, H. (2004). Hourly wind power variations in the Nordic countries. Wind Energy: An International Journal for Progress, and Applications in Wind Power Conversion Technology, 8(2), pp. 173 - 95.

Hove, T., Madiye, L. & Musademba, D. (2014). Mapping wind power density for Zimbabwe: a suitable Weibull-parameter calculation method. Journal of Energy in Southern Africa, 25(4), pp. 37 - 47.

Hrayshat, E. S. (2007). Wind resource assessment of the Jordanian southern region. Renewable Energy, 32(11), pp. 1948 - 60.

Huang, H. Y., Capps, S. B., Huang, S. C. & Hall, A. (2015). Downscaling near-surface wind over complex terrain using a physically-based statistical modeling approach. Climate Dynamics, 44 (1), pp. 529 - 42.

Hui, C. & Zheng, X. T. (2018). Uncertainty in Indian Ocean Dipole response to global warming: the role of internal variability. Climate Dynamics, 51(9-10), pp. 3597 - 3611.

Iacono, M. J. (2009). Why is the Wind Speed Decreasing?, Milton, Massachusetts: Blue Hill Meteorological Observatory.

IEA. (2018). Renewables 2018: Market analysis, and forecast from 2018 to 2023, Paris: International Energy Association.

IEC. (2019). Wind energy generation systems - Part 1: Design requirements, Geneva: IEC.

IEC. (2020). Wind energy generation systems: IEC 61400-15 ED1, Geneva: IEC.

International Energy Agency. (2016). Egypt: Feed-in tariff for wind, and solar PV projects, Paris: IEA.

International Energy Agency. (2016). IEA wind TPC 2015 annual report, Paris: International Energy Agency.

IRENA. (2012). Wind power: volume 1, Power Sector Issue 5/5, Masdar City: International Renewable Energy Association.

IRENA. (2019). RENEWABLE CAPACITY STATISTICS 2019, Abu Dhabi: International Renewable Energy Agency.

Jacob, A. & Rajvanshi, A. K. (2006). Long term weather trends in western Maharashtra, India: Nimbkar Agricultural Research Institute (NARI).

Jacovides, C. P., Theophilou, C., Tymvios, F. S. & Pashiardes, S. (2002). Wind statistics for coastal stations in Cyprus. Theoretical, and applied climatology, 72(3 - 4), pp. 259 - 63.

Jasmine, B. D. J., Cuff, C., Rasmussen, C. & Hesson, A. S. (2018). Teleconnection of atmospheric, and oceanic climate anomalies with Australian weather patterns: a review of data availability. Earth-Science Reviews, 176(1), pp. 117 - 46.

Jenkins, G. M. & Watts, D. G. (1968). Spectral analysis, and its application. San Francisco: Holden-Day.

Jhajharia, D., Shrivastava, S. K., Sarkar, D. S. A. S. & Sarkar, S. (2009). Temporal characteristics of pan evaporation trends under the humid conditions of northeast India. Agricultural, and Forest Meteorology, 149(5), pp. 763 - 70.

Jiang, Y., Luo, Y., Zhao, Z. & Tao, S. (2010). Changes in wind speed over China during 1956–2004. Theoretical, and Applied Climatology, 99(3 -4), p. 421.

Jiménez, P. A., González-Rouco, J. F., Navarro, J., Montávez, J. P., & García-Bustamante, E. (2010). Quality assurance of surface wind observations from automated weather stations. Journal of atmospheric, and Oceanic Technology, 27(7), pp. 1101 - 22.

Jiménez-Muñoz, J. C., Mattar, C., Barichivich, J., Santamaría-Artigas, A., Takahashi, K., Malhi, Y., van der Schrier, G. (2016). Record -breaking warming, and extreme drought in the Amazon rainforest during the course of El Niño 2015–2016. Scientific Reports, 6(9), p. 33130.

Jing, P., O'Brien, T., Streets, D. G. & Patel, P. (2016). Relationship of ground-level ozone with synoptic weather conditions in Chicago. Urban Climate, 17(9), pp. 161 - 75.

Joubert, C. J. (2017). Geographical location optimisation of wind, and solar photovoltaic power capacity in South Africa using mean-variance portfolio theory, and time series clustering, Cape Town: Stellenbosch: Stellenbosch University.

Jung, C. & Schindler, D. (2018). On the inter-annual variability of wind energy generation – A case study from Germany. Applied Energy, 230(11), pp. 845 - 54.

Jung, C., Schindler, D. & Laible, J. (2018). National, and global wind resource assessment under six wind turbine installation scenarios. Energy Conversion, and Management, 165(1), pp. 403 - 15.

Jung, C., Taubert, D. & Schindler, D. (2019). The temporal variability of global wind energy – Long-term trends, and inter-annual variability. Energy Conversion, and Management, 188(5), pp. 462 - 72.

Jury, M. R. & Diab, R. (1989). Wind energy potential in the Cape coastal belt. South African Geographical Journal, 71(1), pp. 3 - 11.

Jury, M. R. (1988). Case studies of the response, and spatial distribution of wind-driven upwelling off the coast of Africa: 29–34 south. Continental Shelf Research, 8(11), pp. 1257 - 71.

Jury, M. R. (2018). Climate trends across South Africa since 1980. Water SA, 44(2), pp. 297 - 307.

Justus, C. G. & Mikhail, A. (1976). Height variation of wind speed, and wind distributions statistics. Geophysical Research Letters, 3(5), pp. 261 - 4.

Kahn, E. (1979). The reliability of distributed wind generators. Electric Power Systems Research, 2(1), pp. 1 - 14.

Kainkwa, R. M. (2010). Wind energy development in the African Great Lakes Region to supplement the hydroelectricity in the locality: a case study from Tanzania. World Academic in Science, Engineering, and Technology, 61(10), pp. 214 - 18.

Karnauskas, K. B., Lundquist, J. K. & Zhang, L. (2018). Southward shift of the global wind energy resource under high carbon dioxide emissions. Nature Geoscience, 11(1), pp. 38 - 43.

Kasatkina, E. A., Shumilov, O. I. & Krapiec, M. (2007). On periodicities in long term climatic variations near 68 ◦ N, 30 ◦ E. Advances in Geoscience, 13(08), pp. 25 - 9.

Katinas, V., Gecevicius, G. & Marciukaitis, M. (2018). An investigation of wind power density distribution at location with low, and high wind speeds using statistical model. Applied energy, 218(5), pp. 442 - 51.

Ke, R.-Y., Wang, B., Wei, Y.-M. & Yuan, X.-C. (2014). China's regional assessment of renewable energy vulnerability to climate change. Renewable, and Sustainable Energy Reviews, 14 (40), pp. 185 - 95.

Keevallik, S. & Soomere, T. (2009). Seasonal, and diurnal variations of wind parameters at Pakri. Estonian Journal of Engineering, 15(3), pp. 227 - 39.

Keimig, F. T. Bradley, R. S. (2002). Recent changes in wind chill temperatures at high latitudes in North America. Geophysical research letters, 29(8), pp. 4 - 1.

Kekana, H. & Landwehr, G. (2019). Wind capacity factor calculator. Journal of Energy in Southern Africa, 30(2), pp. 118 - 25.

Kendall, M. G. (1975). Rank Correlation Methods. 1 ed. London, UK: Charles Griffin.

Key, J. R. & Chan, A. C. K. (1999). Multidecadal global, and regional trends in 1000 mb, and 500 mb cyclone frequencies. Geo Physical Research Letters, 26(14), pp. 2053 - 6.

Keyhani, A., Ghasemi-Varnamkhasti, M., Khanali, M. & Abbaszadeh, R. (2010). An assessment of wind energy potential as a power generation source in the capital of Iran, Tehran. Energy, 35(1), pp. 188 - 201.

Kim, H. C., Kim, S., Kim, B., Jin, C., Hong, S., Park, R., Stein, A. (2017). Recent increase of surface particulate matter concentrations in the Seoul Metropolitan Area, Korea. Scientific reports, 7(1), p. 4710.

King, J. (2006). Minnesota Public Utilities Commission. [Online] Available at: http://uvig.org/wp-content/uploads/2013/01/windrpt_vol-1.pdf [Accessed 26 08 2018].

Klink, K. (1999). Trends in mean monthly maximum, and minimum surface wind speeds in the coterminous United States, 1961 to 1990. Climate Research, 13(3), pp. 193 - 205.

Klink, K. (2002). Trends, and interannual variability of wind speed distributions in Minnesota. Journal of Climate, 15(22), pp. 3311 - 7.

Klink, K. (2007). Atmospheric circulation effects on wind speed variability at turbine height. journal of applied meteorology, 46(4), pp. 445 - 56.

Kloppers, P. L. (2014). Investigating the relationships between wheat-specific rainfall characteristics, large-scale modes of climate variability, and wheat yields in the Swartland region, South Africa, Cape Town: UCT.

Knowland, K. E., Doherty, R. M., Hodges, K. I. & Ott, L. E. (2017). The influence of mid-latitude cyclones on European background surface ozone. Atmospheric Chemistry, and Physics, 17(20), pp. 12421 - 12447.

Ko, K., Kim, K. & Huh, J. (2010). Variations of wind speed in time on Jeju Island, Korea. Energy, 35(8), pp. 3381 - 7.

Kobashi, T., Box, J. E., Vinther, B. M., Goto-Azuma, K., Blunier, T., White, J. W., Andresen, C. S. (2015). Modern solar maximum forced late twentieth century Greenland cooling. Geophysical research Letters, 42(06), pp. 5992 - 99.

Kodera, K., Coughlin, K. & Arakawa, O. (2007). Possible modulation of the connection between the Pacific, and Indian Ocean variability by the solar cycle. Geopysical research letters, 34(5), p. L03710.

Köse, R. (2004). An evaluation of wind energy potential as a power generation source in Kütahya, Turkey. Energy Conversion, and Management, 45(112), pp. 1631 - 41.

Kramm, G., Mölders, N., Cooney, J. & Dlugi, R. (2019). Near-Surface Wind-Speed Stilling in Alaska during 1984-2016, and Its Impact on the Sustainability of Wind Power. Journal of Power, and Energy Engineering, 7(7), pp. 71 - 124.

Kruger, A. C. (1999). The influence of the decadal-scale variability of summer rainfall on the impact of el Nino, and La Nina events in South Africa. International Journal of Climatology, 19(1), pp. 59 - 68.

Kruger, A. C. (2011). Wind climatology of South Africa relevant to the design of the built environment, Stellenbosch: University of Stellenbosch.

Kruger, A. C., Goliger, A. M., Retief, J. V. & Sekele, S. (2010). Strong wind climatic zones in South Africa. Wind, and Structures, 13 (1), pp. 1 - 19.

Kruger, A. C., Pillay, D. L. & Van Staden, M. (2016). Indicative hazard profile for strong winds in South Africa. South African Journal of Science, 112(1 - 2), pp. 01 - 11.

Kruger, A. C., Retief, J. V. & Goliger, A. M. (2013b). Strong winds in South Africa: Part 2 Mapping of updated statistics. Journal of the South African Institution of Civil Engineering, 55(2), pp. 46 - 58.

Kruger, A. C., Retief, J. V. & M, G. A. (2013a). Strong winds in South Africa: Part 1 Application of estimation methods. Journal of the South African Institution of Civil Engineering, 55(2), pp. 29 - 45.

Kruger, W., Eberhard, A. & Swartz, K. (2018). Renewable Energy Auctions: A Global Overview, Cape Town: Graduate School of Business (GBS).

Laapas, M. & Venäläinen, A. (2017). Homogenization, and trend analysis of monthly mean, and maximum wind speed time series in Finland, 1959–2015. International journal of climatology, 37(14), pp. 4803 - 13.

Labitzke, K. & van Loon, H. (1995). Connections between the troposphere, and stratosphere on a decadal scale. Tellus A: Dynamic Meteorology, and Oceanography, 47(2), pp. 275 - 86.

Lakhraj-Govender, R. & Grab, S. W. (2018). Assessing the impact of El Niño–Southern Oscillation on South African temperatures during austral summer. International Journal of Climatology, 39(1), pp. 143 - 56.

Landberg, L., Myllerup, L., Rathmann, O. & Petersen, E. L. (2003). Wind resource estimation - an Overview. Wind Energy, 6 (3), pp. 261 - 71.

Landry, M., Quedraogo, Y., Gagnon, Y. & Ouedraogo, A. (2017). On the wind resource mapping of Burkina Faso. International Journal of Green Energy, 14(2), pp. 150 - 6.

Lantz, E., Hand, M. & Wiser, R. (2012). IEA wind task 26 WP2: the past, and future cost of wind energy, Colorado: Golden: National Renewable Energy Laboratory.

Lau, K. M. & Sheu, P. J. (1988). Annual cycle, Quasi-Biennial oscillation, and southern oscillation in global precipitation. Journal of geophysical research, 93(D9), pp. 10975 - 10988.

Lavaysse, C., Flamant, C., Evan, A., Janicot, S., & Gaetani, M. (2016). Recent climatological trend of the Saharan heat low, and its impact on the West African climate. Climate Dynamics, 47(11), pp. 3479 - 98.

Lazenby, M. J., Todd, M. C., Chadwick, R. & Wang, Y. (2018). Future Precipitation Projections over Central, and Southern Africa, and the Adjacent Indian Ocean: What Causes the Changes, and the Uncertainty?. Journal of Climate, 31(12), pp. 4807 - 26.

Lennard, C. (2019). Multi-Scale Drivers of the South African Weather, and Climate. In: J. Knight & C. Rogerson, eds. InThe Geography of South Africa. Cham: Springer, pp. 81 - 9.

Lenters, J. D., Kratz, T. K. & Bowser, C. J. (2005). Effects of climate variability on lake evaporation: Results from a long-term energy budget study of Sparkling Lake, northern Wisconsin (USA). Journal of Hydrology, 308(1 - 4), pp. 168- 95.

Li, M. & Li, X. (2005). Investigation of wind characteristics, and assessment of wind energy potential for Waterloo region, Canada. Energy Conversion, and Management, 46(18 - 19), pp. 3014 - 33.

Li, T. & Wang, B. (2003). A Theory for the Indian Ocean Dipole–Zonal Mode. Journal of the atmospheric sciences, 60(17), pp. 2119 - 35.

Lindergren, M., Checkley Jr, D. M., Koslow, J. A., Goericke, R., & Ohman, M. D. (2017). Climate-mediated changes in marine ecosystem regulation during El Niño. 24(2), pp. 796 - 809.

Lindhorst, S., Betzler, C. & Kroon, D. (2019). Wind variability over the northern Indian Ocean during the past 4 million years–Insights from coarse aeolian dust (IODP exp. 359, site U1467, Maldives). Palaeogeography, Palaeoclimatology, Palaeoecology, 536(12), p. 109371.

Lindsey, R. (2009). Climate, and Earth's Energy Budget, Greenbelt, MD: NASA Earth Observatory.

Liu, D., Duan, W., Feng, R. & Tang, Y. (2018). Summer Predictability Barrier of Indian Ocean Dipole Events, and Corresponding Error Growth Dynamics. JGR: Oceans, 123(5), pp. 2625 - 50.

Liu, F., Sun, F., Liu, W., Wang, T., Wang, H., Wang, X., & Lim, W. H. (2019). On wind speed pattern, and energy potential in China. Applied energy, 236(2), pp. 867 - 76.

Liu, X., Zhang, X. J., Tang, Q. & Zhang, X. Z. (2014). Effects of surface wind speed decline on modeled hydrological conditions in China. Hydrology, and Earth System Sciences, 18(8), pp. 2803 - 13.

Liu, Z. & Alexander, M. (2007). Atmospheric bridge, oceanic tunnel, and global climatic teleconnections. Reviews of geophysics, 45(2), p. RG2005.

Lledó, L., Torralba, V. S. A., Ramon, J. & Doblas-Reyes, F. J. (2019). Seasonal forecasts of wind power generation. Renewable Energy, 143(12), pp. 91 - 100.

Lombard, A. & Ferreira, S. L. (2015). The spatial distribution of renewable energy infrastructure in three particular provinces of South Africa. Bulletin of Geography, 30 (30), pp. 71 - 86.

Lu, B., Ren, H., Scafie, A. A., Wu, J., Dunstone, N., Smith, D., Gordon, M. (2018). An extreme negative Indian Ocean Dipole event in 2016: dynamics, and predictability. Nature, 51(1-2), pp. 89 - 100.

Lu, J., Vecchi, G. A. & Reichler, T. (2007). Expansion of the Hadley cell under global warning. Geophysical research letters, 34(6), p. L06805.

Lu, X., McElroy, M. B. & Kiviluoma, J. (2009). Global potential for wind-generated electricity. Proceedings of the National Acadamy of Sciences of the United States of America, 106(27), pp. 10933 - 38.

Lynch, A. H., Curry, J. A., Brunner, R. D. & Maslanik, J. A. (2004). Toward an integrated assessment of the impacts of extreme wind events on Barrow, Alaska. Bulletin of the American Meteorological Society, 85(2), pp. 209 - 22.

Ma, H., Chen, H., Gray, L., Zhou, L., Li, X., Wang, R., & Zhu, S. (2018). Changing response of the North Atlantic/European winter climate to the 11 year solar cycle. Environmental Research Letters, 13(3), p. 034007.

MacLeod, D., Torralba, V., Davis, M. & Doblas-Reyes, F. (2018). Transforming climate model output to forecasts of wind power production: how much resolution is enough?. Meteorological Applications, 25(1), pp. 1 - 10.

Madden, R. A. & Julian, P. R. (1971). Detection of a 40–50 Day Oscillation in the Zonal Wind in the Tropical Pacific. Journal of the Atmospheric Sciences, 28(5), pp. 702 - 8.

Mahlalela, P. T., Blamey, R. C. & Reason, C. J. (2019). Mechanisms behind early winter rainfall variability in the southwestern Cape, South Africa. Climate Dynamics, 53(1 - 2), pp. 21 - 39.

Mahowald, N. M., Ballantine, J. A., Feddema, J. & Ramankutty, N. (2007). Global trends in visibility: implications for dust sources. Atmospheric Chemistry, and Physics, 7(12), pp. 3309 - 39.

Mann, H. B. (1945). Nonparametric tests against trends. Econometrica, 13(6), pp. 245 - 59.

Manyeredzi, T. & Makaka, G. (2018). An Assessment of the Wind Power Generation Potential of Built Environment Wind Turbine (BEWT) Systems in Fort Beaufort, South Africa. Sustainability, 10(5), p. 1346.

Maoyi, M. L., Abiodun, B. J., Prusa, J. M. & Veitch, J. J. (2018). Simulating the characteristics of tropical cyclones over the South West Indian Ocean using a Stretched-Grid Global Climate Model. Climate Dynamics, 50(5 - 6), pp. 1581 - 96.

Mararakanye, N. & Bekker, B. (2019a). Renewable energy integration impacts within the context of generator type, penetration level, and grid characteristics. Renewable, and Sustainable Energy Reviews, 108(06), pp. 441 - 51.

Mararakanye, N. & Bekker, B. (2019b). Investigating renewable energy curtailment as a flexibility resource in the future South African Grid. Johannesburg, CIGRE Southern Africa.

Marchant, R., Mumbi, C., Behera, S. & Yamagata, T. (2006). The Indian Ocean dipole – the unsung driver of climatic variability in East Africa. African Journal of Ecology, 41(1), pp. 4 - 16.

Marshall, A. G., Hemer, M. A., Hendon, H. H. & McInnes, K. L. (2018). Southern annular mode impacts on global ocean surface waves. Ocean Modelling, 129(9), pp. 58 - 74.

Mason, S. J. & Tyson, P. D. (1992). The modulation of sea surface temperature, and rainfall associations over southern Africa with solar activity, and the quasi-biennial oscillation. JGR Atmospheres, 97(D5), pp. 5847 - 56.

McCabe, G. J., Clark, M. P. & Serreze, M. C. (2001). Trends in Northern Hemisphere Surface Cyclone Frequency, and Intensity. Journal of Climate, 14(12), pp. 2763 - 68.

McVicar, T. R., Roderick, M. L., Donohue, R. J., Li, L. T., Van Niel, T. G., Thomas, A., Dinpashoh, Y. (2012). Global review, and synthesis of trends in observed terrestrial near-surface wind speeds: Implications for evaporation. Journal of Hydrology, 416 - 417(12), pp. 182 - 205.

McVicar, T. R., Van Niel, T. G., Li, L. T., Roderick, M. L., Rayner, D. P., Ricciardulli, L., & Donohue, R. J. (2008). Wind speed climatology, and trends for Australia, 1975–2006: Capturing the stilling phenomenon, and comparison with near-surface reanalysis output. Geophysical Research Letters, 35(20), p. L20403.

McVicar, T. R., Van Niel, T. G., Roderick, M. L., Li, L. T., Mo, X. G., Zimmermann, N. E., & Schmatz, D. R. (2010). Observational evidence from two mountainous regions that near-surface wind speeds are declining more rapidly at higher elevations than lower eleva than lower elevations: 1960–2006. Geophysical Research Letters, 37(6), p. L06402.

Meehl, G. A., Shea, D. J. & van Loon, H. (2007). Coupled air-sea response to solar forcing in the Pacific region during northern winter. Journal of Geophysical Research: Atmospheres, 112(D2), pp. 01 - 07.

Mekis, É., Vincent, L. A., Shephard, M. W. & Zhang, X. (2015). Observed trends in severe weather conditions based on humidex, wind chill, and heavy rainfall events in Canada for 1953–2012. Atmosphere-Ocean, 53(4), pp. 383 - 97.

Mentis, D., Hermann, S., Howells, M., Welsch, M., & Siyal, S. H. (2015). Assessing the technical wind energy potential in Africa a GIS-based approach. Renewable Energy, 83(205), pp. 110 - 25.

Mentis, D., Siyal, S. H., Korkovelos, A. & Howells, M. (2017). Estimating the spatially explicit wind generated electricity cost in Africa - A GIS based analysis. Energy Strategy Reviews, 17(September), pp. 45 - 9.

Meque, A. & Abiodun, B. J. (2015). Simulating the link between ENSO, and summer drought in Southern Africa using regional climate models. Climate Dynamics, 44(7 - 8), pp. 1888 - 90.

Mescherskaya, A. V., Eremin, V. V., Baranova, A. A. & Maystrova, V. V. (2006). Change in wind speed in northern Russia in the second half of the twentieth century, from surface, and upper air data. Russian Journal of Meteorology, and Hydrology, 9(1), pp. 46 - 58.

Meshcherskaya, A. V., Getman, I. F., Borisenko, M. M. & Shevkunova, E. I. (2004). Monitoring of wind speed in the Volga, and Ural river basins in the twentieth century. Russian Meteorology, and Hydrology, 3(1), pp. 67 - 74.

Meyer-Renschhausen, M. (2013). Evaluation of feed-in tariff-schemes in African countries. Journal of Energy in Southern Africa, 24(1), pp. 2013 - 51.

Michels, K., Potter, K. N. & Williams, J. R. (1999). Calibration of EPIC for the simulation of wind erosion damage to pearl millet in West Africa. Kansas State, Proceedings Wind Erosion – An International Symposium/Workshop.

Millstein, D., Solomon-Culp, J., Wang, M., Ullrich, P., & Collier, C. (2019). Wind energy variability, and links to regional, and synoptic scale weather. Climate Dynamics, 52(7-8), pp. 4891 - 4906.

Misios, S. (2012). Influences of the 11-year solar cycle on the tropical atmosphere, and oceans, Hamburg: International Max Planck Research School on Earth System Modelling.

Mohamed, A. A. & Elmabrouk, A. M. (2009). Assessment of the wind energy potential on the coast of Tripoli. [Online] Available at: http://www.ontario-sea.org/Storage/27/1865_Assessment_of_the_wind_Energy_Potential_on_the_Coast_of_Tripoli.pdf [Accessed 01 06 2016].

Mohammadi, K. A. & Goudarzi, N. (2018). Study of inter-correlations of solar radiation, wind speed, and precipitation under the influence of El Niño Southern Oscillation (ENSO) in California. Renewable Energy, 120(5), pp. 190 - 200.

Monjid, A. M., Maach, A., Elghanami, D. & Hafid, A. (2015). Wind resource assessment: north, and West of Morocco. Morocco, 3rd International renewable, and sustainable energy.

Moon, I. J., Kim, S. H. & Wang, C. (2015). El Niño, and intense tropical cyclones. Nature, 516 (11), pp. 82 - 85.

Moore, J., Grinsted, A. & Jevrejeva, S. (2006). Is there evidence for sunspot forcing of climate at multi-year, and decadal periods?. Geophysical Research Letters, 33(17), p. L17705.

Moratiel, R., Snyder, R. L., Durán, J. M. & Tarquis, A. M. (2011). Trends in climatic variables, and future reference evapotranspiration in Duero Valley (Spain). Natural Hazards, and Earth System Sciences, 11(6), pp. 1795 - 1805.

Mostafaeipour, A. & Abarghooei, H. (2008). Harnessing wind energy at Manjil area located in north of Iran. Renewable, and Sustainable Energy Reviews, 12(6), pp. 1758 - 66.

Munday, C. & Washington, R. (2018). Systematic climate model rainfall biases over southern Africa: links to moisture circulation, and topography. Journal of Climate, 31(18), pp. 7533 - 7548.

Nagovitsyn, Y. A. & Kuleshova, A. I. (2015). North–South asymmetry of solar activity on a long timescale. Geomagnetism, and Aeronomy, 55(7), pp. 887 - 91.

Naizghi, M. S. & Ouarda, T. B. M. J. (2017). Teleconnections, and analysis of long-term wind speed variability in the UAE. International Journal of Climatology, 37(1), pp. 230 - 48.

Najac, J., Lac, C. & Terray, L. (2011). Impact of climate change on surface winds in France using a statistical-dynamical downscaling method with mesoscale modelling. International Journal of Climatology, 31(3), pp. 415 - 30.

Nchaba, T. (2013). Verification of gridded seasonal wind speed forecasts over South Africa, Cape Town: University of Cape Town.

Ncwane, S. & Folly, K. A. (2020). A Review of the Impact of Integrating Wind Generation on Transient Stability. Cape Town, IEEE.

Neuberger, J. (1981). Coriolis force revisited. American Journal of Physics, 49(8), pp. 782-784.

Nfah, E. M. & Ngundam, J. M. (2008). Modelling of wind/diesel/battery hybrid power systems for far North Cameroon. Meteorogical Society, 49(6), pp. 1295 - 1301.

Ng, B., Cai, W., Cawan, T. & Daohua, B. (2018). Influence of internal climate variability on Indian Ocean Dipole properties. Scientific reports, 8(1), pp. 1 - 8.

Ni, Y. & Li, M. (2016). Wind pressure data reconstruction using neural network techniques: A comparison between BPNN, and GRNN. Measurement, 88(6), pp. 468 - 76.

Nigam, T., Pant, V. & Prakash, K. R. (2018). Impact of Indian ocean dipole on the coastal upwelling features off the southwest coast of India. Ocean dynamics, 68(6), pp. 633 - 76.

NOAA. (2019a). Antarctic Oscillation (AAO). [Online] Available at: https://www.cpc.ncep.noaa.gov/products/precip/CWlink/daily_ao_index/aao/aao.shtml [Accessed 31 May 2019].

NOAA. (2019b). Dipole Mode Index (DMI). [Online] Available at: https://www.esrl.noaa.gov/psd/gcos_wgsp/Timeseries/DMI/ [Accessed 31 May 2019].

NOAA. (2019c). El Niño / Southern Oscillation (ENSO): Cold & Warm Episodes by Season. [Online] Available at: http://origin.cpc.ncep.noaa.gov/products/analysis_monitoring/ensostuff/ONI_v5.php [Accessed 31 May 2019].

NOAA. (2019d). Sunspot Index. [Online] Available at: https://www.esrl.noaa.gov/psd/gcos_wgsp/Timeseries/SUNSPOT/ [Accessed 31 May 2019].

Nogueira Júnior, F. D., Pagotto, M. A., Roig, F. A., Lisi, C. S., & Ribeiro, A. D. (2018). Responses of tree-ring growth in Schinopsis brasiliensis to climate factors in the dry forests of northeastern Brazil. Trees, 32(6), pp. 453 - 464.

Ntsadu, N. (2019). Using normalised cross correlation, and variance to determine the source of voltage unbalance exceedances in Eskom networks with wind farms. Journal of Energy in Southern Africa, 30(2), pp. 64 - 79.

O'Higgins, R. C. (2007). Savannah woodland degradation assessments in Ghana: integrating ecological indicators with local perceptions. Earth Environmental, 3(07), pp. 246 - 81.

Ogolo, E. O. (2011). Regional trend analysis of pan evaporation in Nigeria (1970 to 2000). Journal of Geography, and Regional Planning, 4(10), pp. 566 - 77.

Oguntunde, P. G., Abiodun, B. J., olukunle, O. J. & Olufayoa, A. A. (2011). Trends, and variability in pan evaporation, and other climatic variables at Ibadan, Nigeria, 1973–2008. Meteorlogical applications, 19(4), pp. 464 - 72.

Olaofe, Z. O. (2017). Modeling, and sensitivity of the seasonal ocean winds to local effects at west, and south coasts of South Africa. Sustainable Energy Technologies, and Assessments, 19(2), pp. 24-41.

Olaofe, Z. O. (2018). Review of energy systems deployment, and development of offshore wind energy resource map at the coastal regions of Africa. Energy, 161(10), pp. 1096 - 1114.

Ordóñez, C., Barriopedro, D., García-Herrera, R., Sousa, P. M., & Schnell, J. L. (2017). Regional responses of surface ozone in Europe to the location of high-latitude blocks, and subtropical ridges. Atmospheric Chemistry, and Physics, 17(4), pp. 3111 - 31.

Ouammi, A., Dagdougui, H., Sacile, R. & Mimet, A. (2010). Monthly, and seasonal assessment of wind energy characteristics at four monitored locations in Liguria region (Italy). Renewable, and Sustainable Energy Reviews, 14(7), pp. 1959 - 68.

Owens, M. J., Lockwood, M., Hawkins, E., Usoskin, I., Jones, G. S., Barnard, L., Fasullo, J. (2017). The Maunder minimum, and the Little Ice Age: an update from recent reconstructions, and climate simulations. Journal of Space Weather, and Space Climate, 7(A33).

Ozdogan, M. & Salvucci, G. D. (2004). Irrigation induced changes in potential evapotranspiration in southeastern Turkey: Test, and application of Bouchet's complementary hypothesis. Water Resources Research, 40(4), p. W04301.

Ozer, P. (1996). Evolution des directions et des vitesses des vents de 1951 à 1994 sur la façade Atlantique de l'Afrique de l'Ouset du sud du Senegal au nord de la Mauritanie. Journal of International Climatology, 9(96), pp. 479 - 86.

Palaiologou, P., Kalabokidis, K., Haralambopoulos, D., Feidas, H., & Polatidis, H. (2011). Wind characteristics, and mapping for power production in the Island of Lesvos, Greece. Computers & geosciences, 37(7), pp. 962 - 72.

Papadopoulos, K. H. & Helmis, C. G. (1999). Evening, and morning transition of katabatic flows. Boundary-Layer Meteorology, 99 (92), pp. 195 - 227.

Papaioannou, G., Kitsara, G. & Athanasatos, S. (2011). Impact of global dimming, and brightening on reference evapotranspiration in Greece. Journal of Geophysical Research: Atmospheres, 116(D09107), pp. 1 - 13.

Patra, A. & Bhaskaran. P. (2016). Trends in wind-wave climate over the head Bay of Bengal region. International Journal of Climatology, 36(13), pp. 4222 - 40.

Pei, W., Chen, Y., Sheng, K., Deng, W., Du, Y., Qi, Z., & Kong, L. (2015). Temporal -spatial analysis, and improvement measures of Chinese power system for wind power curtailment problem. Renewable, and Sustainable Energy Reviews, 49(9), pp. 148 - 68.

Pepler, A., Dowdy, A. & Hope, P. (2018). A global climatology of surface anticyclones, their variability, associated drivers, and long-term trends. Climate Dynamics, 52(9 - 10), pp. 5397 - 5412.

Perry, S. J., McGregor, S., Gupta, A. S., England, M. H., & Maher, N. (2020). Projected late 21st century changes to the regional impacts of the El Niño-Southern Oscillation. Climate Dynamics, 54(1 - 2), pp. 395 - 412.

Persaud, S., Flynn, D. & Fox, B. (1999). Potential for wind generation on the Guyana coastlands. Renewable Energy, 18(2), pp. 175 - 89.

Philippon, N., Rouault, M., Richard, Y. & Favre, A. (2011). The influence of ENSO on winter rainfall in South Africa. International Journal of Climatology, 32(15), pp. 2333 - 47.

Pirazzoli, P. A. & Tomasin, A. (2003). Recent near-surface wind changes in the central Mediterranean, and Adriatic areas. International Journal of Climatology: A Journal of the Royal Meteorological Society, 23(8), pp. 963 - 73.

Pishgar-Komleh, S. H., Keyhani, A. & Sefeedpari, P. (2015). Wind speed, and power density analysis based on Weibull, and Rayleigh distributions. Renewable, and Sustainable Energy Reviews, 42 (2), pp. 313 - 22.

Pohl, B. (2010). Relationships between the Antarctic Oscillation, the Madden–Julian Oscillation, and ENSO, and Consequences for Rainfall Analysis. Journal of Climate, 23(2), pp. 238 - 54.

Pollet, B. G., Staffell, I. & Adamson, K. A. (2015). Structure of the rnergy sector in South Africa. In: The energy landsCape in the Republic of South Africa. London: Springer International Publishing, pp. 21 - 9.

Pomposi, C., Funk, C., Shukla, S., Harrison, L., & Magadzire, T. (2018). Distinguishing southern Africa precipitation response by strength of El Niño events, and implications for decision-making. Environmental Research Letters, 13(7), p. 074015.

Prestes, A., Klausner, V., Rojahn da Silva, I., Ojeda-González, A., & Lorensi, C. (2018). Araucaria growth response to solar, and climate variability in South Brazil. Annales Geophysicae, 36(05), pp. 717 - 29.

Prikryl, P., Muldrew, D. B. & Sofko, G. J. (2009b). The influence of solar wind on extratropical cyclones - Part 2: A link mediated by auroral atmospheric gravity waves?. Annales Geophysicae, 27(1), pp. 31 - 57.

Prikryl, P., Rusin, V. & Rybansk, M. (2009a). The influence of solar wind on extratropical cyclones – Part 1: Wilcox effect revisited. Annales Geophysicae, 27(1), pp. 1 - 30.

Pryor, S. C. & Barthelmie, R. J. (2013). Assessing the vulnerability of wind energy to climate change, and extreme events. Climatic Change, 121(1), pp. 79 - 91.

Pryor, S. C. & Ledolter, J. (2010). Addendum to "Wind speed trends over the contiguous United States". Journal of Geophysical Research: Atmospheres, 115(D10), p. D10103.

Pryor, S. C., Barthelmie, R. J. & Schoof, J. T. (2005). The impact of non-stationarities in the climate system on the definition of 'a normal wind year': a case study from the Baltic. International Journal of Climatology, 05(25), pp. 735 - 52.

Pryor, S. C., Barthelmie, R. J., Young, D. T. & Takle, D. T. (2009). Wind speed trends over the contiguous United States. Journal of Geophysical Research, 09 (114), p. D14105.

Pryor, S. C., Barthelmine, R. J. & Schoof, J. T. (2006). Inter-annual variability of wind indices across Europe. Wind Energy, 9(1-2), pp. 27 - 38.

Rahimzadeh, F., Noorian, A. M., Pedram, M. & Kruk, M. C. (2011). Wind speed variability over Iran, and its impact on wind power potential: a case study for Esfehan Province. meteorological Applications, 18(2), pp. 198 - 210.

Randel, W. J. & Wu, F. (2007). A stratospheric ozone profile data set for 1979–2005: Variability, trends, and comparisons with column ozone data. Journal of geophysical research, 112(D6), p. D06313.

Rasmussen, D. J., Holloway, T. & Nemet, G. F. (2011). Opportunities, and challenges in assessing climate change impacts on wind energy—a critical comparison of wind speed projections in California. Environmental Research Letters, 6(2), p. 024008.

Raspopov, O. M., Dergachev, V. A. & Kolström, T. (2004). Periodicity of climate conditions, and solar variability derived from dendrochronological, and other palaeoclimatic data in high latitudes. Palaeogeography, Palaeoclimatology, Palaeoecology, 209(1 - 4), pp. 127 - 39.

Rauthe, M. & Paeth, H. (2004). Relative importance of Northern Hemisphere circulation modes in predicting regional climate change. Journal of Climate, 17(21), pp. 4180 - 9.

Reason, C. J. & Rouault, M. (2005). Links between the Antarctic Oscillation, and winter rainfall over western South Africa. Geophysical Research Letters, 32(7), pp. 1 - 4.

Reason, C. J. (2001). Subtropical Indian Ocean SST dipole events, and southern African rainfall. Geophysical research Letters, 28(11), pp. 2225 - 7.

Reason, C. J. C. (2019). Storm Hazards in Sub-Saharan Africa. Natural, and Human-Induced Hazards, and Disasters in Africa. In: G. Mulugeta & T. Simelane, eds. Natural, and Human-Induced Hazards, and Disasters in Africa. Pretoria: Africa institute of South Africa, p. 112.

Reason, C. J., Rouault, M., Melice, J. L. & Jagedheesha, D. (2002). Interannual winter rainfall variability in SW South Africa, and large scale ocean–atmosphere interactions. Meteorology, and Atmospheric Physics, 80(1-4), pp. 19 - 29.

Reba, M. L., Marks, D., Seyfried, M., Winstral, A., Kumar, M., & Flerchinger, G. (2011). A long - term data set for hydrologic modeling in a snow-dominated mountain catchment. Water Resources Research, 47(7), pp. 1 - 7.

Recio, M., Rodríguez-Rajo, F. J., Jato, M. V., Trigo, M. M., & Cabezudo, B. (2009). The effect of recent climatic trends on Urticaceae pollination in two bioclimatically different areas in the Iberian Peninsula: Malaga, and Vigo. Climatic Change, 97(1-2), pp. 215 - 28.

Rehman, S. (2004). Wind energy resources assessment for Yanbo, Saudi Arabia. Energy Conversion, and Management, 45(13- 14), pp. 2019 - 32.

Rehman, S., El-Amin, I. M., Ahmad, F., Shaahid, S. M., Al-Shehri, A. M., & Bakhashwain, J. M. (2007). Wind power resource assessment for Rafha, Saudi Arabia. Renewable, and Sustainable Energy Reviews, 11(5), pp. 937 - 50.

Ren, G., Liu, J., Wan, J., Guo, Y., & Yu, D. (2017). Overview of wind power intermittency: Impacts, measurements, and mitigation solutions. Applied Energy, 204(10), pp. 47-65.

Ren, G., Wan, J., Liu, J., Yu, D., & Soder, L. (2018). Analysis of wind power intermittency based on historical wind power data. Energy, 150(5), pp. 482 - 92.

Resmi, E. A., Murugavel, P., Dinesh, G., Balaji, B., Leena, P. P., Mercy, V., Prabha, T. V. (2019). Observed diurnal, and intraseasonal variations in boundary layer winds over Ganges valley. Journal of Atmospheric, and Solar-Terrestrial Physics, 188(7), pp. 11 - 25.

Rienecker, M., Suarez, M., Todling, R., Bacmeister, J., Takacs, L., Liu, H. C., Stajner, I. (2008). Technical Report Series on Global Modeling, and Data Assimilation: The GEOS-5 Data Assimilation System Documentation of Versions 5.0. 1, 5.1. 0., and 5.2. 0, Greenbelt, USA: NASA.

Robeson, S. M. & Shein, K. A. (1997). Spatial coherence, and decay of wind speed, and power in the north-central United States. Physical Geography, 18(6), pp. 479 - 95.

Roderick, M. L., Rotstayn, L. D., Farquhar, G. D. & Hobbins, M. T. (2007). On the attribution of changing pan evaporation. Geophysical research letters, 34(17), p. L17403.

Rodrigues, R. R. (2015). The Impact of ENSO on the South Atlantic Subtropical Dipole Mode. Journal of Climate, 28(7), pp. 2691 - 2705.

Rosales-Asensioa, E., Borge-Diezb, D., Blanes-Peirób, J. J. & Pérez-Hoyosc, A. (2019). Review of wind energy technology, and associated market, and economic. Renewable, and Sustainable Energy Reviews, 101(3), pp. 415 - 427.

Rouault, M., Pohl, B. & Peven, P. (2010). Coastal oceanic climate change, and variability from 1982 to 2009 around South Africa. African Journal of Marine Science, 32(2), pp. 237 - 46.

Routson, C. C., McKay, N. P., Kaufman, D. S., Erb, M. P., Goosse, H., Shuman, B. N., Ault, T. (2019). Mid -latitude net precipitation decreased with Arctic warming during the Holocene. Nature, 568(7750), pp. 83 - 87.

Sabziparvar, A. A., Mirmasoudi, S. H., Tabari, H., Nazemosadat, M. J., & Maryanaji, Z. (2011). ENSO teleconnection impacts on reference evapotranspiration variability in some warm climates of Iran. International Journal of Climatology, 31(11), pp. 1710 - 23.

Safari, B. & Gasore, J. (2010). A statistical investigation of wind characteristics, and wind energy potential based on the Weibull, and Rayleigh models in Rwanda. Renewable Energy, 12(35), pp. 2874 - 80.

Saji, N. H. & Yamagata, T. (2003). Possible impacts of Indian Ocean Dipole mode events on global climate. Climate Research, 25(2), pp. 151 - 61.

Saji, N. H., Ambrizzi, T. & Ferraz, S. E. (2005). Indian Ocean Dipole mode events, and austral surface air temperature anomalies. Dynamics of Atmospheres, and Oceans, 39(1-2), pp. 87 - 101.

Saji, N. H., Goswami, B., Vinayachandran, P. & Yamagata, T. (1999). A dipole mode in the tropical Indian Ocean. Nature, 401, pp. 360-63.

Sang, Y. F., Wang, Z. & Liu, C. (2013). Discrete wavelet-based trend identification in hydrologic time series. Hydrological Processes, 27(14), pp. 2021 - 31.

Sato, K., Inoue, J., Yamazaki, A., Kim, J. H., Makshtas, A., Kustov, V., Dethloff, K. (2018). Impact on predictability of tropical, and mid-latitude cyclones by extra Arctic observations. Scientific reports, 8(1), pp. 1 - 8.

SAWS. (2015). About Climate at SAWS. [Online] Available at: http://www.weathersa.co.za/climate [Accessed 09 February 2015].

SAWS. (2019). Historical Synpotic Charts. [Online] Available at: http://www.weathersa.co.za/home/historicalsynoptic [Accessed 31 May 2019].

Schindler, D., Jung, C. & Buchholz, A. (2016). Using highly resolved maximum gust speed as predictor for forest storm damage caused by the high-impact winter storm Lothar in Southwest Germany. Royal Meyeorological Society, 17(8), pp. 462 - 9.

Schlipf, D., Rettenmeier, A., Haizmann, F., Hofsäß, M., Courtney, M., & Cheng, P. W. (2012). Model based wind vector field reconstruction from lidar data. Bremen, Proceedings of the 11th German Wind Energy Conference DEWEK 2012, 7th-8th November 2012.

Schulze-Makuch, D. & Irwin, L. N. (2018). Energy Sources, and Life. In: S. P. Books, ed. Life in the Universe. Switzerland: Springer, Cham, pp. 75 - 100.

Schumann, E. H. (1992). Interannual wind variability on the south, and east coasts of South Africa. JGR Atmospheres, 97(D18), pp. 20397 - 403.

Scott, R. C., Nicolas, J. P., Bromwich, D. H., Norris, J. R., & D, L. (2019). Meteorological drivers, and large-scale climate forcing of West Antarctic surface melt. Journal of Climate, 32(3), pp. 665 - 84.

Sen, P. K. (1968). Estimates of the regression coefficient based on Kendall's tau. Journal of the American statistical association, 63(324), pp. 1379 - 89.

Shaner, M. R., Davis, S. J., Lewis, N. S. & Caldeira, K. (2018). Geophysical constraints on the reliability of solar, and wind power in the United States. Energy & Environmental Science, 11(4), pp. 914 - 25.

Sharma, P. K., Warudkar, V. & Ahmed, S. (2019). A comparative analysis of wind resource parameters using WAsP, and windPRO. International journal of green energy, 16(2), pp. 152 - 66.

Shen, L., Mickley, L. J. & Tai, A. P. K. (2015). Influence of synoptic patterns on surface ozone variability over the eastern United States from 1980 to 2012. Atmospheric Chemistry, and Physics, 15(19), pp. 10925 - 38.

Shen, L., Zhao, C., Ma, Z., Li, Z., Li, J., & Wang, K. (2019). Observed decrease of summer sea-land breeze in Shanghai from 1994 to 2014, and its association with urbanization. Atmospheric Research, 227(10), pp. 198 - 209.

Shenbin, C., Yunfeng, L. & Thomas, A. (2006). Climatic change on the Tibetan Plateau: potential evapotranspiration trends from 1961–2000. Climatic change, 76(3 - 4), pp. 291 - 319.

Shi, P., Zhang, G., Kong, F., Chen, D., Azorin-Molina, C., & Guijarro, J. A. (2019). Variability of winter haze over the Beijing-Tianjin-Hebei region tied to wind speed in the lower troposphere, and particulate sources. Atmospheric Research, 215(01), pp. 1 - 11.

Shuab, Z. R., Liab, Q. S., Hec, Y. C. & Chand, P. W. (2018). Observational study of veering wind by Doppler wind profiler, and surface weather station. Journal of Wind Engineering, and Industrial Aerodynamics, 178(7), pp. 18 - 25.

Shumway, R. H. & Stoffer, D. S. (2011). Time series regression, and exploratory data analysis. In: In: Time Series Analysis, and its Applications. New York: Springer, pp. 47 - 82.

Simonsen, T. K. & Stevens, B. G. (2004). Regional wind energy analysis for the Central United States, Grand Forks: Energy & Environmental Research Center.

Slingo, J., Spencer, H., Hoskins, P. B. & Black, E. (2004). The meteorology of the Western Indian Ocean, and the influence of the East African Highlands. Philosophical Transactions of the Royal Society A, 363(1826), pp. 25 - 42.

Slot, R. M., Svenningsen, L., Sørensen, J. D. & Thøgersen, M. L. (2018). Importance of Shear in Site Assessment of Wind Turbine Fatigue Loads. Journal of Solar Energy Engineering, 140(4), p. 041012.

Sniderman, J. K., Brown, J. R., Woodhead, J. D., King, A. D., Gillett, N. P., Tokarska, K. B., Meinshausen, M. (2019). Southern Hemisphere subtropical drying as a transient response to warming. Nature Climate Change, 9(3), pp. 232 - 36.

Solari, G. (2019). Wind Science, and Engineering. In: Cham, ed. Wind Meteorology, Micrometeorology, and Climatology. 1 ed. Garmisch-Partenkirchen, Germany: Springer, pp. 325 - 440.

Soler-Bientz, R., Watson, S. & Infield, D. (2010). Wind characteristics on the Yucatán Peninsula based on short term data from meteorological stations. Energy Conversion, and Management, 51(4), pp. 754 - 64.

Solomom, S., Daniel, J. S., Neely, R. R. & Vernier, J. P. (2011). The persistently variable "background" stratospheric aerosol layer, and global climate change. Science, 333 (6044), pp. 866 - 70.

Song, Z. W., Zhang, H. L., Snyder, R. L., Anderson, F. E., & Chen, F. (2010). Distribution, and trends in reference evapotranspiration in the North China Plain. Journal of Irrigation, and Drainage Engineering, 136(4), pp. 240 - 7.

Sonwa, D. J., Dieye, A., El Mzouri, E. H., Majule, A., Mugabe, F. T., Omolo, N., Brooks, N. (2017). Drivers of climate risk in African agriculture. Climate, and Development, 9(5), pp. 383 - 98.

Sorensen, P., Litong-Palima, M., Hahmann, A. N., Heunis, S., Ntusi, M., & Hansen, J. C. (2018). Wind power variability, and power system reserves in South Africa. J. energy South. Afr., 29(1), pp. 59-71.

Soukharev, B. E. & Hood, L. L. (2006). Solar cycle variation of stratospheric ozone: Multiple regression analysis of long-term satellite data sets, and comparisons with models. Journal of geophysical research, 111(D20), p. D20314.

Sousa, P. M., Blamey, R., Reason, C., Ramos, A. M., & Trigo, R. M. (2018). The "Day Zero" Cape Town drought, and the poleward migration of moisture corridors. Environmental Research Letters, 13(12), p. 124025.

Spinoni, J., Vogt, J., Naumann, G., Carrao, H., & Barbosa, P. (2015). Towards identifying areas at climatological risk of desertification using the Köppen–Geiger classification, and FAO aridity index. International Journal of Climatology, 35(9), pp. 2210 - 22.

StatsSA. (2019). P4141 - Electricity generated, and available for distribution. [Online] Available at: http://www.statssa.gov.za/?s=P4141%20&sitem=publications [Accessed 7 Sept 2019].

Stutton, J. R. (1905). The Winds of East London. Quarterly Journal of the Royal Meteorological Society, 31(134), pp. 133 - 149.

Stutton, J. R. (1908). The Working Value of the Wind at Kimberley. Agricultural Journal of the union of South Africa, 33(4).

Stutton, J. R. (1910). The working value of the wind at East London. Agricultural Journal of the Union of South Africa, 37(3), pp. 282 - 83.

Sun, X., Renard, B., Thyer, M. & Westra, S. (2015). A global analysis of the asymmetric effect of ENSO on extreme precipitation. Journal of Hydrology, 530 (11), pp. 51 - 65.

Tahir, N. A., Omer, D. A., Lateef, D. D., Ahmad, D. A., Salih, S. H., & Khal, L. H. (2019). Diversity, and Population Structure Analysis of Faba Bean (Vicia faba L.) Accessions Using SSR Markers. Journal of Agricultural Science, and Technology, 21(2), pp. 463 - 74.

Takatama, K., Minobe, S., Inatsu, M. & Small, J. R. (2015). Diagnostics for near-surface wind response to the gulf stream in a regional atmospheric model. Journal of Climate, 28 (1), pp. 235 - 55.

Tang, B., Tong, L., Kang, S. & Zhang, L. (2011). Impacts of climate variability on reference evapotranspiration over 58 years in the Haihe river basin of north China. Agricultural Water Management, 98(10), pp. 1660 - 70.

Tchinda, R. & Kaptouom, E. (2003). Wind energy in Adamaoua, and North Cameroon provinces. Energy Conversion, and Management, 44(6), pp. 845 - 57.

Tchinda, R., Kendjio, J., Kaptouom, E. & Njomo, D. (2000). Estimation of mean wind energy available in far north Cameroon. Energy conversion management, 41(17), pp. 1917 - 29.

Technical University of Denmark. (2018). Global wind atlas. [Online] Available at: https://globalwindatlas.info/ [Accessed 01 07 2019].

The Wind Power. (2019). Worldwide Wind Farms. [Online] Available at: https://www.thewindpower.net/country_list_en.php [Accessed 6 July 2019].

Thompson, D. W. J. & Wallace, J. M. (1998). The Arctic Oscillation signature in the wintertime geopotential height, and temperature fields. Geophysical research letters, 25(9), pp. 1297 - 1300.

Thomson, D. W., Soloman, S., Kushner, P. J., England, M. H., Grise, K. M., & Karoly, D. J. (2011). Signatures of the Antarctic ozone hole in Southern Hemisphere surface climate change. Nature Geoscience, 4(11), pp. 741 - 49.

Thopil, M. S., Bansal, R. C., Zhang, L. & Sharma, G. (2018). A review of grid connected distributed generation using renewable energy sources in South Africa. Energy Strategy Reviews, 21(8), pp. 88-97.

Tian, Q., Huang, G., Hu, K. & Niyogi, D. (2019). Observed, and global climate model based changes in wind power potential over the Northern Hemisphere during 1979–2016. Energy, 167(1), pp. 1224 - 35.

Tinsley, B. A. (1991). Interpretation of Short-Term Solar Variability Effects in the Troposphere. Journal of geomagnetism, and geoelectricity, 43(2), pp. 775 - 83.

Trouet, V., Babst, F. & Meko, M. (2018). Recent enhanced high-summer North Atlantic Jet variability emerges from three-century context. Nature communications, 9(1), p. 180.

Tuller, S. E. (2004). Measured wind speed trends on the West coast of Canada. International Journal of Climatology, 04 (24), pp. 1359 - 74.

Tyson, P. D. & Preston-Whyte, R. A. (2000). The Weather, and Climate of Southern Africa, London: Oxford University Press.

Ummenhofer, C. C., Gupta, A. S., Taschetto, A. S. & England, M. H. (2009). Modulation of Australian Precipitation by Meridional Gradients in East Indian Ocean Sea Surface Temperature. Journal of Climate, 22(21), pp. 5597 - 5610.

Ummenhofer, C. C., Sen Gupta, A., England, M. H. & Reason, C. J. (2009). Contributions of Indian Ocean sea surface temperatures to enhanced East African rainfall. Journal of Climate, 22(4), pp. 933 - 1013.

Vaas, F. & Kim, H. G. (2008). Application of Neural Network for Long-Term Correction of Wind Data. 신재생에너지, 4(4), pp. 23 - 9.

Vaideanu, P., Dima, M. & Voiculescu, M. (2018). Atlantic Multidecadal Oscillation footprint on global high cloud cover. Theoretical, and Applied Climatology, 134(3-4), pp. 1245 - 56.

van Vuuren, C. Y. & Vermeulen, H. J. (2019). Wind resource clustering based on statistical Weibull characteristics. Wind Engineering, 43(4), pp. 126 - 43.

Vautard, R., Cattiaux, J., Yiou, P., Thépaut, J. N., & Ciais, P. (2010). Northern hemisphere atmospheric stilling partly attributed to increased surface roughness. Nature geoscience, 3(11), pp. 756 - 61.

Verdon-kidd, D. C. (2018). On the classification of different flavours of Indian Ocean Dipole events. International Journal of Climatology, 38(13), pp. 4924 - 37.

Vinayachandran, P. N., Lizuka, S. & Yamagata, T. (2002). Indian Ocean dipole mode events in an ocean general circulation model. Deep Sea Research Part II: Topical Studies in Oceanography, 49(7-8), pp. 1573 - 96.

Vuillermoz, E., Cabini, E., Verza, G. P. & Tartari, G. (2006). Summary Report 1994 - 2006 of Pyramid Meteorological Network, Khumbu Valley, Nepal, Bergamo, Italy: SHARE Project, Ec-K2-CNR Committee.

Walker, G. T. & Bliss, E. (1924). World Weather II. Mem. Roy. Meteor., 24(1), pp. 275-506.

Walker, G. T. & Bliss, E. (1932). World weather V. Mem. Roy. Meteor., 4(36), pp. 53-84.

Wan, H., Wang, X. L. & Swail, V. R. (2010). Homogenization, and trend analysis of canadian near-surface wind speeds. Journal of Climate, 10 (23), pp. 1209 - 225.

Wang, B., Wu, R. & FU, X. (2000). Pacific-East Asian teleconnection: How does ENSO affect East Asian climate?. Journal of climate, 13(9), pp. 1517 - 1536.

Wang, F. K. & Du, T. C. T. (2000). Using principal component analysis in process performance for multivariate data. Omega, 28(2), pp. 185 - 94.

Wang, J., Qin, S., Jin, S. & Wu, J. (2015). Estimation methods review, and analysis of offshore extreme wind speeds, and wind energy resources. Renewable, and Sustainable Energy Reviews, 42 (1), pp. 26 - 42.

Warudkar, V., Sharma, P. K. & Ahmed, S. (2019). Analysis of a terrain characteristic using WAsP, and windPRO. Energy Procedia, 158(2), pp. 1223 - 8.

WASA. (2015). Online data projects. [Online] Available at: http://www.wasa.csir.co.za/ProjectListText.aspx?&Rnd=658864 [Accessed 10 February 2015].

Watson, S. J., Kritharas, P. & Hodgson, G. J. (2015). Wind speed variability across the UK between 1957, and 2011. Wind Energy, 18(1), pp. 21 - 42.

Webster, P. J., Moore, A. M., Loschnigg, J. P. & Leben, R. R. (1999). Coupled ocean atmosphere dynamics in the Indian Ocean during 1997-98. Nature, 401(6751), pp. 356 - 60.

Weldon, D. & Reason, C. J. (2014). Variability of rainfall characteristics over the South Coast region of South Africa. Theoretical, and Applied Climatology, 115(1-2), pp. 177 - 85.

Wents, F. Z., Ricciardulli, L., Hilburn, K. & Mears, C. (2007). How much more rain will global warming bring?. Science, 317(5835), pp. 233 - 35.

Westra, S., White, C. J. & Kiem, A. S. (2016). Introduction to the special issue: historical, and projected climatic changes to Australian natural hazards. Climatic change, 139(1), pp. 1 - 19.

William, J. E. & Thomson, R. E. (1997). Data analysis methods in physical oceanography. Tunbridge Wells, Kent: Gray Publishing.

Willmott, C. J., Ackleson, S. G., Davis, R. E., Feddema, J. J., Klink, K. M., Legates, D. R., O'donnell, J. M., Rowe, C. (1985). Statistics for the evaluation, and comparison of models. Journal of Geophysical Research: Oceans, 90(C5), pp. 8995 - 9005.

WindEurope. (2017). Wind in power: 2016 European statistics, Brussels: WindEurope.

Windgiant. (2013). Roughness Classes, usable wind in %. [Online] Available at: http://www.windgigant.eu/wg/index.php/en/technics/other-theme/182-rauhigkeitsklassen-nutzbare-energie-im-wind-in [Accessed 09 April 2015].

World Energy Council. (2017). World energy resources 2016, London: World Energy Council.

World Wind Energy Association. (2018a). Global Wind Installations. [Online] Available at: https://library.wwindea.org/global-statistics-2018-preliminary/ [Accessed 30 06 2019].

World Wind Energy Association. (2018b). Wind Turbines Database. [Online] Available at: https://library.wwindea.org/wind-turbines-database-top-10-oem/ [Accessed 30 06 2019].

Wright, J. G., Bischof-Niemz, T., Catitz, j. R., Mushwana, C., & van Heerden, R. (2017). Future wind deployment scenarios for South Africa, Pretoria: CSIR.

Wright, M. A. & Grab, S. W. (2017). Wind speed characteristics, and implications for: Wind power generation: Cape regions, South Africa. South African Journal of Science, 113(7/8), pp. 1 - 8.

Xie, k., Liao, Q., Tai, H. & Hu, B. (2017). Non-Homogeneous Markov Wind Speed Time Series Model Considering Daily, and Seasonal Variation Characteristics. IEEE Transactions on Sustainable Energy, 8(3), pp. 1281-90.

Xu, M., Chang, C., FU, C. & Qi, Y. (2006). Steady decline of East Asian monsoon winds 1969 - 2000: evidence from direct ground measurements of wind speed. Journal of Geophysical Research, 06(111), p. D24111.

Yanfei, L., Huipeng, S., Fengze, H., Zhu, D., & Hui, L. (2019). Smart wind speed forecasting approach using various boosting algorithms, big multi-step forecasting strategy. Renewable Energy, 135(05), pp. 540 - 53.

Yang, X., Hou, Y. & Chen, B. (2011). Observed surface warming induced by urbanization in east China. Journal of Geophysical Research: Atmospheres, 116(D14113), pp. 1 - 12.

Yin, Y., Wu, S. & Dai, E. (2010). Determining factors in potential evapotranspiration changes over China in the period 1971–2008. Chinese Science Bulletin, 55(29), pp. 3329 - 37.

You, Q., Kang, S., Flügel, W. A., Pepin, N., Yan, Y., & Huang, J. (2010). Decreasing wind speed, and weakening latitudinal surface pressure gradients in the Tibetan Plateau. Climate Research, 42(1), pp. 57 - 64.

Young, I. R. & Ribal, A. (2019). Multiplatform evaluation of global trends in wind speed, and wave height. Science, 364(6440), pp. 548 - 52.

Young, I. R., Zieger, S. & Babanin, A. V. (2011). Global trends in wind speed, and wave height. Science, 332(11), pp. 451 - 55.

Yu, B. & Zwiers, F. (2007). The impact of combined ENSO, and PDO on the PNA climate: A 1,000 -year climate modeling study. Climate Dynamics, 29(7-8), pp. 837 - 51.

Yuen, C. K. & Fraser, D. (1979). Digital Spectral Analysis. 1 ed. East Melbourne: C.S.I.R.O.

Zambrano, F., Lillo-Saavedra, M., Verbist, K. & Lagos, O. (2016). Sixteen years of agricultural drought assessment of the BioBío Region in Chile using a 250 m resolution Vegetation Condition Index (VCI). Remote Sensing, 8(6), p. 530.

Zhai, D. L., Yu, H., Chen, S. C., Ranjitkar, S., & Xu, J. (2019). Responses of rubber leaf phenology to climatic variations in Southwest China. International journal of biometeorology, 63(5), pp. 607 - 16.

Zhang, G., Azorin-Molina, C., Shi, P., Lin, D., Guijarro, J., Kong, F., & Chen, D. (2019). Impact of near-surface wind speed variability on wind erosion in the eastern agro-pastoral transitional zone of Northern China, 1982–2016. Agricultural, and Forest Meteorology, 271(06), pp. 102 - 15.

Zhang, X., Wang, L., Wang, W., Cao, D., Wang, X., & Ye, D. (2015). Long -term trend, and spatiotemporal variations of haze over China by satellite observations from 1979 to 2013. Atmospheric Environment, 119(10), pp. 362 - 73.

Zhang, Y., Chen, B., Pan, G. & Zhao, Y. (2019). A novel hybrid model based on VMD-WT, and PCA-BP-RBF neural network for short-term wind speed forecasting. Energy Conversion, and Management, 195(9), pp. 180 - 97.

Zhang, Y., Liu, C., Tang, Y. & Yang, Y. (2007). Trends in pan evaporation, and reference, and actual evapotranspiration across the Tibetan Plateau. Journal of Geophysical Research: Atmospheres, 112(D12), p. D12110.

Zhang, Z., Wang, K., Chen, D., L. J., & Dickinson, R. (2019). Increase in surface friction dominates the observed surface wind speed decline during 1973-2014 in the Northern Hemisphere lands. Journal of Climate, 32(21), pp. 7421 - 35.

Zheng, H., Liu, X., Liu, C., Dai, X., & Zhu, R. (2009). Assessing contributions to panevaporation trends in Haihe River Basin, China. Journal of Geophysical Research: Atmospheres, 114(D24105), pp. 1 - 12.

Zhou, W., Xuexi, T., Zhou, G. & Liang, P. (2015). Possible effects of climate change of wind on aerosol variation during winter in Shanghai, China. Particuology, 20 (06), pp. 80 - 88.

Zinke, J., Dullo, W. C., Heiss, G. A. & Eisenhauer, A. (2004). ENSO, and Indian Ocean subtropical dipole variability is recorded in a coral record off southwest Madagascar for the period 1659 to 1995. Earth, and Planetary Science Letters, 228(1-2), pp. 177 - 94.

Zuo, H., Li, D., Hu, Y., Bao, Y., & Lü, S. (2005). Characteristics of climatic trends, and correlation between pan-evaporation, and environmental factors in the last 40 years over China. Chinese Science Bulletin, 50(12), pp. 1235 - 41.